

CHALMERS TEKNISKA HÖGSKOLAS  
HANDLINGAR

TRANSACTIONS OF CHALMERS UNIVERSITY OF TECHNOLOGY  
GOTHENBURG, SWEDEN

Nr 34

(Avd. Elektroteknik 3)

1944

ON THE PROPAGATION OF  
RADIO WAVES

BY

OLOF E. H. RYDBECK



GÖTEBORG  
N. J. GUMPERTS BOKHANDEL A.-B.

PRINTED IN SWEDEN

CHALMERS TEKNISKA HÖGSKOLAS  
HANDLINGAR

TRANSACTIONS OF CHALMERS UNIVERSITY OF TECHNOLOGY  
GOTHENBURG, SWEDEN

Nr 34

(Avd. Elektroteknik 3)

1944

# ON THE PROPAGATION OF RADIO WAVES

BY

OLOF E. H. RYDBECK



GÖTEBORG 1944  
ELANDERS BOKTRYCKERI AKTIEBOLAG

To

*Karl G. Eliasson, E. E.,*

*a pioneer in Swedish broadcasting.*

## Introduction and Summary.

The transmission of radio waves in inhomogeneous media is a problem of considerable theoretical and practical interest. An important contribution to the subject was made in 1930 by P. S. EPSTEIN [1]. EPSTEIN'S work which was based on what might be called an EPSTEIN layer was further developed in 1939 by K. RAWER [2] with special reference to practical applications. At about the same time the present author studied the transmission properties of the parabolic layer in the penetration frequency region. The results were subsequently published [3].

In the present memoir the transmission properties of the parabolic layer are studied throughout the long, medium, and short wave ranges. Suitable expansions of the wave functions are developed for this purpose and it is also possible to investigate the accuracy of the phase integral method originally developed by T. L. ECKERSLEY [4].

The transmission of radio waves round the earth surrounded by a concentric parabolic layer is a problem of considerable interest in this connexion. General formulae are obtained for the transmission of horizontally and vertically polarized waves. These formulae are applicable to any kind of layer provided its wave functions and their circuit relation have been found. The original series solution has been transformed into the physically simplest possible form. This makes it possible to split up the solution in subsidiary waves. This has already been done in the reflector free case by B. VAN DER POL and H. BREMMER in 1937 [5]. Following G. N. WATSON [6] the series solution is transformed into a contour integral in the long wave case. The residue series subsequently obtained is studied in detail and numerical examples are shown. For medium and short waves the subsidiary waves are transformed by the stationary phase method to yield the amplitude and phase of the geometrical optical ray. The bridging between the long wave and the medium wave cases is also discussed.

It is also of considerable interest to study the attenuation coefficient in long wave transmission. In the case of horizontal polariza-

tion for example it is found that there normally is little difference between the inhomogeneous and homogeneous layers in the true long wave case. Reasonable D-layer data yield attenuation coefficients in good agreement with the empirical AUSTIN ones. As an illustration of the actual nature of the propagation the magnitude of the ratio between the actual field and the so called primary field has been plotted as a function of the sender-receiver distance in a typical long wave case. This demonstrates the crude approximation of the AUSTIN formula. A further study of the individual terms of the residue series then shows how radially standing waves are produced between reflector and ground as selected by the proper values or poles of the residue series. It is found that low order waves are guided mainly by the reflecting shell contrary to the high order waves where ground and reflector have a symmetrical attenuation influence.

Finally the transmission properties of the parabolic layer are studied from an ionospheric point of view. The influence of the electronic collisional frequency upon the transmission coefficients and the so called virtual height is discussed theoretically and numerically with special reference to practical conditions. Numerical results are shown for layers of variable thickness. In conclusion as a by-product the transmission properties of the extremely thin layer have been deduced with special reference to the discussion of the nature of the so called abnormal E-reflections.

\* \* \*

This investigation has partly been the result of a Swedish Government Grant for technical research. The author's thanks are due, and are cordially extended, to H. L. KNUDSEN, E. E., who assisted with some of the numerical computations, and to TORSTEN JÖNSSON, M. PH., who kindly assisted in correcting the proof.

Finally the author wishes to express his thanks to the Chalmers Publications Committee which generously facilitated the publication of this memoir.

O. E. H. R.

*Laboratory of Electrical Communication and Electronics 1944.*

## General Considerations.

To begin with we introduce the following notations, viz.

$e$ = magnitude of the charge of electron, $m$ = mass of electron, $c_0$ = the velocity of light, $N$ = electron density in electrons $\text{cm}^{-3}$ , $\omega$ = angular wave frequency, $\omega_H$ = angular gyro frequency of the electron in the terrestrial magnetic field, of strength $H_m$ , $\left(\omega_H = \frac{e H_m}{m c_0}\right)$ , $\nu$ = electron collisional frequency, $\Theta_P$ = angle between the wave normal and $\overline{H}_m$ , the propagation angle, $\overline{E}$ = electric field vector of the wave, $\overline{H}$ = magnetic field vector of the wave, $\overline{P}$ = the polarization vector and $\overline{D}$ = the displacement vector.	(1)
---	-----

As an introduction we make a short recapitulation of the equations of motion of the electron. We assume that all dependent variables contain time only in the factor  $e^{-j\omega t}$ . The equations of motion of an electron with displacement components,  $\xi$ ,  $\eta$ ,  $\zeta$ , along the  $z$ ,  $x$ , and  $y$  axes then become

$-m\omega^2\xi = -eE_z + j\omega m\nu\xi + j\frac{\omega e H_m}{c_0} \cdot \sin\Theta_P \cdot \eta,$ $-m\omega^2\eta = -eE_x + j\omega m\nu\eta + j\frac{\omega e H_m}{c_0} \cdot \cos\Theta_P \cdot \zeta - j\frac{\omega e H_m}{c_0} \cdot \sin\Theta_P \cdot \xi,$ $-m\omega^2\zeta = -eE_y + j\omega m\nu\zeta - j\frac{\omega e H_m}{c_0} \cdot \cos\Theta_P \cdot \xi.$	(2)
---	-----

Here we have chosen the  $z$  axis to be the direction of propagation and  $x$  is given such a direction that  $H_m$  has no component along it.

Since  $P_z = -N e \xi$ ,  $P_x = -N e \eta$ ,  $P_y = -N e \zeta$ , the equations of motion become

$$\left. \begin{aligned} -\frac{E_z}{4\pi} &= x_0^2 \left(1 + j \frac{\nu}{\omega}\right) P_z + j \gamma_T P_x, \\ -\frac{E_x}{4\pi} &= x_0^2 \left(1 + j \frac{\nu}{\omega}\right) P_x - j \gamma_T P_z + j \gamma_L P_y, \\ -\frac{E_y}{4\pi} &= x_0^2 \left(1 + j \frac{\nu}{\omega}\right) P_y - j \gamma_L P_x, \end{aligned} \right\} \quad (3)$$

where

$$\frac{1}{X} x_0^2 = \frac{\omega^2}{\omega_c^2}, \quad \gamma_T = x_0^2 \frac{\omega_H}{\omega} \cdot \sin \Theta_P, \quad \text{and} \quad \gamma_L = x_0^2 \frac{\omega_H}{\omega} \cdot \cos \Theta_P.$$

$\omega_c = \left(\frac{4\pi e^2 N}{m}\right)^{\frac{1}{2}}$  is the so-called critical frequency at which the refractive index of the friction-free ionized medium is reduced to zero when  $\omega_H = 0$ .

We assume that the electron density is a function of  $z$  only, i. e., we have a plane ionosphere. Since  $\text{div}(\bar{D}) = 0$ , this means that  $\frac{\delta}{\delta z}(D_z) = 0$ , or  $D_z = E_z + 4\pi P_z = 0$ , as constant fields are out of consideration. By (3) the expressions for  $E_x$  and  $E_y$  then become

$$\left. \begin{aligned} -\frac{E_x}{4\pi} &= \left\{ x_0^2 \left(1 + j \frac{\nu}{\omega}\right) + \frac{\gamma_T^2}{1 - x_0^2 \left(1 + j \frac{\nu}{\omega}\right)} \right\} P_x + j \gamma_L P_y, \\ -\frac{E_y}{4\pi} &= x_0^2 \left(1 + j \frac{\nu}{\omega}\right) P_y - j \gamma_L P_x. \end{aligned} \right\} \quad (3a)$$

Now for a certain value,  $\bar{u}$ , of the ratio  $P_y/P_x$ , the ratios  $E_x/P_x$  and  $E_y/P_y$  become identical and consequently belong to the same wave-solution. One immediately finds that two  $\bar{u}$  values are possible, viz.

$$\left. \begin{aligned} \bar{u}_1 &= j [\delta_u - (\delta_u^2 + 1)^{\frac{1}{2}}], \quad \bar{u}_2 = j [\delta_u + (\delta_u^2 + 1)^{\frac{1}{2}}], \quad \text{and} \quad \bar{u}_1 \bar{u}_2 = 1, \\ \text{where} \\ \delta_u &= \frac{\gamma_T^2}{2\gamma_L} \cdot \frac{1}{1 - x_0^2 \left(1 + j \frac{\nu}{\omega}\right)} = \frac{1}{2} \cdot \frac{\sin^2 \Theta_P}{\cos \Theta_P} \cdot \frac{\omega \omega_H}{\omega_c^2 - \omega^2 - j \omega \nu}. \end{aligned} \right\} \quad (4)$$

As  $\omega_c$  is a function of  $z$ , the ratios  $\bar{u}$  are not independent of height. This means, as we shall see, that the two wave-solutions corresponding to  $\bar{u}_1$  and  $\bar{u}_2$  generally are not independent of each other. Since  $E_x/P_x = E_y/P_y$ , we have

$$E_y^{(1)}/E_x^{(1)} = \bar{u}_1, \quad E_x^{(2)}/E_y^{(2)} = \bar{u}_2. \quad (4 a)$$

Neglecting for a moment the collisional friction ( $\nu^2$  generally  $\ll \omega^2$ ), one finds from (4) that wave-solution 2 has right-hand polarization

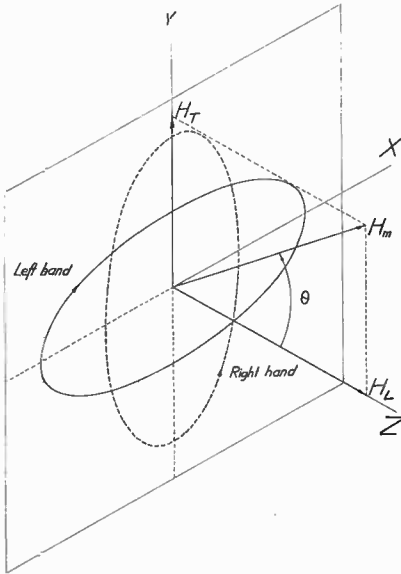


Fig. 1. The Polarization of the Waves.

for  $\omega < \omega_c$ , plane polarization for  $\omega = \omega_c$  and left-hand polarization for  $\omega > \omega_c$  as is well known. For wave-solution 1 the conditions are reversed because  $\bar{u}_1 \bar{u}_2 = 1$ , i. e. the polarization is left-hand, when  $\omega < \omega_c$  etc. In both cases the polarization is elliptical when  $\omega \neq \omega_c$ , except if  $\theta_p = 0, \pi/2, \pi, 3\pi/2$  etc. Finally reference is made to Fig. 1 which illustrates the orientation of the axes and the polarization of the waves.

Since  $-\pi/2 < \theta_p < \pi/2$  for down-coming waves in the northern hemisphere and  $\pi/2 < \theta_p < 3\pi/2$  in the southern hemisphere, the polarization is left-handed in the northern hemisphere when it is right-handed in the southern hemisphere and vice versa.

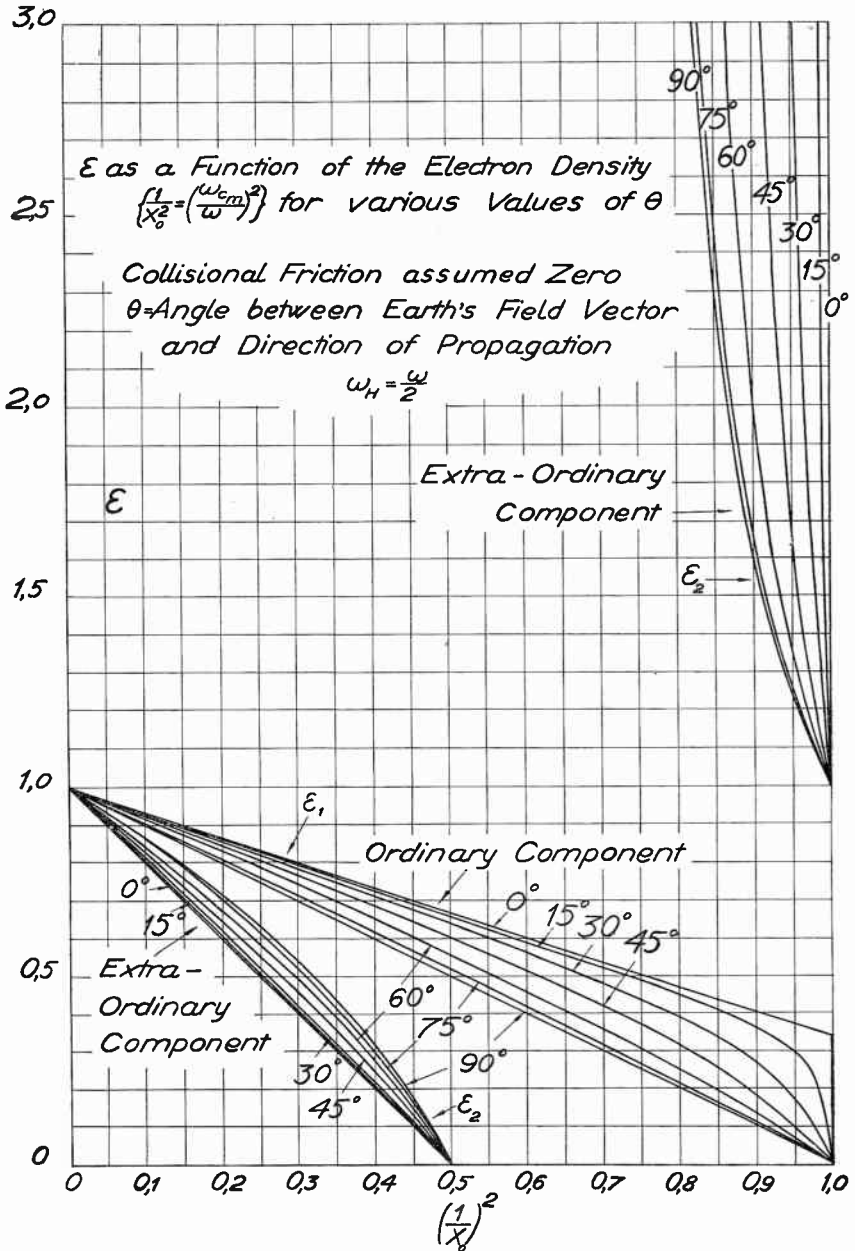


Fig. 2.1)

1) Computed by the author's former colleague, J. DE BETTENCOURT, S. M., Harvard University.

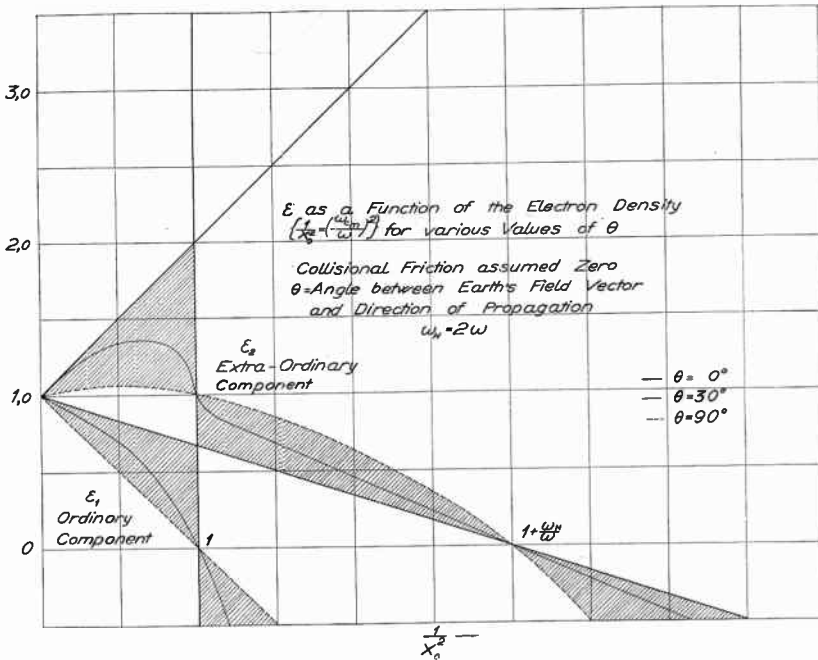


Fig. 3.

Remembering that  $\bar{D} = \bar{E} + 4\pi\bar{P}$ , we obtain from (3 a) and (4)

$$\left. \begin{aligned}
 D_x^{(1)} &= E_x^{(1)} \cdot \left\{ 1 - \frac{1}{x_0^2 \left( 1 + j \frac{\nu}{\omega} \right) + \frac{\gamma_T^2}{1 - x_0^2 \left( 1 + j \frac{\nu}{\omega} \right)} + j \gamma_L \bar{u}_1} \right\} = E_x^{(1)} \cdot \varepsilon_1(z) \\
 D_x^{(2)} &= E_x^{(2)} \cdot \left\{ 1 - \frac{1}{x_0^2 \left( 1 + j \frac{\nu}{\omega} \right) + \frac{\gamma_T^2}{1 - x_0^2 \left( 1 + j \frac{\nu}{\omega} \right)} + j \frac{\gamma_L}{\bar{u}_1}} \right\} = E_x^{(2)} \cdot \varepsilon_2(z),
 \end{aligned} \right\} (5)$$

where  $\varepsilon(z)$  denotes the »dielectric constant».

For the sake of completeness we have as figs 2 and 3 included the familiar graphical representation of  $\varepsilon_1$  and  $\varepsilon_2$  as functions of  $(\omega_0/\omega)^2$  for the two characteristic cases  $\omega_H/\omega = 1/2$  and 2.

Let us now make use of MAXWELL'S equations. They can in this case be written

$$\left. \begin{aligned} -j\omega D_x &= -c_0 \frac{d}{dz} (H_y), & -j\omega D_y &= c_0 \frac{d}{dz} (H_x), \\ -j\omega H_x &= c_0 \frac{d}{dz} (E_y), & -j\omega H_y &= -c_0 \frac{d}{dz} (E_x). \end{aligned} \right\} (6 a)$$

They yield

$$\left. \begin{aligned} -\frac{\omega^2}{c_0^2} D_x &= \frac{d^2}{dz^2} (E_x), & \text{and} \\ -\frac{\omega^2}{c_0^2} D_y &= \frac{d^2}{dz^2} (E_y). \end{aligned} \right\} (6 b)$$

But as  $D_x = \epsilon_1 E_x^{(1)} + \epsilon_2 E_x^{(2)}$ , etc., (6 b) yields<sup>1</sup>

$$\begin{aligned} \frac{d^2 E_x^{(1)}}{dz^2} - \frac{d}{dz} (\bar{u}^2) \cdot \frac{dE_x^{(1)}}{dz} + \left( \frac{\omega^2}{c^2} \cdot \epsilon_1 - \frac{\bar{u}}{1 - \bar{u}^2} \frac{d^2 \bar{u}}{dz^2} \right) E_x^{(1)} &= - \frac{\frac{d^2 \bar{u}}{dz^2} \cdot E_y^{(2)} + 2 \frac{d\bar{u}}{dz} \cdot \frac{dE_y^{(2)}}{dz}}{1 - \bar{u}^2}, \\ \frac{d^2 E_y^{(2)}}{dz^2} - \frac{d}{dz} (\bar{u}^2) \cdot \frac{dE_y^{(2)}}{dz} + \left( \frac{\omega^2}{c^2} \cdot \epsilon_2 - \frac{\bar{u}}{1 - \bar{u}^2} \frac{d^2 \bar{u}}{dz^2} \right) E_y^{(2)} &= - \frac{\frac{d^2 \bar{u}}{dz^2} \cdot E_x^{(1)} + 2 \frac{d\bar{u}}{dz} \cdot \frac{dE_x^{(1)}}{dz}}{1 - \bar{u}^2}. \end{aligned}$$

To get rid of the first-order derivative we make the following substitution, viz.

$$\left. \begin{aligned} E_x^{(1)} &= \Pi_1 e^{+\frac{1}{2} \int \frac{d}{dz} (\bar{u}^2) \cdot dz} = (1 - \bar{u}^2)^{-\frac{1}{2}} \cdot \Pi_1, & \text{and similarly} \\ E_y^{(2)} &= (1 - \bar{u}^2)^{-\frac{1}{2}} \cdot \Pi_2. \end{aligned} \right\} (7)$$

The wave-equations therefore reduce to

$$\left. \begin{aligned} \frac{d^2 \Pi_1}{dz^2} + \left( \frac{\omega^2}{c_0^2} \epsilon_1 + \frac{\left(\frac{d\bar{u}}{dz}\right)^2}{(1 - \bar{u}^2)^2} \right) \Pi_1 &= -\Pi_2 \cdot \frac{d}{dz} \left( \frac{\frac{d\bar{u}}{dz}}{1 - \bar{u}^2} \right) - 2 \frac{\frac{d}{dz} \Pi_2 \cdot \frac{d\bar{u}}{dz}}{1 - \bar{u}^2}, \\ \frac{d^2 \Pi_2}{dz^2} + \left( \frac{\omega^2}{c_0^2} \epsilon_2 + \frac{\left(\frac{d\bar{u}}{dz}\right)^2}{(1 - \bar{u}^2)^2} \right) \Pi_2 &= -\Pi_1 \cdot \frac{d}{dz} \left( \frac{\frac{d\bar{u}}{dz}}{1 - \bar{u}^2} \right) - 2 \frac{\frac{d}{dz} \Pi_1 \cdot \frac{d\bar{u}}{dz}}{1 - \bar{u}^2}. \end{aligned} \right\} (8)$$

<sup>1</sup> Note:  $\bar{u} = \bar{u}_1$ .

We get two coupled wave-equations. We first of all wish to find out when the coupling terms disappear. To that end it is convenient to express  $\bar{u}$  in  $\delta_u$ . From (4) we have

$$\frac{\frac{d\bar{u}}{dz}}{1-u^2} = j \frac{\frac{d\delta_u}{dz}}{2(1+\delta_u^2)}. \tag{9}$$

This expression and its derivative are equal to zero only when  $\theta_P = 0, \pi$  and  $\frac{\pi}{2}, \frac{3\pi}{2}$ . In the first cases, longitudinal transmission, both waves are circularly polarized. In the second cases, transverse transmission, which corresponds to the condition at the magnetic equator, the two components are plane polarized at right angles. For the two cases, longitudinal and transverse transmission, the coupling between the equations disappear and we have

$$\left. \begin{aligned} \text{and, } \frac{d^2 H_1}{dz^2} + \frac{\omega^2}{c_0^2} \epsilon_1 H_1 &= 0, \\ \frac{d^2 H_2}{dz^2} + \frac{\omega^2}{c_0^2} \epsilon_2 H_2 &= 0. \end{aligned} \right\} \tag{8 a}$$

$[\theta_P = 0, \pi/2, \pi, 3\pi/2]$

When  $\theta_P$  does not have any of the above values the coupling has to be considered. The problem, however, is extremely complicated on account of the fact that  $\epsilon(z)$  is not a simple function of  $z$  even for linear electron density distributions. As a matter of fact (8 a) can be solved exactly in a few cases only when  $\epsilon$  has the values corresponding to  $\theta_P = 0, \pi/2, \pi, 3\pi/2$ . When this is the case the phase integral equations connecting the true and virtual heights for one of the waves can be solved as has already been shown [3]. These cases, viz. transverse and longitudinal transmission, are therefore of most immediate interest. They are of practical importance at or near the magnetic equator and the magnetic poles.

When  $\theta_P$  does not have the above characteristic values the wave-equations (8) in the first approximation have to be solved by the W.K.B.-method neglecting the coupling terms. The approximate solutions when the coupling is considered are then obtained in the usual way by the method of the variation of the constants. A treatment of this case, which always must be approximate, is outside the scope of the present communication. The reader is referred to an interesting paper by FÖRSTERLING [7] on this subject.

Let us now return to the cases of transverse and longitudinal transmission. We obtain from (4) and (5) the familiar relations,

$$\varepsilon_1 = 1 - \frac{\omega_c^2}{\omega(\omega + j\nu)}, \text{ for the transverse case,} \quad (10 \text{ a})$$

and

$$\varepsilon_2 = 1 - \frac{\omega_c^2}{\omega(\omega - \omega_H + j\nu)}, \text{ for the longitudinal case.} \quad (10 \text{ b})$$

$(\omega \gg \omega_H)$

$\varepsilon_1$  refers to the ordinary wave and  $\varepsilon_2$  to the extra-ordinary one. It is clear from (10 a) and (10 b) that we only need to study the transmission of the extra-ordinary wave in the longitudinal case as we then merely put  $\omega_H = 0$  in order to get the ordinary wave in the transverse case.

### On the Wave Functions of the Parabolic Layer.

For the parabolic layer we write

$$\omega_c^2 = \omega_{cm}^2 \left[ 1 - \left( \frac{z}{\Delta h_m} \right)^2 \right], \quad (11)$$

where  $\Delta h_m$  is the layer half-thickness and  $z$  is counted from the apex of the layer, positive downwards. Eq. (8 a) then becomes

$$\frac{d^2 H}{dV^2} + \left( j\varrho - \frac{V^2}{4} \right) H = 0, \quad (12)$$

where

$$\varrho = \alpha \left[ e^{-j\Psi} - x^2 \Delta e^{+j\Psi} \right], \quad (13)$$

$$V = e^{j\frac{\pi}{4}} \frac{z}{\Delta h_m} (4\alpha)^{\frac{1}{2}} e^{-j\frac{\Psi}{2}} = e^{j\frac{\pi}{4}} u, \quad (14)$$

$$x^2 = \frac{|\omega(\omega - \omega_H)|}{\omega_{cm}^2} = \frac{\omega_r^2}{\omega_{cm}^2}, \quad (15)$$

$$\Psi = \frac{1}{2} \arctan \left( \frac{\nu}{\omega - \omega_H} \right),^1) \quad (16)$$

$$\Delta = \left[ 1 + \left( \frac{\nu}{|\omega - \omega_H|} \right)^2 \right]^{\frac{1}{2}}, \quad (17)$$

<sup>1)</sup> Note: When  $\omega < \omega_H$ , we define  $2\Psi = \pm \pi - \arctan \left( \frac{\nu}{\omega_H - \omega} \right)$ .

$$\alpha = \frac{\pi \Delta h_m}{\lambda_{em}} \left[ \frac{\omega}{(|\omega - \omega_H|) \Delta} \right]^{\frac{1}{2}}, \text{ with } \lambda_{em} = \frac{2\pi c_0}{\omega_{em}}. \quad (18)$$

We know already that the solutions of (12) are WEBER's functions of the parabolic cylinder, viz., in the notation of WHITTAKER,

$$D\left(u e^{j \frac{\pi}{4}}\right), D\left(u e^{-j \frac{\pi}{4}}\right), \text{ and } D\left(u e^{j \frac{3\pi}{4}}\right) \quad (19)$$

$j\rho - \frac{1}{2} \qquad -j\rho - \frac{1}{2} \qquad -j\rho - \frac{1}{2}$

$e^{-j\omega t} D\left(u e^{j \frac{\pi}{4}}\right)$ , for example, represents the up-going, primary wave when  $\omega > \omega_H$ .

The author has already shown [3] that in that case the important circuit relation connecting the waves is

$$\underbrace{D\left(u e^{j \frac{\pi}{4}}\right)}_{\text{up-going wave}} = \underbrace{\frac{\Gamma\left(j\rho + \frac{1}{2}\right)}{(2\pi)^{\frac{1}{2}}} e^{\frac{\pi\rho}{2} + j \frac{\pi}{4}} \cdot D\left(u e^{-j \frac{\pi}{4}}\right)}_{\text{reflected wave}} + \underbrace{\frac{\Gamma\left(j\rho + \frac{1}{2}\right)}{(2\pi)^{\frac{1}{2}}} e^{-\frac{\pi\rho}{2} - j \frac{\pi}{4}} \cdot D\left(u e^{j \frac{3\pi}{4}}\right)}_{\text{refracted wave}}. \quad (20)$$

This circuit relation only connects one up-going wave with its reflected and refracted components. Actually, there is an infinite number of waves (generally with decreasing amplitude) since the waves always experience a slight reflection at the bottom and top

of the layer, if  $\frac{d\varepsilon}{dz}$  has a discontinuity there. We must, therefore,

before we proceed discuss the influence of the reflection at the boundaries of the layer. To that end we refer to Fig. 4. This shows plots of  $\varepsilon(z)$  for  $\nu = 0$ . When  $\omega_{em} < \omega < \omega_H$  the layer is optically denser than the surrounding medium for the extra-ordinary component corresponding to  $\varepsilon_2(z)$  (see fig. 3). When  $\omega > \omega_H$  the layer is optically thinner. The last case is the important one as far as the present ionospheric exploration is concerned.

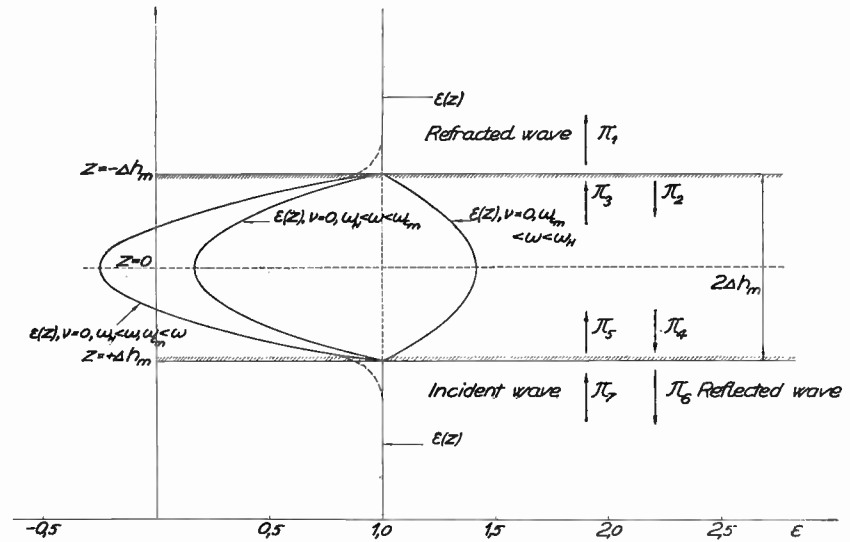


Fig. 4. A schematic representation of the transmission of waves through the inhomogeneous layer.

Our immediate task is to find a relation between the incident wave,  $\Pi_7$ , the reflected wave,  $\Pi_6$ , and the refracted wave,  $\Pi_1$ .

At the boundaries we require that the tangential components of  $\vec{E}$  and  $\vec{H}$  be continuous.

Since by (6 a)

$$-j\omega H_x = \frac{\delta E_y}{\delta z}, \text{ and } -\epsilon j\omega E_y = \frac{\delta H_x}{\delta z}$$

this further means that  $\frac{\delta E_y}{\delta z}, \frac{1}{\epsilon} \cdot \frac{\delta H_x}{\delta z}$ , etc. are continuous.

The wave functions  $\Pi_2, \Pi_3, \Pi_4$  and  $\Pi_5$  are parabolic cylinder functions when  $\epsilon(z)$  is parabolic.

Let us for the moment throw the up-going wave, which in the case of  $\omega > \omega_H$  is  $D \left( u e^{j \frac{\pi}{4}} \right)$ , in the form

$$D \left( u e^{j \frac{\pi}{4}} \right) = A(\rho) e^{-j\phi(z)}, \tag{21}$$

which we assume will hold near the boundaries. The other components accordingly become

$$D \left( u e^{-j \frac{\pi}{4}} \right) = A e^{+j \psi(z)}, \text{ and } D \left( u e^{j \frac{3\pi}{4}} \right) = A e^{+j \psi(-z)}. \quad (21 \text{ a})$$

$$-j \rho - \frac{1}{2} \qquad \qquad \qquad -j \rho - \frac{1}{2}$$

Since the first two of these wave functions are complex conjugates when  $\text{Im}(\rho) = 0$ , we infer that

$$[\text{Im} \{ \Phi(z) \}]_{\nu=0} = 0.$$

The internal complex reflexion factor,  $R$ , according to the circuit (20) therefore becomes

$$R = \frac{\Gamma \left( j \rho + \frac{1}{2} \right)}{(2\pi)^{\frac{1}{2}}} \exp. \left[ \frac{\pi \rho}{2} + j \left\{ \frac{\pi}{4} + 2 \Phi(z) \right\} \right].$$

Making use of the multiplication rule for the  $\Gamma$ -function we obtain

$$R = 2^{\frac{1}{2}} \frac{\Gamma(2j\rho)}{\Gamma(j\rho)} \exp. \left[ \frac{\pi \rho}{2} + j \left\{ \frac{\pi}{4} + 2 \Phi(z) - \rho \ln 4 \right\} \right]. \quad (22)$$

The reflection factor,  $|R|$ , consequently becomes

$$|R| = 2^{\frac{1}{2}} \frac{|\Gamma(2j\rho)|}{|\Gamma(j\rho)|} \exp. \left[ \frac{\pi}{2} - 2 \text{Im} \{ \Phi(z) \} \right]. \quad (22 \text{ a})$$

In the non-dissipative case  $\text{Im}(\rho) = 0$ ,  $\text{Im} \{ \Phi(z) \} = 0$ , and

$$|R|^2 = \frac{e^{\pi \rho}}{2 \cosh \pi \rho} = \frac{1}{1 + e^{-2\pi \rho}}, \nu = 0. \quad (22 \text{ b})$$

This result is immediately obtained from the circuit relation when  $\nu = 0$ , since from it

$$\frac{|R|^2}{1 - |R|^2} = |e^{2\pi \rho}|, \nu = 0, \quad (22 \text{ c})$$

which is the same as (22 b). The internal refraction coefficient,  $T$ , by the circuit relation becomes

$$T = R \exp. \left\{ -\pi \rho - j \frac{\pi}{2} \right\} = R e^{-\check{\gamma}}. \quad (23)$$

Introducing the notation

$$k = \frac{2\pi}{\lambda}, \tag{24}$$

where  $\lambda$  is the wave-length in the surrounding medium, we write the advancing wave on top of the layer,

$$\left. \begin{aligned} E_{y_1} &= \Pi_1 e^{-j\omega t} = A_1 \exp. [-j\{\omega t + k(z + \Delta h_m) - \Phi(\Delta h_m)\}], \\ \text{and the other waves} \\ E_{y_2} &= \Pi_2 e^{-j\omega t} = A_2 \exp. [-j\{\omega t + \Phi(-z) - 2\Phi(\Delta h_m)\}], \\ E_{y_3} &= \Pi_3 e^{-j\omega t} = A_3 \exp. [-j\{\omega t - \Phi(-z)\}], \\ E_{y_4} &= \Pi_4 e^{-j\omega t} = A_4 \exp. [-j\{\omega t - \Phi(z) + 2\Phi(\Delta h_m)\}], \\ E_{y_5} &= \Pi_5 e^{-j\omega t} = A_5 \exp. [-j\{\omega t + \Phi(z)\}], \\ E_{y_6} &= \Pi_6 e^{-j\omega t} = A_6 \exp. [-j\{\omega t - k(z - \Delta h_m) + \Phi(\Delta h_m)\}], \\ \text{and} \\ E_{y_7} &= \Pi_7 e^{-j\omega t} = A_7 \exp. [-j\{\omega t + k(z - \Delta h_m) + \Phi(\Delta h_m)\}]. \end{aligned} \right\} \tag{25}$$

Our boundary requirements at the top yield  $A_1 = A_2 + A_3$  and

$$A_1 = (A_2 - A_3) \frac{1}{k} \left\{ \frac{\delta \Phi(-z)}{\delta z} \right\}_{z = -\Delta h_m} = (A_3 - A_2) \frac{1}{k} \left\{ \frac{\delta \Phi(z)}{\delta z} \right\}_{z = \Delta h_m}$$

Further introducing

$$\mu = \frac{k}{\left\{ \frac{\delta \Phi(z)}{\delta z} \right\}_{z = \Delta h_m}},$$

we have

$$A_1 = A_3 \frac{2}{1 + \mu} = A_3 t_0, \tag{26}$$

and

$$A_2 = A_3 \frac{1 - \mu}{1 + \mu} = A_3 r_0,$$

where  $t_0$  is the transmission factor and  $r_0$  the reflection factor in direction out of the layer. We next obtain from the circuit relation (20)

$$\Pi_3 = \Pi_2 R + \Pi_5 R e^{-\tilde{r}}, \text{ and } \Pi_4 = \Pi_5 R + \Pi_2 R e^{-\tilde{r}}.$$

This yields

$$A_5 = A_3 \frac{1 - r_0 R}{R} \exp. \{ \check{\gamma} + j 2 \Phi (\Delta h_m) \}$$

and

$$A_4 = A_5 \left\{ R + \frac{r_0 R^2}{1 - r_0 R} e^{-2\check{\gamma}} \right\}.$$

At the bottom of the layer the boundary conditions yield

$$A_7 + A_6 = A_5 + A_4, \text{ and } (A_7 - A_6) \mu = A_5 - A_4, \text{ i. e.,}$$

$$A_6 = A_7 \frac{r_i + R + \frac{r_0 R^2 e^{-2\check{\gamma}}}{1 - r_0 R}}{1 - r_0 R + \frac{r_i r_0 R^2 e^{-2\check{\gamma}}}{1 - r_0 R}} = A_7 \cdot R_{eff},$$

and

$$A_1 = A_7 e^{-j 2 \Phi (\Delta h_m)} \frac{t_i t_0 T}{1 - R (r_0 - r_i) - r_i r_0 R^2 (1 - e^{-2\check{\gamma}})} = A_7 e^{-j 2 \Phi (\Delta h_m)} T_{eff},$$

where  $r_i = -r_0 =$  reflection factor in direction into the layer,

$t_i = \mu t_0 =$  transmission factor into the layer,

$R_{eff} =$  effective reflection factor of the layer in the surrounding medium,

and  $T_{eff} =$  effective refraction or transmission factor of the layer in the surrounding medium.

It is immediately clear from (28) that these effective coefficients contain a complexity of waves. After expansion and collection of the first few terms only we obtain

$$R_{eff} = r_i + t_i t_0 [R + R^2 r_0 + R^3 r_0^2 + \dots + R^2 r_0 e^{-2\check{\gamma}} \{1 + 3 R r_0 + \dots\} + R^4 r_0^2 e^{-4\check{\gamma}} \{1 + \dots\} + \dots], \quad (28 a)$$

and

$$T_{eff} = t_i R e^{-\check{\gamma}} t_0 [1 + R 2 r_0 + R^2 3 r_0^2 + \dots + R^2 r_0^2 e^{-2\check{\gamma}} \{1 + 4 R r_0 + \dots\} + R^4 r_0^4 e^{-4\check{\gamma}} \{1 + \dots\} + \dots]. \quad (28 b)$$

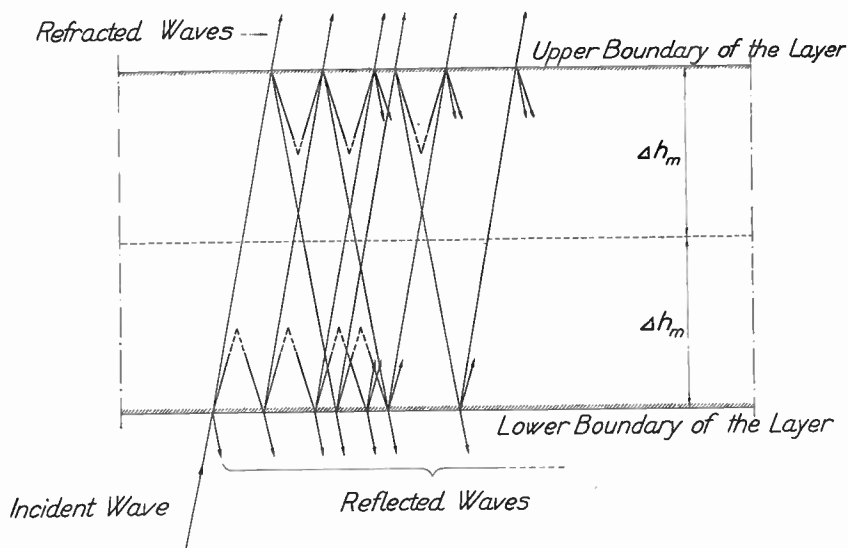


Fig. 5.

The paths corresponding to these waves are schematically shown in fig. 5. In the case of the optically thin layer, i. e.,  $\text{Re}(\epsilon) < 1$ , which is the common case in the radio exploration of the ionosphere,  $|r_0|$  generally is very small and  $\rho$  real when  $\nu = 0$ . In most practical cases the layer also is many critical wavelengths thick and so only the term  $t_i t_0 R \approx R$  in  $R_{eff}$  is of importance, i. e., only the first reflexion within the layer is considered. In the exceptional case,  $\omega_{c_m} < \omega < \omega_H$ ,  $\rho$  is purely imaginary when  $\nu = 0$ . The consequence of this is that several waves in (28 a) and (28 b) have to be considered, i. e. the layer can show the colour effect of thin or of thick plates. This is characteristic for the denser layers. To this we will have occasion to return later.

Relation (22 c) can be thrown into the more instructive form

$$|R| = \left[ 1 + e^{-\frac{\pi^2 \Delta h_m}{\lambda c_m} \left( \frac{\omega}{\omega - \omega_H} \right)^{\frac{1}{2}} (1 - x^2)} \right]^{-\frac{1}{2}} ; \nu = 0, \omega > \omega_H. \quad (29)$$

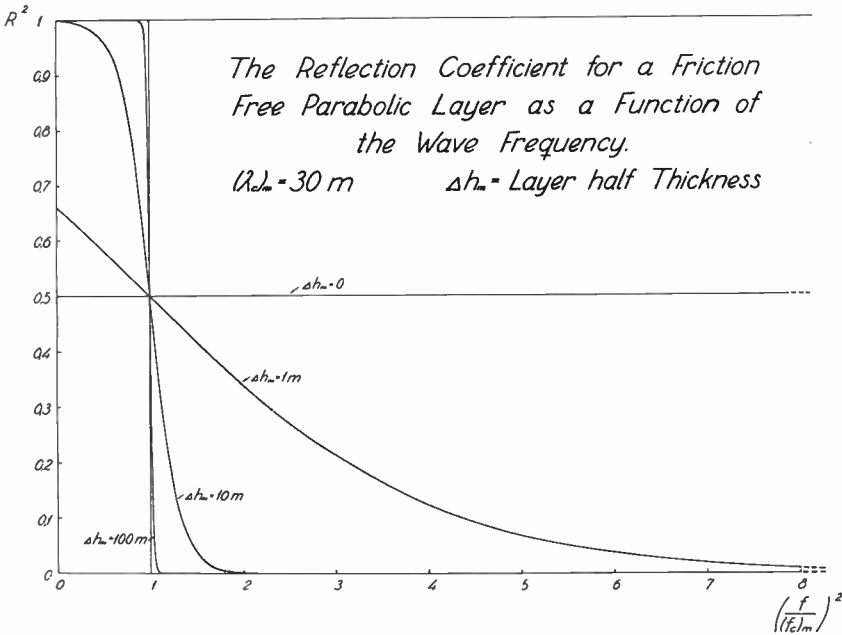


Fig. 6.  
 (Note:  $f = \omega/2\pi$ )

In order to demonstrate the character of relation (29) we reproduce in fig. 6 a plot of  $|R|^2$  for  $\omega_H = 0$ , as a function of  $x^2 = \frac{\omega^2}{\omega_{cm}^2}$ , which has already been shown in earlier communications [3].

\* \* \*

In this connexion it should not be out of place to discuss the case of oblique incidence briefly. To that end we have to put  $\omega_H = 0$ . For the sake of simplicity we only discuss horizontal polarization, viz. the electric vector perpendicular to the stratification of the layer. We arbitrarily denote the axis of the electric vector the  $y$ -axis. Moreover, we consider only plane waves parallel to the direction

$y$  so that  $\frac{\delta}{\delta y} = 0$ . MAXWELL's equations become

$$-j \frac{\omega \epsilon(z)}{c_0} E_y = \frac{\delta H_x}{\delta z} - \frac{\delta H_z}{\delta x},$$

$$j \frac{\omega}{c_0} H_x = - \frac{\delta E_y}{\delta z},$$

$$j \frac{\omega}{c_0} H_z = \frac{\delta E_y}{\delta x}.$$

These equations obviously lead to the rigorous equation of wave motion

$$\nabla^2 E_y + \left(\frac{\omega}{c_0}\right)^2 \varepsilon(z) E_y = 0$$

with boundary requirements that  $E_y$  and  $\frac{\delta E_y}{\delta z}$  be continuous.

Giving the separation constant such a value that the wave gets an angle of incidence,  $\varphi$ , we accordingly write

$$E_y = \Pi \exp. \{-j(\omega t - kx \sin \varphi)\}, \quad (30)$$

and

$$\frac{d^2 \Pi}{dz^2} + \left(\frac{\omega}{c_0}\right)^2 \left\{ \cos^2 \varphi - \frac{e^{-j2\varphi}}{x^2 \Delta} \left(1 - \left(\frac{z}{\Delta h_m}\right)^2\right) \right\} \Pi = 0. \quad (31)$$

The wave functions become  $D\left(u e^{j\frac{\pi}{4}}\right)$ , etc., as before, where

$$j\rho - \frac{1}{2}$$

we instead of  $\Phi(z)$  write  $\Phi(\varphi, z)$ . With the exception of  $x^2$  the parameters remain unchanged. We find

$$x^2 = \left(\frac{\omega \cos \varphi}{\omega_{c_m}}\right)^2. \quad (32)$$

Whenever  $\nu = 0$ , the other parameters will not contain  $\omega$ , and therefore with respect to the wave functions

$$\frac{\delta}{\delta \varphi} = - \tan \varphi \cdot \omega \frac{\delta}{\delta \omega}, \quad (33)$$

when  $\nu = 0$ . This is an important relation.

Let us for the sake of simplicity only study one of the primary waves. At the lower boundary we have the incident wave

$$\left. \begin{aligned}
 & \Pi_1 e^{-j\omega t} = A_1 \exp. [-j\{\omega t + k z \cos \varphi - k x \sin \varphi + \Phi(\varphi, \Delta h_m)\}], \\
 & \text{the reflected wave} \\
 & \Pi_2 e^{-j\omega t} = A_2 \exp. [-j\{\omega t - k z \cos \varphi - k x \sin \varphi + \Phi(\varphi, \Delta h_m)\}], \\
 & \text{and the refracted wave} \\
 & \Pi_3 e^{-j\omega t} = A_3 \exp. [-j\{\omega t + \Phi(\varphi, z) - k x \sin \varphi\}].
 \end{aligned} \right\} (34)$$

The boundary requirements yield

$$\left. \begin{aligned}
 & r_i = - \frac{1 - \mu \cos \varphi}{1 + \mu \cos \varphi}, \\
 & \text{and} \\
 & t_i = \frac{2 \mu \cos \varphi}{1 + \mu \cos \varphi}.
 \end{aligned} \right\} (35)$$

As before  $|r_i|$  generally is small.

The internally reflected, down-coming wave will be

$$\Pi_4 e^{-j\omega t} = t_i t_0 R e^{+j k x_1 \sin \varphi} \cdot \Pi_1 e^{-j\omega t}, \quad (36)$$

where  $x_1$  is the distance between the points of entrance and withdrawal. The reflection factor becomes

$$r = t_i t_0 R e^{+j k x_1 \sin \varphi}. \quad (36 a)$$

When  $\nu = 0$ ,  $\text{Im}(t_i) = 0$  and  $\text{Im}(t_0) = 0$ . Thus when  $\nu = 0$

$$\xi_r = \text{Phase}(r) = \text{Phase}(R) + k x_1 \sin \varphi.$$

If the time of travel is  $\tau$ , the total phase change becomes

$$\xi_r - \omega \tau = \Gamma_0.$$

At the point of withdrawal the following relations must hold, viz.

$$\frac{\delta \Gamma_0}{\delta \omega} = 0, \text{ and } \frac{\delta \Gamma_0}{\delta \varphi} = 0,^1. \quad (37)$$

By (33) this yields

$$\tau \approx \frac{1}{\cos^2 \varphi} \frac{\delta}{\delta \omega} \{ \text{Phase}(R) \}, \quad (38 a)$$

and

$$x_1 = c_0 \tau \sin \varphi. \quad (38 b)$$

<sup>1</sup>) This relation has to be used with great care whenever  $|R|$  varies considerably within the main spectrum of the transmitted signal.

This proves the BREIT-TUVE theorem [8] when  $\nu = 0$  also for the general case that the methods of the geometrical optics cannot be applied<sup>1)</sup>. It should be stressed, however, that relations (37) are the general relations from which the point of withdrawal ( $x_1$ ) is determined even in the moderately dissipative case.

The methods we have used in this section are, of course, generally applicable even to layers of different shape. When the wave functions corresponding to (19) have been found the main problem is to find the circuit relation. The  $R$  and  $\tilde{\gamma}$  values determined from such a relation can equally well be used in relations (28), (36), etc.

Returning to the parabolic layer, our next step will be to obtain suitable expansions of the wave-functions from which  $\Phi(z)$  and  $R$  can be obtained.

### On the Expansions of the Parabolic Wave Functions.

The parameters  $\varrho$  and  $u$ , (13), (14), are small or large depending upon the wave frequency used and the dimensions of the layer. It is obvious that the properties of the wave functions will depend to a great extent upon the magnitude of  $\frac{\pi \Delta \hbar_m}{\lambda_{cm}}$ . When  $\Delta \approx 1$  (low losses) and  $\omega > \omega_H$ , the character of the solution will be notably different if  $x^2 < 1$  or  $> 1$ .

a)  $\frac{\pi \Delta \hbar_m}{\lambda_{cm}} < 1$ . This case (thin layer) is not of immediate practical interest. For the sake of completeness, however, we write down WHITTAKER's expression in KUMMER-functions [10].

One has with the notation  $\ln = \log \text{ nat}$ .

$$D \left( u e^{j \frac{\pi}{4}} \right) = e^{-j \left( \frac{u^2}{4} - \frac{\rho}{2} \ln 2 \right)} \pi^{\frac{1}{2}} \left[ \frac{2^{-\frac{1}{4}} {}_1F_1 \left\{ \frac{1-2j\varrho}{4}; \frac{1}{2}; j \frac{u^2}{2} \right\}}{\Gamma \left( \frac{3-2j\varrho}{4} \right)} - \frac{1}{2^{\frac{1}{4}}} u e^{j \frac{\pi}{4}} \right. \\ \left. \frac{{}_1F_1 \left\{ \frac{3-2j\varrho}{4}; \frac{3}{2}; j \frac{u^2}{2} \right\}}{\Gamma \left( \frac{1-2j\varrho}{4} \right)} \right]; \quad -\pi < \text{Phase}(u) < \frac{\pi}{2}. \quad (39)$$

<sup>1)</sup> Compare D. R. HARTREE: *Optical and Equivalent Paths in a Stratified Medium*, [9].

We check this relation by letting  $\omega_{c_m}$  tend to zero. Although

$$|\varrho| \rightarrow \infty, \varrho u^2 \rightarrow -\left(\frac{\omega z}{c_0}\right)^2 = -\left(\frac{2\pi z}{\lambda}\right)^2. \text{ Therefore}$$

$${}_1F_1\left(\frac{1-2j\varrho}{4}; \frac{1}{2}; j\frac{u^2}{2}\right) \rightarrow \cos\left(\frac{2\pi z}{\lambda}\right), \text{ and } {}_1F_1\left(\frac{3-2j\varrho}{4}; \frac{3}{2}; j\frac{u^2}{2}\right) \rightarrow \frac{\lambda}{2\pi z} \sin\left(\frac{2\pi z}{\lambda}\right).$$

Since  $\frac{\Gamma\left(\frac{3-2j\varrho}{4}\right)}{\Gamma\left(\frac{1-2j\varrho}{4}\right)} \rightarrow \left(-\frac{\varrho}{2}\right)^{\frac{1}{2}} e^{j\frac{\pi}{4}}$ , the terms within the brackets

tend to  $\frac{2^{-\frac{1}{4}} e^{j\frac{2\pi z}{\lambda}}}{\Gamma\left(\frac{3-2j\varrho}{4}\right)}$ , which shows that relation (39) yields the

proper up-going wave.

b)  $u$  is large and  $\varrho$  is small, i. e. the layer is many critical wavelengths thick,  $x^2 \approx 1$ , and  $\nu$  limited. This means that  $\omega$  ( $\omega \approx \omega_H$ )  $\approx \omega_{c_m}^2$ , which expresses that  $\omega$  lies in the penetration frequency region.

By WHITTAKER's integral representation [11],<sup>1)</sup>

$$D\left(u e^{j\frac{\pi}{4}}\right) = -\frac{\Gamma\left(j\varrho + \frac{1}{2}\right)}{2\pi j} e^{-j\frac{u^2}{4}} \int_{-\infty}^{(0+)} e^{-ut} e^{j\frac{\pi}{4} - \frac{t^2}{2}} (-t)^{-j\varrho - \frac{1}{2}} dt, \quad (40)$$

and the HANKEL formula,

$$\frac{1}{\Gamma(z)} = -\frac{1}{2\pi j} \int_{-\infty}^{(0+)} (-t)^{-z} e^{-t} dt, \text{ we immediately obtain, after ex-}$$

pansion of  $e^{-\frac{t^2}{2}}$  in powers of  $t^2$ , the asymptotic expansion of WHITTAKER,

<sup>1)</sup> Note:  $\ln(-t)$  is defined purely real when  $t$  is on the negative side of the real axis.

$$D \left( u e^{j \frac{\pi}{4}} \right) \sim e^{-j \left( \frac{u^2}{4} - \varrho \ln u + \frac{\pi}{8} \right)} e^{-\frac{\pi \rho}{4}} \left[ \frac{1}{(u)^{\frac{1}{2}}} \left[ 1 - j \frac{\left( \varrho + j \frac{1}{2} \right) \left( \varrho + j \frac{3}{2} \right)}{2u} - \frac{\left( \varrho + j \frac{1}{2} \right) \left( \varrho + j \frac{3}{2} \right) \left( \varrho + j \frac{5}{2} \right) \left( \varrho + j \frac{7}{2} \right)}{2 \cdot 4 u} + \dots \right] \right]; \quad -\pi < \text{Phase}(u) < \frac{\pi}{2}, \quad (41)$$

This expansion is useful only when  $|\varrho| \ll |2u^2|$ , which limits the practical frequency range of the solution.

c) Both  $u$  and  $\varrho$  are large, but  $\varrho < \frac{u^2}{4}$ . This corresponds, for example, to the general cases of a thick layer and a wave frequency lower than the penetration frequency but higher than the gyrofrequency, or a wave frequency higher than the penetration frequency.

We make the following transformation, viz.  $t = \tau e^{j \frac{\pi}{4}}$ . Relation (40) then becomes

$$D \left( u e^{j \frac{\pi}{4}} \right) = - \frac{\Gamma \left( j \varrho + \frac{1}{2} \right)}{2 \pi} e^{\frac{1}{4} \pi \rho} e^{-j \left( \frac{u^2}{4} + \frac{3\pi}{8} \right)} \int_{\infty \cdot e^{-j \frac{\pi}{4}}}^{(0+)} e^{-j \left\{ u \tau + \frac{\tau^2}{2} + \varrho_1 \ln(-\tau) \right\}} d\tau, \quad (42)$$

where

$$\varrho_1 = \varrho - j \frac{1}{2}. \quad (43)$$

In order to obtain a suitable expansion from this we have to use the classical method of steepest descents [12]. We introduce the notation

$$W = -j \left\{ u \tau + \frac{\tau^2}{2} + \varrho_1 \ln(-\tau) \right\}. \quad (44)$$

Now we try to select a contour of integration such that it passes through a point, where  $\frac{dW}{d\tau} = 0$ , and further has the property that

$$\text{Im}(W) = \text{const.}$$

<sup>1)</sup> To obtain the form of the expansion for values of Phase  $u$  not comprised in this sector it is practical to make use of the circuit relation (20).

The points, where  $\frac{dW}{d\tau} = 0$ , are saddle points or passes on the  $\text{Re}(W)$ -surface. Our choice of the contour is finally determined from the consideration that the curve must descend on both sides of the pass. Generally if the curve ascended,  $\text{Re}(W)$  would tend to  $+\infty$  and the integral would diverge.

The physical interpretation of the choice of contour is that on it the interference effects have been evaded because  $\text{Im}(W) = \text{const.}$

We obtain the stationary points from

$$\frac{dW}{d\tau} = -j \left\{ u + \tau + \frac{\varrho_1}{\tau} \right\} = 0, \text{ which yields two points,}$$

$$\tau_A = -\frac{u}{2} + \left( \frac{u^2}{4} - \varrho_1 \right)^{\frac{1}{2}}, \tag{45 a}$$

and

$$\tau_B = -\frac{u}{2} - \left( \frac{u^2}{4} - \varrho_1 \right)^{\frac{1}{2}}. \tag{45 b}$$

It is further convenient to introduce

$$\Omega_1 = W(\tau_A) - W(\tau) = W_A - W, \tag{46}$$

and

$$\Omega_2 = W(\tau_B) - W(\tau) = W_B - W.$$

This transformation is of course a conformal representation except at the stationary points. Since

$$\frac{d^2W}{d\tau^2} = -j \left\{ 1 - \frac{\varrho_1}{\tau^2} \right\}, \tag{47}$$

then  $\frac{d^2W}{d\tau^2} \neq 0$  at the stationary points, except when  $\varrho_1 = \frac{u^2}{4}$ .

When  $\varrho_1 \neq \frac{u^2}{4}$ , therefore, the stationary points are branch points

of the first order. In the special case,  $\varrho_1 \approx \frac{u^2}{4}$ , which from the beginning was excluded (wave frequency equal to magnetic gyro frequency), a special treatment is needed. To this we will return later on.

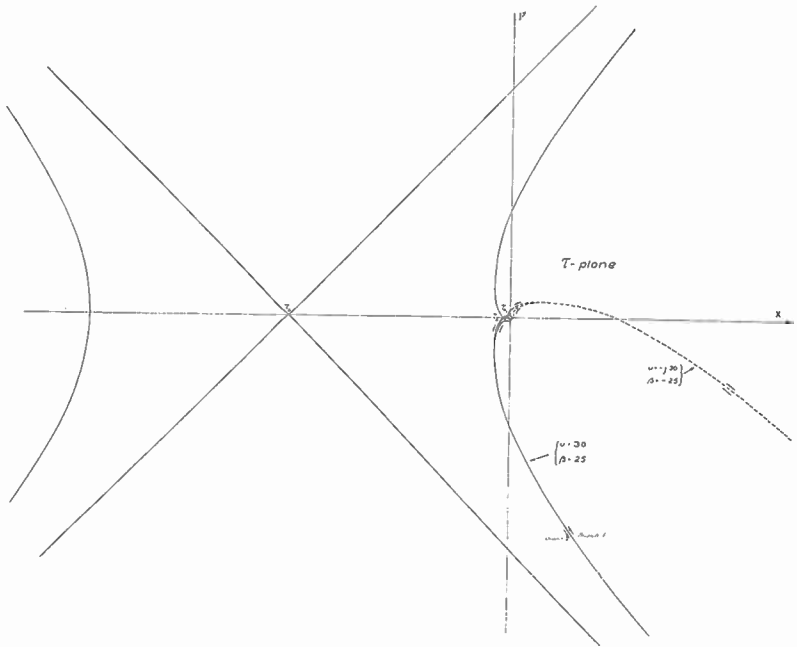


Fig. 7. The contours  $\text{Im}(W) = \text{const.}$  through the stationary points.

Fig. 7 shows a plot of the contours  $\text{Im}(W) = \begin{cases} \text{Im}(W)_{\tau = \tau_A} \\ \text{Im}(W)_{\tau = \tau_B} \end{cases}$ , for  $u = 30$  and  $\rho = 25$ . Point  $\tau_B$  must be discarded as it does not yield a proper contour.

Fig. 8 shows the contours close to the origin. The proper branches are marked by  $I_1$  and  $I_2$ . A few adjacent constant phase curves have also been plotted in order to show the nature of the saddle-region. A further discussion of the contour for complex  $u$  is outside the scope of the present communication, even though it is an interesting mathematical topic.

At the stationary point

$$W = W(\tau_A) = W_A = -j \left\{ -\frac{u^2}{4} + \frac{u}{2} \left( \frac{u^2}{4} - \rho_1 \right)^{\frac{1}{2}} + \rho_1 \left( \ln \{-\tau_A\} - \frac{1}{2} \right) \right\}. \quad (48)$$

The integral representation (40 a) then becomes



Next we discuss the expansions of  $\tau$  or of  $\frac{d\tau}{d\Omega_1}$  in ascending powers of  $\Omega$  for the two branches, from the stationary point. Since  $\Omega_1$  and  $\frac{d\Omega_1}{d\tau}$  vanish at the stationary point, the expansion of  $\Omega$  in  $\tau$  begins with a term in  $(\tau - \tau_A)^2$ . By reversion we can write

$$\tau - \tau_A = \sum_{n=0}^{\infty} \frac{a_n}{n+1} \Omega_1^{\frac{1}{2}(n+1)}, \tag{50 a}$$

for branch  $I_1$ , and

$$\tau - \tau_A = \sum_{n=0}^{\infty} \frac{a_n}{n+1} \Omega_1^{\frac{1}{2}(n+1)} e^{j\pi(n+1)}, \tag{50 b}$$

for branch  $I_2$  since a half circuit round the stationary point in the  $\tau$ -plane corresponds to a single circuit round the origin in the  $\Omega_1$ -plane.

This expansion should be valid almost up to  $\tau_B$ , where  $\left| \frac{d\tau}{d\Omega} \right| \rightarrow \infty$ .

We have from (50 a) and (50 b)

$$\left( \frac{d\tau}{d\Omega_1} \right)_{I_1} - \left( \frac{d\tau}{d\Omega_1} \right)_{I_2} = \sum_{n=0}^{\infty} a_{2n} \Omega_1^{n-\frac{1}{2}}. \tag{51}$$

But

$$a_{2n} = \frac{1}{2\pi j} \int_{\Omega_1^{(0+,0+)}}^{\tau_A^{(+)}} \frac{d\tau}{\Omega_1^{n+\frac{1}{2}}} d\Omega_1 = \frac{1}{2\pi j} \int_{\tau_A^{(+)}}^{\tau_A^{(+)}} \frac{d\tau}{[W_A - W]^{n+\frac{1}{2}}}. \tag{52}$$

Since

$$(W - W_A)^{n+\frac{1}{2}} = (\tau - \tau_A)^{2n+1} \left\{ \frac{1}{2!} \left( \frac{d^2 W}{d\tau^2} \right) + \dots \right\}^{n+\frac{1}{2}}, \tag{52}$$

$\tau = \tau_A$

(52) yields the familiar relation

$$a_{2n} = \frac{1}{(2n)!} \left[ \frac{d^{2n}}{d\tau^{2n}} \frac{(\tau - \tau_A)^{2n+1}}{(W_A - W)^{n+\frac{1}{2}}} \right]_{\tau = \tau_A}. \tag{53}$$

<sup>1)</sup> The double circuit in the  $\Omega_1$ -plane is necessary in order to dispose of the fractional powers of  $\Omega_1$ .

This yields the following values of the first coefficients, viz.

$$\left. \begin{aligned} a_0 &= e^{j \frac{\pi}{4}} (2)^{\frac{1}{2}} (\eta - 1)^{-\frac{1}{2}}, \\ a_2 &= e^{j \frac{3\pi}{4}} (2)^{\frac{1}{2}} (\eta - 1)^{-\frac{7}{2}} \tau_A^{-2} \eta (\eta + 9) \frac{1}{6}, \\ a_4 &= e^{j \frac{5\pi}{4}} (2)^{\frac{1}{2}} (\eta - 1)^{-\frac{13}{2}} \tau_A^{-4} \eta \left( \frac{\eta^3}{18} + \eta^2 + \frac{89}{2} \eta + 40 \right) \frac{1}{12}, \end{aligned} \right\} (54)$$

where  $\eta = \frac{\rho_1}{\tau_A^2}$ .

Since  $\left| \frac{d\tau}{d\Omega_1} \right| \rightarrow 0$  and  $(W - W_A) \rightarrow -\infty$ , when  $\tau \rightarrow e^{-j \frac{\pi}{4}} \cdot \infty$ , irrespective of the phase of  $u$ , we get by WATSON'S lemma [13]

$$J_1 \sim - \sum_{n=0}^M a_{2n} \Gamma \left( n + \frac{1}{2} \right).$$

We therefore obtain the following asymptotic expansion of the wave function, viz.

$$\begin{aligned} \left( u e^{j \frac{\pi}{4}} \right) \sim & \frac{\Gamma \left( j \varrho + \frac{1}{2} \right)}{(2\pi)^{\frac{1}{2}}} (\eta - 1)^{-\frac{1}{2}} e^{\frac{\pi}{4} \varrho} e^{-j \left( \frac{u}{2} \left( \frac{u^2}{4} - \varrho_1 \right)^{\frac{1}{2}} + \varrho_1 \left( \ln \{-\tau_A\} - \frac{1}{2} \right) + \frac{\pi}{8} \right)} \\ & \cdot \left[ 1 + e^{j \frac{\pi}{2}} (\eta - 1)^{-3} \tau_A^{-2} \eta (\eta + 9) \frac{1}{12} + \right. \\ & \left. + e^{j \pi} (\eta - 1)^{-6} \tau_A^{-4} \eta \left( \frac{\eta^3}{18} + \eta^2 + \frac{89}{2} \eta + 40 \right) \frac{1}{16} + \dots \dots \dots \right]. \end{aligned} \quad (55)$$

To convince us that the expansion actually represents the up-going wave, we let  $\omega_{em} \rightarrow 0$ , i. e. we reduce the electron density to zero. Making use of relations (13) to (18) one finds that the parts of the wave-phase containing  $\frac{z}{\Delta h_m}$  tend to  $-\frac{2\pi z}{\lambda}$  as expected.

d) Both  $u$  and  $\varrho$  are large but  $\varrho_1 \approx \frac{u^2}{4}$ . This case has to be treated

separately on account of the fact that for  $\varrho_1 = \frac{u^2}{4}$ ,  $\frac{d^2 W}{d\tau^2} = 0$ , and the stationary point becomes a branch point of the second order.

We introduce

$$\beta = \frac{u^2}{4} - \varrho_1. \quad (56)$$

This yields  $\tau_A = -\frac{u}{2} + (\beta)^{\frac{1}{2}}$ , and the new stationary point becomes  $\bar{\tau}_A = \tau_A - (\beta)^{\frac{1}{2}} = -\frac{u}{2} = \bar{\tau}_B$ . We also introduce the notations

$$\bar{W} = W - j\beta \ln \{-\tau\} = -j \left\{ u\tau + \frac{\tau^2}{2} + \frac{u^2}{4} \ln \{-\tau\} \right\}, \quad (57 a)$$

and

$$\bar{W}_A = W_A - j\beta \ln \{-\bar{\tau}_A\} = -j \left\{ -\frac{3u^2}{8} + \frac{u^2}{4} \ln \frac{u}{2} \right\}. \quad (57 b)$$

We further introduce  $\Omega_3 = \bar{W}_A - \bar{W}$ . Accordingly

$$D \left( u e^{j\frac{\pi}{4}} \right) = - \frac{\Gamma \left( j\varrho + \frac{1}{2} \right)}{2\pi} e^{\frac{\pi}{4}\rho} e^{-j \left\{ -\frac{u^2}{8} + \frac{u^2}{4} \ln \frac{u}{2} + \frac{3}{8}\pi \right\}} \cdot J_3, \\ j\rho - \frac{1}{2}$$

$$\text{where } J_3 = \int_{\text{Proper contours}} e^{-\Omega_3} \cdot \Phi_0(\Omega_3) d\Omega_3, \text{ and } \Phi_0(\Omega_3) = \frac{e^{j\beta \ln \{-\tau\}}}{j \left\{ u + \tau + \frac{u^2}{4\tau} \right\}}.$$

In order to secure a wider selection of proper contours we write  $\Omega_3 = e^{j\zeta} \Omega_4$ ,<sup>1)</sup> (58)

Since  $|\Phi_0(\Omega_4)| \rightarrow |\tau|^{-\frac{3}{2} - \alpha x^2 \sin \Psi} \cdot \exp. \left\{ \frac{\pi}{4} (\alpha x^2 \cos \Psi) \right\}$ , when  $z = \Delta h_m$ , and  $\tau \rightarrow \infty \cdot e^{-j\frac{\pi}{4}}$ , we only have to require that  $\cos \zeta < 0$  in order to be able to use WATSON'S lemma on a contour where

$$\text{Im}(\Omega_4) = \text{const.} = 0.$$

<sup>1)</sup> This method is used for instance to avoid two stationary points on the contour for one of the DEBYE expansions of the cylinder functions of large argument and order.

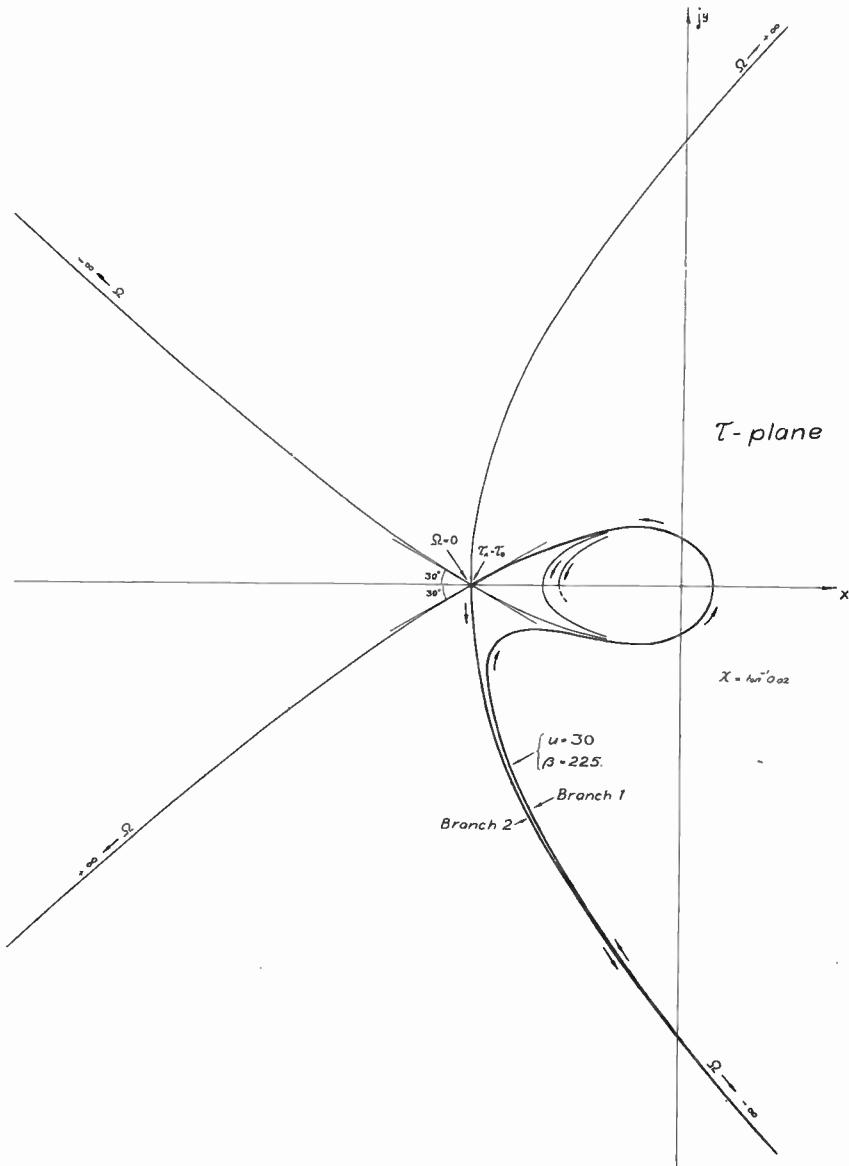


Fig. 9. The  $\text{Im}(\Omega_4) = 0$  contours through the stationary point.  
 (Note:  $\tau_A$  means  $\bar{\tau}_A$ ,  $\Omega$  means  $-\Omega_3$ )

Fig. 9 shows a plot of the contour through the stationary point,  $\bar{\tau}_A$ , for  $u = 30$ , and  $\zeta = 0$ , ( $q \approx 225$ ). Since  $u^2$  is equal to the layer thickness in radians ( $\omega_H = 0$ ), at the critical frequency, the above case corresponds to a layer about 144 critical wave-lengths thick.

$J_3$  gets the form

$$J_3 = \int_{\text{Branch 1}} e^{-e^{j\zeta} \Omega_4} \Phi_0(e^{+j\zeta} \Omega_4) e^{j\zeta} d\Omega_4 + \int_{\text{Branch 2}} e^{-e^{j\zeta} \Omega_4} \Phi_0(e^{+j\zeta} \Omega_4) e^{j\zeta} d\Omega_4.$$

Since  $(\Omega_4)_{\tau = \bar{\tau}_A} = 0$ ,  $\left(\frac{d\Omega_4}{d\tau}\right)_{\tau = \bar{\tau}_A} = 0$ ,  $\left(\frac{d^2\Omega_4}{d\tau^2}\right)_{\tau = \bar{\tau}_A} = 0$ , but  $\left(\frac{d^3\Omega_4}{d\tau^3}\right)_{\tau = \bar{\tau}_A} \neq 0$ , the same applies to the derivatives of  $\frac{1}{\Phi_0}$  and we get by inversion

$$\Phi_0 = \sum_{n=1}^{\infty} b_n \Omega_4^{\frac{n}{3}-1}. \tag{59}$$

As further

$$\Phi_0 - \Phi_0 = \sum_{\text{Branch 1}} b_n \Omega_4^{\frac{n}{3}-1} \left(1 - e^{j\frac{4\pi}{3}n}\right), \tag{60}$$

in accordance with fig. 9, we finally get

$$J_3 = -2j e^{j\zeta} \int_0^{\infty} e^{-e^{j\zeta} \Omega_4} \sum_{n=1}^{\infty} b_n e^{-j\frac{\pi}{3}n} \sin \frac{n\pi}{3} \cdot \Omega_4^{\frac{n}{3}-1} \cdot d\Omega_4.$$

By WATSON'S lemma, therefore,

$$J_3 \sim - \sum_{n=0}^m b_n e^{j\zeta} \cdot 2j e^{-j\frac{n}{3}(\pi + \zeta)} \sin \frac{n\pi}{3} \cdot \Gamma\left(\frac{n}{3}\right) = - \sum_{n=1}^m c_n \Gamma\left(\frac{n}{3}\right).$$

This time we have to make a triple circuit round the image of the stationary point in the  $\Omega_4$ -plane in order to determine  $b_n$ . We accordingly have

$$b_n = \frac{1}{6\pi j} \int_{(0+, 0+, 0+)} \frac{\Phi_0 d\Omega_4}{(\Omega_4)^{\frac{n}{3}}} = \frac{e^{-j\zeta}}{6\pi j} \int_{(\tau_A+)} e^{j\left(\beta \ln \{-\tau\} + \frac{n\zeta}{3}\right)} \frac{d\tau}{(\bar{W}_A - \bar{W})^{\frac{n}{3}}}, \tag{61}$$

or in analogy with (53)

$$b_n = \frac{e^{-j\zeta}}{3(n-1)!} \left\{ \frac{d^{n-1}}{d\tau^{n-1}} \frac{e^{j\beta \ln\{-\tau\}} (\tau - \tau_A)^n}{[\bar{W}_A - \bar{W}]^{\frac{n}{3}}} \right\}_{\tau = \bar{\tau}_A} e^{+j\frac{\zeta n}{3}}. \tag{62}$$

This relation then yields

$$\begin{aligned} &= 1 \cdot \\ &= -e^{-j\frac{\pi}{6}} \left(\frac{3u}{2}\right)^{-\frac{2}{3}} \left(j\beta + \frac{1}{2}\right) 3 \cdot \\ &= 0 \\ &= e^{-j\frac{3\pi}{6}} \left(\frac{3u}{2}\right)^{-\frac{6}{3}} \left[ (j\beta)^3 - \frac{11}{20}(j\beta)^2 - \frac{1}{40} \right] \frac{9}{2} \cdot \\ &= -e^{-j\frac{4\pi}{6}} \left(\frac{3u}{2}\right)^{-\frac{8}{3}} \left[ (j\beta)^4 - (j\beta)^3 - (j\beta)^2 + \frac{j\beta}{2} + \frac{67}{560} \right] \frac{27}{4} \cdot \\ &= 0 \cdot \\ &= \dots \end{aligned} \left. \vphantom{\begin{aligned} &= 1 \cdot \\ &= -e^{-j\frac{\pi}{6}} \left(\frac{3u}{2}\right)^{-\frac{2}{3}} \left(j\beta + \frac{1}{2}\right) 3 \cdot \\ &= 0 \\ &= e^{-j\frac{3\pi}{6}} \left(\frac{3u}{2}\right)^{-\frac{6}{3}} \left[ (j\beta)^3 - \frac{11}{20}(j\beta)^2 - \frac{1}{40} \right] \frac{9}{2} \cdot \\ &= -e^{-j\frac{4\pi}{6}} \left(\frac{3u}{2}\right)^{-\frac{8}{3}} \left[ (j\beta)^4 - (j\beta)^3 - (j\beta)^2 + \frac{j\beta}{2} + \frac{67}{560} \right] \frac{27}{4} \cdot \\ &= 0 \cdot \\ &= \dots \end{aligned}} \right\} \cdot \begin{aligned} &e^{j\left(\beta \ln \frac{u}{2} + \frac{\pi}{3}\right)} \cdot \\ &\left(\frac{3u}{2}\right)^{\frac{1}{3}} 3^{-\frac{1}{2}} \cdot \end{aligned} \tag{63}$$

We therefore get the following asymptotic expansion, viz.

$$\begin{aligned} D(u e^{j\frac{\pi}{4}}) &\sim \frac{\Gamma\left(j\varrho + \frac{1}{2}\right)}{2\pi} \left(\frac{3u}{2}\right)^{\frac{1}{3}} 3^{-\frac{1}{2}} e^{-\frac{3\pi}{4}} \varrho \cdot \\ &e^{-j\left\{-\frac{u^2}{8} + \left(\frac{u^2}{4} - \beta\right) \ln \frac{u}{2} + \frac{1}{24}\pi\right\}} \left[ \Gamma\left(\frac{1}{3}\right) - \Gamma\left(\frac{2}{3}\right) e^{-j\frac{\pi}{6}} \cdot \right. \\ &\left. \left(\frac{3u}{2}\right)^{-\frac{2}{3}} \left(j\beta + \frac{1}{2}\right) 3 + \Gamma\left(\frac{1}{3}\right) e^{-j\frac{3\pi}{6}} \left(\frac{3u}{2}\right)^{-\frac{6}{3}} \left[ (j\beta)^3 - \frac{11}{20}(j\beta)^2 - \frac{1}{40} \right] \frac{3}{2} - \right. \\ &\left. - \Gamma\left(\frac{2}{3}\right) e^{-j\frac{4\pi}{6}} \left(\frac{3u}{2}\right)^{-\frac{8}{3}} \left[ (j\beta)^4 - (j\beta)^3 - (j\beta)^2 + \frac{j\beta}{2} + \frac{67}{560} \right] \frac{9}{2} + \dots \right]. \tag{64} \end{aligned}$$

\* \* \*

The last two expansions, (55) and (64), of the function of the parabolic cylinder correspond to the DEBYE expansions of the functions of the circular cylinder,  $Z_p(z)$ , for  $p$  and  $z$  large, when  $p < z$  or  $p \approx z$ .

It should be pointed out already here that expansion (64) is useful only in a very narrow frequency range. In its limited usefulness it is strikingly similar to the DEBYE expansion in the exceptional case  $p \approx z$ . Since (64) has such a narrow frequency range we will find it desirable to secure a bridging relation between (55) and (64). To this problem we will return in a later section when the general characteristics of the transmission of radio waves round the world have been discussed. It is namely advantageous to obtain first the general expression for the spherical reflection coefficient of the parabolic layer.

We have not endeavoured to make a theoretical investigation of the expansions (55) and (64) when  $\text{Im}(u) \neq 0$  and  $\text{Im}(\varrho) \neq 0$ , i. e., when  $\nu > 0$ . Such an investigation would chiefly concern the  $\text{Im}(W) = \text{const.}$  paths and it must be considered outside the scope of the present communication which mainly deals with problems where the phase angles of  $u$  and  $\varrho$  are quite small.

### **The Transmission of Radio Waves round a Spherical Earth surrounded by a Radially Inhomogeneous Concentric Reflecting Shell.**

So far we have only discussed the transmission of waves in the inhomogeneous plane layer. From the point of view of ionospheric investigation this is the important case. For long-distance radio communication, however, the reflecting earth also has to be considered. The dominant wave functions of the appropriate solutions are few for the longest radio waves in practice. For the shorter waves, however, each solution is made up of a very large number of important wave-functions which give the wave its ray-like character. For numerical calculations the transition from diffractive waves to ray waves presents difficulties. Unfortunately, the transition occurs in a widely used wave range.

## Transmission of Radio Waves round the Earth

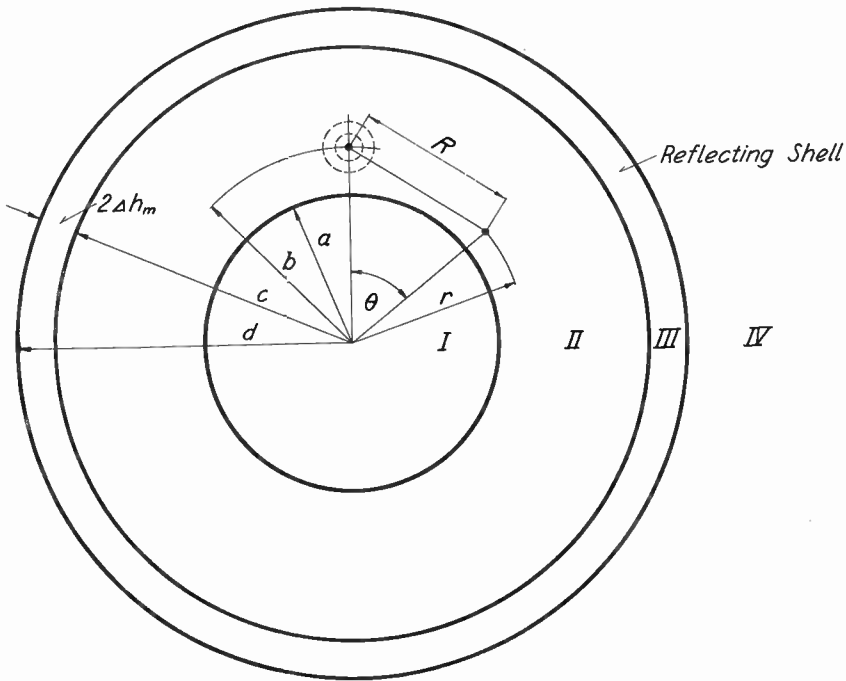


Fig. 10.

The problem of the transmission of vertically polarized radio waves between the earth and a concentric, homogeneous reflector of finite conductivity was treated in 1919 by WATSON [6] in a classical paper. The results were, however, not established in a form useful for immediate numerical computation. In the light of our present knowledge of the inhomogeneous character of the reflecting shells Watson's original treatment has to be extended. KENRICK indicated in 1928 [14] that the general characteristic of Watson's result should not be invalidated by the presence of an inhomogeneous reflecting shell. In the present section we wish to incorporate, as completely as the present available space permits, the reflecting properties of the inhomogeneous layer into the wave solution. This solution is further presented in a new and simplified form which permits a more physical interpretation of the solution.

Let us first consider the simplest case, viz. horizontal polarization. In this case the waves are transmitted by a small horizontal loop carrying an electric current. Such a loop is equivalent to a fictitious magnetic dipole perpendicular to the plane of the loop.

The radiation field is symmetrical to the dipole-earth centre axis. The electric field lines are circles around this axis and the magnetic field lines are contained in the meridian planes. This problem has already been treated by miss M. GRAY [15] in the reflector free case.

We express the field of the current loop in terms of a radial HERTZIAN vector. We have in m. k. s. units

$$\Pi = \Pi_r(r, \theta) = \frac{J S k}{4 \pi} \cdot z_0 \cdot \frac{r}{b} \cdot U = A \cdot \frac{r}{b} \cdot U, \quad (65)$$

where  $r$  denotes the distance to the centre of the spherical earth of radius  $a$  (see fig. 10),  $\theta$  is the angular distance from the sender,  $z_0$  is the characteristic impedance of free space,  $120 \pi$  ohms, and  $J$  is the electric current in the small loop of area  $S$ . The »primary field» is

$$U = U_{pr} = e^{j k R} / j k R.$$

In spherical coordinates we further have

$$H_r = k^2 \Pi + \frac{\delta^2}{\delta r^2} (\Pi); H_\theta = \frac{1}{r} \frac{\delta^2}{\delta r \delta \theta} (\Pi); H_\varphi = 0;$$

and

$$E_r = E_\theta = 0; E_\varphi = z_0 \frac{j \omega A}{c_0} \frac{\delta U}{\delta \theta}. \quad (66)$$

One further finds that  $U$  satisfies the rigorous wave-equation also when  $\epsilon$  is a function of  $r$ , i. e., when the reflector is radially inhomogeneous. This is a characteristic feature when the polariza-

tion is horizontal as is already well known from the oblique incidence case of the plane reflector (compare p. 20).

Thus

$$\nabla^2 U + k_q^2 U = 0,$$

where

$k_q = k_1$  for  $r < a$ ,  $k_q = k_2 = k$  for  $a < r < c$ ,  $k_q = k_3$  for  $c < r < d$ , and  $k_q = k_4 = k$  for  $r > d$ . Here  $c$  and  $d$  denote the radial distance from the centre to the lower and upper boundaries of the reflecting shell.

Since the time factor is  $e^{-j\omega t}$ , we have

$$\left. \begin{aligned} k_1^2 &= \frac{\omega^2}{c_0^2} (\epsilon_1 + j 60 \sigma_1 \lambda) = k^2 (\epsilon_1 + j 60 \sigma_1 \lambda), \\ k_3^2 &= \frac{\omega^2}{c_0^2} \epsilon(r). \end{aligned} \right\} \quad (67)$$

As before  $\epsilon$  denotes the dielectric »constant» (terrestrial magnetic field assumed zero) and  $\sigma_1$  is the conductivity in mhos per meter.

Separating the wave-equation we get

$$U = \sum_0^\infty f_n(kr) P_n(\cos \theta), \quad (68)$$

where  $f_n(kr) = f(\bar{z})$  is a solution of

$$\frac{d^2}{d\bar{z}^2} \{ \bar{z} f_n(\bar{z}) \} + \left[ \epsilon_t(r) - \frac{n(n+1)}{\bar{z}^2} \right] \bar{z} f_n(\bar{z}) = 0. \quad (69)$$

When the layer thickness is small compared to  $r$  it is apparent from (69) that there is little difference between the plane and spherical cases as far as the reflector is concerned.

The general notation  $\varepsilon_t(r) = \varepsilon(r) + j 60 \sigma_1 \lambda$  has been introduced for the sake of convenience. For  $\varepsilon_t(r) = \text{constant}$  (i. e. for  $r < c$ ,  $r > d$ ) the radial functions are the well-known three dimensional functions

$$\left. \begin{aligned} \frac{\zeta_n^{(1)}(kr)}{kr} &= \left(\frac{\pi}{2kr}\right)^{\frac{1}{2}} H_{n+\frac{1}{2}}^{(1)}(kr); & \frac{\zeta_n^{(2)}(kr)}{kr} &= \left(\frac{\pi}{2kr}\right)^{\frac{1}{2}} H_{n+\frac{1}{2}}^{(2)}(kr); \\ \text{and} \\ \frac{\Psi_n(kr)}{kr} &= \left(\frac{\pi}{2kr}\right)^{\frac{1}{2}} J_{n+\frac{1}{2}}(kr) = \frac{1}{2} \left[ H_{n+\frac{1}{2}}^{(1)}(kr) + H_{n+\frac{1}{2}}^{(2)}(kr) \right]. \end{aligned} \right\} \quad (70)$$

In the range  $c < r < d$  (the reflecting layer) we assume that the radial functions corresponding to the incident, the reflected and the refracted waves, viz.

$$\frac{\xi_n^{(1)}(kr)}{kr}; \quad \frac{\xi_n^{(2)}(kr)}{kr}; \quad \text{and} \quad \frac{\xi_n^{(3)}(kr)}{kr}; \quad (71)$$

are known. Since these solutions are not linearly independent we must have

$$\xi_n^{(1)}(kr) = A_n \xi_n^{(2)}(kr) + B_n \xi_n^{(3)}(kr). \quad (72)$$

When the reflection at the boundary of the layer is neglected (this is a permissible approximation for most wave-lengths) then the internal spherical reflection factor of the layer becomes

$$R_3 = e^{j\delta_3} = -\frac{A_n \xi_n^{(2)}(kc)}{\xi_n^{(1)}(kc)} = \left| \frac{A_n \xi_n^{(2)}(kc)}{\xi_n^{(1)}(kc)} \right| e^{j \text{Re}(\delta_3)}, \quad (73)$$

For the parabolic layer the radial functions (71) can be obtained with sufficient approximations from the parabolic cylinder functions. Since  $\Delta h_m \ll c$ , (69) becomes

$$\left. \begin{aligned} \frac{d^2 \{z f_m(z)\}}{dz^2} + \left[ 1 - \frac{n(n+1)}{k^2 p^2} - \underbrace{\left\{ \frac{n(n+1)}{k^2 p^2} \right\}^2}_{\nu_1} \Delta x^2 e^{+j2\psi} \left( \frac{\Delta h_m}{p} \right)^2 - \right. \\ \left. - \frac{e^{-j2\psi}}{\Delta x^2} \left\{ 1 - \left( \frac{z_1}{\Delta h_m} \right)^2 \right\} \right] f_m(z) = 0, \end{aligned} \right\} \quad (70 \text{ a})$$

where  $p = c + \Delta h_m \approx c$  and  $z_1 = z - \underbrace{\Delta h_m \frac{\Delta h_m n(n+1)}{p k^2 p^2}}_{\nu_2} \Delta x^2 e^{j2\psi}$ .

The corrections  $\nu_1$  and  $\nu_2$  generally can be neglected for the dimensions obtaining in the radio case and it appears from a comparison with (31) that the spherical and the plane reflection coefficients even for a fairly thick layer are approximately identical to this degree of approximation when  $n(n+1) \neq k^2 p^2$ . It further appears the well-known fact that

$$\sin^2 \varphi_p \approx \frac{n(n+1)}{k^2 p^2} \approx \frac{\left(n + \frac{1}{2}\right)^2}{k^2 p^2}. \tag{74}$$

Except for small angles  $n \gg 1$  and therefore  $n + \frac{1}{2} \approx kp \sin \varphi_p$ .

\* \* \*

If the HERTZIAN-function were unaffected by the presence of the earth of the reflecting shell, the value of  $U$  should be

$$U = U_{pr} = \frac{e^{jkR}}{jkR}. \tag{75}$$

the so-called »primary field». By the well known addition theorem for the three-dimensional, spherical functions one has

$$\left. \begin{aligned} \frac{e^{jkR}}{jkR} &= \frac{1}{k^2 r b} \sum_{n=0}^{\infty} (2n+1) \zeta_n^{(1)}(kr) \Psi_n(kb) P_n(\cos \theta), \quad (r \geq b) \\ \frac{e^{jkR}}{jkR} &= \frac{1}{k^2 r b} \sum_{n=0}^{\infty} (2n+1) \zeta_n^{(1)}(kb) \Psi_n(kr) P_n(\cos \theta), \quad (r \leq b). \end{aligned} \right\} \tag{76}$$

If we take account of the presence of the earth and of the reflecting shell we denote the disturbance in the primary function by  $U_1, U_2$ , etc. The appropriate forms are

$$\left. \begin{aligned} U_1 &= \frac{1}{k^2 r b} \sum_{n=0}^{\infty} (2n+1) a_n \Psi_n(k_1 r) P_n(\cos \theta), \\ U_2 &= \frac{1}{k^2 r b} \sum_{n=0}^{\infty} (2n+1) \{b_n \Psi_n(kr) + c_n \zeta_n^{(1)}(kr)\} P_n(\cos \theta), \\ U_3 &= \frac{1}{k^2 r b} \sum_{n=0}^{\infty} (2n+1) d_n \{ \underset{\text{near the lower boundary in the reflecting shell,}}{\xi_n^{(1)}(kr) - A_n \xi_n^{(2)}(kr)} \} P_n(\cos \theta), \\ U_3 &= \frac{1}{k^2 r b} \sum_{n=0}^{\infty} (2n+1) d_n \cdot \underset{\text{near the upper boundary in the reflecting shell,}}{B_n \xi_n^{(3)}(kr)} P_n(\cos \theta), \\ U_4 &= \frac{1}{k^2 r b} \sum_{n=0}^{\infty} (2n+1) d_n B_n \frac{\xi_n^{(3)}(kd)}{\zeta_n^{(1)}(kd)} \cdot \zeta_n^{(1)}(kr) P_n(\cos \theta), \end{aligned} \right\} \tag{77}$$

<sup>1)</sup> Note: For the sake of simplicity the upper boundary reflection is neglected.

The boundary requirements that the tangential components of  $\overline{E}$  and  $\overline{H}$  be continuous, i. e.  $U$  and  $\frac{\delta}{\delta r} (r U)$  be continuous, therefore yield for the determination of the coefficients  $a, b, c, d$  the equations

$$\left. \begin{aligned} U_{pr} + U_2 &= U_1; (r = a), \\ \frac{\delta}{\delta r} (r U_{pr} + r U_2) &= \frac{\delta}{\delta r} (r U_1); (r = a), \\ U_{pr} + U_2 &= U_3; (r = c), \\ \frac{\delta}{\delta r} (r U_{pr} + r U_2) &= \frac{\delta}{\delta r} (r U_3); (r = c). \end{aligned} \right\} \quad (78)$$

Remembering the WRONSKIAN

$$\Psi_n(z) \zeta_n^{(1)'}(z) - \Psi_n'(z) \zeta_n^{(1)}(z) = j,$$

we find the wave function  $U$  at the surface of the earth ( $U = U_{pr} + U_2$ )

$$U = \frac{j}{k^2 a b} \sum (2n + 1) \frac{e_n}{g_n} P_n(\cos \theta), \quad (79)$$

where

$$e_n = \Psi_n(kb) \zeta_n^{(1)'}(kc) - \Psi_n'(kc) \zeta_n^{(1)}(kb) - \frac{\zeta_n^{(1)'}(kc)}{\zeta_n^{(1)}(kc)} a_n \{ \Psi_n(kb) \zeta_n^{(1)}(kc) - \Psi_n(kc) \zeta_n^{(1)}(kb) \}, \quad (80 a)$$

and

$$\begin{aligned} g_n &= \Psi_n'(ka) \zeta_n^{(1)'}(kc) - \Psi_n'(kc) \zeta_n^{(1)'}(ka) + \beta_n \{ \Psi_n'(kc) \zeta_n^{(1)}(ka) - \Psi_n(ka) \zeta_n^{(1)'}(kc) \} - \\ &- \frac{\zeta_n^{(1)'}(kc)}{\zeta_n^{(1)}(kc)} a_n [ \Psi_n'(ka) \zeta_n^{(1)}(kc) - \Psi_n(kc) \zeta_n^{(1)'}(ka) + \\ &+ \beta_n \{ \Psi_n(kc) \zeta_n^{(1)}(ka) - \Psi_n(ka) \zeta_n^{(1)}(kc) \} ], \end{aligned} \quad (80 b)$$

where

$$a_n = \frac{k_3}{k} \cdot \frac{\zeta_n^{(1)}(kc) \zeta_n^{(1)'}(kc)}{\zeta_n^{(1)'}(kc) \zeta_n^{(1)}(kc)} \cdot \frac{1 - A_n \frac{\zeta_n^{(2)'}(kc)}{\zeta_n^{(1)'}(kc)}}{1 - A_n \frac{\zeta_n^{(2)}(kc)}{\zeta_n^{(1)}(kc)}} = -j \tan \frac{\delta_y}{2}; \quad (80 c)$$

and

$$\beta_n = \frac{k_1 \Psi_n'(k_1 a)}{k \Psi_n(k_1 a)} \tag{80 d}$$

When  $\frac{\xi_n^{(2)' }(\bar{z})}{\xi_n^{(2)}(\bar{z})} \approx \frac{\xi_n^{(1)' }(\bar{z})}{\xi_n^{(1)}(\bar{z})} \approx \frac{\zeta_n^{(1)' }(k c)}{\zeta_n^{(1)}(k c)}$ , as generally is the case in an important region of the  $n/\bar{z}$  — plane, it appears from (73 a) that  $\delta_y = \delta_3$ . Since a factor of the type  $e^{j\delta_3}$  indicates reflection in the shell, it is advantageous to rearrange (80 a) and (80 b) somewhat so that the various waves contained in  $\frac{e_n}{g_n}$  will be easily separated.

Making use of (79) we obtain after several transformations

$$\frac{e_n}{g_n} = \frac{\zeta_n^{(1)}(k b)}{\zeta_n^{(1)' }(k a) - \beta_n \zeta_n^{(1)}(k a)} \cdot \underbrace{\frac{1 - j e^{j \delta_y} \left\{ \frac{\zeta_n^{(2)}(k b)}{\zeta_n^{(1)}(k b)} \zeta_n^{(1)}(k c) \zeta_n^{(1)' }(k c) - \Delta \right\}}{1 + j e^{j \delta_y} \left\{ \frac{\zeta_n^{(2)}(k a)}{\zeta_n^{(1)}(k a)} \zeta_n^{(1)}(k c) \zeta_n^{(1)' }(k c) R_1 + \Delta \right\}}}_{k_n} \tag{81}$$

where  $R_1$  is a complex reflection factor to be specified shortly and  $\Delta = \frac{1}{2} \{ \zeta_n^{(1)}(k c) \zeta_n^{(2)' }(k c) + \zeta_n^{(1)' }(k c) \zeta_n^{(2)}(k c) \}$  which generally is a very small quantity and therefore often can be neglected (generally of the order of magnitude  $\frac{\lambda}{2 \pi c}$ ). The solution therefore finally becomes

$$U = \frac{j}{k^2 a b} \sum_{n=0}^{n=\infty} (2n + 1) \frac{\zeta_n^{(1)}(k b)}{\zeta_n^{(1)}(k a)} \frac{P_n(\cos \theta)}{\frac{\zeta_n^{(1)' }(k a)}{\zeta_n^{(1)}(k a)} - \frac{k_1 \Psi_n'(k_1 a)}{k \Psi_n(k_1 a)}} k_n \tag{82}$$

With the reflecting shell absent,  $k_n = 1$ , we are returned to the familiar solution of the diffraction of electromagnetic waves round the earth. In this case  $\zeta_n^{(1)}(k b)/\zeta_n^{(1)}(k a)$  evidently becomes the height-gain factor.

We further have

$$R_1 = \frac{-\frac{\zeta_n^{(2)' }(k a)}{\zeta_n^{(2)}(k a)} + \frac{k_1 \Psi_n'(k_1 a)}{k \Psi_n(k_1 a)}}{\frac{\zeta_n^{(1)' }(k a)}{\zeta_n^{(1)}(k a)} - \frac{k_1 \Psi_n'(k_1 a)}{k \Psi_n(k_1 a)}} = -\eta_1 \tag{83}$$

This complex reflection-refraction factor must contain all reflected and refracted waves in the earth. One finds that (83) permits the expansion

$$R_1 = R_{21} + T_{21} T_{12} \sum_{m=0}^{\infty} R_{12}^m \left\{ \frac{\zeta_n^{(1)}(ka)}{\zeta_n^{(2)}(ka)} \right\}^{m+1}, \quad (83 \text{ a})$$

where  $R_{21}$  and  $T_{21}$  are the spherical reflection and refraction coefficients in direction into the earth, and  $R_{12}$ ,  $T_{12}$  are the corresponding coefficients in direction out of the earth, viz.

$$\left. \begin{aligned} R_{21} &= \frac{-\frac{\zeta_n^{(2)'}(ka)}{\zeta_n^{(2)}(ka)} + \frac{k_1}{k} \frac{\zeta_n^{(2)'}(k_1 a)}{\zeta_n^{(2)}(k_1 a)}}{\frac{\zeta_n^{(1)'}(ka)}{\zeta_n^{(1)}(ka)} - \frac{k_1}{k} \frac{\zeta_n^{(2)'}(k_1 a)}{\zeta_n^{(2)}(k_1 a)}}, \\ T_{21} &= 1 + R_{21}, \\ R_{12} &= \frac{-\frac{\zeta_n^{(1)'}(ka)}{\zeta_n^{(1)}(ka)} + \frac{k_1}{k} \frac{\zeta_n^{(1)'}(k_1 a)}{\zeta_n^{(1)}(k_1 a)}}{\frac{\zeta_n^{(1)'}(ka)}{\zeta_n^{(1)}(ka)} - \frac{k_1}{k} \frac{\zeta_n^{(2)'}(k_1 a)}{\zeta_n^{(2)}(k_1 a)}}, \\ T_{12} &= 1 + R_{12}. \end{aligned} \right\} \quad (83 \text{ b})$$

and

Generally  $-\zeta_n^{(2)'}(ka) / \zeta_n^{(2)}(ka) \approx \zeta_n^{(1)'}(ka) / \zeta_n^{(1)}(ka)$  (i. e.,  $\Delta \approx 0$ ) and  $R_{12} \approx -R_{21}$ .

\* \* \*

Since  $n/ka \approx \sin \varphi_a < 1$  and both  $n$  and  $ka$  are very large, it is necessary to make use of the appropriate DEBYE-WATSON expansions of the BESSEL-functions. In the region of the  $n/\bar{z}$ -plane of most immediate interest in this connexion they are

$$\zeta_n^{(2)}(\bar{z}) \sim \left\{ 1 - \frac{\left(n + \frac{1}{2}\right)^2}{\bar{z}^2} \right\}^{-\frac{1}{4}} \exp \cdot \left[ \mp j \int_{n + \frac{1}{2}}^{\bar{z}} \left\{ 1 - \frac{\left(n + \frac{1}{2}\right)^2}{x^2} \right\}^{\frac{1}{2}} dx - \frac{\pi}{4} \right]. \quad (84)$$

Remembering that  $\zeta_n(\bar{z})$  is a solution of (69) for  $\epsilon_t(r) = 1$ , it is at once apparent that (84) is nothing else but a W.K.B.-approximation. It therefore breaks down in the bridging region where  $n/\bar{z} \approx 1$  and where the NICHOLSON-WATSON formulae will have to be used. We will have occasion to return to this question later.

As further for  $n$  very large and real

$${}_{n}(\cos \theta) \sim \frac{1}{\left\{2\pi\left(n + \frac{1}{2}\right)\sin\theta\right\}^{\frac{1}{2}}} \cdot \frac{e^{j\left\{\left(n + \frac{1}{2}\right)\theta - \frac{\pi}{4}\right\}} + e^{-j\left\{\left(n + \frac{1}{2}\right)\theta - \frac{\pi}{4}\right\}}}{2} \quad (85)$$

( $\theta$  not too near 0 or  $\pi$ )

waves travelling clockwise round the earth will be of the type

$$\exp. \left[ j \left\{ \left( n + \frac{1}{2} \right) \theta \mp \int_{n+\frac{1}{2}}^{kr} \left\{ 1 - \frac{\left( n + \frac{1}{2} \right)^2}{x^2} \right\}^{\frac{1}{2}} dx \right\} \right] = \exp. (jS).$$

But this is nothing else than the abbreviated action function  $S$  which is the solution of the HAMILTON-JACOBI differential equation [3]

$$\sum_{x,y,z} \left( \frac{\delta S}{\delta x} \right)^2 = 1.$$

This illustrates the physical character of the asymptotic solution involving the DEBYE-expansions. The factor  $\zeta_n^{(1)}(k_1 a) / \zeta_n^{(2)}(k_1 a)$  occurring in (83) thus denotes the phase retardation and attenuation experienced by a wave of incidence characterized by  $n$  when traversing the earth.

\* \* \*

We proceed with the transformation of the solution and introduce the notation.

$$\bar{p} = \frac{k}{k_3} \cdot \frac{1 + R_3}{1 + R_3 \frac{\xi_n^{(2)}(kc) \xi_n^{(1)}(kc)}{\xi_n^{(1)}(kc) \xi_n^{(2)}(kc)}} \quad (86)$$

We thus obtain from (80 c).

$$e^{j \delta_y} = \frac{-\frac{\xi_n^{(1)'}(k c)}{\xi_n^{(1)}(k c)} + \bar{p} \cdot \frac{\zeta_n^{(1)'}(k c)}{\zeta_n^{(1)}(k c)}}{\frac{\xi_n^{(1)'}(k c)}{\xi_n^{(1)}(k c)} + \bar{p} \cdot \frac{\zeta_n^{(1)'}(k c)}{\zeta_n^{(1)}(k c)}}. \quad (87 \text{ a})$$

Again remembering the WRONSKIAN and observing that  $\Delta = -j + \zeta_n^{(1)'}(k c) \zeta_n^{(2)}(k c)$ , we further find

$$1 + j \Delta e^{j \delta_y} = -j \zeta_n^{(1)'}(k c) \zeta_n^{(2)}(k c) \frac{\frac{\xi_n^{(1)'}(k c)}{\xi_n^{(1)}(k c)} - \bar{p} \frac{\zeta_n^{(2)'}(k c)}{\zeta_n^{(2)}(k c)}}{\frac{\xi_n^{(1)'}(k c)}{\xi_n^{(1)}(k c)} + \bar{p} \frac{\zeta_n^{(1)'}(k c)}{\zeta_n^{(1)}(k c)}}. \quad (87 \text{ b})$$

Relation (81) therefore after transformation yields the important result

$$k_n = \frac{1 + R_4 \frac{\zeta_n^{(2)}(k b) \zeta_n^{(1)}(k c)}{\zeta_n^{(1)}(k b) \zeta_n^{(2)}(k c)}}{1 - R_1 R_4 \frac{\zeta_n^{(1)}(k c) \zeta_n^{(2)}(k a)}{\zeta_n^{(2)}(k c) \zeta_n^{(1)}(k a)}}, \quad (88)$$

where

$$R_4 = \frac{-\frac{\xi_n^{(1)'}(k c)}{\xi_n^{(1)}(k c)} + \bar{p} \frac{\zeta_n^{(1)'}(k c)}{\zeta_n^{(1)}(k c)}}{\frac{\xi_n^{(1)'}(k c)}{\xi_n^{(1)}(k c)} - \bar{p} \frac{\zeta_n^{(2)'}(k c)}{\zeta_n^{(2)}(k c)}}. \quad (89)$$

Introducing the spherical boundary reflection coefficients

$$R_{23} = \frac{-\frac{\xi_n^{(1)'}(k c)}{\xi_n^{(1)}(k c)} + \frac{k}{k_3} \cdot \frac{\zeta_n^{(1)'}(k c)}{\zeta_n^{(1)}(k c)}}{\frac{\xi_n^{(1)'}(k c)}{\xi_n^{(1)}(k c)} - \frac{k}{k_3} \cdot \frac{\zeta_n^{(2)'}(k c)}{\zeta_n^{(2)}(k c)}}, \quad (90 \text{ a})$$

and

$$R_{32} = \frac{-\frac{\xi_n^{(2)'}(k c)}{\xi_n^{(2)}(k c)} + \frac{k}{k_3} \cdot \frac{\zeta_n^{(2)'}(k c)}{\zeta_n^{(2)}(k c)}}{\frac{\xi_n^{(1)'}(k c)}{\xi_n^{(1)}(k c)} - \frac{k}{k_3} \cdot \frac{\zeta_n^{(2)'}(k c)}{\zeta_n^{(2)}(k c)}}, \quad (90 \text{ b})$$

we find that (89) permits the expansion

$$R_4 = R_{23} + R_3 \frac{(1 + R_{23})(1 + R_{32})}{1 - R_3 R_{23}} = R_{23} + R_3 T_{23} T_{32} (1 + R_3 R_{23} + R_3^2 R_{23}^2 + \dots). \quad (91)$$

It is thus apparent from relation (91) that the complex reflection factor  $R_4$  contains all waves due to internal reflection and lower boundary reflection in the layer. Further putting  $\check{\gamma} = \infty$  in (28) we infer that  $R_{eff}$  is the plane equivalent of the spherical coefficient  $R_4$ .

If we have two reflecting shells, (A) (radii c, d) and (B) (radii e, f), and  $\frac{\zeta_n^{(1)}(ke) \zeta_n^{(2)}(kd)}{\zeta_n^{(1)}(kd) \zeta_n^{(2)}(ke)} = \Delta_{ed}$ , we similarly obtain

$$R_4 \approx R_4^{(A)} + \frac{R_4^{(B)} \Delta_{ed} (T_4^{(A)})^2}{1 - R_4^{(A)} R_4^{(B)} \Delta_{ed}}. \quad (91 a)$$

Therefore for short waves (no boundary reflection)

$$R_4 \approx R_3^{(A)} + R_3^{(B)} \Delta_{ed} (T_3^{(A)})^2 = R_3^{(A)} + R_3^{(AB)}. \quad (91 b)$$

\* \* \*

It is sometimes convenient to separate the ground and sky waves in (82), (88). To make the result more general, we raise the receiver to a point a distance  $r - a$  above the ground. We therefore get

$$U(r, \theta) = \underbrace{\frac{e^{jkR}}{jkR} + \frac{1}{k^2rb} \sum_{n=0}^{\infty} (2n+1) \zeta_n^{(1)}(kb) \zeta_n^{(1)}(kr) \frac{1}{2} \left\{ \frac{\zeta_n^{(2)}(ka)}{\zeta_n^{(1)}(ka)} R_1 - 1 \right\} P_n(\cos \theta)}_{\text{The ground waves}} + \frac{1}{k^2rb} \sum_{n=0}^{\infty} (2n+1) \zeta_n^{(1)}(kb) \zeta_n^{(2)}(ka) \frac{1}{2} \left\{ \frac{\zeta_n^{(2)}(kr)}{\zeta_n^{(2)}(ka)} + \frac{\zeta_n^{(1)}(kr)}{\zeta_n^{(1)}(ka)} R_1 \right\} R_4 \frac{\zeta_n^{(1)}(kc)}{\zeta_n^{(2)}(kc)} + \frac{\left\{ \frac{\zeta_n^{(2)}(kb)}{\zeta_n^{(1)}(kb)} + \frac{\zeta_n^{(2)}(ka)}{\zeta_n^{(1)}(ka)} R_1 \right\} P_n(\cos \theta)}{1 - R_1 R_4 \frac{\zeta_n^{(2)}(ka) \zeta_n^{(1)}(kc)}{\zeta_n^{(1)}(ka) \zeta_n^{(2)}(kc)}}. \quad (a < r < c) \quad (92)$$

The sky waves

The ground waves have been treated thoroughly by VAN DER POL and BREMMER in the case of vertical polarization [5]. We therefore leave them aside. So much more so as this communication primarily deals with the transmission of radio waves in the atmosphere.

Grouping the reflection factors in a physical order we can write the sky waves as

$$\begin{aligned}
 U_s(r, \theta) = & \frac{1}{2 k^2 r b} \sum_{n=0}^{\infty} (2n + 1) \frac{\zeta_n^{(1)}(kc)}{\zeta_n^{(1)}(kb)} R_4 \frac{\zeta_n^{(2)}(kb)}{\zeta_n^{(2)}(kc)} \cdot \zeta_n^{(1)}(kb) \zeta_n^{(2)}(ka) \cdot \\
 & \cdot \left[ 1 + \sum_{p=0}^{\infty} \left\{ \left[ R_{21} + T_{21} T_{12} \sum_{n=0}^{\infty} R_{12}^m \left\{ \frac{\zeta_n^{(1)}(ka)}{\zeta_n^{(2)}(ka)} \right\}^{m+1} \right] \frac{\zeta_n^{(1)}(kc)}{\zeta_n^{(1)}(ka)} R_4 \frac{\zeta_n^{(2)}(ka)}{\zeta_n^{(1)}(ka)} \right\}^p \right] \cdot \\
 & \cdot \left[ \frac{\zeta_n^{(2)}(kr)}{\zeta_n^{(2)}(ka)} + \frac{\zeta_n^{(1)}(kr)}{\zeta_n^{(1)}(ka)} \left\{ R_{21} + T_{21} T_{12} \sum_{q=0}^{\infty} R_{12}^q \left\{ \frac{\zeta_n^{(1)}(ka)}{\zeta_n^{(2)}(ka)} \right\}^{q+1} \right\} \right] P_n(\cos \theta) + \\
 & + \frac{1}{2 k^2 r b} \sum_{n=0}^{\infty} (2n + 1) \zeta_n^{(1)}(kb) \zeta_n^{(2)}(ka) \left\{ R_{21} + T_{21} T_{12} \sum_{q=0}^{\infty} R_{12}^q \left\{ \frac{\zeta_n^{(1)}(ka)}{\zeta_n^{(2)}(ka)} \right\}^{q+1} \right\} \left\{ \frac{\zeta_n^{(1)}(kc)}{\zeta_n^{(1)}(ka)} \right\} R_4 \cdot \\
 & \cdot \frac{\zeta_n^{(2)}(ka)}{\zeta_n^{(2)}(kc)} \left[ 1 + \sum_{p=0}^{\infty} \left\{ \left[ R_{21} + T_{21} T_{12} \sum_{m=0}^{\infty} R_{12}^m \left\{ \frac{\zeta_n^{(1)}(ka)}{\zeta_n^{(2)}(ka)} \right\}^{m+1} \right] \frac{\zeta_n^{(1)}(kc)}{\zeta_n^{(1)}(ka)} R_4 \right\}^p \right] \cdot \\
 & \cdot \frac{\zeta_n^{(2)}(ka)}{\zeta_n^{(2)}(kc)} \left[ \frac{\zeta_n^{(2)}(kr)}{\zeta_n^{(2)}(ka)} + \frac{\zeta_n^{(1)}(kr)}{\zeta_n^{(1)}(ka)} \left\{ R_{21} + T_{21} T_{12} \sum_{q=0}^{\infty} R_{12}^q \left\{ \frac{\zeta_n^{(1)}(ka)}{\zeta_n^{(2)}(ka)} \right\}^{q+1} \right\} \right] P_n(\cos \theta). \quad (92 a)
 \end{aligned}$$

The first group of waves contains all those which experience their first reflection in the shell. The waves in the second group experience their first reflection (and refraction) at the earth.

At the earth the wave is broken up in one direct reflected wave ( $R_{21}$ ) and indirect reflected waves which are twice refracted ( $T_{21}$ ,  $T_{12}$ ) and  $q$  times reflected on the inside  $\left( R_{12}^q \left\{ \frac{\zeta_n^{(1)}(ka)}{\zeta_n^{(2)}(ka)} \right\}^{q+1} \right)$ . The indirect reflected waves are, of course, unimportant in the radio

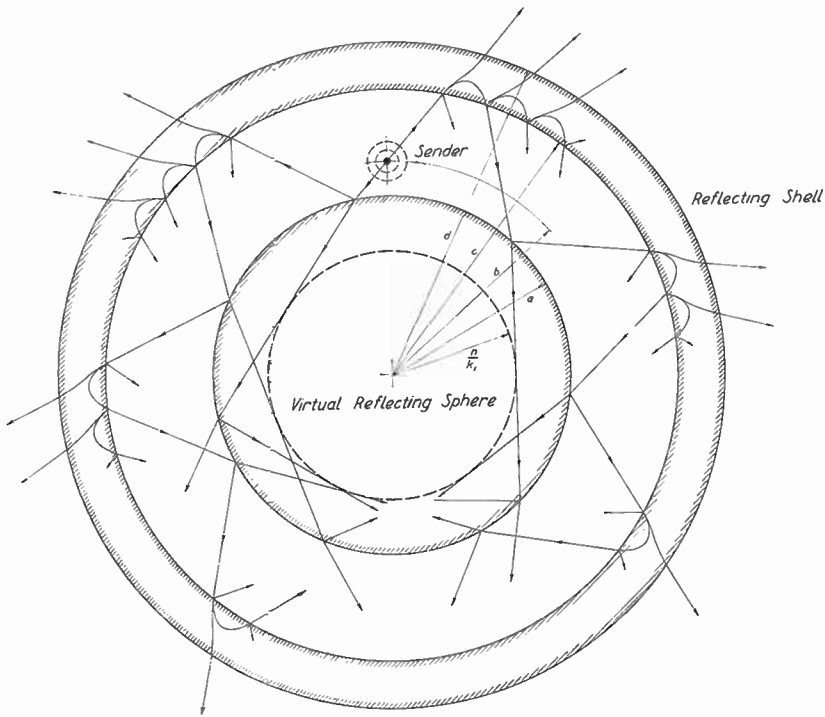


Fig. 11.

case. Finally as a demonstration of the separation of the various waves fig. 11 depicts the first few waves of each group. This should not be taken to mean that actual ray treatment is permissible.

As will be shown  $\frac{2(c - a)}{\lambda} = \frac{2h}{\lambda} \gg 1$  in order that the ray methods may be used.

\* \* \*

Next let us study the case of vertical polarization. The waves are transmitted by a small vertical current element, a fictitious electric dipole. The radiation field is symmetrical to the dipole — earth centre axis as before. The magnetic field lines are circles around this axis and the electric field lines are contained in the meridian planes.

If the strength of the current element is  $\Delta K$  meter-amperes we have the HERTZIAN vector (radial)

$$H^1 = H_r^1 = \Delta K \cdot \frac{z_0}{4\pi} \cdot \frac{r}{b} \cdot U^1 = A_1 \cdot \frac{r}{b} \cdot U^1, \quad (93)$$

with a primary field  $U_{pr}^1 = e^{jkR}/jkR$ , in the homogeneous medium.

This time one finds that  $U$  does not satisfy the rigorous wave-equation when the medium is radially in homogeneous. With

$$U^1 = \sum_0^{\infty} f_n^1(kr) P_n(\cos \theta)$$

we have instead of (69), ( $\bar{z} = kr$ )

$$\frac{d^2}{d\bar{z}^2} \{\bar{z} f_n^1(\bar{z})\} - \frac{1}{\varepsilon_t} \frac{d\varepsilon_t}{d\bar{z}} \frac{d}{d\bar{z}} \{\bar{z} f_n^1(\bar{z})\} + \left[ \overbrace{\varepsilon_t(r) - \frac{n(n+1)}{\bar{z}^2}}^{\varepsilon_{t_n}} \right] \bar{z} f_n^1(\bar{z}) = 0. \quad (94)$$

$\underbrace{\hspace{10em}}_{\sin^2 \varphi_r}$

One further easily finds that

$$\frac{d^2}{d\bar{z}^2} \{\bar{z} f_n^1(\bar{z})\} - \frac{1}{\varepsilon_{t_n}} \cdot \frac{d\varepsilon_{t_n}}{d\bar{z}} \frac{d}{d\bar{z}} \{\bar{z} f_n^1(\bar{z})\} + \varepsilon_{t_n} \cdot \bar{z} f_n^1(\bar{z}) = 0, \quad (94 \text{ a})$$

is satisfied by  $\frac{d}{d\bar{z}} \{\bar{z} f_n(\bar{z})\}$ , where  $f_n(\bar{z})$  is a solution of (69). Thus

$\bar{z} f_0^1(z) = \text{const.} \cdot \frac{d}{d\bar{z}} \{\bar{z} f_0(\bar{z})\}$ . This holds for  $n \approx 0$ , i. e., for vertical incidence as expected.

Similarly to (71) we introduce three radial functions

$$\frac{\xi_{n_1}^{(1)}(kr)}{kr}; \quad \frac{\xi_{n_1}^{(2)}(kr)}{kr}; \quad \text{and} \quad \frac{\xi_{n_1}^{(3)}(kr)}{kr} \quad (95)$$

which build up  $f_n^1(kr)$ . In the circuit relation similar to (72) the coefficients may be  $A_n^1$  and  $B_n^1$ , i. e., the internal spherical reflection coefficient of the layer becomes

$$R_3^1 = e^j \delta_3^1 = - \frac{A_n^1 \xi_{n_1}^{(2)}(kr)}{\xi_{n_1}^{(1)}(kr)} \quad (96)$$

Utilizing the fact that when  $\lambda \ll \Delta h_m$  (short wave case) as will later be shown on p. 97

$$\frac{1}{\xi_n^{(1)}} \cdot \frac{d \xi_n^{(1)}}{d r} \approx - \frac{1}{\xi_n^{(2)}} \cdot \frac{d \xi_n^{(2)}}{d r} \approx j k \cos \varphi_p, \tag{97}$$

we obtain from (94) and (94 a) the approximate result

$$f_n^1(kr) \approx \text{const.} \left( \frac{\varepsilon_t}{\varepsilon_{t_n}} \right)^{\frac{1}{2}} \cdot \frac{d}{d r} \{f_n(kr)\}, \tag{98}$$

when  $\cos^2 \varphi_r > 0$  and not too small. When (97) holds we have  $A_{n_1} \approx A_n$  and therefore by virtue of (97)  $R_3^1 \approx -R_3$ . Therefore when the layer is very many wave-lengths thick (approximately diffraction-free transmission) the ionospheric reflection properties for horizontal and vertical polarization are practically identical.

In spherical coordinates we further have

$$E_r = k^2 \Pi^1 + \frac{1}{\varepsilon_t} \frac{\delta^2 \Pi^1}{\delta r^2} - \frac{1}{\varepsilon_t^2} \frac{\delta \varepsilon_t}{\delta r} \frac{\delta \Pi^1}{\delta r}; \quad E_\theta = \frac{1}{\varepsilon_t r} \frac{\delta^2 \Pi^1}{\delta r \delta \theta}; \quad E_\varphi = 0;$$

and

$$H_r = H_\theta = 0; \quad H_\varphi = -j \frac{k}{z_0} \frac{A}{b} \frac{\delta U^1}{\delta \theta}. \tag{99}$$

At the boundaries  $U^1$  and  $\frac{1}{\varepsilon_t} \frac{\delta}{\delta r} (r U^1)$  must be continuous. This yields

$$U = \frac{1}{k^2 a b} \sum_{n=0}^{n=\infty} (n + 1/2) \zeta_n^{(1)}(kb) \zeta_n^{(2)}(kr) \left\{ 1 + R_1^1 \frac{\zeta_n^{(2)}(ka)}{\zeta_n^{(1)}(ka)} \cdot \frac{\zeta_n^{(1)}(kr)}{\zeta_n^{(2)}(kr)} \right\} \cdot \frac{1 + R_4^1 \frac{\zeta_n^{(1)}(kc)}{\zeta_n^{(2)}(kc)} \cdot \frac{\zeta_n^{(2)}(cb)}{\zeta_n^{(1)}(cb)}}{1 - R_1^1 R_4^1 \frac{\zeta_n^{(1)}(kc)}{\zeta_n^{(2)}(kc)} \cdot \frac{\zeta_n^{(2)}(ka)}{\zeta_n^{(1)}(ka)}} \cdot P_n(\cos \theta), \tag{100}$$

$(b > r > a)$

where

$$R_1^1 = \frac{-\frac{\zeta_n^{(2)'}(ka)}{\zeta_n^{(2)}(ka)} + \frac{k}{k_1} \cdot \frac{\Psi_n'(k_1 a)}{\Psi_n(k_1 a)}}{\frac{\zeta_n^{(1)'}(ka)}{\zeta_n^{(1)}(ka)} - \frac{k}{k_1} \cdot \frac{\Psi_n'(k_1 a)}{\Psi_n(k_1 a)}} = -\frac{\zeta_n^{(2)'}(ka)}{\zeta_n^{(2)}(ka)} \frac{\zeta_n^{(1)}(ka)}{\zeta_n^{(1)'}(ka)} \cdot \eta_1^1, \quad (101)$$

and

$$R_4^1 = \frac{-\frac{\xi_n^{(1)'}(kc)}{\xi_n^{(1)}(kc)} + \bar{p}^1 \frac{\zeta_n^{(1)'}(kc)}{\zeta_n^{(1)}(kc)}}{\frac{\xi_n^{(1)'}(kc)}{\xi_n^{(1)}(kc)} - \bar{p}^1 \frac{\zeta_n^{(2)'}(kc)}{\zeta_n^{(2)}(kc)}}, \quad (102)$$

with

$$\bar{p}^1 = \frac{k_3}{k} \cdot \frac{1 + R_3^1}{1 + R_3 \frac{\xi_{n_1}^{(2)'}(kc)}{\xi_{n_1}^{(1)'}(kc)} \frac{\xi_{n_1}^{(1)}(kc)}{\xi_{n_1}^{(2)}(kc)}}. \quad (103)$$

Similarly to  $R_1$ ,  $R_1^1$  permits the expansion

$$R_1^1 = R_{21}^1 + T_{21}^1 T_{12}^1 \sum_{m=0}^{m=\infty} (R_{12}^1)^m \left\{ \frac{\zeta_n^{(1)}(ka)}{\zeta_n^{(2)}(ka)} \right\}^{m+1}, \quad (104)$$

where

$$R_{21}^1 = \frac{-\frac{\zeta_n^{(2)'}(ka)}{\zeta_n^{(2)}(ka)} + \frac{k}{k_1} \cdot \frac{\zeta_n^{(2)'}(k_1 a)}{\zeta_n^{(2)}(k_1 a)}}{\frac{\zeta_n^{(1)'}(ka)}{\zeta_n^{(1)}(ka)} - \frac{k}{k_1} \cdot \frac{\zeta_n^{(2)'}(k_1 a)}{\zeta_n^{(2)}(k_1 a)}}, \quad (105)$$

$$T_{21}^1 = \left( \frac{k}{k_1} \right)^2 (1 + R_{21}^1), \text{ etc.} \quad (106)$$

These are the spherical reflection and refraction coefficients for vertical polarization.

### The Transformation of the Series.

The series for  $U(r, \theta)$  converges very slowly, since the main contribution comes from terms with  $n$  of order  $ka$ . It is therefore convenient to follow WATSON and transform the series into a continuous integral over  $n$ . We obtain

$$(a, \theta) = \frac{1}{k^2 ab} \int_c \frac{n}{\cos(n\pi)} \cdot \frac{e_{n-\frac{1}{2}}}{g_{n-\frac{1}{2}}} P_{n-\frac{1}{2}} \{ \cos(\pi - \theta) \} dn + \frac{1}{k^2 ab} \int_0^{j\infty} \frac{n}{\cos(n\pi)} \left\{ \frac{e_{n-\frac{1}{2}}}{g_{n-\frac{1}{2}}} - \frac{e_{-n-\frac{1}{2}}}{g_{-n-\frac{1}{2}}} \right\} \cdot P_{n-\frac{1}{2}} \{ \cos(\pi - \theta) \} dn \tag{107}$$

The contour of integration  $c$  in the complex  $n$ -plane lies wholly in the first quadrant and encloses all poles lying there since there are no poles in the fourth quadrant. The last integral is zero when

$\frac{e_{n-\frac{1}{2}}}{g_{n-\frac{1}{2}}}$  is an even function of  $n$ .

An approximation especially suitable when  $k_1 a$  has a great imaginary part (i. e., the radio case) is

$$\frac{\Psi'_n(k_1 a)}{\Psi_n(k_1 a)} \approx \frac{\zeta_n^{(2)'}(k_1 a)}{\zeta_n^{(2)}(k_1 a)}$$

which means nothing else than that the indirect reflected waves are very weak.

Since 
$$\zeta_{-n-\frac{1}{2}}^{(1)}(z) = e^{\pm j n \pi} \zeta_{n-\frac{1}{2}}^{(1)}(z)$$

and by (13)  $e_{-n-\frac{1}{2}} = e_{+n-\frac{1}{2}}$ ,

we have by virtue of (40) under these circumstances

$$\frac{e_\nu}{g_\nu} \approx \frac{e_{-\nu-1}}{g_{-\nu-1}},$$

where  $\nu = n - \frac{1}{2}$ .

In the radio case, therefore, we should be sufficiently justified in neglecting the last integral of (107).

To evaluate the contour integral of (107) we need a knowledge of the poles of  $\frac{e_\nu}{g_\nu}$ . Apparently the only poles are those of

$$\underbrace{\left\{ \frac{\zeta_\nu^{(1)'}(ka)}{\zeta_\nu^{(1)}(ka)} - \frac{k_1}{k} \cdot \frac{\Psi'_\nu(k_1 a)}{\Psi_\nu(k_1 a)} \right\}}_{\Phi_1} \underbrace{\left\{ 1 - R_1 R_4 \frac{\zeta_\nu^{(1)}(kc) \zeta_\nu^{(2)}(ka)}{\zeta_\nu^{(2)}(kc) \zeta_\nu^{(1)}(ka)} \right\}}_{\Phi_2} = g_\nu.$$

The poles of  $\Phi_1$  and  $R_1$  are the same, viz. the poles corresponding to the case without reflecting shell. These poles have been investigated thoroughly by VAN DER POL and BREMMER [16] for vertical and by MISS M. GRAY for horizontal polarization [15]. When the shell

is poorly reflecting,  $|R_4| \ll 1$ , the poles of  $\Phi_2$  are only slightly displaced from those of  $\Phi_1$ . When the reflecting power increases the poles of  $\Phi_2$  are found on a curve entirely different from that of  $\Phi_1$ . One similarity remains, however, viz. that the important poles are found near  $n \sim ka$  as in the reflector-free case. This introduces certain difficulties as will presently be shown. WATSON in his original contribution to the subject, for example, did not proceed

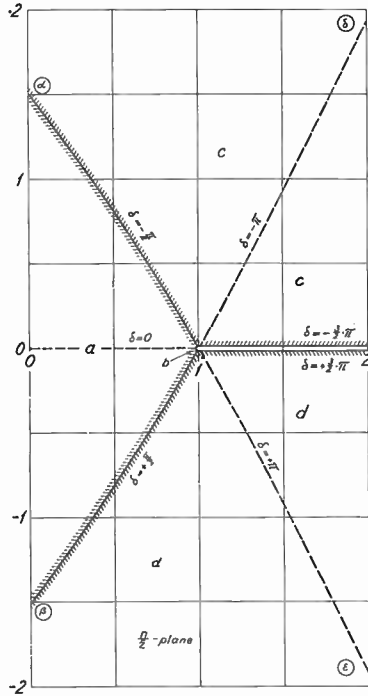


Fig. 12. The division of the  $\frac{n}{z}$  — plane for  $\bar{z}$  real and positive.

so far as to make a closer examination of these important poles possible. Without a sufficient knowledge of these poles the numerical computation of the transmission problem becomes approximate and uncertain.

Before we proceed let us study briefly the types of expansions we have to use in the first and fourth quadrants of the  $n/\bar{z}$ -plane. Introducing the notation

$$S_{\nu}^{(1)}(\bar{z}) = \left\{ 1 - \frac{n^2}{\bar{z}^2} \right\}^{-\frac{1}{4}} \cdot \exp. \left[ \mp j \left\{ \int_{\frac{n}{\bar{z}}}^{\bar{z}} \left\{ 1 - \frac{n^2}{x^2} \right\}^{\frac{1}{2}} dx - \frac{\pi}{4} \right\} \right], \quad (108)$$

we get the following asymptotic DEBYE-WATSON representation [17] of the three-dimensional functions in the regions *a*), *c*), and *d*) of fig. 12, viz.

Function	Region <i>a</i> )	Region <i>c</i> )	Region <i>d</i> )
$\left(\frac{\pi \bar{z}}{2}\right)^{\frac{1}{2}} H_{\nu}^{(1)}(\bar{z})$	$S_{\nu}^{(1)}(\bar{z})$	$S_{\nu}^{(1)}(\bar{z}) - S_{\nu}^{(2)}(\bar{z})$	$S_{\nu}^{(1)}(\bar{z})$
$\left(\frac{\pi \bar{z}}{2}\right)^{\frac{1}{2}} H_{\nu}^{(2)}(\bar{z})$	$S_{\nu}^{(2)}(\bar{z})$	$S_{\nu}^{(2)}(\bar{z})$	$S_{\nu}^{(2)}(\bar{z}) - S_{\nu}^{(1)}(\bar{z})$
$\left(\frac{\pi \bar{z}}{2}\right)^{\frac{1}{2}} J_{\nu}(\bar{z})$	$\frac{1}{2} \{S_{\nu}^{(1)}(\bar{z}) + S_{\nu}^{(2)}(\bar{z})\}$	$\frac{1}{2} S_{\nu}^{(1)}(\bar{z})$	$\frac{1}{2} S_{\nu}^{(2)}(\bar{z})$

TABLE I

Region *a*), where the majority of the poles will be found, evidently corresponds to the earlier mentioned (84).

It is to be noted that the root  $\left\{\frac{\bar{z}^2}{n^2} - 1\right\}^{\frac{1}{2}}$  is defined as lying in the same quadrant as  $\frac{\bar{z}}{n}$ . Writing

$$\gamma_r = \int_n^{kr} \left\{1 - \frac{n^2}{x^2}\right\}^{\frac{1}{2}} dx = e^{j\delta}, \tag{109}$$

this leads to the orientation of the conformal representation of the  $\gamma$ -plane as shown by the boundary lines and dashed lines in fig. 12. Along the dashed lines, therefore,  $|S_{\nu}^{(1)}(\bar{z})| = |S_{\nu}^{(2)}(\bar{z})|$ , and one of the three-dimensional functions has an oscillatory character.  $H_{\nu}^{(1)}(\bar{z})$ , for example, is oscillatory on the branch *b*) — (8). This is of importance also in the study of the shadow side of the caustic.

The DEBYE-WATSON expansions break up in the neighbourhood of the branch-point  $\frac{n}{\bar{z}} = 1$ . In the transition region *b*) we therefore have to make use of the NICHOLSON-WATSON formulae [18] involving cylinder functions of order  $\frac{1}{3}$ , <sup>1)</sup>. They are preferably transformed in the following suitable form, viz.

<sup>1)</sup> For a comparative study of the bridging problem the reader is referred to the *Transactions of Chalmers University*, 3, p. 30, 1942 and to p. 86 of this communication.

$$\left(\frac{\pi \bar{z}}{2}\right)^{\frac{1}{2}} H_{\nu}^{(1)}(\bar{z}) \sim \left(\frac{\pi \bar{z}}{6}\right)^{\frac{1}{2}} \frac{\bar{z}}{n} \left\{1 - \frac{n^2}{\bar{z}^2}\right\}^{\frac{3}{4}} H_{\frac{1}{3}}^{(1)}(\varrho_r) \cdot e^{\mp j \left(\frac{5}{12} \pi - \varrho_r\right)} S_{\nu}^{(1)}(\bar{z}), \quad (110)$$

where

$$\varrho_r = \frac{n}{3} \left\{ \frac{(kr)^2}{n^2} - 1 \right\}^{\frac{3}{2}}, \text{ and as before } kr = \bar{z}.$$

Since

$$\frac{d}{d\varrho} \left\{ \varrho^{\frac{1}{3}} H_{\frac{1}{3}}^{(1)}(\varrho) \right\} = e^{\mp j \frac{2}{3} \pi} \varrho^{\frac{1}{3}} H_{\frac{2}{3}}^{(1)}(\varrho), \text{ one has}$$

$$\frac{\zeta_{\nu}^{(2)'}(\bar{z})}{\zeta_{\nu}^{(1)'}(\bar{z})} \sim \frac{1}{\bar{z}} \pm j \frac{3 \varrho_r}{\bar{z}} + e^{\mp j \frac{2}{3} \pi} \frac{\bar{z}}{n} \left(\frac{3}{n}\right)^{\frac{1}{3}} \frac{\varrho_r^{\frac{2}{3}} H_{\frac{2}{3}}^{(1)}(\varrho_r)}{\varrho_r^{\frac{1}{3}} H_{\frac{1}{3}}^{(1)}(\varrho_r)}, \quad (111)$$

where the first term may safely be neglected.

Finally

$$S_{\nu}^{(1)}(\bar{z}) S_{\nu}^{(1)'}(\bar{z}) \sim e^{\mp j 2 \gamma_r} \quad (112)$$

\* \* \*

Let us next investigate a few of the reflection coefficients. Making use of (83 b) and (110), (111) we get for example

$$\frac{\zeta_{\nu}^{(2)}(ka)}{\zeta_{\nu}^{(1)}(ka)} R_{21}^1 = - \frac{\zeta_{\nu}^{(2)'}(ka)}{\zeta_{\nu}^{(1)'}(ka)} \cdot \frac{1 - \frac{k}{k_1} \alpha^*}{1 + \frac{k}{k_1} \alpha} = - \frac{\zeta_{\nu}^{(2)'}(ka)}{\zeta_{\nu}^{(1)'}(ka)} \cdot \eta_{21}^1, \quad (113)$$

where

$$\alpha^* \left. \begin{matrix} a \\ a \end{matrix} \right\} = \frac{\left\{1 - \frac{n^2}{(k_1 a)^2}\right\}^{\frac{1}{2}}}{\left\{1 - \frac{n^2}{(ka)^2}\right\}^{\frac{1}{2}}} \cdot e^{\pm j \frac{\pi}{6}} \cdot \frac{H_{\frac{1}{3}}^{(1)}(\varrho_a)}{H_{\frac{2}{3}}^{(1)}(\varrho_a)}, \text{ and } \varrho_a = \frac{n}{3} \left\{ \frac{(ka)^2}{n^2} - 1 \right\}^{\frac{3}{2}}. \quad (114)$$

When  $n/ka$  lies in section a) of fig. 12 and  $|\varrho_a| \gg 1$ , it is obvious that the expression for  $R_{21}^1$  reduces to the plane FRESNEL coefficient for vertical polarization, i. e.,

$$R_{21}^1 \approx \frac{\left[ k_1 \left\{ 1 - \frac{n^2}{(k a)^2} \right\}^{\frac{1}{2}} - k \left\{ 1 - \frac{n^2}{(k_1 a)^2} \right\}^{\frac{1}{2}} \right]}{\left[ k_1 \left\{ 1 - \frac{n^2}{(k a)^2} \right\}^{\frac{1}{2}} + k \left\{ 1 - \frac{n^2}{(k_1 a)^2} \right\}^{\frac{1}{2}} \right]} \quad (113 a)$$

Region a);  
not too close to b).

When  $n/ka$  lies in section c) of fig. 12, it is convenient to write

$$\left. \begin{matrix} \alpha \\ \alpha^* \end{matrix} \right\} = \frac{\left\{ 1 - \frac{n^2}{(k_1 a)^2} \right\}^{\frac{1}{2}}}{\left\{ \frac{n^2}{(k a)^2} - 1 \right\}^{\frac{1}{2}}} \cdot e^{\mp j \frac{\pi}{6}} \frac{I_{-\frac{1}{3}}(\bar{\varrho}_a) + e^{\mp j \frac{\pi}{3}} I_{\frac{1}{3}}(\bar{\varrho}_a)}{I_{-\frac{2}{3}}(\bar{\varrho}_a) + e^{\pm j \frac{\pi}{3}} I_{\frac{2}{3}}(\bar{\varrho}_a)}, \quad (114 a)$$

where  $\bar{\varrho}_a = \varrho_a e^{j \frac{3}{2} \pi}$ .

When the losses are moderate, and this is the only case to be discussed in this connexion,  $|k_1 a| \gg n$ , and  $\left\{ 1 - \frac{n^2}{(k_1 a)^2} \right\}^{\frac{1}{2}} \approx 1$ .

For  $n = ka$ ,  $\eta_{21}^1$  therefore becomes

$$(\eta_{21}^1)_{n=ka} = \frac{1 - \frac{k}{k_1} \left( \frac{ka}{6} \right)^{\frac{1}{3}} \Gamma\left(\frac{1}{3}\right) \left\{ \Gamma\left(\frac{2}{3}\right) \right\}^{-1} e^{j \frac{\pi}{6}}}{1 - \frac{k}{k_1} \left( \frac{ka}{6} \right)^{\frac{1}{3}} \Gamma\left(\frac{1}{3}\right) \left\{ \Gamma\left(\frac{2}{3}\right) \right\}^{-1} e^{-j \frac{\pi}{6}}}$$

For the homogeneous reflector (WATSON-case) we get similarly to (113) from (102) that

$$R_4^1 = R_{23}^1 = - \frac{\zeta_{\nu}^{(1), (k c)}}{\zeta_{\nu}^{(1), (k c)}} \cdot \frac{\zeta_{\nu}^{(2), (k c)}}{\zeta_{\nu}^{(2), (k c)}} \cdot \frac{1 - \frac{k}{k_3} \beta}{1 + \frac{k}{k_3} \beta^*} = - \frac{\zeta_{\nu}^{(1), (k c)}}{\zeta_{\nu}^{(1), (k c)}} \cdot \frac{\zeta_{\nu}^{(2), (k c)}}{\zeta_{\nu}^{(2), (k c)}} \cdot \eta_{23}^1, \quad (115)$$

where

$$\left. \begin{matrix} \beta^* \\ \beta \end{matrix} \right\} \approx \frac{\left\{ 1 - \frac{n^2}{(k_3 c)^2} \right\}^{\frac{1}{2}}}{\left\{ 1 - \frac{n^2}{(k c)^2} \right\}^{\frac{1}{2}}} e^{\pm j \frac{\pi}{6}} \frac{H_{\frac{1}{3}}^{(1)}(\varrho_c)}{H_{\frac{2}{3}}^{(1)}(\varrho_c)}, \quad \text{and } \varrho_c = \frac{n}{3} \left\{ \frac{(k c)^2}{n^2} - 1 \right\}^{\frac{3}{2}}. \quad (116)$$

When further  $n/kc$  lies in section a) of fig. 12 and  $|\varrho_c| \gg 1$ ,  $R_{23}^1$  reduces to the plane FRESNEL-coefficient.

When  $n/kc$  lies in section c) it is convenient to write similarly to (92 a)

$$\left. \begin{array}{l} \beta \\ \beta^* \end{array} \right\} = \frac{\left\{ 1 - \frac{n^2}{(k_3 c)^2} \right\}^{\frac{1}{2}}}{\left\{ \frac{n^2}{(k c)^2} - 1 \right\}^{\frac{1}{2}}} e^{\mp j \frac{\pi}{6}} \frac{I_{-\frac{1}{3}}(\bar{\varrho}_c) + e^{\mp j \frac{\pi}{3}} I_{\frac{1}{3}}(\bar{\varrho}_c)}{I_{-\frac{2}{3}}(\bar{\varrho}_c) + e^{\pm j \frac{\pi}{3}} I_{\frac{2}{3}}(\bar{\varrho}_c)}, \quad (117 \text{ a})$$

where  $\bar{\varrho}_c = \varrho_c \cdot e^{j \frac{3\pi}{2}}$ .

It is also convenient to write

$$R_{23}^1 = e^{j \varphi_{23}^1} \cdot \eta_{23}^1. \quad (118 \text{ a})$$

When  $n$  real =  $n^0 < kc$ ,  $\varrho_c = \varrho_c^0$ , and

$$\varphi_{23}^1 = \varphi_{23}^{10} = \frac{\pi}{3} + 2 [\text{Phase} \{H_{\frac{2}{3}}^{(1)}(\varrho_c^0)\} - \text{Phase} \{H_{\frac{1}{3}}^{(1)}(\varrho_c^0)\}].$$

For  $n^0 > kc$  the above expression is conveniently written

$$\varphi_{23}^{10} = \frac{\pi}{3} + 2 \text{Phase} \left\{ \frac{I_{-\frac{2}{3}}(|\varrho_c^0|) + e^{j \frac{\pi}{3}} I_{\frac{2}{3}}(|\varrho_c^0|)}{I_{-\frac{1}{3}}(|\varrho_c^0|) + e^{-j \frac{\pi}{3}} I_{\frac{1}{3}}(|\varrho_c^0|)} \right\}.$$

Fig. 13 shows a plot of  $\varphi_{23}^1$ ,  $|\eta_{23}^1|$  and  $\text{Phase} \{\eta_{23}^1\}$  as functions of  $n^0 - kc = \Delta n^0$ , for  $\lambda = 5 \text{ km}$  and  $\left| \frac{k}{k_3} \right| \approx 0,125$ , which roughly corresponds to  $\omega_c = 2\pi \cdot 0,768 \cdot 10^6 \text{ sec}^{-1}$  and  $\nu = 10^6 \text{ sec}^{-1}$  for the  $D$ -layer.

It is also convenient to throw  $\frac{\zeta_{\nu}^{(2)}(ka)}{\zeta_{\nu}^{(1)}(ka)} R_{21}^1$  in the form

$$\frac{\zeta_{\nu}^{(2)}(ka)}{\zeta_{\nu}^{(1)}(ka)} R_{21}^1 = j e^{j(\varphi_{21}^1 - 2\gamma_a)} \cdot \eta_{21}^1 \quad (118 \text{ b})$$

Spherical Reflection Coefficient  $R'_{23}$  as a Function of  $\Delta n^\circ$  for  
 $h=60 \text{ km}$ ,  $\lambda=5 \text{ km}$ ,  $\omega_c=2\pi \cdot 0,768 \cdot 10^6 \text{ sec}^{-1}$  and  $\nu=10^6 \text{ sec}^{-1}$

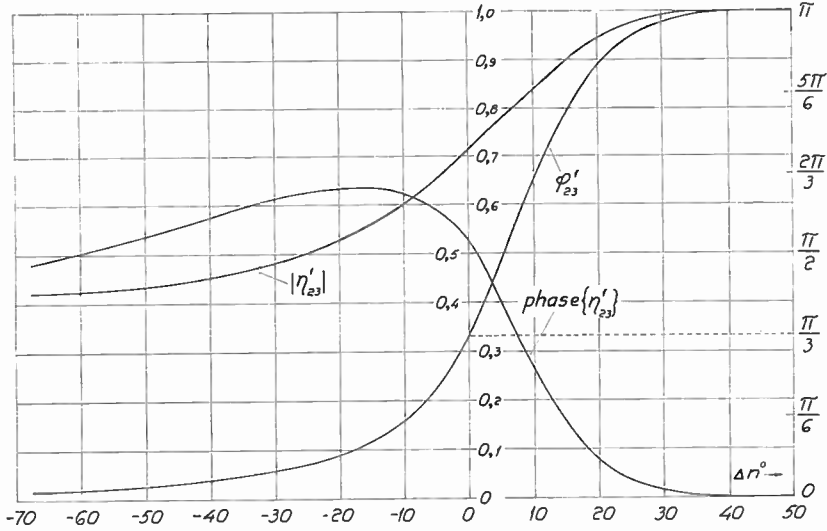


Fig. 13.

For  $n$  real and  $\leq ka$  we find by means of (88), (89) that

$$\varphi_{21}^{10} = -\frac{7}{6} \pi + 2 \varrho_a^0 - 2 \text{Phase} \left\{ H_{\frac{2}{3}}^{(1)}(\varrho_a^0) \right\},$$

or  $\varphi_{21}^{10} = -\frac{\pi}{12}$ , when  $n = ka$ .  $|\varphi_{21}^{10}|$  decreases monotonically to become

zero when  $\varrho_a \gg 1$ . For  $\varrho_a = 1$ ,  $\varphi_{21}^{10} \approx -\frac{\pi}{40}$  (or  $-4,5^\circ$ ).

### The Poles of the Watson Case.

Quite generally the poles or proper values,  $n_s = \nu_s + \frac{1}{2}$ , of the solution, for vertical polarization for example, must satisfy the relation

$$\ln \left\{ R_1^1 R_4^1 \frac{\zeta_{\nu_s}^{(2)}(ka) \zeta_{\nu_s}^{(1)}(kc)}{\zeta_{\nu_s}^{(1)}(ka) \zeta_{\nu_s}^{(2)}(kc)} \right\} = j 2 s \pi. \quad (s = \dots, 2, 1, 0, -1, -2, \dots) \quad (119)$$

The physical interpretation of this important relation is simple. The proper values select only those waves which do not cancel out by mutual radial interference.

In the WATSON case the pole selecting relation can also be written

$$\ln \left\{ \eta_1^1 \eta_{23}^1 \cdot \frac{\zeta_{\nu_s}^{(1)'}(k c) \zeta_{\nu_s}^{(2)'}(k a)}{\zeta_{\nu_s}^{(2)'}(k c) \zeta_{\nu_s}^{(1)'}(k a)} \right\} = j 2 s \pi, \tag{120}$$

where  $\eta_1^1$  is defined by relation (101).

Making use of relations (110) and (111) we have

$$\frac{\zeta_{\nu_s}^{(1)'}(k c) \zeta_{\nu_s}^{(2)'}(k a)}{\zeta_{\nu_s}^{(2)'}(k c) \zeta_{\nu_s}^{(1)'}(k a)} \sim \frac{H_{\frac{2}{3}}^{(1)}(\varrho_c) H_{\frac{2}{3}}^{(2)}(\varrho_a)}{H_{\frac{2}{3}}^{(2)}(\varrho_c) H_{\frac{2}{3}}^{(1)}(\varrho_a)} \exp. \left[ j 2 \left\{ (\gamma_c - \gamma_a) - (\varrho_c - \varrho_a) \right\} \right]. \tag{121}$$

These expressions yield the formal Phase Integral Relations

$$\left. \begin{aligned} \int_{ka}^{kc} \left\{ 1 - \frac{n^2}{x^2} \right\}^{\frac{1}{2}} dx &= s \pi + \delta_{14}, \quad \{ \text{Re}(n) \leq ka \}, \\ \int_n^{kc} \left\{ 1 - \frac{n^2}{x^2} \right\}^{\frac{1}{2}} dx &= s \pi + \delta_{14}, \quad \{ kc \geq \text{Re}(n) \geq ka \}, \end{aligned} \right\} \tag{122}$$

where

$$- \delta_{14} = j \frac{1}{2} \ln \left\{ \frac{H_{\frac{2}{3}}^{(1)}(\varrho_a) H_{\frac{2}{3}}^{(2)}(\varrho_c)}{H_{\frac{2}{3}}^{(2)}(\varrho_a) \cdot H_{\frac{2}{3}}^{(1)}(\varrho_c)} \right\} + \varrho_a - \varrho_c - j \frac{1}{2} \ln \eta_1^1 \eta_{23}^1; \{ \text{Re}(n) \leq ka \},$$

and

$$- \delta_{14} = j \frac{1}{2} \ln \left\{ \frac{H_{\frac{2}{3}}^{(1)}(\varrho_a) H_{\frac{2}{3}}^{(2)}(\varrho_c)}{H_{\frac{2}{3}}^{(2)}(\varrho_a) \cdot H_{\frac{2}{3}}^{(1)}(\varrho_c)} \right\} - \varrho_c - j \frac{1}{2} \ln \eta_1^1 \eta_{23}^1; \{ kc \geq \text{Re}(n) \geq ka \}.$$

When  $|\delta_{14}| \approx j \frac{1}{2} \ln \eta_1^1 \eta_{23}^1$ , i. e., when  $\text{Re}(n) < ka$ , the proper values are selected by the radial phase integral of the geometrical optics already demonstrated on p. 45.

When  $n$  real and  $< ka$ , we denote  $\delta_{14}$  by  $\delta_{14}^0$  and obtain

$$-\delta_{14}^0 = \text{Phase} \left\{ H_{\frac{2}{3}}^{(1)}(\varrho_c^0) \right\} - \text{Phase} \left\{ H_{\frac{2}{3}}^{(1)}(\varrho_a^0) \right\} + \varrho_a^0 - \varrho_c^0,$$

and when further  $n$  real and  $ka \leq n \leq kc$  we find

$$-\delta_{14}^0 = \text{Phase} \left\{ H_{\frac{2}{3}}^{(1)}(\varrho_c^0) \right\} + \frac{\pi}{2} - \arctan \frac{3^{\frac{1}{2}} I_{\frac{2}{3}}(|\varrho_a^0|)}{2 I_{-\frac{2}{3}}(|\varrho_a^0|) + I_{\frac{2}{3}}(|\varrho_a^0|)} - \varrho_c^0. \tag{123}$$

Since  $(\varrho_c^0)_{n=ka} \approx \frac{11\pi}{\lambda_{km}}$ , it is obvious that even for waves as long as 5 km,  $\delta_{14}^0$  is with a good degree of approximation given by

$$-\delta_{14}^0 = -\frac{7}{12}\pi + \varrho_a^0 - \text{Phase} \left\{ H_{\frac{2}{3}}^{(1)}(\varrho_a^0) \right\}, \tag{123 a}$$

*Graphical Representation of the Solution of the Phase Integral*

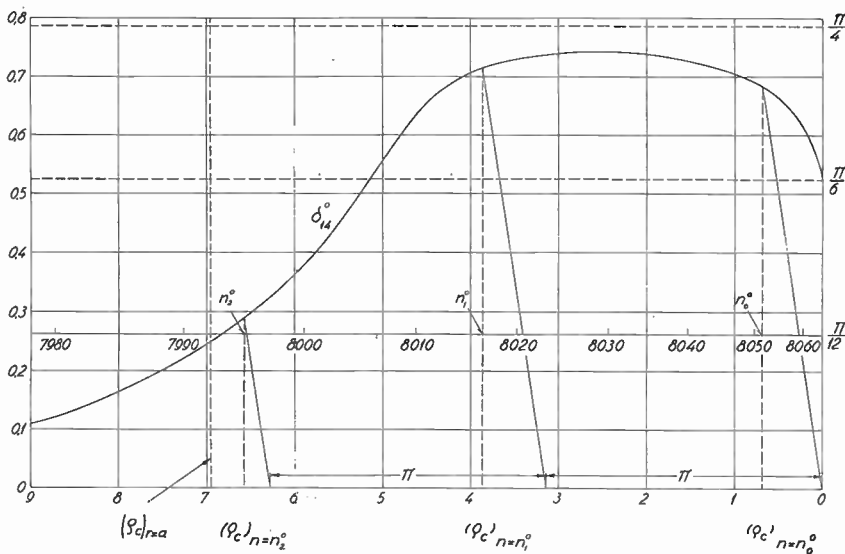


Fig. 14. A plot of  $\delta_{14}^0$  as a function of  $n$ .  $\{\text{Im}(n) = 0\}$ .

[Note:  $(\varrho_c)_{r=a}$  means  $(\varrho_c)_{n=ka}$ ]

when  $n$  real and  $\leq ka$ . It is further apparent from (123) that  $\delta_{14}^0 \approx \frac{\pi}{4}$  midway between  $ka$  and  $kc$  for waves which are not too long, since  $I_{\frac{2}{3}}(|\varrho_a|) \approx I_{-\frac{2}{3}}(|\varrho_a|)$  when  $|\varrho_a| \gg 1$ .

Fig. 14 shows a plot of  $\delta_{14}^0$  as a function of  $n$ , when  $\text{Im}(n) = 0$ . This plot was made with the aid of tables of BESSEL functions of order  $\pm \frac{2}{3}$ , presented at the end of this communication.

\* \* \*

For poles with  $\text{Re}(n)$  sufficiently smaller than  $ka$  (i. e. the majority of the poles)  $\delta_{14}^0 = 0$  and (122) yields

$$\int_{ka}^{kc} \left\{ 1 - \frac{n^2}{x^2} \right\}^{\frac{1}{2}} dx = s \pi + j \frac{1}{2} \ln \eta_1^1 \eta_{23}^1$$

where  $s$  necessarily is a positive integer (in accordance with the orientation of fig. 12) and sufficiently large, so that  $|\varrho_a| > 1$ . Since under these circumstances  $R_1^1 = \eta_1^1$  and  $R_{23}^1 = \eta_{23}^1$  {i. e., we are well inside region  $a$ ) and the first term in the asymptotic expansion of  $H_{\frac{1}{3}}^{(1)}(\varrho_a)$  occurring in the NICHOLSON-WATSON formula leads to  $S_y^{(1)}(\bar{z})$ , we have proved that, when  $s$  is sufficiently large, the poles are actually determined by the phase-integral which has been used so successfully by ECKERSLEY in the treatment of radio transmission problems.

Written in the familiar manner the phase-integral relation therefore becomes

$$2 \int_{ka}^{kc} \left\{ 1 - \frac{n^2}{x^2} \right\}^{\frac{1}{2}} dx - j \ln R_1^1 - j \ln R_{23}^1 = 2 s \pi, \quad (124)$$

when  $|\varrho_a| > 1$ . Even for waves as long as 5 km the  $s$ -value corresponding to the pole closest to  $ka$ , i. e. 2, makes  $s \pi$  considerably larger than  $\frac{\pi}{12}$  and it is therefore almost possible to use this phase integral relation up to  $ka$ . Unfortunately the most important poles (i. e. the poles with the smallest imaginary part when losses are

introduced) may lie between  $ka$  and  $kc$  where the application of this classical phase integral relation (124) is no longer permissible.

For the higher order poles it is, however, an extremely useful relation. Since

$$\left\{ 1 - \frac{4n^2}{k(a+c)^2} \right\}^{\frac{1}{2}} kh$$

is a very close approximation to the phase integral when  $\frac{c-a}{c} \ll 1$ , the phase-integral relation yields

$$n_s \approx \frac{k(c+a)}{2} \left[ 1 - \frac{1}{(kh)^2} \left\{ s^2 \pi^2 - \frac{1}{4} \ln^2 \eta_1^1 \eta_{23}^1 \right\} - j \frac{s \pi}{(kh)^2} \ln \eta_1^1 \eta_{23}^1 \right]^{\frac{1}{2}} \quad (125)$$

which we call *Relation I*.

When  $s$  is not too large and the losses are moderate a good approximation to (125) is

$$\approx \frac{k(c+a)}{2} \left\{ \left[ 1 - \frac{1}{(kh)^2} \left\{ s^2 \pi^2 - \frac{1}{4} \ln^2 \eta_1^1 \eta_{23}^1 \right\} \right]^{\frac{1}{2}} - j \frac{\frac{s \pi}{2 (kh)^2} \cdot \ln \eta_1^1 \eta_{23}^1}{\left[ 1 - \frac{1}{(kh)^2} \left\{ s^2 \pi^2 - \frac{1}{4} \ln^2 \eta_1^1 \eta_{23}^1 \right\} \right]^{\frac{1}{2}}} \right\} \quad (125 a)$$

Neglecting the losses for a moment we infer from (125) that the maximum number of proper values corresponding to real no-loss poles is

$$s_{\max} = \frac{kh}{\pi} = \frac{2h}{\lambda}$$

as was already shown by WATSON [6].

Long-wave transmission therefore has comparatively few important poles which is an indication of the fact that no real rays are formed. Finally (125) shows that there are infinitely many poles along the positive imaginary axis. These are, of course, practically unimportant.

Denoting the no-loss pole by  $n_s^0$  we write

$$n_s = n_s^0 + \Delta n_s, \quad (126)$$

i. e.,  $\Delta n_s$  is the change in  $n_s$  due to the introduction of the losses.

For  $s$  not too large we therefore have

$$\Delta n_s \approx j \frac{a+c}{2} \cdot \frac{\cot \varphi_s}{h} \left( -\frac{1}{2} \right) \ln \eta_1^1 \eta_{23}^1, \quad (126 \text{ a})$$

where  $\varphi_s = \arcsin \left\{ \frac{2 n_s}{k(c+a)} \right\}$ .

For long-waves  $\frac{k}{k_1} \approx \left| \frac{k}{k_1} \right| e^{-j \frac{\pi}{4}}$ , and  $\left| \frac{k}{k_3} \right| \approx e^{-j \frac{\pi}{4}}$ .

This yields for vertical polarization

$$\begin{aligned} \text{Im} (\Delta n_s) \approx \frac{a+c}{8h} \cot \varphi_s \cdot \left[ \ln \left\{ \frac{\cos^2 \varphi_s^1 + \left| \frac{k}{k_1} \right|^2 + \sqrt{2} \left| \frac{k}{k_1} \right| \cos \varphi_s^1}{\cos^2 \varphi_s^1 + \left| \frac{k}{k_1} \right|^2 - \sqrt{2} \left| \frac{k}{k_3} \right| \cos \varphi_s^1} \right\} + \right. \\ \left. + \ln \left\{ \frac{\cos^2 \varphi_s^3 + \left| \frac{k}{k_3} \right|^2 + \sqrt{2} \left| \frac{k}{k_3} \right| \cos \varphi_s^3}{\cos^2 \varphi_s^3 + \left| \frac{k}{k_3} \right|^2 - \sqrt{2} \left| \frac{k}{k_3} \right| \cos \varphi_s^3} \right\} \right], \quad (126 \text{ b}) \end{aligned}$$

where  $\varphi_s^1 = \arcsin \left( \frac{n_s}{ka} \right)$ ; etc. This relation is identical with WATSON'S which, however, only considered the ground losses. It is shown by the above relations that the ground and reflector losses are contained symmetrically in  $\Delta n_s$ . It is apparent from (126 b) that there is a number of poles with only slightly increasing imaginary part. This is most easily seen for small losses when

$$\text{Im} (\Delta n_s) \approx \frac{a+c}{4h} \cdot \frac{\sqrt{2}}{\sin \varphi_s} \left\{ \left| \frac{k}{k_1} \right| + \left| \frac{k}{k_3} \right| \right\}, \left( \left| \frac{k}{k_1} \right| \ll 1, \left| \frac{k}{k_3} \right| \ll 1 \right). \quad (126 \text{ a})$$

since  $\varphi_s^1 \approx \varphi_s \approx \varphi_s^3$ . As  $\sin \varphi_s \approx 1$  for the lower order poles,  $\text{Im} (\Delta n_s)$  is changing rather slowly and consequently for shorter waves a considerable number of terms must be evaluated in the residue series.

The remaining poles  $n_s^0$  close to  $ka$  and between  $ka$  and  $kc$  are easily obtained from relations (122), (123), and (123 a).

Since in the region  $ka - kc$

$$\int_n^{kc} \left\{ 1 - \frac{n^2}{x^2} \right\}^{\frac{1}{2}} dx \approx \varrho_c, \quad (127)$$

the no-loss poles between  $ka$  and  $kc$  are simply obtained graphically from

$$\varrho_c - s\pi = \delta_{14}^0(\varrho_c).$$

The construction of the poles is shown in fig. 14 for  $h = 60$  km and  $\lambda = 5$  km.

The remaining important task is to find expressions for the corresponding  $\Delta n_s$ -values.

We must have

$$j \frac{1}{2} \ln \eta_1^1 \eta_{23}^1 = \int_{n_s^0}^{n_s^0 + \Delta n_s} \int_{ka}^{kc} \left(1 - \frac{n^2}{x^2}\right)^{\frac{1}{2}} dx - \delta_{14}.$$

Fortunately it is not necessary to make use of many terms in the expansion of the above relation when the losses are small. Making use of the WRONSKIAN and remembering the derivation rules for order  $\frac{1}{3}$  and  $\frac{2}{3}$  functions we get for the two cases:

$$\begin{aligned} & 1) \ n_s^0 \leq ka \\ & - \Delta n_s \left[ \left\{ \frac{2(kc - n_s^0)}{kc} \right\}^{\frac{1}{2}} \cdot \frac{2}{\pi \varrho_c^0} \cdot \frac{1}{\{|H_{\frac{2}{3}}^{(1)}(\varrho_c^0)|\}^2} \right. \\ & \cdot \left. \left\{ 1 + \underbrace{\left\{ \left| \frac{H_{\frac{1}{3}}^{(1)}(\varrho_c^0)}{H_{\frac{2}{3}}^{(1)}(\varrho_c^0)} \right| \cos \left( \frac{\pi}{3} + \beta_c^0 \right) (\varrho_c^0)^{\frac{1}{3}} \left( \frac{3}{kc} \right)^{\frac{1}{3}} - \frac{1}{(3 \varrho_c^0)^{\frac{2}{3}}} \cdot \frac{1}{(kc)^{\frac{1}{3}}} \right\}}_{\varepsilon_c} \Delta n_s \right\} - \right. \\ & \left. - \left\{ \frac{2(ka - n_s^0)}{kc} \right\}^{\frac{1}{2}} \cdot \frac{2}{\pi \varrho_a^0} \cdot \frac{1}{\{|H_{\frac{2}{3}}^{(1)}(\varrho_a^0)|\}^2} \right. \\ & \left. \cdot \left. \left\{ 1 + \underbrace{\left\{ \left| \frac{H_{\frac{1}{3}}^{(1)}(\varrho_a^0)}{H_{\frac{2}{3}}^{(1)}(\varrho_a^0)} \right| \cos \left( \frac{\pi}{3} + \beta_a^0 \right) (\varrho_a^0)^{\frac{1}{3}} \left( \frac{3}{ka} \right)^{\frac{1}{3}} - \frac{1}{(3 \varrho_a^0)^{\frac{2}{3}}} \cdot \frac{1}{(ka)^{\frac{1}{3}}} \right\}}_{\varepsilon_a} \Delta n_s \right\} \right] \approx \\ & \approx j \frac{1}{2} \ln \eta_1^1 \eta_{23}^1, \end{aligned} \tag{128}$$

where

$$\left. \begin{aligned} \beta_c^0 &= \text{Phase} \left\{ H_{\frac{1}{3}}^{(1)}(\varrho_c^0) \right\} - \text{Phase} \left\{ H_{\frac{2}{3}}^{(1)}(\varrho_c^0) \right\}, \\ \text{and} \\ \beta_a^0 &= \text{Phase} \left\{ H_{\frac{1}{3}}^{(1)}(\varrho_a^0) \right\} - \text{Phase} \left\{ H_{\frac{2}{3}}^{(1)}(\varrho_a^0) \right\}. \end{aligned} \right\} (128 a)$$

The correction terms  $\varepsilon_c$  and  $\varepsilon_a$  are very small for normal losses when  $n^0 < kc$  and  $ka$  respectively. For  $|\varrho| \approx 0$  one has  $\varepsilon \approx 0$ .  $\varepsilon$  gets its maximum for  $\varrho \approx 0,4$  where  $\varepsilon_{\max} \approx 0,15$ .

Since normal reflection losses may correspond to  $|\Delta n_s| \approx 5$  for a wave-length of 5 km the order of magnitude of the error omitting  $\varepsilon$  is about 5–6 %. It can therefore often be neglected for practical purposes.

$$\begin{aligned} & 2) \ n_s^0 \geq ka. \\ & -\Delta n_s \left[ \left\{ \frac{2(kc - n_s^0)}{ka} \right\}^{\frac{1}{2}} \cdot \frac{2}{\pi \varrho_c^0} \cdot \frac{1}{\left\{ \left| H_{\frac{2}{3}}^{(1)}(\varrho_c^0) \right| \right\}^2} \right. \\ & \cdot \left. \left\{ 1 + \underbrace{\left\{ \left| \frac{H_{\frac{1}{3}}^{(1)}(\varrho_c^0)}{H_{\frac{2}{3}}^{(1)}(\varrho_c^0)} \right| \cos \left( \frac{\pi}{3} + \beta_c^0 \right) (\varrho_c^0)^{\frac{1}{3}} \left( \frac{3}{kc} \right)^{\frac{1}{3}} - \frac{1}{(3 \varrho_c^0)^{\frac{2}{3}}} \cdot \frac{1}{(kc)^{\frac{1}{3}}} \right\}}_{\varepsilon_c} \Delta n_s \right\} + \right. \\ & \left. + \left\{ \frac{2(n_s^0 - ka)}{ka} \right\}^{\frac{1}{2}} \cdot \frac{2}{\pi |\varrho_a^0|} \cdot \frac{1}{\left\{ \left| H_{\frac{2}{3}}^{(1)}(|\varrho_a^0|) \right| \right\}^2} \right. \\ & \cdot \left. \left\{ 1 - \underbrace{\left\{ |\alpha_1| \cos \left( \frac{\pi}{3} + \beta_a^0 \right) (|\varrho_a^0|)^{\frac{1}{3}} \left( \frac{3}{ka} \right)^{\frac{1}{3}} - \frac{1}{(3 |\varrho_a^0|)^{\frac{2}{3}}} \cdot \frac{1}{(ka)^{\frac{1}{3}}} \right\}}_{-\varepsilon_a} \Delta n_s \right\} \right] \approx \\ & \approx j \frac{1}{2} \ln \eta_1^1 \eta_{23}^1. \end{aligned} \quad (129)$$

where  $H_{\frac{2}{3}}^{(1)}(|\varrho_a^0|)$  is defined by

$$\left. \begin{aligned}
 H_{\frac{2}{3}}^{(1)}(|\varrho_a^0|) &\approx \frac{I_{-\frac{2}{3}}(|\varrho_a^0|) + e^{j\frac{\pi}{3}} I_{\frac{2}{3}}(|\varrho_a^0|)}{\sin \frac{\pi}{3}}, \\
 \alpha_1 &= \frac{I_{-\frac{1}{3}}(|\varrho_a^0|) + e^{-j\frac{\pi}{3}} I_{\frac{1}{3}}(|\varrho_a^0|)}{I_{-\frac{2}{3}}(|\varrho_a^0|) + e^{j\frac{\pi}{3}} I_{\frac{2}{3}}(|\varrho_a^0|)}, \\
 \bar{\beta}_a &= \text{Phase } (\alpha_1).
 \end{aligned} \right\} \quad (129 \text{ a})$$

and

$\epsilon_a$  is much larger in this case when  $|\varrho_a| \gg 1$ .

As

$$\left| \frac{2}{\pi \varrho_a} \frac{1}{\{H_{\frac{2}{3}}^{(1)}(|\varrho_a|)\}^2} \right| \approx e^{-2|\varrho_a|},$$

when  $|\varrho_a| \gg 1$ , this increase in  $\epsilon_a$  is not important.

As a primary and very useful approximation we therefore have  
*Relation II*

$$n_s = j \frac{-\frac{1}{2} \ln \eta_1^1 \eta_{23}^1}{\left\{ \frac{2(kc - n_s^0)}{kc} \right\}^{\frac{1}{2}} \frac{2}{\pi \varrho_c^0} \frac{1}{\{H_{\frac{2}{3}}^{(1)}(\varrho_c^0)\}^2} - \left\{ \frac{2(n_s^0 - ka)}{ka} \right\}^{\frac{1}{2}} \frac{2}{\pi \varrho_a^0} \frac{1}{\{H_{\frac{2}{3}}^{(1)}(\varrho_a^0)\}^2}} \quad (n_s^0 \leq ka) \quad (128 \text{ b})$$

and *Relation III*

$$n_s = j \frac{-\frac{1}{2} \ln \eta_1^1 \eta_{23}^1}{\left\{ \frac{2(kc - n_s^0)}{kc} \right\}^{\frac{1}{2}} \frac{2}{\pi \varrho_c^0} \frac{1}{\{H_{\frac{2}{3}}^{(1)}(\varrho_c^0)\}^2} + \left\{ \frac{2(n_s^0 - ka)}{ka} \right\}^{\frac{1}{2}} \frac{2}{\pi |\varrho_a^0|} \frac{1}{\{H_{\frac{2}{3}}^{(1)}(|\varrho_a^0|)\}^2}} \quad (n_s^0 \geq ka) \quad (129 \text{ b})$$

$$\frac{2}{\pi Q} \frac{1}{(H_{2/3}^{(n)}(\rho)) ^2}$$

$$-\frac{2}{\pi \cdot |\rho|} \frac{1}{(H_{2/3}^{(n)}(|\rho|)) ^2}$$

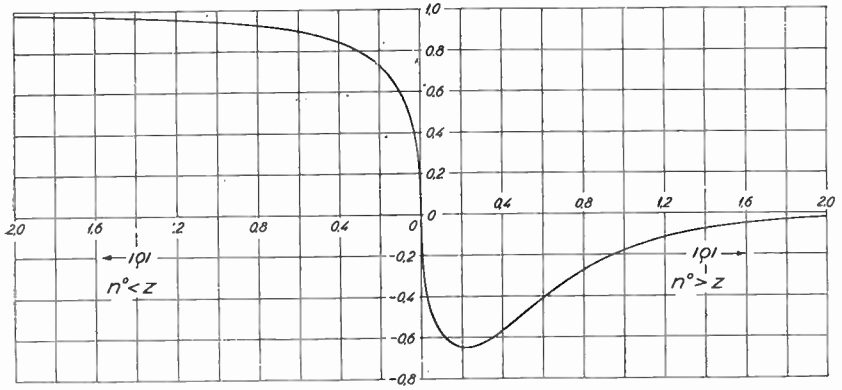


Fig. 15.

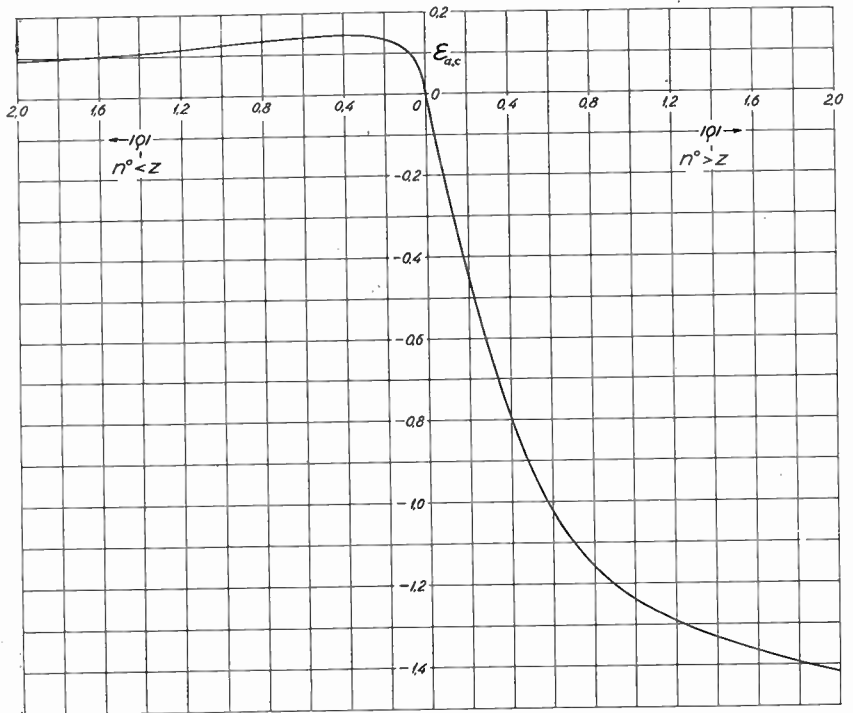


Fig. 16.

In order to make *Relations* I and II useful even for slide-rule computations we have in fig. 15 plotted

$$\frac{2}{\pi \varrho} \cdot \frac{1}{\{|H_{\frac{2}{3}}^{(1)}(\varrho)|\}^2} \text{ and } -\frac{2}{\pi |\varrho|} \cdot \frac{1}{\{|H_{\frac{2}{3}}^{(1)}(|\varrho|)\}^2}$$

through the necessary range of  $|\varrho|$ -values.

It is also convenient to be able to estimate quickly the magnitude of the corrections introduced by  $\varepsilon_c$  and  $\varepsilon_a$ . To that end we have further in fig. 16 plotted  $\varepsilon$  as a function of  $\varrho$  for the important range of values.

It is further easily shown (compare fig. 15) that *Relation* II yields the same results as *Relation* I in the form (125 a) when  $|\varrho_a| \gg 1$ .

Our present results have all been based on the NICHOLSON-WATSON formulae. For the higher order poles these formulae become identical with the DEBYE-WATSON representations, as has already been mentioned. The highest order poles (which are the least important ones) will, however, be situated near the imaginary axis in region c) where formally a different DEBYE-WATSON representation holds. Since  $S_v^{(2)}(\bar{z}) \ll S_v^{(1)}(\bar{z})$  in this region, the result is in reality correct.

### The Numerical Evaluation of the Poles.

In the deduction of *Relations* I and II we have tacitly assumed the losses to be so small that

$$\left\{ \ln \eta_1^1 \eta_{23}^1 \right\}_{n_s^0} \approx \left\{ \ln \eta_1^1 \eta_{23}^1 \right\}_{n_s}$$

When this is not the case the corrections may be worked out by successive approximations. To estimate the corrections we evaluate

$$\frac{d}{dn} (\ln \eta_1^1 \eta_{23}^1).$$

We find

$$\frac{d}{dn} (\ln \eta_1^1 \eta_3^1) = - \frac{\frac{k}{k_1}}{\left(1 - \frac{k}{k_1} \alpha^*\right) \left(1 + \frac{k}{k_1} \alpha\right)} \left\{ \mu_1(\varrho_a^0) + \frac{k}{k_1} \left(\frac{k a}{3}\right)^{\frac{1}{3}} \mu_2(\varrho_a^0) \right\} -$$

$$- \frac{\frac{k}{k_3}}{\left(1 - \frac{k}{k_3} \beta\right) \left(1 + \frac{k}{k_3} \beta^*\right)} \left\{ \mu_1(\varrho_c^0) - \frac{k}{k_3} \left(\frac{k c}{3}\right)^{\frac{1}{3}} \mu_2(\varrho_c^0) \right\}, \quad (130)$$

where

$$\mu_1(\varrho) = \left[ \frac{H_{\frac{1}{3}}^{(1)}(\varrho)}{H_{\frac{2}{3}}^{(1)}(\varrho)} \right]^2 e^{j \frac{\pi}{6}} + \left[ \frac{H_{\frac{1}{3}}^{(2)}(\varrho)}{H_{\frac{2}{3}}^{(2)}(\varrho)} \right]^2 e^{-j \frac{\pi}{6}}, \quad (130 a)$$

and

$$\mu_2(\varrho) = \varrho^{-\frac{1}{3}} \left[ \frac{H_{\frac{1}{3}}^{(1)}(\varrho)}{H_{\frac{2}{3}}^{(1)}(\varrho)} e^{j \frac{\pi}{3}} - \frac{H_{\frac{1}{3}}^{(2)}(\varrho)}{H_{\frac{2}{3}}^{(2)}(\varrho)} e^{-j \frac{\pi}{3}} \right] \left[ 1 - \frac{H_{\frac{1}{3}}^{(1)}(\varrho) H_{\frac{1}{3}}^{(2)}(\varrho)}{H_{\frac{2}{3}}^{(1)}(\varrho) H_{\frac{2}{3}}^{(2)}(\varrho)} \right]. \quad (130 b)$$

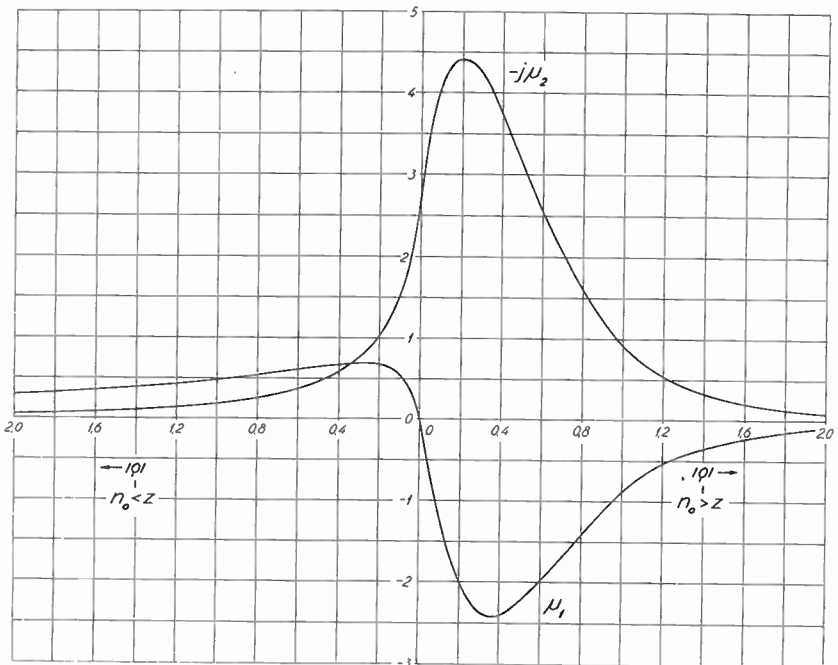


Fig. 17.

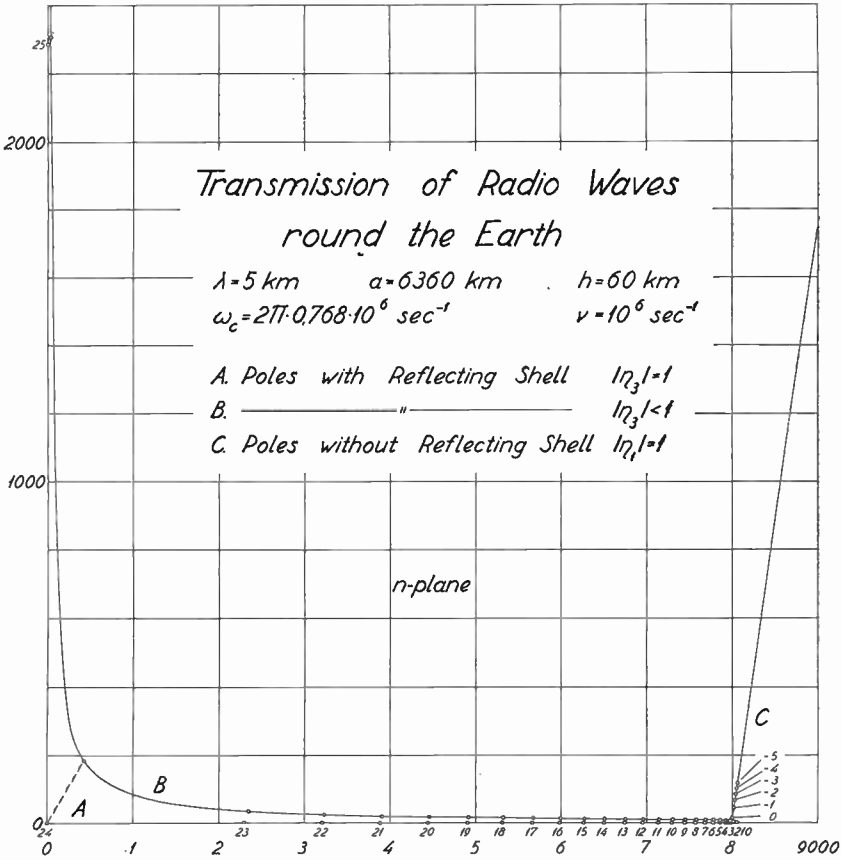


Fig. 18.  
( $\eta_3$  means  $\eta_{23}^1$ )

Since for long-waves  $\frac{k}{k_1} \approx \left| \frac{k}{k_1} \right| e^{-j\frac{\pi}{4}}$  and  $\frac{k}{k_3} \approx \left| \frac{k}{k_3} \right| e^{-j\frac{\pi}{4}}$ , both  $\mu_1$  and  $\mu_2$  will tend to change  $\text{Im}(\Delta n_s)$ . For the sake of convenience for numerical computations we have in fig. 17 shown  $\mu_1$  and  $\mu_2$  as functions of  $\rho$ .

It is obvious that the corrections become considerable when the losses are no longer small. Writing therefore our original Relations II and III as

$$\Delta n_s = j \frac{1}{A_{II III}} \left\{ \ln \eta_1^1 \eta_3^1 \right\}, \quad (n = n_s), \quad (131)$$

*Comparison of the Position  
of the more Important Poles*

$\lambda = 5 \text{ km}$      $a = 6360 \text{ km}$      $h = 60 \text{ km}$   
 $\omega_c = 2\pi \cdot 0.768 \cdot 10^6 \text{ sec}^{-1}$      $\nu = 10^6 \text{ sec}^{-1}$

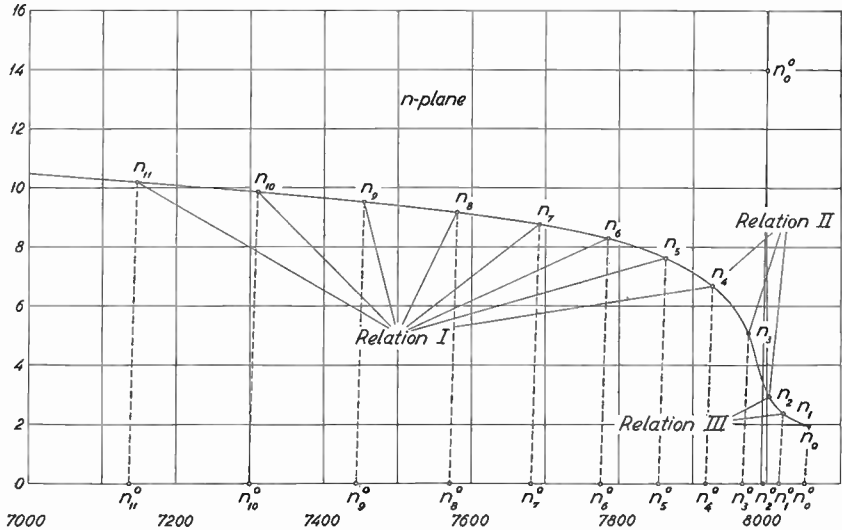


Fig. 19.  
(Vertical polarization)

we therefore get the parallell relation

$$\Delta n_s = j \frac{-\frac{1}{2} \{ \ln \eta_1^1 \eta_3^1 \}}{B_{II \text{ III}}}, \quad (n = n_s^0), \tag{132}$$

where

$$B_{II \text{ III}} = A_{II \text{ III}} + j \frac{1}{2} \left[ \frac{d}{dn} \{ \ln \eta_1 \eta_{23} \} \right]_{n_s^0}. \tag{132 a}$$

The numerical evaluation of the lower order poles is quite conveniently made if curves of  $B_{II \text{ III}}$  are first plotted throughout the necessary range. Fig. 18 shows a plot of the poles for transmission at a wave-length of 5 km between water and a  $D$ -layer with height 60 km and reflection characteristics as shown in fig. 13. In this case the dominating losses are ionospheric which makes the computation fairly simple. The corresponding poles for transmission round

a reflector-free, perfectly reflecting sphere are shown for comparison.

They are all situated on the curve Phase  $\int_n^{ka} \left\{ 1 - \frac{n^2}{x^2} \right\}^{\frac{1}{2}} dx = -\pi$ .

Fig. 19 finally shows the lower order poles near  $ka$  and  $kc$ . Poles of order 0, 1, 2 have been computed by means of *Relation III* in the form (132), poles of order 3, 4 have been computed by means of *Relation II*, and poles 4, 5, 6, . . . finally by means of *Relation I*. *Relations II* and *I* yield the same result for  $s = 4$ . The order of magnitude of the correction due to  $\mu_1$  and  $\mu_2$  is a few per cent for the lowest order poles.

It should be pointed out in this connexion that the character of the curve on which the poles are situated becomes different round  $ka$  if the ground losses dominate. This is immediately clear from an inspection of fig. 13.

### The Residue Series.

The next and final step when the poles have been determined is to evaluate the residue series (107). Developing  $\{\cos n\pi\}^{-1}$  as

$$\frac{1}{\cos n\pi} = 2 e^{j\pi n} \sum_{l=0}^{\infty} e^{j\pi l(2n+1)}, \tag{133}$$

which is valid over the integration path, we get from (107) in the familiar way

$$U(a, \theta) = \frac{4\pi j}{k^2 ab} \sum_{l=0}^{\infty} e^{j\pi l} \sum_{s=1}^{\infty} n_s e^{j\pi n_s(2l+1)} \frac{e_{\nu_s}}{\Phi_1(n_s) \Phi_3(n_s)} \cdot P_{\nu_s} \{ \cos(\pi - \theta) \}, \tag{134}$$

where

$$\Phi_3(n_s) = \left\{ \frac{\delta}{\delta n} \Phi_2(n) \right\}_{n_s}.$$

One finds for vertical polarization for example that

$$\begin{aligned} \Phi_3(n_s) = 2j & \left[ \left\{ \frac{2(kc - n_s)}{kc} \right\}^{\frac{1}{2}} \frac{2}{\pi \varrho_c} \cdot \frac{1}{H_{\frac{2}{3}}^{(1)}(\varrho_c) H_{\frac{2}{3}}^{(2)}(\varrho_c)} - \left\{ \frac{2(ka - n_s)}{ka} \right\}^{\frac{1}{2}} \frac{2}{\pi \varrho_a} \cdot \frac{1}{H_{\frac{2}{3}}^{(1)}(\varrho_a) H_{\frac{2}{3}}^{(2)}(\varrho_a)} \right. \\ & - j \frac{1}{2} \frac{\frac{k}{k_1}}{\left(1 - \frac{k}{k_1} \alpha^*\right) \left(1 + \frac{k}{k_3} \alpha\right)} \left\{ \mu_1(\varrho_a) + \frac{k}{k_1} \left(\frac{k\alpha}{3}\right)^{\frac{1}{3}} \mu_2(\varrho_a) \right\} - j \frac{1}{2} \frac{\frac{k}{k_3}}{\left(1 - \frac{k}{k_3} \beta\right) \left(1 + \frac{k}{k_3} \beta^*\right)} \\ & \left. \cdot \left\{ \mu_1(\varrho_c) - \frac{k}{k_3} \left(\frac{kc}{3}\right)^{\frac{1}{3}} \mu_2(\varrho_c) \right\} \right]. \quad (135) \end{aligned}$$

It should be remarked here that it is generally sufficiently accurate to put

$$\Phi_3(n_s) \approx \Phi_3(n_s^0)$$

for normal losses. An approximation of this kind naturally is not permissible as regards the evaluation of  $\Delta n_s$ . When the losses are moderate and the above approximation therefore can be used the evaluation of (135) is at least comparatively simple.

For larger  $s$ -values, when Relation I can be used, one finds for moderate losses that

$$\Phi_3(n_s) = 2j \frac{n_s}{\left\{ \frac{k(a+c)}{2} \right\}^2} \cdot \frac{kh}{\left\{ 1 - \frac{n_s^2}{\left( \frac{k(a+c)}{2} \right)^2} \right\}^{\frac{1}{2}}} \approx 2j \frac{1}{\frac{k(a+c)}{2}} \cdot \frac{kh}{s\pi} \left\{ \left( \frac{kh}{s\pi} \right)^2 - 1 \right\}^{\frac{1}{2}}. \quad (13)$$

This can also be obtained from (135) when  $\varrho_a^0 \gg 1$  and  $\mu_1$  and  $\mu_2$  can be put equal to zero.

When  $\theta$  is not too close to 0 or  $\pi$ , and since  $n$  is of the order of magnitude of  $ka$  for the important terms we make use of the asymptotic expansion of  $P_n(\cos \theta)$ , (85). Remembering that the time factor is  $e^{-j\omega t}$  the sum of the waves travelling clock-wise round the earth becomes

$$U(a, \theta) \sim \left( \frac{8\pi}{\sin \theta} \right)^{\frac{1}{2}} \frac{e^{j\frac{3\pi}{4}}}{k^2 ab} \sum_{l=0}^{\infty} e^{j\pi l} \sum_{s=0}^M n_s^{\frac{1}{2}} e^{jn_s(\theta + l2\pi)} \cdot \frac{e_{\nu_s}}{\Phi_1(n_s) \Phi_3(n_s)}$$

In the radio case we neglect waves which have made complete revolutions round the earth and therefore finally have,

$$e^{-j\omega t} U(a, \theta) \sim \left( \frac{8\pi}{\sin \theta} \right)^{\frac{1}{2}} \frac{e^{j\frac{3\pi}{4}}}{k^2 ab} \sum_{s=1}^M n_s^{\frac{1}{2}} \frac{e_{\nu_s}}{\Phi_1(n_s) \Phi_3(n_s)} e^{j(n_s \theta - \omega t)}, \tag{137}$$

which is a familiar form.  $M$  is taken sufficiently large to include all important poles.

The attenuation is  $\text{Im}(\Delta n_s) \cdot \theta$  and the tangential phase-velocity  $\frac{ka}{\text{Re}(n_s)} \cdot c_0$ . The important terms therefore have a surface phase-velocity practically equal to  $c_0$ .

For small losses we have for the higher order poles and vertical polarization according to (126 a) an attenuation coefficient

$$\beta_s = \frac{\text{Im}(\Delta n_s)}{a} \approx \frac{1}{\sqrt{2} h \sin \varphi_s} \left\{ \left| \frac{k}{k_1} \right| + \left| \frac{k}{k_3} \right| \right\}, \tag{138 a}$$

or for long waves

$$\beta \approx \frac{1}{h} \left\{ \left( \frac{1}{2\sigma_1} \right)^{\frac{1}{2}} + \left( \frac{\nu}{2\omega_c^2} \right)^{\frac{1}{2}} \right\} \omega^{\frac{1}{2}}. \tag{138 b}$$

This is similar to the well-known attenuation coefficient from the AUSTIN-COHEN formula in its original form. This formula had  $\beta \approx 2,75 \cdot 10^{-6} \cdot f^{\frac{1}{2}} \text{ km}^{-1}$  for transmission over sea-water. For a collision frequency of  $0,25 \cdot 10^6 \text{ sec}^{-1}$ ,  $f_c$  must be about 0,85 Mc/s for a layer height of 60 km in order to be in rough accord with the AUSTIN-COHEN value.

For horizontal polarization we similarly to (138 a) obtain

$$\beta_s \approx \frac{\cos^2 \varphi_s}{\sqrt{2} h \sin \varphi_s} \left\{ \left| \frac{k}{k_1} \right| + \left| \frac{k}{k_3} \right| \right\}, \tag{138 c}$$

i. e., a considerably smaller attenuation coefficient than in the case of vertical polarization.

For the inhomogeneous layer,  $\delta_{14}$  in the phase relation gets a different value with a correspondingly different  $\Delta n_s$ . We will return to this question later after we have made use of the parabolic cylinder functions to determine the actual value of the reflection coefficient.

For short waves the number of necessary terms of the residue series becomes very large and the evaluation of the series becomes completely unpractical. Therefore it becomes necessary and practical to treat separately each wave contained in (92 a). It is convenient to make use of the stationary phase treatment of the wave functions.

### The Treatment of the Separate Wave Groups.

We arbitrarily pick out a wave group which has experienced  $p + 1$  reflections at the surface of the earth and  $p + 1$  reflections including the last one, in the reflecting shell. From (86) and the relation following, this wave group becomes

$$U_p^1 = \frac{1}{2 k^2 r^2 b} \sum_{n=0}^{\infty} (2n + 1) \zeta_n^{(1)}(kb) \zeta_n^{(2)}(ka) \left\{ R_{21}^1 \frac{\zeta_n^{(1)}(kc)}{\zeta_n^{(1)}(ka)} R_3^1 \frac{\zeta_n^{(2)}(ka)}{\zeta_n^{(2)}(kc)} \right\}^{p+1} \cdot \frac{\zeta_n^{(2)}(kr)}{\zeta_n^{(2)}(ka)} \cdot P_n(\cos \Theta). \quad (139)$$

As a consequence of the relation

$$\zeta_{-n-\frac{1}{2}}^{(1)}(z) = e^{\pm j n \pi} \zeta_{n-\frac{1}{2}}^{(2)}(z),$$

(compare p. 53) the sum (139) transforms to the integral

$$U_p^1 = \int_{-\infty + j\kappa}^{+\infty + j\kappa} h \left( n - \frac{1}{2} \right) \zeta_\nu^{(1)}(kb) \zeta_\nu^{(2)}(kr) \left\{ - \frac{\zeta_\nu^{(2)'}(ka) \zeta_\nu^{(1)}(kc)}{\zeta_\nu^{(1)'}(ka) \zeta_\nu^{(2)}(kc)} e^{j \operatorname{Re}(\partial_3)} \right\}^{p+1} \cdot \frac{1}{2} \cdot P_\nu \{ \cos(\pi - \Theta) \} \frac{n dn}{\cos n \pi}, \quad (139 a)$$

where

$$h \left( n - \frac{1}{2} \right) = \frac{1}{j k^2 r b} (\eta_{21}^1)^{p+1} e^{-(p+1) \operatorname{Im}(\partial_3)},$$

and  $\kappa$  is a small positive quantity.

It is convenient to make use of KELVIN's principle of the stationary phase in order to evaluate (139 a) when the angle of incidence at the

earth is less than  $\frac{\pi}{2}$ , i. e. when  $n < ka$ . When this is the case, and when

$\omega_{c_m} > \omega \sin \Psi_{c_0}$ ,  $h \left( n - \frac{1}{2} \right)$  is varying so slowly through the stationary phase region that one is well justified to treat it as a constant, which is a considerable simplification.

Remembering that

$$\frac{\zeta_v^{(2)'}(ka)}{\zeta_v^{(1)'}(ka)} \sim - \frac{H_{\frac{2}{3}}^{(2)}(\varrho_a)}{H_{\frac{2}{3}}^{(1)}(\varrho_a)} e^{-j \left( \frac{7}{6} \pi - 2 \varrho_a \right)} \cdot \frac{S_v^{(2)}(ka)}{S_v^{(1)}(ka)} = -j e^{-j 2 (\gamma_a + \check{\beta}_a)}, \quad (140)$$

with

$$2 \check{\beta}_a = \frac{7}{6} \pi - 2 \varrho_a - j \ln \frac{H_{\frac{2}{3}}^{(1)}(\varrho_a)}{H_{\frac{2}{3}}^{(2)}(\varrho_a)}, \quad (140 \text{ a})$$

and further dropping the counter clock-wise waves and neglecting waves with more than one revolution, we obtain

$$\frac{1}{p} \sim \int_{-\infty}^{(0-)} \frac{h \left( n - \frac{1}{2} \right)}{(2 \pi \sin \Theta)^{\frac{1}{2}}} n^{\frac{1}{2}} \left\{ \mathcal{P}_{x=b, r} \left( \frac{\pi k x}{6} \right)^{\frac{1}{2}} \left( \frac{n}{3} \right)^{\frac{1}{3}} \cdot \left| \varrho_x^{\frac{1}{3}} H_{\frac{1}{3}}^{(1)}(\varrho_x) \right| \right\} \cdot e^{j \left( \frac{\pi}{4} + F \right)} d n, \quad (141)$$

where

$$= n \Theta + \gamma_b - 2 (p + 1) \gamma_a + 2 (p + 1) \{ \gamma_c + \text{Re} (\delta_3^1) \} - \gamma_r - 2 (p + 1) \check{\beta}_a + \delta_b - \delta_r, \quad (141 \text{ a})$$

and 
$$\delta_b = \frac{5}{12} \pi - \varrho_b + \text{Phase} \left\{ \varrho_b^{\frac{1}{3}} H_{\frac{1}{3}}^{(1)}(\varrho_b) \right\}. \quad (141 \text{ b})$$

Introducing

$$k b \cdot \cos \Psi_b = k a \cdot \cos \Psi_a = k c \cdot \cos \Psi_c = k r \cdot \cos \Psi_r = n, \quad (142)$$

making use of a relation which is an alternative form of (109)

$$\gamma_a = n \{ \tan \Psi_a - \Psi_a \}, \quad (143)$$

further of (33), and of (38 a) one finds since  $R_3^1 \approx -R_3$  that the stationary phase point  $n = n_0$  (or the corresponding angles  $\Psi_{b_0}$ ,  $\Psi_{a_0}$ , etc.), which is obtained from  $\frac{\delta F}{\delta n} = 0$ , for vertical or horizontal polarization must satisfy the approximate relation

$$\theta \approx \left[ \frac{\Psi_b}{\frac{\pi \varrho_b}{2} \frac{H_1^{(1)}(\varrho_b)}{3} \frac{H_1^{(2)}(\varrho_b)}{3}} - 2(p+1) \frac{\Psi_a}{\frac{\pi \varrho_a}{2} \frac{H_2^{(1)}(\varrho_a)}{3} \frac{H_2^{(2)}(\varrho_a)}{3}} + 2(p+1) \left\{ \Psi_c + \frac{\Delta h_v}{c} \cdot \cot \Psi_c \right\} - \frac{\Psi_r}{\frac{\pi \varrho_r}{2} \frac{H_1^{(1)}(\varrho_r)}{3} \frac{H_1^{(2)}(\varrho_r)}{3}} \right]_{n = n_0}, \quad (144)$$

where  $\Delta h_v$  is the virtual ionospheric height ( $\Delta h_v \approx \frac{x_1}{2} \tan \Psi_c$ , with  $x_1$  as defined on p. 23 and  $\varphi_c = \frac{\pi}{2} - \Psi_c$ ). When  $\varrho_a > 1$ , i. e., when

$$\Psi_a > \left( \frac{3 \lambda}{2 \pi a} \right)^{\frac{1}{3}},$$

or for a wave-length of about 600 m when  $\Psi_a > 2^\circ$ , then

$$\theta = \Psi_{b_0} - 2(p+1) \Psi_{a_0} + (p+1) \left\{ 2 \Psi_{c_0} + \frac{x_1}{c} \right\} - \Psi_{r_0}. \quad (145)$$

With (142), which is nothing else than the law of refraction, (145) is readily interpreted as determining the geometrical properties of a ray between the sender and the receiver. This is demonstrated by fig. 20.

The smaller  $\lambda$  is the smaller will be the lower limit of  $\Psi_a$  and the approach to geometrical optics becomes better.

When (145) holds we have

$$U_p^1 \sim \frac{e^{j \frac{\pi}{4} h \left( n_0 - \frac{1}{2} \right)}}{(2 \pi \sin \theta)^{\frac{1}{2}}} \left( \frac{ka \cos \Psi_{a_0}}{\sin \Psi_{b_0} \sin \Psi_{r_0}} \right)^{\frac{1}{2}} e^{j S_0} \cdot \int_{-\infty}^{(0-)} \exp. j \left\{ \underbrace{\frac{\delta \theta (\Delta n)^2}{\delta n 2!} + \frac{\delta^2 \theta (\Delta n)^3}{\delta n^2 3!} \dots}_{\Delta F} \right\} \cdot d(\Delta n), \quad (146)$$

$p=2$

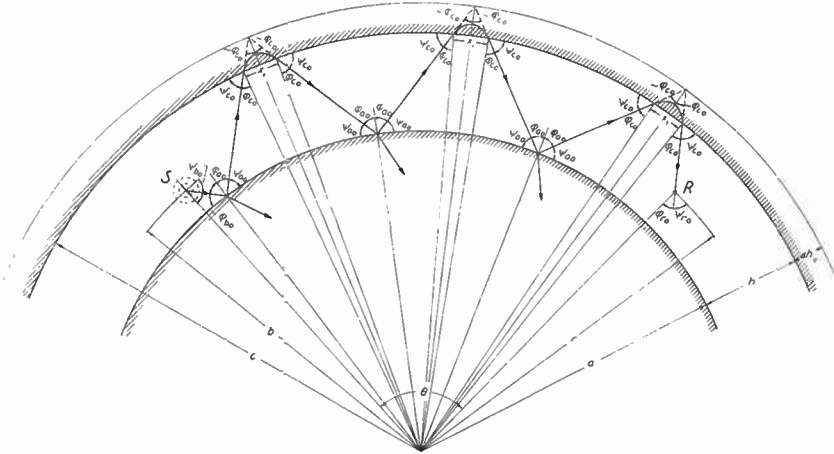


Fig. 20.

where

$$\Delta n = n_0 - n,$$

$$= kb \cdot \sin \Psi_{b_0} - 2(p + 1) ka \cdot \sin \Psi_{a_0} + (p + 1) \{ 2kc \cdot \sin \Psi_{c_0} + \text{Re}(\delta_3^1) \} - kr \cdot \sin \Psi_{r_0}, \quad (147)$$

$$\frac{\delta \Theta}{\delta n} = -\frac{1}{kb \cdot \sin \Psi_{b_0}} + \frac{2(p + 1)}{ka \cdot \sin \Psi_{a_0}} - 2(p + 1) \left\{ \frac{1}{kc \cdot \sin \Psi_{c_0}} - \frac{h_v}{kc^2 \cdot \sin^3 \Psi_{c_0}} \left( 1 - \cos^2 \Psi_{c_0} \frac{\omega}{h_v} \frac{dh_v}{d\omega} \right) \right\} + \frac{1}{kr \cdot \sin \Psi_{r_0}}, \quad (147 a)$$

and

$$\frac{\delta^2 \Theta}{\delta n^2} = n_0 \left[ \frac{-1}{(kb)^3 \sin^3 \Psi_{b_0}} + \frac{2(p + 1)}{(ka)^3 \sin^3 \Psi_{a_0}} - 2(p + 1) \left\{ \frac{1}{(kc)^3 \sin^3 \Psi_{c_0}} - \frac{3 h_v}{k^3 c^4 \sin^5 \Psi_{c_0}} \cdot \left( 1 - \frac{\omega}{h_v} \frac{dh_v}{d\omega} \left( 1 + \frac{\cos^2 \Psi_{c_0}}{3} - \frac{\cos^2 \Psi_{c_0}}{3} \cdot \frac{\omega}{dh_v} \cdot \frac{d^2 h_v}{d\omega^2} \right) \right) \right\} + \frac{1}{(kr)^3 \sin^3 \Psi_{r_0}} \right]. \quad (147 b)$$

Regarding the path of integration we require  $\text{Im}(\Delta F) = 0$  at least in the neighbourhood of  $n_0$ . Examples of such paths will be shown in connexion with the discussion of the bridging approximation of the parabolic cylinder functions.

Neglecting higher than third order terms in the phase expansion we obtain the third order approximation

$$U_p^1 \sim \frac{(\eta_{21}^1)^{p+1} e^{(p+1)\text{Im}(\delta_3^1)}}{j k^2 r b} \cdot \left\{ \frac{\pi}{6} \frac{ka \cos \Psi_{a_0}}{\sin \Psi_{b_0} \sin \Psi_{r_0} \sin \Theta} \right\}^{\frac{1}{2}} \cdot \frac{\delta \Theta}{\delta n} \cdot \frac{\delta^2 \Theta}{\delta n^2} \cdot \exp. j \left\{ \frac{5}{12} \pi - \frac{1}{3} \frac{\left(\frac{\delta \Theta}{\delta n}\right)^3}{\left(\frac{\delta^2 \Theta}{\delta n^2}\right)^2} \right\} \cdot H_{\frac{1}{3}}^{(1)} \left\{ \frac{1}{3} \frac{\left(\frac{\delta \Theta}{\delta n}\right)^3}{\left(\frac{\delta^2 \Theta}{\delta n^2}\right)^2} \right\} \cdot e^{j S_0}. \quad (148)$$

When

$$\frac{1}{3} \frac{\left(\frac{\delta \Theta}{\delta n}\right)^3}{\left(\frac{\delta^2 \Theta}{\delta n^2}\right)^2} = \Gamma \gg 1,$$

(148) becomes

$$U_p^1 \sim \frac{(R_{21}^1)^{p+1} (|R_3^1|)^{p+1}}{j k (r b)^{\frac{1}{2}}} \cdot \left\{ \frac{\tan \varphi_{b_0}}{\sin \Theta \cdot \frac{\delta \Theta}{\delta \varphi_r}} \right\}^{\frac{1}{2}} \cdot e^{j S_0}, \quad (148 \text{ a})$$

which is the result of the second order approximation. Thus (148 a) yields the amplitude and phase, i. e. the iconal  $S_0$  of the geometrical optical ray. This amplitude is as a matter of fact also easily obtained from elementary geometrical considerations. The ray formula breaks down, however, in the neighbourhood of the caustic where  $\frac{\delta \Theta}{\delta n} \approx 0$  and (148) has to be used.

On the other side of the caustic, where  $H_{\frac{1}{3}}^{(1)}(\Gamma)$  is oscillatory, we find

$$U_p^1 \sim \frac{(R_{21}^1)^{p+1} (|R_3^1|)^{p+1}}{j k (r b)^{\frac{1}{2}} r} \cdot \left\{ \frac{-\tan \varphi_{b_0}}{\sin \Theta \frac{\delta \Theta}{\delta \varphi_r}} \right\}^{\frac{1}{2}} \cdot e^{j S_0} \cdot \left\{ 1 - e^{2j \left(\Gamma + \frac{\pi}{4}\right)} \right\},$$

when  $\Gamma \ll -1$ . (148 b)

When  $\frac{\delta \theta}{\delta \varphi_r} < 0$ , the receiver is generally reached by two rays. When further  $\Gamma \ll -1$ , the phase difference between these two rays becomes  $-2 \left( \Gamma - \frac{\pi}{4} \right)$ . By purely geometrical considerations one finds that on this side of the caustic the geometrical phase difference actually equals  $-2 \Gamma$ . This was shown already by VAN DER POL and BREMMER [5]. The geometrical treatment, however, does not yield the constant phase difference  $\frac{\pi}{2}$ .

\* \* \*

It is of considerable interest to investigate if actual focusing of the ray is possible or not. From (147 a) we have approximately

$$\frac{\delta \theta}{\delta n} \approx \frac{2(p+1)}{(kc)^2 \sin^3 \Psi_{c_0}} \left\{ h + h_v \left( 1 - \cos^2 \Psi_{c_0} \frac{\omega}{h_v} \frac{dh_v}{d\omega} \right) \right\}. \quad (149)$$

It is immediately clear that in the case of negligible dispersion focusing is never possible.

For a parabolic layer. of half-thickness  $\Delta h_m$ , we find

$$\frac{\delta \theta}{\delta n} \approx \frac{2(p+1) \Delta h_m}{(kc)^2 \sin^3 \Psi_{c_0}} \left\{ \frac{h}{\Delta h_m} + W(\underline{\alpha}, \underline{y}) \right\}, \quad (149 a)$$

where

$$W(\underline{\alpha}, \underline{y}) = \frac{\underline{\alpha} \underline{y}}{2} \left\{ y^2 \ln \left( \frac{1 + \underline{\alpha} \underline{y}}{1 - \underline{\alpha} \underline{y}} \right) - 2 \frac{\underline{\alpha} \underline{y}}{1 - (\underline{\alpha} \underline{y})^2} \right\},$$

with

$$\underline{\alpha} = \frac{\omega}{\omega_{c_m}}, \quad \text{and} \quad \underline{y} = \sin \Psi_{c_0}.$$

Fig. 21 shows a plot of  $W(\underline{\alpha}, \underline{y})$  for various values of  $\underline{\alpha}$ . It is seen that for  $\frac{h}{\Delta h_m} = 2,5$  (a typical day-time value for the  $F_2$ -layer in the equatorial regions) focusing never occurs when penetration is impossible at any angle, i. e. when  $\underline{\alpha} < 1$ . Focusing becomes

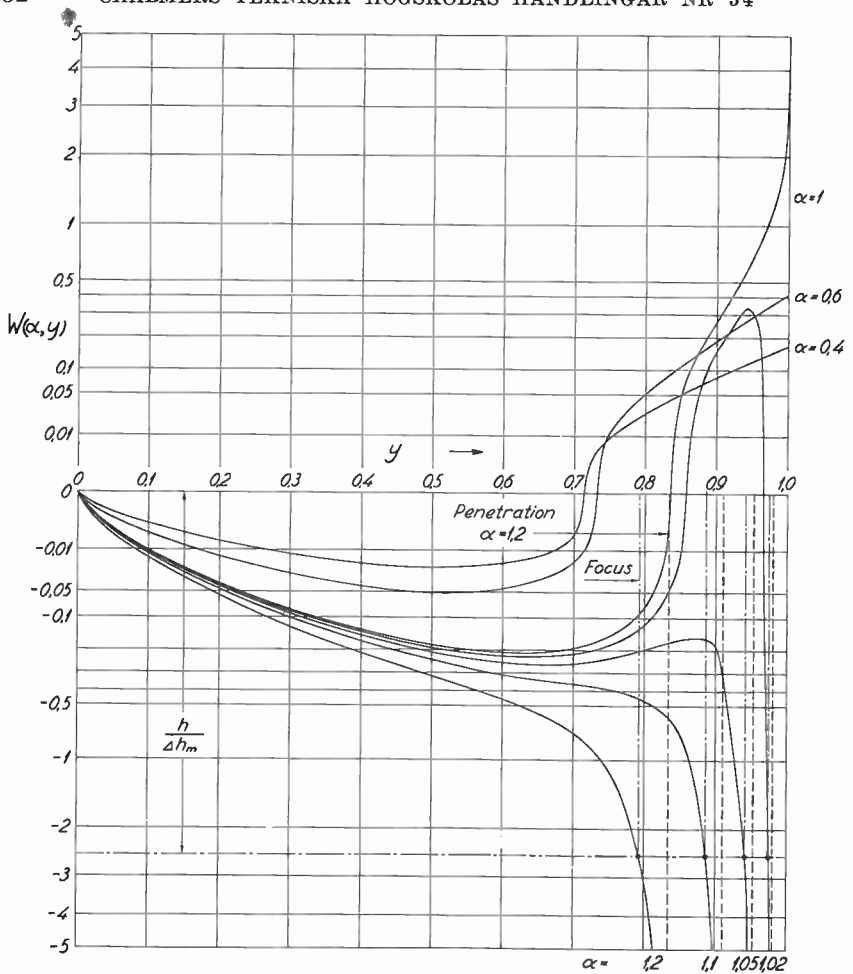


Fig. 21.

possible first when a considerable proportion of the high elevation rays escape into space. The focusing angle further does not differ much from the critical or penetration angle. The difference between them becomes very small in the case of the  $E$ -layer, for which

$$\frac{h}{\Delta h_m} \approx 20.$$

The silent zone will therefore be surrounded by a concentric caustic circle. It should not be forgotten, however, that the generally rapid increase of  $\text{Im}(\delta_3)$  near penetration makes the focusing effect practically unimportant.

\* \* \*

So far we have not said anything about the wave-length limit of the ray treatment. We have seen that the second order approximation yields the ray amplitude and ray phase of geometrical optics as expected (when  $\frac{\delta \theta}{\delta n} > 0$ ).

The wave-length limit therefore is determined by the requirement that  $F > 1$ , say  $F \geq \pi$ . Considering the practically important case that  $\underline{a} \underline{y} < 1$ , we have approximately from (147 b) and (149) that

$$s_{\max} = \frac{2k}{\lambda} \geq \frac{13,5}{p+1} \cdot \frac{\cos^2 \Psi_{a_0}}{\sin \Psi_{a_0}} \cdot (\Psi_{a_0} > 0). \quad (150)$$

Thus we have found an approximate expression for the minimum number of poles or proper values required in order to justify the ray treatment (compare p. 63). When therefore the long wave formulae (the residue series) become unpractical to handle the ray method automatically becomes permissible. It should be noted that this is true even though the ray treatment is not permissible within the inhomogeneous ionized shell itself. Its properties (which depend upon its inhomogeneous character) are contained in  $\delta_3$ , which has to be obtained from the circuit relation (72) which holds under all circumstances.

### The Field Strength from the Dipole Element.

Applying (99) to (148 a) one easily finds for vertical polarization for example when the ray treatment is permissible that

$$E_r \approx A_1 k^2 \cdot \cos^2 \Psi_{r_0} \cdot \left(\frac{r}{b} U^1\right); \quad E_\theta \approx A_1 k^2 \cdot \sin \Psi_{r_0} \cdot \cos \Psi_{r_0} \cdot \left(\frac{r}{b} U^1\right);$$

$$E_t = (E_r^2 + E_\theta^2)^{\frac{1}{2}} \approx A_1 k^2 \cdot \cos \Psi_{r_0} \cdot \left(\frac{r}{b} U^1\right); \quad H_\varphi \approx \frac{A_1}{z_0} k^2 \cdot \cos \Psi_{r_0} \cdot \left(\frac{r}{b} U^1\right), \quad (151)$$

indicating that POYNTING's vector is parallel to the ray direction in fig. 20.

So far we have only studied one of the four different wave groups which may reach the receiver after  $p + 1$  reflections in the shell. Collecting the wave groups we get instead of (139) the complete expression

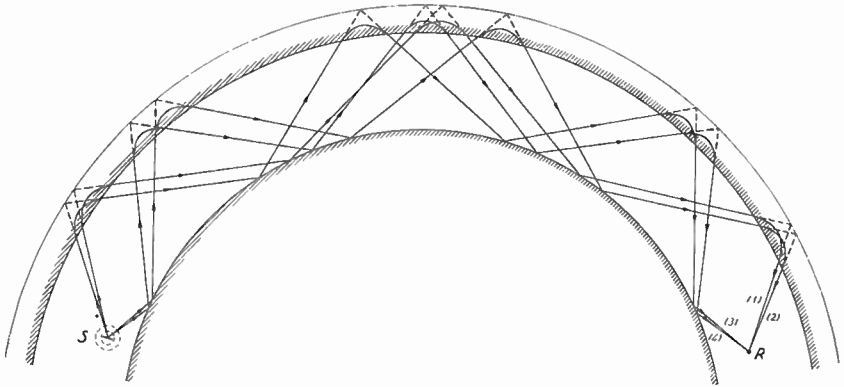
$p=2$ 

Fig. 22.

$$U_p^1 = \frac{1}{2 k^2 r b} \sum_{n=0}^{\infty} (2n+1) \zeta_n^{(2)}(kb) \zeta_n^{(1)}(kc) R_3^1 \frac{\zeta_n^{(2)}(ka)}{\zeta_n^{(2)}(kc)} \left\{ R_{21}^1 \frac{\zeta_n^{(1)}(kc)}{\zeta_n^{(1)}(ka)} R_3^1 \cdot \frac{\zeta_n^{(2)}(ka)}{\zeta_n^{(1)}(kc)} \right\}^p \frac{\zeta_n^{(2)}(kr)}{\zeta_n^{(2)}(ka)} \cdot \left\{ 1 + R_{21}^1 \frac{\zeta_n^{(1)}(kb) \zeta_n^{(2)}(ka)}{\zeta_n^{(2)}(kb) \zeta_n^{(1)}(ka)} \right\} \left\{ 1 + R_{21}^1 \frac{\zeta_n^{(1)}(kr) \zeta_n^{(2)}(ka)}{\zeta_n^{(2)}(kr) \zeta_n^{(1)}(ka)} \right\} P_n(\cos \theta). \quad (152)$$

Of the last two bracketed expressions the first one introduces the influence of the ground at the sending side and the other one quite similarly introduces the influence of the ground at the receiving side. As a matter of fact (152) is symmetrical in  $r$  and  $b$ , as is (139), proving the reciprocity, i. e. that receiver and sender may be exchanged without affecting the result.

Again making use of the principle of the stationary phase we obtain from (134) the four rays shown in fig. 22. Introducing the iconal  $S_1$  for the ray with  $p$  ground reflections,  $S_2 = S_1 + \Delta S_2$ , and  $S_3 = S_1 + \Delta S_3$  for the two rays with  $p+1$  ground reflections, and finally  $S_4 \approx S_1 + \Delta S_2 + \Delta S_3$  for the fourth ray, which experiences  $p+2$  ground reflections, and remembering that  $\frac{\delta \theta}{\delta \varphi_r}$  is to a close approximation the same for the four rays, we obtain

$$\left. \begin{matrix} \Delta E_r \\ \Delta E_\theta \end{matrix} \right\} \sim \frac{30k\Delta K}{j(rb)^{\frac{1}{2}}} \frac{r}{b} (R_{21}^1)^p (|R_3^1|)^{p+1} \left\{ \frac{\tan \varphi_{b_0}}{\sin \theta \frac{\delta \theta}{\delta \varphi_{r_0}}} \right\}^{\frac{1}{2}} e^{j S_1} \underbrace{\left\{ 1 + R_{22}^1 e^{j \Delta S_2} \right\}}_{\bar{\eta}_1} \cdot \cos \Psi_{b_0} \cdot \underbrace{\left\{ 1 \pm R_{22}^1 e^{j \Delta S_3} \right\}}_{\bar{\eta}_2^{(r)}} \frac{\cos \Psi_{r_0}}{\sin \Psi_{r_0}} \quad (153)$$

where  $\Delta K$  is the strength of the dipole element. It is of special interest to note that the directive radiation characteristic of the vertical dipole element above ground in (153) is  $\bar{\eta}_1 \cdot \cos \Psi_{b_0}$  or practically the same as in the plane case.

For a vertical wire of length  $2l$  (with arbitrary current distribution) we consequently find, if  $S_0$  is the iconal referred to the centre of the antenna, that

$$\left. \begin{matrix} \Delta E_r \\ \Delta E_\theta \end{matrix} \right\} \sim \frac{30k}{j(rb)^{\frac{1}{2}}} \frac{r}{b} (R_{21}^1)^p (|R_3^1|)^{p+1} \left\{ \frac{\text{tg } \varphi_{b_0}}{\sin \theta \frac{\delta \theta}{\delta \varphi_{r_0}}} \right\}^{\frac{1}{2}} \bar{\eta}_2^{(r)} e^{j S_0} \int_{-l}^{+l} e^{j(S_1 - S_0)} \bar{\eta}_1 \cdot \cos \Psi_{b_0} dK, \quad (153 a)$$

where

$$\int_{-l}^{+l} e^{j(S_1 - S_0)} \eta_1 \cos \Psi_{b_0} dK = f_l(\Psi_{b_0}) I_{\max}, \quad (153 b)$$

is the effective vertical radiation characteristic of the antenna with maximum current  $I_{\max}$ .

Since  $b^{\frac{3}{2}} / r^{\frac{1}{2}} \approx a$ , we finally obtain

$$\left. \begin{matrix} \Delta E_r \\ \Delta E_\theta \end{matrix} \right\} \sim \frac{30k}{a} (|R_{21}^1|)^p (|R_3^1|)^{p+1} \left\{ \frac{\tan \varphi_{b_0}}{\sin \theta \frac{\delta \theta}{\delta \varphi_{r_0}}} \right\}^{\frac{1}{2}} \left| \bar{\eta}_2^{(r)} \right| \cdot |f_l(\Psi_{b_0})| I_{\max} \dots \text{Volts/meter}, \quad (153 c)$$

with  $\lambda, (rb)^{\frac{1}{2}}, |f_l(\Psi_{b_0})|$  in meters and  $I_{\max}$  in amperes. Similar formulae are easily obtained for horizontal polarization.

In order to compare (153 c) with the result of the plane case we write

$$|E_r| \sim \frac{30k^2}{S_0} (|R_{21}^1|)^p (|R_3^1|)^{p+1} \left| \bar{\eta}_2^{(r)} \right| \cdot |f_l(\Psi_{b_0})| I_{\max} \cdot c_p \dots \text{Volts/meter} \quad (153 d)$$

with  $S_0/k$  in meters, and where  $c_p$  is a focusing or convergence factor,

$$c_p = \left\{ \frac{S_0^2}{k^2 r b} \frac{\tan \varphi_{b_0}}{\sin \theta \frac{\delta \Theta}{\delta \varphi_{r_0}}} \right\}^{\frac{1}{2}}. \quad (154)$$

If  $c_p \approx 1$  the result is approximately the same as that of the plane case.

Neglecting the dispersion (i. e.,  $\frac{d h_v}{d \omega}$ ) we find from (147 a) that

$$c_p \approx \left\{ \frac{S_0 \sin \varphi_{a_0}}{ka \sin \theta} \right\}^{\frac{1}{2}}.$$

Since  $\frac{h + h_v}{a} \ll 1$ , the above expression yields  $c_p \approx 1$  as expected in the case of negligible dispersion.

Finally it should be emphasized again that when focusing becomes appreciable, i. e.  $c_p \gg 1$ , the formulae (153) which are second order approximations break down and the more accurate third order approximation (148) has to be used.

## The Reflection Coefficient of the Parabolic Layer.

In order to consider the case of radio wave propagation round a homogeneous earth surrounded by a concentric parabolic layer we have to study the parabolic wave-functions more closely. If we omit the in this connexion unimportant frequency range near penetration we can make use of expansions (55) and (64) for the thick layer.

Unfortunately expansion (64) has properties very similar to the DEBYE-expansion for  $H_n^{(2)}(z)$  in the exceptional case  $z \approx n \gg 1$ . This seems to lie in the nature of the method of expansion used. It should be remarked at this point that it was therefore necessary to use the NICHOLSON-WATSON-approximation (110) (HANKEL-approximation) instead of the corresponding DEBYE-expansion (*Tangent*-approximation) in order to obtain the poles of the residue series in the exceptional region  $n \approx ka$ .

We will accordingly find it convenient to investigate the possibilities of finding a suitable bridging approximation between the more exact (55) and (64). We once more turn to the method of the station-

ary phase and the third order approximation leading to the AIRY-type integrals. The integral appearing in (42) can then be written

$$I_1 \approx (\bar{\tau}_A)^{-\frac{1}{2}} e^{\bar{\bar{W}}_A} \int_{c_1} \exp. \left[ j \left\{ \frac{d^2 \Theta}{d\tau^2} \cdot \frac{(\Delta \tau)^2}{2!} + \frac{d^3 \Theta}{d\tau^3} \cdot \frac{(\Delta \tau)^3}{3!} \right\} \right] \cdot d(\Delta \tau), \quad (155)$$

where

$$\frac{d^2 \Theta}{d\tau^2} = -2 \cdot \frac{\frac{u^2}{4} - \varrho - \frac{u}{2} \left\{ \frac{u^2}{4} - \varrho \right\}^{\frac{1}{2}}}{\bar{\tau}_A^2}, \quad (155 a)$$

$$\frac{d^3 \Theta}{d\tau^3} = -2 \cdot \frac{\varrho}{\bar{\tau}_A^3}, \quad (155 b)$$

$$-\bar{\tau}_A = \frac{u}{2} - \left\{ \frac{u^2}{4} - \varrho \right\}^{\frac{1}{2}},$$

and

$$-\bar{\bar{W}}_A = j \left[ \frac{u \bar{\tau}_A}{2} + \varrho \left\{ \ln(-\bar{\tau}_A) - \frac{1}{2} \right\} \right].$$

The slow variation of  $(\tau)^{-\frac{1}{2}}$  has been neglected in the bridging region.

The next problem concerns the path of integration. A glance at fig. 8 shows that we have to approach  $\bar{\tau}_A$  along the axis of reals from the positive side  $\{\text{Re}(\bar{\bar{W}}_A) = 0 \text{ in this contour}\}$  and then take the first  $\text{Re}(\bar{\bar{W}}_A) = 0$  contour to the left.

In the same manner the integral corresponding to  $D \left( u e^{-j\frac{\pi}{4}} \right)_{-j\rho - \frac{1}{2}}$  becomes

$$I_2 \approx -(\bar{\tau}_A)^{-\frac{1}{2}} e^{-\bar{\bar{W}}_A} \int_{c_2} \exp. \left[ j \left\{ -\frac{d^2 \Theta}{d\tau^2} \cdot \frac{(\Delta \tau)^2}{2!} + \frac{d^3 \Theta}{d\tau^3} \frac{(\Delta \tau)^3}{3!} \right\} \right] \cdot d(\Delta \tau). \quad (156)$$

The contours which have a familiar shape are shown slightly deformed in fig. 23. For these contours the result is well known and we have

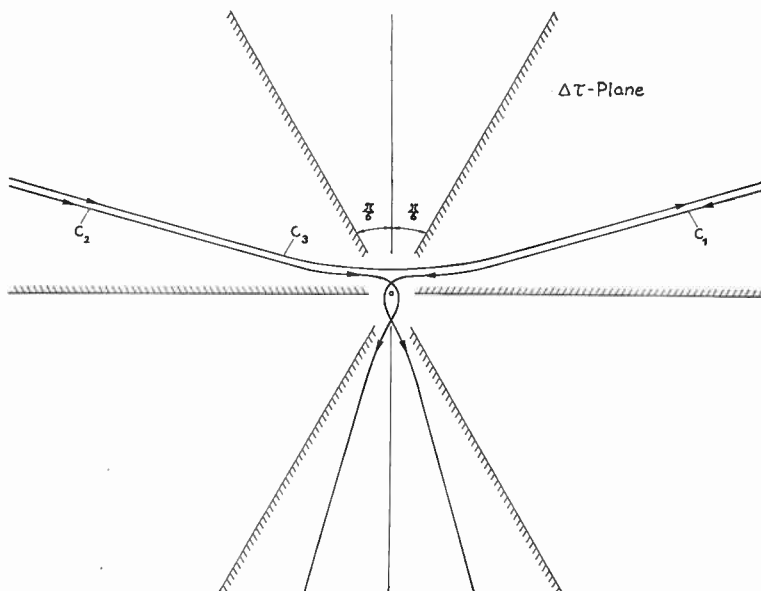


Fig. 23. Paths of integration for the third order bridging approximations.

$$\left. \begin{matrix} I_1 \\ I_2 \end{matrix} \right\} = -(\bar{\tau}_A)^{-\frac{1}{2}} \cdot \frac{\pi}{3^{\frac{1}{2}}} \cdot \frac{\frac{d^2 \Theta}{d\tau^2}}{\frac{d^3 \Theta}{d\tau^3}} \cdot \exp \left\{ \pm \bar{W}_A \pm j \left( \Gamma - \frac{\pi}{6} \right) \right\} \cdot H_{\frac{1}{3}}^{(2)}(\Gamma), \quad (157)$$

where

$$\Gamma = \frac{1}{3} \frac{\left( \frac{d^2 \Theta}{d\tau^2} \right)^3}{\left( \frac{d^3 \Theta}{d\tau^3} \right)^2}. \quad (157 \text{ a})$$

Integration along path  $c_3$  yields a wave of oscillatory amplitude. When  $\frac{\delta \Theta}{\delta n} < 0$  [in (148)] the path of integration is switched from  $c_2$  to  $c_3$ , i. e., one is on the oscillatory side of the caustic.

In accordance with (42) our bridging approximations thus become

$$D \left( u e^{\pm j \frac{\pi}{4}} \right) \sim \frac{\Gamma \left( \pm j \varrho + \frac{1}{2} \right)}{2 \cdot 3^{\frac{1}{2}}} \cdot (-\bar{\tau}_A)^{-\frac{1}{2}} \cdot \frac{d^2 \Theta}{d\tau^2} \cdot \frac{1}{d\tau^3} \cdot \exp. \left[ \frac{\pi}{4} \varrho \pm \left\{ \bar{W}_A + j \left( \Gamma - \frac{13\pi}{24} - \frac{u^2}{4} \right) \right\} \right] \cdot H_{\frac{1}{3}}^{(2)}(\Gamma). \quad (158)$$

Using the HANKEL-expansion for  $H_{\frac{1}{3}}^{(2)}$  when  $\Gamma \gg 1$ , we find that (147) becomes

$$D \left( u e^{j \frac{\pi}{4}} \right) \sim \frac{\Gamma \left( j \varrho + \frac{1}{2} \right)}{(2\pi)^{\frac{1}{2}}} (\bar{\eta} - 1)^{-\frac{1}{2}} (-\bar{\tau}_A)^{-\frac{1}{2}} \cdot \exp. \left[ \frac{\pi}{4} \varrho + \bar{W}_A - j \left( \frac{u^2}{4} + \frac{\pi}{8} \right) \right] \cdot \left[ 1 + e^{j \frac{\pi}{2}} (\bar{\eta} - 1)^{-3} \cdot \bar{\tau}_A^{-2} \cdot \frac{10 \bar{\eta}^2}{12} + \dots \right], \quad (158 \text{ a})$$

where  $\bar{\eta} = \frac{\varrho}{\bar{\tau}_A^2}$ .

This differs from (55) only in the second and following terms. In the bridging region however,  $\eta \approx 1$ , and  $10 \eta^2 \approx \eta(\eta + 9)$ .

When  $\Gamma \ll 1$ ,

$$H_{\frac{1}{3}}^{(2)}(\Gamma) \approx e^{j \frac{\pi}{2}} \cdot \left( \frac{\Gamma}{2} \right)^{-\frac{1}{3}} \cdot \frac{\Gamma \left( \frac{1}{3} \right)}{\pi} \left\{ 1 - \frac{3 \Gamma \left( \frac{2}{3} \right)}{\Gamma \left( \frac{1}{3} \right)} e^{j \frac{\pi}{3}} \left( \frac{\Gamma}{2} \right)^{\frac{2}{3}} \right\}.$$

This yields when  $|y| \ll 1$

$$D \left( u e^{j \frac{\pi}{4}} \right) \sim \frac{\Gamma \left( j \varrho + \frac{1}{2} \right)}{2 \pi 3^{\frac{1}{2}}} \cdot \left( \frac{3u}{2} \right)^{\frac{1}{3}} \cdot (-\bar{\tau}_A)^{-\frac{1}{2}} \cdot \exp. \left[ \frac{\pi \varrho}{4} + \bar{W}_A - j \left( \frac{\pi}{24} + \frac{u^2}{4} \right) \right] \cdot \left\{ 1 - e^{j \frac{\pi}{3}} 3 \left( \frac{3u}{2} \right)^{-\frac{2}{3}} \bar{\beta} \frac{\Gamma \left( \frac{2}{3} \right)}{\Gamma \left( \frac{1}{3} \right)} + \dots \right\}, \quad (158 \text{ b})$$

where  $\bar{\beta} = \frac{u^2}{4} - \varrho$ .

This differs from (64) only in the third and following terms. The bridging approximation therefore must be considered good.

\* \* \*

Let us first determine the internal reflection coefficient,  $R$ .  
The circuit relation (20) immediately yields ( $\omega > \omega_H$ )

$$R = \frac{\Gamma \left( -j \varrho + \frac{1}{2} \right)}{(2 \pi)^{\frac{1}{2}}} \exp. \left\{ \frac{\pi}{2} \varrho + j \left( -\frac{\pi}{2} + \frac{u^2}{2} \right) - 2 \overline{W}_A \right\} e^{-j \left( 2 \Gamma - \frac{5}{6} \pi \right)} \cdot \frac{H_{\frac{1}{3}}^{(1)}(\Gamma)}{H_{\frac{1}{3}}^{(2)}(\Gamma)} \quad (1)$$

When  $\Gamma \gg 1$  and  $|\text{Phase } \Gamma| < \pi$ , we therefore have

$$R = \frac{\Gamma \left( -j \varrho + \frac{1}{2} \right)}{(2 \pi)^{\frac{1}{2}}} \exp. \left\{ \frac{\pi \varrho}{2} + j \left( -\frac{\pi}{2} + \frac{u^2}{2} \right) - 2 \overline{W}_A \right\} \quad (159 \text{ a})$$

When the losses are small ( $\sin \Psi \approx \Psi$ ) and  $x^2 \approx 1$  (penetration frequency region) we find  $\eta \approx 2j \left( \Psi + \frac{1}{4\alpha} \right)^{-1}$ . Therefore when the layer is thick,  $|\eta| \gg 1$  and

$$\left| \frac{\eta(\eta + 9)}{\tau_A^2 (\eta - 1)^3} \right| \approx \frac{2}{1 + 4\alpha\Psi}$$

When the losses are small (55) thus is not quite reliable in the penetration frequency region. The same is especially true of (159 a). As the study of the reflection coefficient in that particular region is of interest only in connexion with ionospheric investigations we preferably defer it to a later chapter. The transition from (159 a) to the corresponding relation in the penetration frequency region will there be shown.

When  $|\varrho| \gg 1$  we have

$$\frac{\Gamma \left( -j \varrho + \frac{1}{2} \right)}{(2 \pi)^{\frac{1}{2}}} e^{\frac{\pi \varrho}{2}} \sim e^{j \{ \varrho - \varrho \ln \varrho \}} \quad (160)$$

This yields

$$R = e^{j 2 \xi + 2 \bar{\gamma}} \quad (161)$$

with

$$2 \xi = u \left( \frac{u^2}{4} - \varrho \right)^{\frac{1}{2}} + \varrho \ln \left\{ \frac{(-\bar{v}_A)^2}{\varrho} \right\} - \frac{\pi}{2}, \quad (161 a)$$

and

$$2 \bar{\gamma} = -j \left[ 2 \Gamma - \frac{5}{6} \pi + j \ln \left\{ \frac{H_{\frac{1}{3}}^{(1)}(\Gamma)}{H_{\frac{1}{3}}^{(2)}(\Gamma)} \right\} \right]. \quad (161 b)$$

Except for very long waves (when the boundary reflection dominates as will soon be shown) we therefore have

$$R \approx e^{j 2 \xi}. \quad (161 c)$$

Introducing  $y^2 = x^2 \Delta$ , and  $\bar{y} = y e^{j \Psi}$ , we have

$$2 \xi = \alpha e^{-j \Psi} \left[ 2 \bar{y} - (1 - \bar{y}^2) \ln \left\{ \frac{1 + \bar{y}}{1 - \bar{y}} \right\} \right] - \frac{\pi}{2}. \quad (*) \quad (162)$$

and

$$\Gamma = \frac{2}{3} \alpha y^3 e^{j 2 \Psi} \cdot \frac{1 - \bar{y}}{(1 + \bar{y})^2}. \quad (163)$$

Further (if the oblique incidence case is included)

$$\left( \frac{d \xi}{d z} \right)_{z = \Delta h_m} = k \cdot \cos \varphi = \left( \frac{d \Phi}{d z} \right)_{z = \Delta h_m}, \quad (164)$$

which by (35) indicates that except for long waves there is no boundary reflection.

From (162) we obtain

$$|R| \approx e^{-\text{Im}(2 \xi)} = \left\{ \frac{1 + \frac{2 y}{1 + y^2} \cos \Psi}{1 - \frac{2 y}{1 + y^2} \cos \Psi} \right\}^{-\frac{\alpha}{2} \sin \Psi \cdot (1 + y^2)} \cdot \exp \left\{ \alpha \cos \Psi \cdot (1 - y^2) \cdot \arctan \left( \sin \Psi \cdot \frac{2 y}{1 - y^2} \right) \right\}, \quad (y < 1) \quad (165)$$

\*) For oblique incidence  $y$  has to be replaced by  $y \cos \varphi$ .

and

$$|R| \approx \left\{ \frac{1 + \frac{2y}{1+y^2} \cos \Psi}{1 - \frac{2y}{1+y^2} \cos \Psi} \right\}^{-\frac{\alpha}{2} \sin \Psi \cdot (1+y^2)} \exp. \left\{ \alpha \cos \Psi \cdot (y^2 - 1) \arctan \left( \sin \Psi \cdot \frac{2y}{y^2 - 1} \right) - \alpha \pi \cos \Psi \cdot (y^2 - 1) \right\}. \quad (y > 1) \quad (165)$$

For  $\nu = 0$  (no losses), (165) yields  $|R| \approx 1$  and (166) yields  $|R| \approx \exp. \{-\alpha \pi (y^2 - 1)\} = \exp. (\pi \varrho)$ . Contrary to the classical theories there thus still is some reflection for frequencies considerably above the penetration frequency (at which  $y^2 = 1$ ).

This is entirely consistent with (22) which yields

$$|R| \approx \exp. (\pi \varrho)$$

when  $\varrho \ll -1$ .

When the losses are so low that  $\Psi \approx \frac{1}{2} \frac{\nu}{\omega - \omega_H}$ , and this is practically always the case, then

$$|R| \approx \left\{ \frac{1+y}{1-y} \right\}^{-\frac{\nu}{\omega - \omega_H} \cdot a \cdot \frac{1+y^2}{2}} \cdot e^{-\frac{\nu}{\omega - \omega_H} \cdot a y}, \quad \left\{ y < 1, \frac{\nu^2}{(\omega - \omega_H)^2} \ll 1 \right\}. \quad (165)$$

and

$$|R| \approx \left\{ \frac{y+1}{y-1} \right\}^{-\frac{\nu}{\omega - \omega_H} \cdot a \cdot \frac{1+y^2}{2}} \cdot e^{-\frac{\nu}{\omega - \omega_H} \cdot a y - \overbrace{\alpha \pi (y^2 - 1)}^{\text{Penetration coefficient}}}. \quad \left\{ y > 1, \frac{\nu^2}{(\omega - \omega_H)^2} \ll 1 \right\}. \quad (166)$$

According to (23) we have the internal refraction coefficient

$$|T| \approx \left\{ \frac{1+y}{1-y} \right\}^{-\frac{\nu}{\omega - \omega_H} \cdot a \cdot \frac{1+y^2}{2}} \cdot e^{-\frac{\nu}{\omega - \omega_H} \cdot a y - \alpha \pi (1 - y^2)}, \quad \left\{ y < 1, \frac{\nu^2}{(\omega - \omega_H)^2} \ll 1 \right\} \quad (167)$$

$$|T| \approx \left\{ \frac{y+1}{y-1} \right\}^{-\frac{\nu}{\omega - \omega_H} \cdot a \cdot \frac{1+y^2}{2}} \cdot e^{-\frac{\nu}{\omega - \omega_H} \cdot a y}. \quad \left\{ y > 1, \frac{\nu^2}{(\omega - \omega_H)^2} \ll 1 \right\} \quad (167)$$

It is of interest to study — Im (2 ξ) for small y-values. One finds from (165) that when

$$y \ll 1, \quad 2 \xi \approx \Gamma. \tag{168}$$

According to (159) therefore when

$$y \ll 1, \quad R \approx \frac{H_{\frac{1}{3}}^{(1)}(\Gamma)}{H_{\frac{1}{3}}^{(2)}(\Gamma)} \cdot e^{j \frac{\pi}{3}}, \tag{169}$$

i. e.,

$$R \approx e^{-j \frac{2}{3} \pi} \cdot \exp. \left\{ \frac{\Gamma \left(\frac{2}{3}\right)}{\Gamma \left(\frac{1}{3}\right)} 3^{\frac{5}{6}} \alpha^{\frac{2}{3}} y^2 e^{j \left(\frac{\pi}{2} + \frac{4}{3} \psi\right)} \right\}, \tag{169 a}$$

when

$$(|\Gamma|)^2 \ll 1.$$

### On the Application of the Phase Integral.

Consider the solution of

$$\frac{d^2 \Pi}{dz^2} + k^2 \varepsilon(z) \Pi = 0,$$

where ε(z) is a slowly varying function with zero at z = z<sub>1</sub>, such that ε > 0 for z > z<sub>1</sub> and ε < 0 for z < z<sub>1</sub>.

The asymptotic solutions in the form of W.B.K.-approximations\* are joined in the region of z = z<sub>1</sub> by expressions involving HANKEL functions of order  $\frac{1}{3}$ . One asymptotic form for z > z<sub>1</sub> is

$$(k^2 \varepsilon)^{-\frac{1}{4}} \cos \left\{ \int_z^{z_1} k \varepsilon^{\frac{1}{2}} dz - \frac{\pi}{4} \right\} \tag{170}$$

containing the standing wave produced by imaginary reflection at the branch point of ε<sup>1/2</sup>. The complex phase difference between the up-going and down-coming waves is

\* They should be called *Jeffreys'-approximations*, since H. JEFFREYS seems to have used them first (*Proc. Lond. Math. Soc.*, ser. 3, 23, p. 428, 1924).

$$\int_{c_1} k \varepsilon^{\frac{1}{2}} dz - \frac{\pi}{2} = 2 \bar{\Phi}, \quad (170 \text{ a})$$

where the contour  $c_1$  must be chosen from  $z$  round the branch point of  $\varepsilon^{\frac{1}{2}}$  and back. This differs from the result of the ray treatment which does not contain the constant phase factor due to the exponential tail (in the region  $z > z_1$ ), and which further only has any real significance for a path along the axis of reals. When the medium is dissipative, therefore, the ray theory cannot be used [3].

We have for a parabolic layer

$$\varepsilon = 1 - (\bar{y})^2 \left\{ 1 - \left( \frac{z}{\Delta h_m} \right)^2 \right\},$$

so that the vertical incidence phase difference becomes

$$-k \Delta h_m \frac{1 - (\bar{y})^2}{\bar{y}} \int_{c_1} (u^2 - 1)^{\frac{1}{2}} du - \frac{\pi}{2} = 2 \bar{\Phi}, \quad (170 \text{ b})$$

where

$$u = \frac{z}{\Delta h_m} \left\{ 1 - (\bar{y})^2 \right\}^{\frac{1}{2}}.$$

One immediately finds  $\bar{\Phi} = \xi$ . For the thick layer, therefore, phase integration round the branch point of  $\sqrt{\varepsilon_{t_n}}$  generally is a very good approximation (even for considerable losses).\*)

We have so far not said anything about the fact that the symmetrical layer actually has two branch points  $z_1$  and  $-z_1$ .

We have the incident wave  $f_i(z) = e^{-j\bar{\Phi}}$ , the reflected wave  $f_r(z) = e^{-j\bar{\Phi}} \cdot \exp. \left\{ \int_{c_1} k \varepsilon^{\frac{1}{2}} dz - \frac{\pi}{2} \right\}$ , and the refracted wave  $f_t(z) = e^{-j\bar{\Phi}} \exp. \left\{ \int_{c_2} k \varepsilon^{\frac{1}{2}} dz \right\} = f_r(-z)$ .

The corresponding connexion formula is\*\*)

$$\underbrace{c_i \cdot f_i + f_r}_{z > z_1} \rightarrow \underbrace{f_r}_{z < -z_1}. \quad (171)$$

\*) Except for very long waves when  $|T| \ll 1$  (169).

\*\*) This is nothing else than the asymptotic form of the circuit relation of the wave-equation.

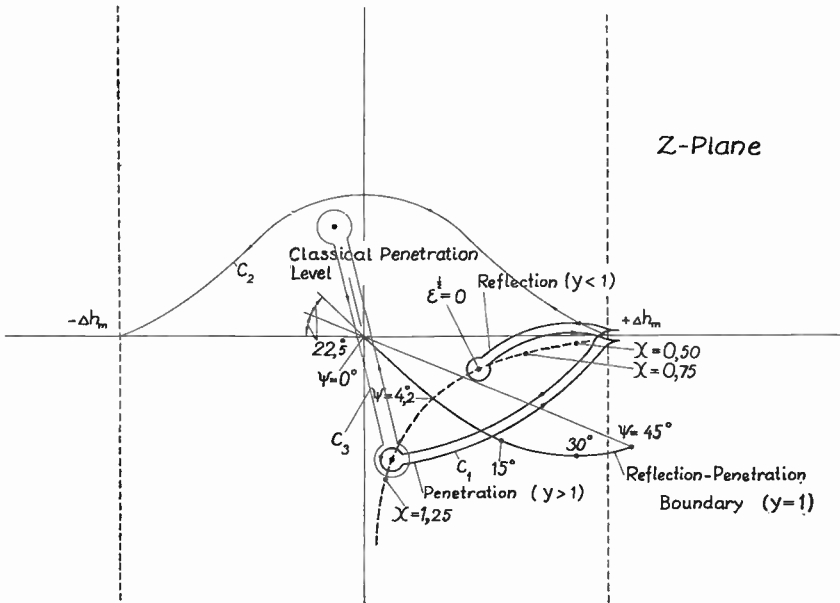


Fig. 24. Countours of integration for the phase integrals.

An examination of the so-called STOKES regions will show that if there is a good path  $c_2$  passing around the reflection (branch) points  $z_1$  and  $-z_1$  from the lower to the upper layer boundary without enclosing other possible zeros of  $\epsilon$ , the existence of this connection formula can be established [19]. The derivation of such connection formulae is the important question in the treatment of the transmission of matter-waves through potential barriers.

One finds that in the non-dissipative case

$$1 - (|c_i|)^2 = - \left| \exp. \left\{ \int_{c_3} k \epsilon^{\frac{1}{2}} dz \right\} \right|.$$

In the case of the parabolic layer  $\left| \exp. \left\{ \int_{c_3} k \epsilon^{\frac{1}{2}} dz \right\} \right| = -2\pi\rho$ .

Thus

$$(|R|)^2 = \frac{1}{1 + e^{-2\pi\rho}}. \quad (y = 0)$$

This is identical with the exact relation (22 b).

In the discussion of the transmission of radio waves round the earth we found that the proper values  $n_s$  (proper angles) were selected according to the relation

$$j 2 \pi s = \ln \left\{ R_1 R_4 \frac{\zeta_{\nu_s}^{(1)}(k c) \zeta_{\nu_s}^{(2)}(k a)}{\zeta_{\nu_s}^{(2)}(k c) \zeta_{\nu_s}^{(1)}(k a)} \right\}. \tag{172}$$

When  $n < k a$  and the DEBYE-(W. K. B.-) approximation can be used, the relation selecting the proper angles therefore becomes

$$2 \pi s = \oint k \varepsilon^{\frac{1}{2}} d r - \pi \tag{173}$$

corresponding to the familiar BOHR-SOMMERFELD phase integral relation

$$\left( s + \frac{1}{2} \right) h = \oint p d q. \tag{174}$$

The exact relation (172), however, selects not only the elevation of the wave front but also determines the intensity of the wave which is expressed by the residue series. In that respect it corresponds to the later wave mechanical improvements of (174).

### The Boundary Reflection of the Parabolic Layer.

When the main portion of the energy is returned at the boundary of the layer we speak of boundary reflection. It is of importance for long waves when  $|\Gamma| < 1$ .

We find

$$\left( \frac{d \Gamma}{d z} \right)_{z = \Delta h_m} = k \cos \varphi_c \cdot \left( \frac{1 - \bar{y} \cos \varphi_c}{1 + \bar{y} \cos \varphi_c} \right)^2. \tag{175}$$

Applying (89) we therefore find

$$\left[ \frac{1}{k} \cdot \frac{d}{d z} \ln \left\{ D \left( u e^{\pm j \frac{\pi}{4}} \right) \right\} \right]_{z = \Delta h_m} = \mp j \left\{ 1 - \left( \frac{1 - \bar{y} \cos \varphi_c}{1 + \bar{y} \cos \varphi_c} \right)^2 + \frac{H_{\frac{2}{3}}^{(1)}(\Gamma)}{H_{\frac{1}{3}}^{(1)}(\Gamma)} \cdot e^{\mp j \frac{\pi}{6}} \right\}.$$

$$\left. \left( \frac{1 - \bar{y} \cos \varphi_c}{1 + \bar{y} \cos \varphi_c} \right)^2 \right\} \cos \varphi_c \approx \mp j \frac{H_{\frac{2}{3}}^{(1)}(I)}{H_{\frac{1}{3}}^{(1)}(I)} e^{\mp j \frac{\pi}{6}} \cdot \cos \varphi_c = \mp j \frac{1}{\Lambda^{(2)}}. \quad (176)$$

The complex reflection coefficient for horizontal polarization thus becomes

$$R_4 = - \frac{1 - \Lambda^{(2)} \bar{\gamma} \bar{p}}{1 + \Lambda^{(2)} \bar{\gamma}^* \bar{p}} = - \eta_4, \quad (177)$$

where

$$\left. \begin{array}{l} \bar{\gamma}^* \\ \bar{\gamma} \end{array} \right\} = e^{\mp j \frac{\pi}{6}} \frac{H_{\frac{2}{3}}^{(1)}(\varrho_c)}{H_{\frac{1}{3}}^{(1)}(\varrho_c)} \cos \varphi_c, \quad (178)$$

and

$$\bar{p} = \frac{1 + R_3}{1 - R_3 \frac{\Lambda^{(2)}}{\Lambda^{(1)}}}. \quad (179)$$

Since  $\varrho_c > 1$ , except for the first pole, we put  $\bar{\gamma} = 1 = \bar{\gamma}^*$  in order to be able easily to study the qualities of the layer as a boundary reflector.

Thus

$$R_{23} \approx \frac{1 - \Lambda^{(2)}}{1 + \Lambda^{(2)}} \cdot (\varphi_c < 90^\circ). \quad (177 \text{ a})$$

For  $|I| \gg 1$ ,  $\Lambda^{(2)} = 1$  and  $R_{23} = 0$ . Appreciable boundary reflection only occurs when  $|I| < 1$ .

When  $y \ll 1$ , (169) and (179) yield

$$\bar{p} \approx \frac{1 + e^{j \frac{\pi}{3}} \frac{H_{\frac{1}{3}}^{(1)}(I)}{H_{\frac{1}{3}}^{(2)}(I)}}{1 + e^{-j \frac{\pi}{3}} \frac{H_{\frac{2}{3}}^{(1)}(I)}{H_{\frac{2}{3}}^{(2)}(I)}}. \quad (179 \text{ a})$$

When  $|\Gamma| \ll 1$ , therefore

$$\bar{p} \approx -e^{j \frac{\pi}{3}},$$

and

$$R_4 \approx - \frac{1 + j y \cos \varphi_c \cdot \left(\frac{\alpha e^{j 2 \Psi}}{3}\right)^{\frac{1}{3}} \frac{\Gamma(\frac{1}{3})}{\Gamma(\frac{2}{3})}}{1 - j y \cos \varphi_c \cdot \left(\frac{\alpha e^{j 2 \Psi}}{3}\right)^{\frac{1}{3}} \frac{\Gamma(\frac{1}{3})}{\Gamma(\frac{2}{3})}} \quad (|\Gamma| \ll 1) \tag{180}$$

When  $\omega_{c_m} \rightarrow \infty$  (sharp layer),  $R_4 \rightarrow e^{-j \pi}$ .

This represents the true long wave case when the polarization is horizontal and  $\omega_H = 0$ . We may arbitrarily make the distinction that for long wave transmission  $|\Gamma| < 1$  and for medium and short wave transmission  $|\Gamma| > 1$ .

\* \* \*

It is of particular interest to study the boundary reflection for a layer with linear increase in electron density, an especially simple case.

The circuit relation connecting the waves (horizontal polarization) is [3]

$$\underbrace{\tilde{x}^{\frac{1}{2}} H_{\frac{1}{3}}^{(2)} \left\{ 2 \left( \frac{\tilde{x}}{3} \right)^{\frac{3}{2}} \right\}}_{\text{up-going wave}} e^{-j \frac{\pi}{6}} = - \underbrace{\tilde{x}^{\frac{1}{2}} H_{\frac{1}{3}}^{(1)} \left\{ 2 \left( \frac{\tilde{x}}{3} \right)^{\frac{3}{2}} \right\}}_{\text{down-coming wave}} e^{j \frac{\pi}{6}} + \underbrace{\frac{3^{\frac{1}{2}}}{\pi} (-\tilde{x})^{\frac{1}{2}} K_{\frac{1}{3}} \left\{ 2 \left( \frac{-\tilde{x}}{3} \right)^{\frac{3}{2}} \right\}}_{\text{surface-wave (exponential tail in non-classical region)}}, \tag{181}$$

where

$$2 \left( \frac{\tilde{x}}{3} \right)^{\frac{3}{2}} = \frac{1}{2} k \int_{c_1} \varepsilon_{t_n}^{\frac{1}{2}} dz = \bar{\Phi} + \frac{\pi}{4}. \tag{181 a}$$

and  $c_1$  is the usual contour round the branch point. Therefore

$$- \left( \frac{d \bar{\Phi}}{dz} \right)_{z=0} = k \cos \varphi_c, \tag{181 b}$$

and

$$\bar{\Phi} + \frac{\pi}{4} = \frac{2}{3} \cos^3 \varphi_c \cdot \frac{\omega^3 \Delta e^{j 2 \Psi}}{c_0 \frac{d}{dz} (\omega_c^2)}. \tag{181 c}$$

By (163)

$$\Gamma \approx \frac{2}{3} \cos^3 \varphi_c \cdot a \left( \frac{\omega}{\omega_{cm}} \right)^3 e^{j 2 \Psi}, \quad (\omega_H = 0)$$

when  $|\Gamma| < 1$ . This differs from  $\bar{\Phi}$  only in the value of the layer constant. For the parabolic layer, however,

$$\left\{ -c_0 \frac{d}{dz} (\omega_c^2) \right\}_{z = \Delta h_m} = \frac{\omega_{cm}^3}{a},$$

and therefore, as expected, the boundary reflecting power of the parabolic layer is the same as that of the linear layer, provided the boundary gradient is the same. We therefore conclude that all layers with a linear term in the electron density distribution function of the boundary region have similar properties as long wave reflectors.

### A Short Note on the Reflection Coefficient of a Layer with Quadratic Increase in Electron Density.

Since the quadratic case is as simple practically as the linear one it is worth while to consider the corresponding reflecting property briefly.\*)

Counting  $z$  positive from the boundary we have

$$\left. \begin{aligned} \omega_c^2 &= \bar{\sigma} z^2, \quad (z > 0) \\ \omega_c^2 &= 0 \quad (z < 0) \end{aligned} \right\} \tag{182}$$

The wave equation becomes (horizontal polarization)

$$\frac{d^2 H}{dx^2} + \left\{ n + \frac{1}{2} - \frac{x^2}{4} \right\} H = 0, \tag{183}$$

---

\*) Reference should here be made to the early but different treatment of this case by HARTREE [20].

where

$$n + \frac{1}{2} = \frac{k \cos^2 \varphi_c}{2 d^{\frac{1}{2}}} = r_0, \tag{183 a}$$

$$x = z (2 k)^{\frac{1}{2}} d^{\frac{1}{4}}, \tag{183 b}$$

and

$$d = \frac{\bar{\sigma}}{\omega^2 \Delta} \cdot e^{-j 2 \eta}. \tag{183 c}$$

The circuit relation becomes

$$e^{-\frac{1}{2} n \pi j} \underbrace{D(-j x)}_{-n-1} = - \underbrace{e^{\frac{1}{2} n \pi j} D(j x)}_{-n-1} - \underbrace{\frac{(2 \pi)^{\frac{1}{2}}}{\Gamma(n+1)} D_n(x)}_{\text{exponential tail}}. \tag{184}$$

up-going wave
down-coming wave
exponential tail.

This immediately yields

$$R = e^{j n \pi} \left\{ \frac{D(j x)}{-n-1} \right\}_{x=0} = e^{j n \pi} = e^{j \left( r_0 \pi - \frac{\pi}{2} \right)}. \tag{185}$$

Performing phase integration round the branch point in the usual manner we obtain

$$2 \bar{\Phi} + \frac{\pi}{2} = k \int_{c_1} \varepsilon_{t_n}^{\frac{1}{2}} dz = r_0 \pi. \tag{186}$$

For the quadratic layer the W.K.B.-approximation is correct for all wave-lengths.

For the linear oscillator in wave mechanics, therefore, (185) immediately yields the correct energy levels, viz.,

$$W_n = \left( m + \frac{1}{2} \right) h \nu_0,$$

where  $\nu_0$  is the classical frequency of free oscillation.

\* \* \*

According to (39)

$$\left[ \frac{d}{dz} \left\{ \ln D(-jx) \right\} \right]_{z=0}^{-n-1} = j \cdot 2 \frac{\Gamma\left(\frac{r_0 + 3/2}{2}\right)}{\Gamma\left(\frac{r_0 + 1/2}{2}\right)} \cdot \left(\frac{\bar{\sigma}}{c_0^2 \Delta}\right)^{1/4} e^{-j\frac{\psi}{2}}. \quad (187)$$

Making use of the STIRLING expansion for the  $\Gamma$ -function we find that for medium waves, when  $|r_0| \gg 1$ ,

$$\left[ \frac{d}{dz} \left\{ \ln D(-jx) \right\} \right]_{z=0}^{-n-1} = j k \cos \varphi_c \cdot \quad (|r_0| \gg 1).$$

There is therefore appreciable boundary reflection only when  $|r_0| < 1$ , which corresponds to the requirement  $|I| < 1$  for the linear and parabolic layers.

Since

$$\bar{p} = -j \tan\left(\frac{r_0\pi}{2} + \frac{\pi}{4}\right)$$

for the quadratic layer, and when further  $\bar{\gamma} = 1$ , we have

$$R_4 = \frac{1 + j \tan\left(\frac{r_0\pi}{2} + \frac{\pi}{4}\right) \cos \varphi_c \cdot \frac{\Gamma\left(\frac{r_0 + 1/2}{2}\right)}{\Gamma\left(\frac{r_0 + 3/2}{2}\right)} \cdot \left(\frac{\Delta}{c_0^2 \bar{\sigma}}\right)^{1/4} \cdot e^{j\frac{\psi}{2}} \cdot \frac{\omega}{2}}{1 - j \tan\left(\frac{r_0\pi}{2} + \frac{\pi}{4}\right) \cos \varphi_c \cdot \frac{\Gamma\left(\frac{r_0 + 1/2}{2}\right)}{\Gamma\left(\frac{r_0 + 3/2}{2}\right)} \cdot \left(\frac{\Delta}{c_0^2 \bar{\sigma}}\right)^{1/4} \cdot e^{j\frac{\psi}{2}} \cdot \frac{\omega}{2}}. \quad (188)$$

When  $b \rightarrow \infty$  (sharp layer),  $R_4 \rightarrow e^{-j\pi}$  as expected for horizontal polarization.

### A Short Discussion of the Case $\omega_{cm} < \omega < \omega_H$ for the Parabolic Layer.

We have

$$\psi = \pm \frac{\pi}{2} - \underbrace{\frac{1}{2} \arctan \frac{\nu}{\omega_H - \omega}}_{\psi_1}. \quad (189)$$

It is convenient to select the plus sign (the other sign will only transform the progressive wave into a standing wave and vice versa), thus

$$\Psi = \frac{\pi}{2} - \Psi_1. \tag{189 a}$$

We find

$$j \varrho = a [(1 + y^2) \cos \Psi_1 + j (1 - y^2) \sin \Psi_1] = n + \frac{1}{2}, \tag{190}$$

i. e., 
$$(n)_{\nu=0} = a (1 + y^2) - \frac{1}{2}.$$

Further 
$$V = \frac{z}{\Delta h_m} \cdot (\pm a)^{\frac{1}{2}} e^{j \frac{\Psi_1}{2}}. \tag{191}$$

The circuit relation

$$D_n(V) = \frac{\Gamma (n + 1)}{(2 \pi)^{\frac{1}{2}}} \left\{ e^{\frac{1}{2} n \pi j} D(j V) + e^{-\frac{1}{2} n \pi j} D(-j V) \right\}_{-n-1}, \tag{192}$$

yields waves progressing in both directions between the branch points,  $\varepsilon^{\frac{1}{2}} = 0$ , i. e., between

$$z = \pm \Delta h_m \left( 1 + y^2 e^{j 2 \Psi_1} \right)^{\frac{1}{2}}.$$

Partial reflection thus does not take place within the layer. Therefore

$$\{R\}_{\omega_{cm} < \omega < \omega_H} = 0,$$

and the internal transmission (refraction) coefficient

$$T = \left\{ \frac{D(-j V)}{-n-1} \right\}_{z = \Delta h_m} \left\{ \frac{D(+j V)}{-n-1} \right\}. \tag{193}$$

We have

$$\Gamma = \frac{2}{3} a y^3 e^{-j 2 \Psi_1} \frac{1 - j \bar{y}_1}{(1 + j \bar{y}_1)^2} \cdot e^{j \pi} = e^{j \pi} \Gamma_1, \tag{194}$$

where

$$\bar{y}_1 = y e^{-j \Psi_1}.$$

Further

$$\begin{aligned} \operatorname{Re}(\xi) = & \frac{a}{2} \left[ 2y - \cos \Psi_1 (1 + y^2) \arctan \left\{ \cos \Psi_1 \cdot \frac{2y}{1 - y^2} \right\} - \right. \\ & \left. - \frac{\sin \Psi_1}{2} (1 - y^2) \ln \left\{ \frac{1 + \frac{2y}{1 + y^2} \sin \Psi_1}{1 - \frac{2y}{1 + y^2} \sin \Psi_1} \right\} \right] - \frac{\pi}{2}, \end{aligned} \quad (195)$$

and

$$\begin{aligned} \operatorname{Im}(\xi) = & \frac{a}{2} \left[ \frac{\cos \Psi_1}{2} (1 + y^2) \ln \left\{ \frac{1 + \frac{2y}{1 + y^2} \sin \Psi_1}{1 - \frac{2y}{1 + y^2} \sin \Psi_1} \right\} - \right. \\ & \left. - \sin \Psi_1 (1 - y^2) \arctan \left\{ \cos \Psi_1 \cdot \frac{2y}{1 - y^2} \right\} \right]. \end{aligned} \quad (196)$$

Thus

$$\{\operatorname{Re}(\xi)\}_{y=0} = \frac{a}{2} \left[ 2y - (1 + y^2) \arctan \left\{ \frac{2y}{1 - y^2} \right\} \right],$$

and

$$\{\operatorname{Im}(\xi)\}_{y=0} = 0.$$

Making use of (158), remembering that

$$H_{\frac{1}{3}}^{(1)}(e^{j\pi} \Gamma_1) = -e^{-j\frac{\pi}{3}} H_{\frac{1}{3}}^{(2)}(\Gamma_1),$$

and introducing

$$\Gamma_1^* = \frac{2}{3} \alpha y^3 e^{-j2\eta_1} \cdot \frac{1 + j\bar{y}_1}{(1 - j\bar{y}_1)^2}, \quad (194 a)$$

we obtain

$$T = e^{j(2\xi + \frac{\pi}{2} + j\pi\rho)} \cdot \exp. \left[ j \left\{ \Gamma_1 + \Gamma_1^* - \frac{5}{6} \pi \right\} \right] \cdot \frac{H_{\frac{1}{3}}^{(2)}(\Gamma_1)}{H_{\frac{1}{3}}^{(1)}(\Gamma_1^*)}, \quad (197)$$

and

$$(|T|)_{\nu=0} = 1.$$

For very long waves therefore ( $|T_1| \ll 1$ )

$$T \approx e^{j\left(\pi\left(n + \frac{1}{2}\right) + \frac{\pi}{6}\right)}. \tag{197 a}$$

When  $|T_1| \gg 1$ ,

$$T \approx e^{j\left(\pi\left(n + \frac{1}{2}\right) + 2\xi + \frac{\pi}{2}\right)}, \tag{197 b}$$

which can also be obtained by phase integration along  $c_2$ .

Finally

$$\begin{aligned} \left[ \frac{1}{k} \frac{d}{dz} \ln \left\{ D(jV) \right\} \right]_{z=\Delta h_m} &= -j \left\{ 1 - \left( \frac{1 - j\bar{y}_1}{1 + j\bar{y}_1} \right)^2 + \right. \\ &+ \left. \frac{H_{\frac{2}{3}}^{(2)}(T_1)}{H_{\frac{1}{3}}^{(2)}(T_1)} e^{-j\frac{\pi}{6}} \cdot \left( \frac{1 - j\bar{y}_1}{1 + j\bar{y}_1} \right)^2 \right\} \approx -j \frac{H_{\frac{2}{3}}^{(2)}(T_1)}{H_{\frac{1}{3}}^{(2)}(T_1)} \cdot e^{-j\frac{\pi}{6}} = \\ &= -j \cdot \frac{1}{\Lambda_1^{(2)}}, \end{aligned} \tag{198}$$

and

$$r_i = - \frac{1 - \Lambda_1^{(2)}}{1 + \Lambda_1^{(2)}} = -r_0. \text{ *)} \tag{199}$$

Introducing

$$T = e^{j\eta_T},$$

and

$$r_0 = e^{j\eta_r}, \quad [\text{Im}(\eta_r) \gg \text{Re}(\eta_r)]$$

the effective transmission and reflection coefficients by (28) approximately become

$$\left. \begin{aligned} T_{eff} &\approx (1 - r_0^2) \frac{T}{1 - r_0^2 T^2} = \frac{\sin \eta_r}{\sin(\eta_r + \eta_T)}, \\ R_{eff} &\approx -r_0 \cdot \frac{1 - T^2}{1 - r_0^2 T^2} = \frac{-\sin \eta_T}{\sin(\eta_r + \eta_T)}. \end{aligned} \right\} \tag{200}$$

\*) Only vertical incidence considered when  $\omega_H \neq 0$ .

In the particular case  $\nu = 0$ ,  $\text{Im}(\eta_T) = 0$ , and the weak reflected wave exhibits the «colours» of thick plates. Since  $|R_{eff}| \ll |T_{eff}|$ , this is not true of the transmission coefficient.

It is interesting to compare the result of (200) to that of EPSTEIN on p. 633 in his fundamental paper *Reflection of Waves in an Inhomogeneous Absorbing Medium* [1].

In the corresponding case EPSTEIN'S numerator in the expression for  $R_{eff}$  is

$$- \sin(-\pi d),$$

where

$$- d = \left\{ \frac{1}{4} + s^2 \varepsilon_3 \right\}^{\frac{1}{2}} - \frac{1}{2}.$$

The variation in dielectric constant is expressed by

$$\varepsilon = 1 + \frac{\varepsilon_3}{4} \cdot \left( \cosh \frac{kz}{2s} \right)^{-2}.$$

The thickness of the layer in  $\frac{\lambda}{2\pi}$  units therefore is proportional to  $s$ . The boundary region may arbitrarily be placed at

$$z = \Delta h_{m_1} = \frac{4s}{k}.$$

For long waves and no absorption this yields

$$- \pi d \approx \frac{\pi^2 \Delta h_{m_1}}{\lambda_{c_m}} \cdot \left( \frac{\omega}{\omega_H} \right)^2,$$

which substantially corresponds to the dominant term in  $\eta_T$ , i. e.,

$$\pi \left( n + \frac{1}{2} \right) \approx \frac{\pi^2 \Delta h_m}{\lambda_{c_m}} \cdot \left( \frac{\omega}{\omega_H} \right)^2.$$

### On the Poles when the Reflecting Shell is Radially Inhomogeneous.

We have for horizontal polarization

$$\Phi_2 = 1 - \eta_1 \eta_4 \frac{\zeta_\nu^{(1)}(kc)}{\zeta_\nu^{(2)}(kc)} \frac{\zeta_\nu^{(2)}(ka)}{\zeta_\nu^{(1)}(ka)}, \tag{201}$$

where  $\eta_1$  as before is expressed by (83) and  $\eta_4$  by (177).

Since

$$\frac{\zeta_y^{(1)}(kc)}{\zeta_y^{(2)}(kc)} \sim \frac{H_{\frac{1}{3}}^{(1)}(\varrho_c)}{H_{\frac{1}{3}}^{(2)}(\varrho_c)} \exp. \left[ j \left\{ 2(\gamma_c - \varrho_c) + \frac{\pi}{3} \right\} \right], \quad (202)$$

these expressions yield the Phase Integral Relations

$$\int_{ka}^{kc} \left\{ 1 - \frac{n^2}{x^2} \right\}^{\frac{1}{2}} dx = s\pi + \delta_{14}, \quad \{\text{Re}(n) \leq ka\}$$

$$\int_n^{kc} \left\{ 1 - \frac{n^2}{x^2} \right\}^{\frac{1}{2}} dx = s\pi + \delta_{14}, \quad \{ka \leq \text{Re}(n) \leq kc\}$$

where

$$\delta_{14} = \varrho_c - \varrho_a + j \frac{1}{2} \ln \left\{ \frac{H_{\frac{1}{3}}^{(1)}(\varrho_c) H_{\frac{1}{3}}^{(2)}(\varrho_a)}{H_{\frac{1}{3}}^{(2)}(\varrho_c) H_{\frac{1}{3}}^{(1)}(\varrho_a)} \right\} + j \frac{1}{2} \ln \eta_1 \eta_4, \quad \{\text{Re}(n) \leq ka\} \quad (203)$$

and

$$\delta_{14} = \varrho_c + j \frac{1}{2} \ln \left\{ \frac{H_{\frac{1}{3}}^{(1)}(\varrho_c) H_{\frac{1}{3}}^{(2)}(\varrho_a)}{H_{\frac{1}{3}}^{(2)}(\varrho_c) H_{\frac{1}{3}}^{(1)}(\varrho_a)} \right\} + j \frac{1}{2} \ln \eta_1 \eta_4 \cdot \{ka \leq \text{Re}(n) \leq kc\}$$

Relations (122) and (203) thus are practically identical for the high order poles.

\* \* \*

Let us now for the sake of completeness show roughly that there can be no poles for  $n^0 > kc$  (no-loss case). For the sake of convenience we further limit ourselves to the parabolic case. We have

$$\frac{H_{\frac{1}{3}}^{(1)}(|\varrho_c^0| e^{-j\frac{3}{2}\pi})}{H_{\frac{1}{3}}^{(2)}(|\varrho_c^0| e^{-j\frac{3}{2}\pi})} = \exp. \left\{ j \left( -\pi - 2 \arctan \frac{3^{\frac{1}{2}} I_{\frac{1}{3}}(|\varrho_c^0|)}{2 I_{-\frac{1}{3}}(|\varrho_c^0|) + I_{\frac{1}{3}}(|\varrho_c^0|)} \right) \right\}, \quad (205)$$

and therefore

$$\frac{H_{\frac{1}{3}}^{(1)}(\varrho_c^0)}{H_{\frac{1}{3}}^{(2)}(\varrho_c^0)} \cdot \frac{H_{\frac{1}{3}}^{(2)}(\varrho_a^0)}{H_{\frac{1}{3}}^{(1)}(\varrho_a^0)} = \exp. \left[ j \left\{ 2 \arctan \frac{3^{\frac{1}{2}} I_{\frac{1}{3}}(|\varrho_a^0|)}{2 I_{-\frac{1}{3}}(|\varrho_a^0|) + I_{\frac{1}{3}}(|\varrho_a^0|)} - \right. \right. \\ \left. \left. - 2 \arctan \frac{3^{\frac{1}{2}} I_{\frac{1}{3}}(|\varrho_c^0|)}{2 I_{-\frac{1}{3}}(|\varrho_c^0|) + I_{\frac{1}{3}}(|\varrho_c^0|)} \right\} \right] = \exp. (jF). \quad (n > kc) \quad (206)$$

Since  $0 < F < \frac{\pi}{3}$  when  $|\varrho_c^0| > 0$ , (201) has no zeros for  $n^0 > kc$ .

\* \* \*

For the higher order poles and horizontal polarization for example we have the same *Relation I* as (125).

*Relation II* becomes in the parallell form for the parabolic layer (compare p. 65)

$$\Delta n_s \left\{ \left( \frac{2(kc - n_s^0)}{kc} \right)^{\frac{1}{2}} \cdot \frac{2}{\pi \varrho_c^0} \cdot \frac{1}{\left\{ \left| H_{\frac{1}{3}}^{(1)}(\varrho_c^0) \right|^2 \right\}} \left\{ 1 - \left| \frac{H_{\frac{2}{3}}^{(1)}(\varrho_c^0)}{H_{\frac{1}{3}}^{(1)}(\varrho_c^0)} \right| \cos \left( \frac{\pi}{3} + \beta_c \right) (\varrho_c^0)^{\frac{1}{3}} \left( \frac{3}{kc} \right)^{\frac{1}{3}} \Delta n_s \right\} - \right. \\ \left. \left\{ \frac{2(ka - n_s^0)}{ka} \right\}^{\frac{1}{2}} \cdot \frac{2}{\pi \varrho_a^0} \cdot \frac{1}{\left\{ \left| H_{\frac{1}{3}}^{(1)}(\varrho_a^0) \right|^2 \right\}} \left\{ 1 - \left| \frac{H_{\frac{2}{3}}^{(1)}(\varrho_a^0)}{H_{\frac{1}{3}}^{(1)}(\varrho_a^0)} \right| \cos \left( \frac{\pi}{3} + \beta_a \right) (\varrho_a^0)^{\frac{1}{3}} \left( \frac{3}{ka} \right)^{\frac{1}{3}} \Delta n_s \right\} + \right. \\ \left. + j \frac{1}{2} \frac{\frac{k}{k_1} \left( \frac{3 \varrho_a}{ka} \right)^{\frac{2}{3}} \left\{ \frac{H_{\frac{2}{3}}^{(1)}(\varrho_a) H_{\frac{2}{3}}^{(2)}(\varrho_a)}{H_{\frac{1}{3}}^{(1)}(\varrho_a) H_{\frac{1}{3}}^{(2)}(\varrho_a)} \right\}^2}{\left( 1 - \frac{k}{k_1 \alpha^*} \right) \left( 1 + \frac{k}{k_1 \alpha} \right)} \left\{ \mu_1(\varrho_a^0) - \frac{k}{k_1} \left( \frac{3 \varrho_a}{ka} \right)^{\frac{2}{3}} \mu_2(\varrho_a^0) \right\} + \right.$$

$$\begin{aligned}
 & + j \frac{1}{2} \frac{\cos \varphi_c}{(1 - \bar{p} \wedge^{(2)} \beta) (1 + \bar{p} \wedge^{(2)} \beta^*)} \cdot \\
 & \cdot \left\{ \frac{H_{\frac{2}{3}}^{(1)}(\varrho_c^0)}{H_{\frac{1}{3}}^{(1)}(\varrho_c^0)} \right\}^2 \left[ \wedge^{(2)} \bar{p} \cos \varphi_c \left\{ \frac{H_{\frac{2}{3}}^{(1)}(\varrho_c^0)}{H_{\frac{1}{3}}^{(1)}(\varrho_c^0)} \right\}^2 \cdot \left\{ \mu_1(\varrho_c^0) - \left( \frac{k c}{3} \right)^{\frac{1}{3}} \cos^2 \varphi_c \cdot \mu_2(\varrho_c^0) \right\} - \right. \\
 & \left. - \left\{ e^{j \frac{\pi}{3}} \frac{H_{\frac{1}{3}}^{(1)}(\varrho_c^0)}{H_{\frac{2}{3}}^{(1)}(\varrho_c^0)} - e^{-j \frac{\pi}{3}} \frac{H_{\frac{1}{3}}^{(2)}(\varrho_c^0)}{H_{\frac{2}{3}}^{(2)}(\varrho_c^0)} \right\} \cdot \frac{3 \Gamma}{k} \cdot \left[ 1 - e^{j \frac{\pi}{3}} \left\{ \frac{H_{\frac{1}{3}}^{(2)}(\Gamma)}{H_{\frac{2}{3}}^{(2)}(\Gamma)} \right\}^2 \right] \right] \Bigg\} = \\
 & = j \frac{1}{2} \left\{ \ln (\eta_1 \eta_4) \right\}_{n = n_s^0}, \tag{207}
 \end{aligned}$$

where  $\eta_1$  is obtained from (83) and  $\eta_4$  from (177). The variation of  $\bar{p}$  has been neglected in the range of *Relations* II and III. *Relation* III is not written out. It is easily obtained from (209) when compared with (134).

### Further Notes on the Residue Series.

If we desire to raise the receiver above ground, i. e.  $r > a$ , we obtain the general expression

$$\left. \begin{aligned}
 \frac{e_\nu}{\Phi_1(n)} &= \frac{1}{2j} \cdot \zeta_\nu^{(1)}(kb) \zeta_\nu^{(2)}(kr) \cdot \left\{ 1 + R_1 \frac{\zeta_\nu^{(2)}(ka)}{\zeta_\nu^{(1)}(ka)} \cdot \frac{\zeta_\nu^{(1)}(kr)}{\zeta_\nu^{(2)}(kr)} \right\} \left\{ 1 + R_4 \cdot \frac{\zeta_\nu^{(1)}(kc)}{\zeta_\nu^{(2)}(kc)} \cdot \frac{\zeta_\nu^{(2)}(kb)}{\zeta_\nu^{(1)}(kb)} \right\}, \\
 &\text{and} \\
 \frac{e_\nu}{\Phi_1(n)} &= \frac{1}{2j} \cdot \zeta_\nu^{(1)}(kr) \zeta_\nu^{(2)}(kb) \cdot \left\{ 1 + R_1 \frac{\zeta_\nu^{(2)}(ka)}{\zeta_\nu^{(1)}(ka)} \cdot \frac{\zeta_\nu^{(1)}(kb)}{\zeta_\nu^{(2)}(kb)} \right\} \left\{ 1 + R_4 \frac{\zeta_\nu^{(1)}(kc)}{\zeta_\nu^{(2)}(kc)} \cdot \frac{\zeta_\nu^{(2)}(kr)}{\zeta_\nu^{(1)}(kr)} \right\}.
 \end{aligned} \right\} \tag{209}$$

Placing the sender on the ground one obtains

$$\left. \begin{aligned}
 \left\{ \frac{e_{\nu_s}}{\Phi_1(n_s)} \right\}_{r=a} &= \frac{1}{2j} \cdot \zeta_{\nu_s}^{(1)}(ka) \zeta_{\nu_s}^{(2)}(ka) (1 + R_1) (1 + R_1) \cdot \frac{1}{R_1}, \\
 &\text{and} \\
 \left\{ \frac{e_{\nu_s}}{\Phi_1(n_s)} \right\}_{r=c} &= \frac{1}{2j} \zeta_{\nu_s}^{(1)}(kc) \zeta_{\nu_s}^{(2)}(ka) (1 + R_1) (1 + R_4).
 \end{aligned} \right\} \tag{209 a}$$

Placing the sender close to the reflector we further obtain

$$\left. \begin{aligned} \left\{ \frac{e_{\nu_s}}{\Phi_1(n_s)} \right\}_{r \rightarrow a} &= \frac{1}{2j} \zeta_{\nu_s}^{(1)}(kc) \zeta_{\nu_s}^{(2)}(ka) (1 + R_1) (1 + R_4), \\ \text{and} \\ \left\{ \frac{e_{\nu_s}}{\Phi_1(n_s)} \right\}_{r \rightarrow c} &= \frac{1}{2j} \zeta_{\nu_s}^{(1)}(kc) \zeta_{\nu_s}^{(2)}(kc) (1 + R_4) (1 + R_4) \cdot \frac{1}{R_4}. \end{aligned} \right\} \quad (209 \text{ b})$$

From these relations we find that the influence of the reflecting properties of ground and shell (layer) is symmetrical when the sender and receiver are placed on the opposite surfaces. When they are placed on the same surface the local reflection coefficient dominates. This holds of course only for a constant  $\theta$ -value.

Returning to the practical case of (209 a) we infer that for high angle (high order) waves and vertical polarization there is not much difference in intensity at the two surfaces when the losses are small.

We have already seen that  $R_1$  and  $R_4$  appear symmetrically in the pole relation. From this one may perhaps be inclined to believe that the reflecting properties of ground and layer have a symmetrical influence upon the attenuation. It is true that the influence is symmetrical for higher order waves. For the lowest order waves, however, the ground properties are only of secondary importance.

For the lowest order pole we have very approximately

$$-\Delta n_0 \left[ \cos \varphi_c \cdot \frac{2}{\pi \zeta_c^0} \cdot \frac{1}{\left\{ \left| H_{\frac{1}{3}}^{(1)}(\varrho_c^0) \right| \right\}^2} \right] \approx j \frac{1}{2} \ln \eta_4. \quad (210)$$

It is worth noting that for this pole  $\eta_1 \approx 1$ . This is borne out by figs. 13 and 14. It is a consequence of the fact that, according to table I on p. 55, when  $\varrho_a = |\zeta_a| \cdot \exp \left\{ -j \frac{2}{3} \pi \right\}$ , ( $n > ka$ ), and  $|\varrho_a| \gg 1$ ,

$$\frac{\zeta_{\nu}^{(1)'}(ka)}{\zeta_{\nu}^{(1)}(ka)} \sim \frac{\zeta_{\nu}^{(2)'}(ka)}{\zeta_{\nu}^{(2)}(ka)}.$$

The reflecting property of the ground therefore should not notably affect the intensity of the lowest order waves. If we put  $k_1 = k$ , i. e., the reflecting sphere is removed, the result is substantially the same.

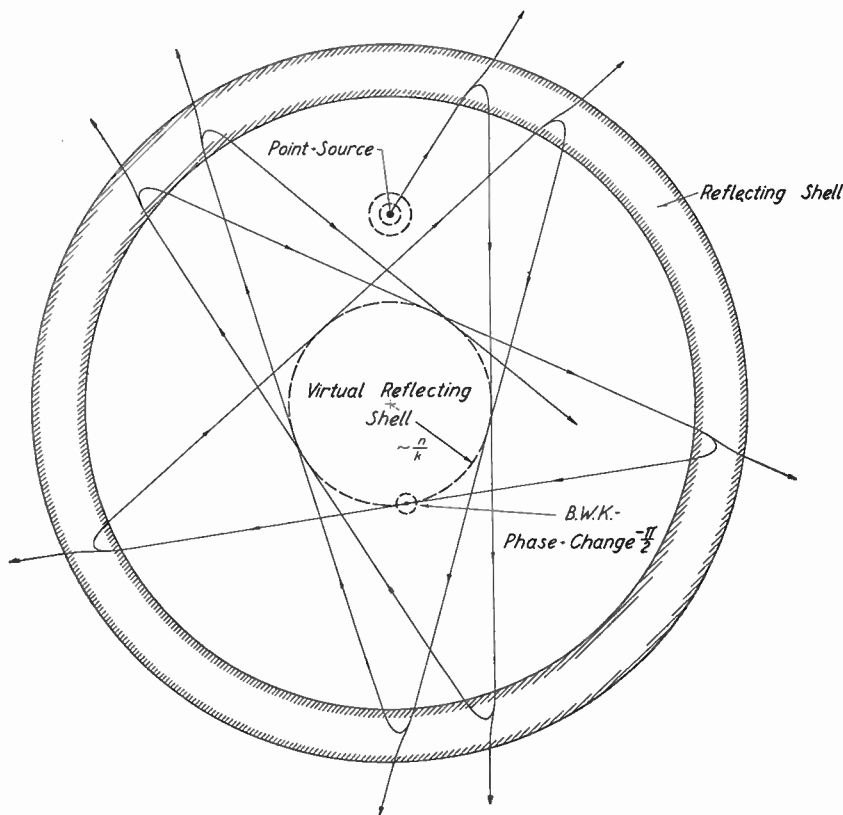


Fig. 25.

The physical meaning of this is clear if we study fig. 25 which depicts how a ray from a point source forms its own virtual reflecting shell. If the wave-length is extremely short a sharp shadow sphere is formed. If a smaller sphere with arbitrary  $k$  is placed concentrically in the shadow sphere it will disturb the picture only if the wave-length is so long that the shadow edge is not sufficiently sharp.

If we make use of the addition theorem (76) we infer that the radially standing wave produced by virtual reflection is

$$\frac{\zeta_v^{(1)}(kb)}{kb} \cdot \frac{\zeta_v^{(2)}(kr) + \zeta_v^{(1)}(kr)}{kr}$$

The phase change down and up becomes

$$\mathcal{E} = \text{Phase} \left\{ \zeta_v^{(1)}(kr) / \zeta_v^{(2)}(kr) \right\}.$$

Since the important  $n$ -values are large we have, when  $kr > n$ , by (84) that

$$\Xi = 2 \gamma_r - \frac{\pi}{2}.$$

The W.K.B.-phase change comes from the exponential tail in the shadow sphere.

When  $kr < n$  we have by table I p. 55

$$\zeta_{\nu}^{(2)}(kr) + \zeta_{\nu}^{(1)}(kr) \sim \frac{1}{2} \cdot \left\{ \frac{n^2}{(kr)^2} - 1 \right\}^{-\frac{1}{4}} \cdot \exp. \left\{ \underbrace{- \int_{kr}^n \left( \frac{n^2}{x^2} - 1 \right)^{\frac{1}{2}} dx}_{-|\gamma_r|} \right\}.$$

Since  $|\gamma_r| \approx \frac{2}{3} \frac{3}{2} (n)^{-\frac{1}{2}} \cdot (k \Delta r)^{\frac{3}{2}}$ , where  $k \Delta r = |n - kr|$ , one infers that the sharpness of the shadow edge increases very rapidly with the wave frequency.

The value of  $\frac{n}{k}$  corresponding to a certain  $\gamma_c$  value for the lowest order poles is

$$\frac{n}{k} \approx c \left\{ 1 - \frac{(3 \varrho_c)^{\frac{2}{3}}}{2} \cdot \omega - \frac{2}{3} \right\}.$$

This is the radius of the virtual reflecting shell. For short waves  $c - n/k \ll h$ , and the lowest order waves (which are guided practically exclusively by the outer shell) will not contribute appreciably to the signal strength even for very long distances. In the long-wave case, however, the low order waves will be important on account of the slow decay of the exponential tail.

Let us consider  $e_{\nu_s} / \Phi_1(n_s)$  for the lowest order terms in the residue series. Remembering that

$$R_1 R_4 \cdot \frac{\zeta_{\nu_s}^{(2)}(ka)}{\zeta_{\nu_s}^{(1)}(ka)} \cdot \frac{\zeta_{\nu_s}^{(1)}(kc)}{\zeta_{\nu_s}^{(2)}(kc)} = e^{j 2 s \pi},$$

we find from (208) for vertical polarization after a few transformations

$$\frac{e_{\nu_s}}{\Phi_1(n_s)} = \frac{2}{j} R_4^1 \cdot \frac{\zeta_{\nu_s}^{(1)}(kc)}{\zeta_{\nu_s}^{(2)}(kc)} \cdot \zeta_{\nu_s}^{(1)}(kb) \left\{ \frac{\psi_{\nu_s}(kb)}{\zeta_{\nu_s}^{(1)}(kb)} + \frac{\psi_{\nu_s}(ka)}{\zeta_{\nu_s}^{(1)}(ka)} \cdot R_{\nu_s}^1 \right\} \cdot \zeta_{\nu_s}^{(1)}(kr) \left\{ \frac{\psi_{\nu_s}(kr)}{\zeta_{\nu_s}^{(1)}(kr)} + \frac{\psi_{\nu_s}(ka)}{\zeta_{\nu_s}^{(1)}(ka)} \cdot R_{\nu_s}^1 \right\}, \quad (211)$$

where

$$R_{\nu_s}^1 = \frac{-\frac{\psi_{\nu_s}(ka)}{\zeta_{\nu_s}^{(1)}(ka)} + \frac{k}{k_1} \frac{\psi_{\nu_s}(k_1a)}{\zeta_{\nu_s}^{(1)}(k_1a)}}{\frac{\zeta_{\nu_s}^{(1)}(ka)}{\zeta_{\nu_s}^{(1)}(ka)} - \frac{k}{k_1} \frac{\psi_{\nu_s}(k_1a)}{\zeta_{\nu_s}^{(1)}(k_1a)}} = \frac{N(R_{\nu_s}^1)}{D(R_{\nu_s}^1)} \quad (212)$$

For the lowest order wave  $|e_a| \gg 1$ , and

$$R_{\nu_s}^1 \approx \frac{1 - \frac{k}{k_1} \frac{\psi_{\nu_s}(k_1a)}{\zeta_{\nu_s}^{(1)}(k_1a)} \cdot \left\{ \frac{n_s^2}{k^2 a^2} - 1 \right\}^{-\frac{1}{2}}}{1 + \frac{k}{k_1} \frac{\psi_{\nu_s}(k_1a)}{\zeta_{\nu_s}^{(1)}(k_1a)} \cdot \left\{ \frac{n_s^2}{k^2 a^2} - 1 \right\}^{-\frac{1}{2}}}.$$

It is especially interesting to note that  $b$  and  $r$  appear symmetrically in (211) indicating the self-evident fact that it is equally profitable to raise the receiver as it is to raise the sender.

After a slight transformation one obtains

$$\zeta_{\nu_s}^{(1)}(kr) \left\{ \frac{\psi_{\nu_s}(kr)}{\zeta_{\nu_s}^{(1)}(kr)} + \frac{\psi_{\nu_s}(ka)}{\zeta_{\nu_s}^{(1)}(ka)} \cdot R_{\nu_s}^1 \right\} = \zeta_{\nu_s}^{(1)}(kr) \left[ \frac{j}{\left\{ \zeta_{\nu_s}^{(1)}(ka) \right\}^2 \cdot D(R_{\nu_s}^1)} + \frac{1}{2} \left\{ \frac{\zeta_{\nu_s}^{(2)}(kr)}{\zeta_{\nu_s}^{(1)}(kr)} - \frac{\zeta_{\nu_s}^{(2)}(ka)}{\zeta_{\nu_s}^{(1)}(ka)} \right\} \right] = L_{\nu_s}^1. \quad (213)$$

For the lowest order waves  $|e_a| \gg 1$ , and

$$L_{\nu_s}^1 \sim \left( \frac{n^2}{k^2 \gamma^2} - 1 \right)^{-\frac{1}{4}} \cdot e^{|\gamma_r| - 2|\gamma_a|} \left[ \frac{1}{1 - j \frac{k}{k_1} \left\{ 1 - \frac{n_s^2}{k_1^2 a^2} \right\}^{\frac{1}{2}} \cdot \left\{ \frac{n_s^2}{k^2 a^2} - 1 \right\}^{-\frac{1}{2}}} + \frac{1}{2} \left( e^{2(|\gamma_a| - |\gamma_r|) - 1} \right) \right]. \quad (213 a)$$

First when  $\exp. (2 |\gamma_a| - 2 |\gamma_r|) \gg 1$ , is it possible to neglect the ground influence in (213). Since

$$|\gamma_a| - |\gamma_r| \approx \left( \frac{4 n_s^2}{k^2 (a + r)^2} - 1 \right)^{\frac{1}{2}} \cdot k (r - a),$$

very long low order waves will keep their surface characteristic a considerable distance above ground. When  $r = c$  we have

$$L_{\nu_s}^1 = \frac{\zeta_{\nu_s}^{(1)}(k c)}{2} \cdot \frac{\zeta_{\nu_s}^{(2)}(k a)}{\zeta_{\nu_s}^{(1)}(k a)} \cdot R_1^1 (1 + R_4^1).$$

This does not contradict what has just been said regarding the ground influence, since  $R_1^1 \approx -1$  for the lowest order wave. Hence we infer that the propagation of the lowest order wave is mainly governed by the properties of the reflecting shell. The ground properties are influential only in the ground neighbourhood.

The intensity of the lowest order wave generally decreases very rapidly when  $r < n_s$  as shown by (213 a). Only for very long waves, for which the decrease is comparatively slow, are the lowest order waves of importance ( $\theta$  fairly large). The contribution from the low order waves appears to be a characteristic feature of the long distance propagation of very long radio waves.

For the higher order waves (high angle) we obtain

$$L_{\nu_s}^1 \sim -\frac{1}{2} \left\{ 1 - \frac{n^2}{k^2 r^2} \right\}^{-\frac{1}{4}} \cdot e^{j \left( \gamma_r - 2 \gamma_a - \frac{\pi}{4} \right)} \left\{ R_1^1 + e^{j (2 \gamma_a - 2 \gamma_r)} \right\}.$$

Since

$$2 \gamma_r - 2 \gamma_a \approx \frac{r - a}{c - a} (2 \gamma_c - 2 \gamma_a),$$

we have

$$\begin{aligned} L_{\nu_s}^1 \sim & -\frac{1}{2} \left\{ 1 - \frac{n^2}{k^2 r^2} \right\}^{-\frac{1}{4}} \cdot e^{-j \left( \gamma_a + \frac{\pi}{4} \right)} \cdot R_1^{\frac{1}{2}} \left\{ R_1^{\frac{1}{2}} \frac{1}{c - a} \cdot R_4^1 \frac{1}{2} \cdot \frac{r - a}{c - a} \cdot e^{j \pi s} \cdot \frac{r - a}{c - a} + \right. \\ & \left. + R_1^1 \frac{1}{2} \frac{c - r}{c - a} \cdot R_4^1 \frac{1}{2} \frac{r - a}{c - a} \cdot e^{-j \pi s} \cdot \frac{r - a}{c - a} \right\}. \end{aligned} \tag{214}$$

Introducing

$$\alpha_0 = \frac{r - a}{c - a} \left\{ \pi s - \frac{1}{2} \text{Phase} (R_4^1) \right\} + \frac{1}{2} \frac{c - r}{c - a} \cdot \text{Phase} (R_1^1),$$

and

$$\beta_0 = -\frac{1}{2} \frac{c - r}{c - a} \cdot \ln |R_1^1| + \frac{1}{2} \frac{r - a}{c - a} \ln |R_4^1|,$$

$$|L_{\nu_s}| \sim \frac{1}{2} \left| \left\{ 1 - \frac{n_s^2}{k^2 r^2} \right\}^{\frac{1}{4}} \cdot e^{-j \left( \gamma_a + \frac{\pi}{4} \right)} \cdot R_1^1 \right|^{\frac{1}{2}} \cdot 2 \left\{ \cos^2 \alpha_0 + \sinh^2 \beta_0 \right\}^{\frac{1}{2}}. \quad (214 a)$$

This demonstrates how radially standing waves (selected by means of the phase integral relation) are set up between ground and shell. In the non-dissipative case equidistant node surfaces are produced in the propagation space. When  $R_1^1 = R_4^1$  it appears from (196 a) that the intensity is practically the same at the ground and at the reflector.

So far we have not said anything about the field strength. Making use of (99) we find that the original residue series (214) can be used providing the following  $e_{\nu_s} / \Phi_1 (n_s)$  expressions are used.

For  $E_r$ :

$$\frac{e_{\nu_s}}{\Phi_1 (n_s)} = \frac{2 A_1 r}{j b} \cdot \left( \frac{n_s}{k r} \right)^2 \cdot R_4^1 \cdot \frac{\zeta_{\nu_s}^{(1)} (k c)}{\zeta_{\nu_s}^{(2)} (k c)} \cdot \zeta_{\nu_s}^{(1)} (k b) \left\{ \frac{\psi_{\nu_s} (k b)}{\zeta_{\nu_s}^{(1)} (k b)} + \frac{\psi_{\nu_s} (k a)}{\zeta_{\nu_s}^{(1)} (k a)} \cdot R_{\nu_s}^1 \right\} \cdot \zeta_{\nu_s}^{(1)} (k r) \left\{ \frac{\psi_{\nu_s} (k r)}{\zeta_{\nu_s}^{(1)} (k r)} + \frac{\psi_{\nu_s} (k a)}{\zeta_{\nu_s}^{(1)} (k a)} \cdot R_{\nu_s}^1 \right\},$$

for  $E_\theta$ :

$$\frac{e_{\nu_s}}{\Phi_1 (n_s)} = \frac{2 A_1 r}{b} \cdot \frac{n_s}{k r} \cdot R_4^1 \cdot \frac{\zeta_{\nu_s}^{(1)} (k c)}{\zeta_{\nu_s}^{(2)} (k c)} \cdot \zeta_{\nu_s}^{(1)} (k b) \left\{ \frac{\psi_{\nu_s} (k b)}{\zeta_{\nu_s}^{(1)} (k b)} + \frac{\psi_{\nu_s} (k a)}{\zeta_{\nu_s}^{(1)} (k a)} \cdot R_{\nu_s}^1 \right\} \cdot \zeta_{\nu_s}^{(1)'} (k r) \cdot \left\{ \frac{\psi_{\nu_s} (k r)}{\zeta_{\nu_s}^{(1)'} (k r)} + \frac{\psi_{\nu_s} (k a)}{\zeta_{\nu_s}^{(1)} (k a)} \cdot R_{\nu_s}^1 \right\}, \quad (2)$$

and for  $H_\varphi$ :

$$\left\{ \frac{e_{\nu_s}}{\Phi_1 (n_s)} \right\}_{H_\varphi} = \frac{k r}{z_0 n_s} \cdot \left\{ \frac{e_{\nu_s}}{\Phi_1 (n_s)} \right\}_{E_r}.$$

We introduce the notations  $\Delta E_r, \Delta E_\theta, \Delta H_\varphi$  for the field strength components corresponding to the individual waves of the residue series. Thus

$$\left. \begin{aligned} \frac{\Delta E_r}{\Delta H_\varphi} &= \frac{n_s}{k r} = \sin \varphi_r, \\ \frac{\Delta E_r}{\Delta E_\theta} &= \frac{n_s}{j k r} \cdot \frac{\psi_{\nu_s}(k r) + \bar{\mu} \zeta_{\nu_s}^{(1)}(k r)}{\psi_{\nu_s}'(k r) + \bar{\mu} \zeta_{\nu_s}^{(1)'}(k r)}, \end{aligned} \right\} \quad (216)$$

and

where

$$\bar{\mu} = \frac{\psi_{\nu_s}(k a)}{\zeta_{\nu_s}^{(1)}(k a)} \cdot R_{\nu_s}^1.$$

We can, of course, also write

$$\frac{E_r}{E_\theta} = \frac{n_s}{j k r} \cdot \frac{\zeta_{\nu_s}^{(1)}(k r)}{\zeta_{\nu_s}^{(1)'}(k r)} \cdot \frac{\frac{\zeta_{\nu_s}^{(2)}(k a)}{\zeta_{\nu_s}^{(1)}(k a)} \cdot R_1^1 + \frac{\zeta_{\nu_s}^{(2)}(k r)}{\zeta_{\nu_s}^{(1)}(k r)}}{\frac{\zeta_{\nu_s}^{(2)}(k a)}{\zeta_{\nu_s}^{(1)}(k a)} \cdot R_1^1 + \frac{\zeta_{\nu_s}^{(2)'}(k r)}{\zeta_{\nu_s}^{(1)'}(k r)}} = \frac{n_s}{j k r} \cdot \frac{\frac{\zeta_{\nu_s}^{(2)}(k c)}{\zeta_{\nu_s}^{(1)}(k c)} + R_4^1 \cdot \frac{\zeta_{\nu_s}^{(2)}(k r)}{\zeta_{\nu_s}^{(1)}(k r)}}{\frac{\zeta_{\nu_s}^{(2)}(k c)}{\zeta_{\nu_s}^{(1)}(k c)} + R_4^1 \cdot \frac{\zeta_{\nu_s}^{(2)'}(k r)}{\zeta_{\nu_s}^{(1)'}(k r)}}. \quad (216 a)$$

In the WATSON-case one easily obtains

$$\left. \begin{aligned} \left( \frac{\Delta E_r}{\Delta E_\theta} \right)_{r=a} &= -j \frac{n_s}{k a} \cdot \frac{k_1}{k} \cdot \frac{\psi_{\nu_s}(k_1 a)}{\psi_{\nu_s}'(k_1 a)} \sim - \frac{n_s}{k a} \cdot \frac{k_1}{k} \cdot \left\{ 1 - \frac{n_s^2}{(k_1 a)^2} \right\}^{\frac{1}{2}}, \\ \left( \frac{\Delta E_r}{\Delta E_\theta} \right)_{r=c} &= -j \frac{n_s}{k c} \cdot \frac{k_3}{k} \cdot \frac{\zeta_{\nu_s}^{(1)}(k_3 c)}{\zeta_{\nu_s}^{(1)}(k_3 c)} \sim \frac{n_s}{k c} \cdot \frac{k_3}{k} \cdot \left\{ 1 - \frac{n_s^2}{(k_3 c)^2} \right\}^{\frac{1}{2}}, \end{aligned} \right\} \quad (216 b)$$

i. e., the electric field of the wave at the surface is rotational and (216 b) yields the familiar ellipses of the electric vector.

Let us further consider the general case  $a < r < c$  for the higher order waves. With the notations of p. 114 we find

$$\frac{\Delta E_r}{\Delta E_\theta} = j \tan \varphi_r \cdot \cot(\alpha_0 + j \beta_0). \quad (216 c)$$

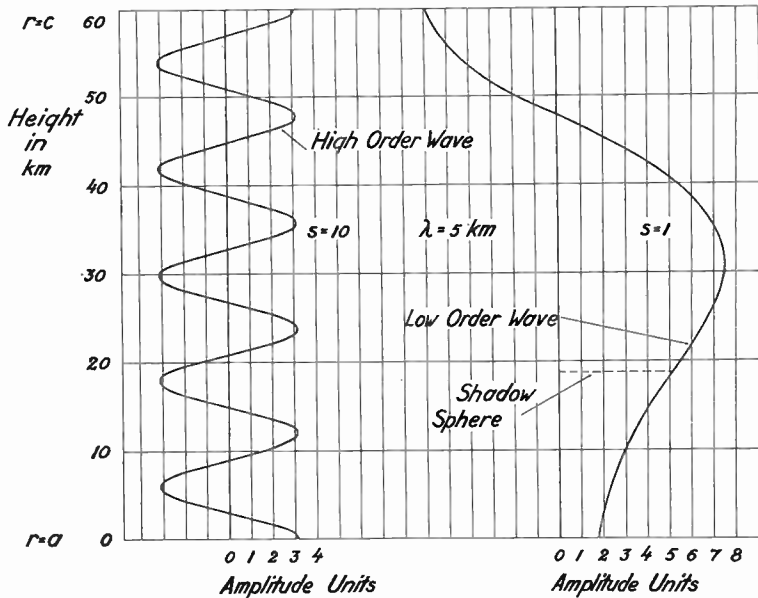


Fig. 26. The low and high order waves in the propagation of long vertically polarized radio waves.

This can also be written

$$\frac{\Delta E_r^-}{\Delta E_\theta} = \tan \varphi_r \cdot \left\{ \frac{\sinh^2 \beta_0 + \cos^2 \alpha_0}{\sinh^2 \beta_0 + \sin^2 \alpha_0} \right\}^{\frac{1}{2}} \exp. \left[ j \left\{ \arctan \left( \frac{\sin 2 \alpha_0}{\sinh 2 \beta_0} \right) \right\} \right]$$

In the nodal surfaces where  $\sin \alpha_0$  or  $\cos \alpha_0$  is zero, one of the axes is vertical. When the losses are small the electric field is practically a purely alternating one in these surfaces.

Denoting the axes of the vector ellipse by  $d_r$  and  $d_\theta$  one further easily finds in the non-dissipative case that

$$d_r^2 + d_\theta^2 = \text{const.} \cdot \sin^2 2 \varphi_r,$$

i. e., the intensity of the individual wave is practically the same from ground to reflector.

As a final illustration of the radial nature of the high and low order waves we have in fig. 26 plotted the variation of  $\Delta E_r$  with height for the two cases. The reflecting shell is homogeneous and the reflection losses have been neglected for the sake of simplicity. The layer height is 60 km and the wave-length is 5 km. The order of the wave, denoted by  $s$ , is also shown in fig. 26.

Making use of the notation  $a \theta = D$ , we have

$$U(r, \theta) \sim \frac{e^{j(kD - \omega t)}}{jD} \cdot \left(\frac{8\pi\theta}{\sin\theta}\right)^{\frac{1}{2}} \cdot \frac{a}{rb} \sum_{s=0}^{s=\infty} (n_s \theta)^{\frac{1}{2}} \cdot \frac{e_{\nu_s}}{\Phi_1(n_s)\Phi_3(n_s)} \cdot e^{j\left(\frac{5}{4}\pi + \frac{\Delta n_s}{a} \cdot D\right)}.$$

Accordingly in practical units (all lengths in meters)

$$E_r(r, \theta) \sim \Delta K \cdot \frac{120\pi}{j\lambda D} \cdot e^{j(kD - \omega t)} \cdot \left(\frac{\theta}{\sin\theta}\right)^{\frac{1}{2}} \cdot \sum_{s=0}^{s=\infty} \frac{a/b}{kb} (2\pi\theta n_s)^{\frac{1}{2}} \cdot \left(\frac{n_s}{kr}\right)^2 \cdot \frac{e_{\nu_s}}{\Phi_1(n_s)\Phi_3(n_s)} \cdot e^{j\left(\frac{4}{5}\pi + \frac{\Delta n_s}{a} D\right)}. \text{ Volts/meter} \quad (217)$$

AUSTIN's formula yields

$$|E| = \Delta K \cdot \frac{120\pi}{\lambda D} \cdot \left(\frac{\theta}{\sin\theta}\right)^{\frac{1}{2}} \cdot e^{-\beta D}. \text{ Volts/meter}$$

AUSTIN's attenuation coefficient  $e^{-\beta D}$  thus must be considered an approximate average of the above sum.

In the case of increased attenuation only the first few terms in the residue series have to be considered and in such a case

$$|E_r(r, \theta)| \approx \Delta K \cdot \frac{120\pi}{\lambda R} \cdot \left| \frac{U^1}{2U_{pr}^1} \right|. \text{ Volts/meter} \quad (218)$$

The power radiated by the vertical current element and by the horizontal loop in free space is

$$P_{\text{watt}} = \frac{\pi z_0}{3} \left(\frac{\Delta K}{\lambda}\right)^2, \text{ and } P_{\text{watt}} = \frac{\pi z_0}{3} \left(\frac{J S k}{\lambda}\right)^2.$$

Relation (218) can therefore also be written in the familiar form

$$\left. \begin{aligned} |E_\varphi(r, \theta)| \\ |E_r(r, \theta)| \end{aligned} \right\} \approx \frac{3 \cdot 10^5}{R_{\text{km}}} \cdot \sqrt{P_{\text{kw}}} \cdot \left\{ \begin{aligned} \left| \frac{U}{U_{pr}} \right| \\ \left| \frac{U^1}{U_{pr}^1} \right| \end{aligned} \right\} \cdot \mu \text{ Volts/meter} \quad (219)$$

We find for the high order waves when the ionospheric intrusion can not be neglected

$$\Phi_3 \approx 2j \cdot \frac{h + \Delta h_0}{c} \cdot \tan \varphi_c \cdot \left( \sin \varphi_c \approx \frac{n_s}{kc} \right) \quad (219)$$

Putting  $\varphi_c \approx \varphi_a = \varphi_s$ , we have for the high order waves when  $k_1 \rightarrow \infty$  and the polarization is vertical

$$\frac{e_{\nu_s}}{\Phi_1(n_s)\Phi_3(n_s)} \approx -\frac{a}{h + \Delta h_v} \cdot \frac{\cos(\gamma_b - \gamma_a) \cdot \cos(\gamma_r - \gamma_a)}{\sin \varphi_s}, \quad (220)$$

and the contribution to  $E_r(r, \theta)$  from the high-order terms ( $s \geq M$ ) becomes

$$\begin{aligned} \Delta E_r^{(M)} \sim \Delta K \cdot \frac{120 \pi}{j \lambda D} \cdot e^{j(kD - \omega t)} \cdot \left(\frac{\theta}{\sin \theta}\right)^{\frac{1}{2}} \cdot \sum_{s=M}^{s=\infty} \left(\frac{2\pi \theta}{ka}\right)^{\frac{1}{2}} \cdot \frac{a}{h + \Delta h_v} \\ \cdot \sin^{\frac{2}{3}} \varphi_s \cdot \cos(\gamma_b - \gamma_a) \cdot \cos(\gamma_r - \gamma_a) \cdot e^{j\left(\frac{\pi}{4} + \frac{\Delta n_s}{a} D\right)} \cdot \left(\frac{h}{a} \ll 1\right). \end{aligned} \quad (221)$$

### The Limiting Case of a Plane Boundary.

In this section we will show how the solution of the problem of the plane boundary can be obtained as a limiting case of the spherical solution. To that end we let  $a \rightarrow \infty$  while keeping constant the quantities  $a\theta = D$ ,  $c - a = h_{ca}$ ,  $b - a = h_{ba}$ ,  $r - a = h_{ra}$ , etc.

Introducing the new variable  $\lambda_1 = k \sin \varphi = \frac{n}{a}$ , we have

$$\lim_{\substack{a \rightarrow \infty \\ b - a = h_{ba}}} \frac{\zeta_{\nu}^{(1)}(kb)}{\zeta_{\nu}^{(1)}(ka)} = e^{-\alpha_2 h_{ba}},$$

where  $\alpha_2 = (\lambda_1^2 - k^2)^{\frac{1}{2}}$ . Further introducing the quantity  $\alpha_1 = (\lambda_1^2 - k_1^2)^{\frac{1}{2}}$ , we find for vertical polarization

$$\lim_{a \rightarrow \infty} \frac{e_{\nu}}{g_{\nu}} = \frac{k}{2\alpha_2} \cdot \frac{e^{-\alpha_2 h_{rb}} \left(1 + r_{21}^1 e^{-\alpha_2 2 h_{ba}}\right) \left(1 + r_4^1 e^{-\alpha_2 2 h_{cr}}\right)}{1 - r_{21}^1 r_4^1 e^{-\alpha_2 2 h_{ca}}}, \quad (h_{ra} > h_{ba})$$

where

$$r_{21}^1 = \frac{k_1^2 \alpha_2 - k^2 \alpha_1}{k_1^2 \alpha_2 + k^2 \alpha_1},$$

is the plane FRESNEL coefficient for vertical polarization and  $r_4^1$  is the plane coefficient for the reflector. In the WATSON case

$$r_4^1 = r_{23}^1 = \frac{k_3^2 a_2 - k^2 a_3}{k_3^2 a_2 + k^2 a_3},$$

where  $a_3 = (\lambda_1^2 - k_3^2)^{\frac{1}{2}}$ .

Since  $\frac{n \, dn}{a \, b} \rightarrow \lambda_1 \, d\lambda_1$ , and

$$\begin{aligned} \lim_{a \rightarrow \infty} \frac{P_\nu \{ \cos(\pi - \theta) \}}{\cos n \pi} &= \lim_{a \rightarrow \infty} \frac{P_\nu \{ \cos(\pi - \theta) \}}{\cos n \pi} = 2j J_0(\lambda_1 D), \\ \text{Im}(n) > 0 & \qquad \qquad \qquad \text{Im}(n) < 0 \end{aligned}$$

[5] we obtain from relation (107)

$$II = \frac{A_1}{j k} \int_0^\infty \frac{\lambda_1 \, d\lambda_1}{a_2} \cdot J_0(D \lambda_1) \cdot \frac{e^{-a_2 h_{rb}} \left( 1 + r_{21}^1 e^{-a_2 h_{ba}} \right) \left( 1 + r_4^1 e^{-a_2 h_{cr}} \right)}{1 - r_{21}^1 r_4^1 e^{-a_2 h_{ca}}} \quad (r > b) \quad (222)$$

If we consider the transmission of waves between two identical reflectors, i. e.,  $r_{21}^1 = r_4^1$ , and if we further place the sender midway between them, we observe that

$$\frac{1 + r_{21}^1 e^{-a_2 h_{ba}}}{1 - r_{21}^1 r_4^1 e^{-a_2 h_{ca}}} = \frac{1}{1 - r_4^1 \cdot 1 \cdot e^{-a_2 h_{ca}}}$$

We thus see that this case is identical with the case of a transmitter on a perfect reflector a distance  $\frac{1}{2} h_{ca}$  from the other reflector as expected for symmetrical reasons.

In the special case  $h_{ba} = 0$ ,  $r_{21}^1 = 1$ , and  $r_4^1 = r_{23}^1$ , we find

$$II = \frac{A_1 e^{j k R}}{j k R} + \frac{2 A_1}{j k} \int_0^\infty \frac{\lambda_1 \, d\lambda_1}{a_2} \cdot J_0(D \lambda_1) \cdot e^{-a_2 h_{ca}} \cdot r_{23}^1 \cdot \frac{\cosh(a_2 h_{ra})}{1 - r_{23}^1 e^{-a_2 h_{ca}}},$$

since according to SOMMERFELD

$$\frac{e^{j k R}}{R} = \int_0^\infty \frac{\lambda_1 \, d\lambda_1}{a_2} \cdot J_0(D \lambda_1) e^{-a_2 h_{ra}} \quad (h_{ra} > 0).$$

This result is found in a slightly different form by ECKERSLEY [4] who, however, appears to have lost a factor  $e^{-a_2 h_{ca}}$  in the numerator.

In the case of perfect reflectors ( $r_{23}^1 = 1 = r_{21}^1$ ) we finally obtain the elementary result

$$H = \frac{A_1}{j k} \sum_{p=0}^{p=\infty} e^{j k R_p} \frac{1}{R_p}.$$

where  $k R_p$  denotes the iconal of a ray of order  $p$ .

### A Short Discussion of the Case of the Poor Reflector.

When the reflecting power of the shell decreases and  $|R_4^1| \ll 1$  it does not appear to be an easy matter to obtain the corresponding value of the low order poles from the previous relation

$$1 - R_1^1 R_4^1 \frac{\zeta_{\nu_s}^{(2)}(ka) \zeta_{\nu_s}^{(1)}(kc)}{\zeta_{\nu_s}^{(1)}(ka) \zeta_{\nu_s}^{(2)}(kc)} = 0.$$

It is obvious that the zeros of  $(\Phi_1 \cdot \Phi_2)$  are also the zeros of

$$\frac{1}{R_1^1} \cdot \frac{\zeta_{\nu_s}^{(1)}(ka)}{\zeta_{\nu_s}^{(2)}(ka)} - R_4^1 \cdot \frac{\zeta_{\nu_s}^{(1)}(kc)}{\zeta_{\nu_s}^{(2)}(kc)}, \tag{223}$$

which is a more suitable expression when  $|R_4^1|$  is small. Introducing a new reflection factor

$$R_1^1 = \frac{\frac{\Psi'_{\nu_s}(ka)}{\Psi_{\nu_s}(ka)} - \beta_n}{-\frac{\Psi'_{-\nu_s-1}(ka)}{\Psi_{-\nu_s-1}(ka)} + \beta_n} = \frac{N(R_1^1)}{D(R_1^1)}, \tag{224}$$

it is easily shown that

$$\frac{\zeta_{\nu_s}^{(2)}(ka)}{\zeta_{\nu_s}^{(1)}(ka)} - \beta_n = \frac{\mp j}{\cos \nu_s \pi} \left\{ 1 - e^{\pm (n_s + 1) j} \frac{\Psi_{\nu_s}(ka)}{\Psi_{-\nu_s-1}(ka)} \cdot R_1^1 \right\} \cdot \Psi_{-\nu_s-1}(ka) \cdot \frac{D(R_1^1)}{\zeta_{\nu_s}^{(1)}(ka)}. \tag{225}$$

This immediately yields

$$\frac{1 - e^{(n_s + 1) \pi j} \frac{\Psi_{\nu_s}(ka)}{\Psi_{-\nu_s-1}(ka)} \cdot \mathbf{R}_1^1}{1 - e^{-(n_s + 1) \pi j} \frac{\Psi_{\nu_s}(ka)}{\Psi_{-\nu_s-1}(ka)} \cdot \mathbf{R}_1^1} = - \frac{\zeta_{\nu_s}^{(2)}(ka)}{\zeta_{\nu_s}^{(1)}(ka)} \cdot \mathbf{R}_1^1, \quad (226)$$

which inserted in (223) leads to the following pole-relation, viz.

$$e^{-(n_s + 1) \pi j} \cdot \frac{\Psi_{\nu_s}(ka)}{\Psi_{-\nu_s-1}(ka)} \cdot \mathbf{R}_1^1 \cdot \frac{1 + \frac{\zeta_{\nu_s}^{(1)}(kc)}{\zeta_{\nu_s}^{(2)}(kc)} \mathbf{R}_4^1 \cdot e^{jn_s \pi}}{1 + \frac{\zeta_{\nu_s}^{(1)}(kc)}{\zeta_{\nu_s}^{(2)}(kc)} \mathbf{R}_4^1} = e^{j2s\pi} \quad (227)$$

It is to be noted, that  $s$  here is not the same  $s$  as appeared in the previous pole relations. When  $\mathbf{R}_4^1 = 0$ , we are left with the relation

$$e^{-(n_s + 1) \pi j} \cdot \frac{\Psi_{\nu_s}(ka)}{\Psi_{-\nu_s-1}(ka)} \cdot \mathbf{R}_1^1 = e^{j2s\pi} \quad (228)$$

This relation which has been found by VAN DER POL and BREMMER [21] yields the poles of the reflector-free case. These poles are all situated in region c) where  $\Psi_{\nu_s}(ka) \approx \frac{1}{2} S_{\nu_s}^{(1)}(ka)$  (except for the lowest order pole where the HANKEL formula has to be used). When this approximation holds one immediately finds  $\mathbf{R}_1^1$  equal to the plane FRESNEL coefficient for vertical polarization. One further obtains the familiar phase integral relation

$$\gamma_a = \int_{n_s}^{ka} \left\{ 1 - \frac{n_s^2}{x^2} \right\}^{\frac{1}{2}} dx = \pi \left( s - \frac{1}{4} \right) + \frac{j}{2} \ln \mathbf{R}_1^1. \quad (229)$$

Removal of the spherical earth is formally effected by putting  $k_1 = k$ . When this is the case we have

$$R_1^1 = \frac{\zeta_{\nu_s}^{(1)}(k a)}{\zeta_{\nu_s}^{(2)}(k a)}, \quad (k = k_1). \tag{230}$$

and therefore

$$R_4^1 \frac{\zeta_{\nu_s}^{(1)}(k c)}{\zeta_{\nu_s}^{(2)}(k c)} = e^{j 2 s \pi}. \quad (k = k_1) \tag{231}$$

For poles not too close to  $k c$  we therefore have

$$\gamma_c = \int_{n_s}^{k c} \left\{ 1 - \frac{n_s^2}{x^2} \right\}^{\frac{1}{2}} dx = \pi \left( s + \frac{1}{4} \right) + \frac{j}{2} \ln R_4^1. \tag{232}$$

Since the first phase integral relation (229) only holds in region  $c$ ) of fig. 12,  $s$  may in this case be restricted to the values  $s = 0, -1, 1-2, -3, \dots$ . The second phase integral relation (232), however, only holds in region  $a$ ) and in this case  $s$  may therefore be restricted to the values  $s = 0, 1, 2, 3, \dots$ .

It is of particular interest to note that formally identical phase integral relations hold for the proper values of the waves guided by the inside of the spherical surface and for the waves diffracted over the outside of the spherical surface.

Returning to the complete pole relation (227) we note that the correction in  $R_1^1$  due to the poor reflector approximately is

$$- R_1^1 \cdot \frac{\frac{\zeta_{\nu_s}^{(1)}(k c)}{\zeta_{\nu_s}^{(2)}(k c)} R_4^1}{1 + \frac{\zeta_{\nu_s}^{(1)}(k c)}{\zeta_{\nu_s}^{(2)}(k c)} \cdot R_4^1},$$

since  $\left| e^{j n_s \pi} \right| \ll 1$ .

When the earth is considered a perfect reflector and  $R_4^1 = 0$ , one has the familiar relation for the lowest order pole

$$n_0 = ka + 0,808 \cdot (ka)^{\frac{1}{3}} e^{j\frac{\pi}{3}}.$$

Therefore for waves not much longer than 1000 m and when  $h$  at least 60 km

$$\gamma_c \approx \frac{ka}{3} \cdot 2^{\frac{3}{2}} \cdot \left(\frac{h}{a}\right)^{\frac{3}{2}} \cdot e^{-j\epsilon_h},$$

where

$$\epsilon_h \approx \frac{(ka)^{\frac{1}{3}}}{kh} \cdot \frac{3^{\frac{3}{2}}}{4} \cdot 0,808.$$

Thus for  $\lambda = 1000$  m

$$\left| R_4^1 \cdot \frac{\zeta_{\nu_s}^{(1)}(kc)}{\zeta_{\nu_s}^{(2)}(kc)} \right| \sim e^{-2 \operatorname{Im}(\gamma_c)} \cdot |R_4^1| \sim 900 \cdot |R_4^1|.$$

This means that even a numerically very small  $R_4^1$  will tend to displace the zero order pole considerably. For  $\lambda = 100$  m,  $-\operatorname{Im}(\gamma_c)$  is  $(10)^{\frac{1}{3}}$  times greater and this effect is even more pronounced as expected.

In the case of a strongly absorbing sphere [5]

$$n_0 = ka + 1,856 \cdot e^{j\frac{\pi}{3}},$$

and the influence of the reflector is still greater. It has thus been shown that even a very poor reflector will tend to change the proper values considerably. This effect is especially considerable for the shorter waves.

## On the Attenuation Coefficient in Long Wave Transmission.

We have already discussed the attenuation coefficient of the high order waves in the special case of a homogeneous reflector (WATSON-case). We are now in a position to extend our study of the attenuation coefficient also to the case of the inhomogeneous reflector when the polarization is horizontal.

Returning to (210) and remembering that for very low losses

$$\eta_4 \approx 1 + j B e^{j \frac{\pi}{6}} \cdot \left| \frac{H_{\frac{2}{3}}^{(1)}(\varrho_c)}{H_{\frac{1}{3}}^{(1)}(\varrho_c)} \right| \cdot 2 \cos \left( \frac{\pi}{6} - \beta_c \right), \quad (233)$$

with

$$B = \left( \frac{|I|}{2} \right)^{\frac{1}{3}} \cdot \frac{\Gamma \left( \frac{1}{3} \right)}{\Gamma \left( \frac{2}{3} \right)} = y \cos \varphi_c \left( \frac{a}{3} \right)^{\frac{1}{3}} \frac{\Gamma \left( \frac{1}{3} \right)}{\Gamma \left( \frac{2}{3} \right)}, \quad (233 a)$$

we obtain the attenuation coefficient

$$\beta_1 \approx \frac{B}{\cos \varphi_c \cdot 2 a} \cdot \frac{\pi \varrho_c^0}{2} \cdot \left| H_{\frac{1}{3}}^{(1)}(\varrho_c^0) \right| \left| H_{\frac{2}{3}}^{(1)}(\varrho_c^0) \right| \cdot \cos \left( \frac{\pi}{6} - \beta_c \right) \approx \frac{B}{2 \cos \varphi_c \cdot a}. \quad (234)$$

Further neglecting the ground losses we get for the higher order waves, in accordance with *Relation I*, for low losses

$$\beta_s \approx \frac{\cos^2 \varphi_c}{2 h \sin \varphi_c} \left( \frac{a}{3} \right)^{\frac{1}{3}} y \frac{\Gamma \left( \frac{1}{3} \right)}{\Gamma \left( \frac{2}{3} \right)} \approx \frac{\cos^2 \varphi_c}{\sqrt{2} h \sin \varphi_c} \cdot \frac{\omega^{\frac{2}{3}} \nu^{\frac{1}{3}}}{\omega_{c_m}} \left\{ \frac{\pi \Delta h_m}{3 \lambda_{c_m}} \right\}^{\frac{1}{3}} \frac{\Gamma \left( \frac{1}{3} \right)}{\sqrt{2} \Gamma \left( \frac{2}{3} \right)}. \quad (235)$$

$(\varrho_a)_s \gg 1.$

In accordance with (138 c) we therefore find

$$\frac{(\beta_s)_{\text{inhomogeneous}}}{(\beta_1)_{\text{homogeneous}}} \approx \left( \frac{\omega}{\nu} \right)^{\frac{1}{6}} \left( \frac{\pi \Delta h_m}{3 \lambda_{c_m}} \right)^{\frac{1}{3}} \frac{\Gamma \left( \frac{1}{3} \right)}{\sqrt{2} \Gamma \left( \frac{2}{3} \right)}, \quad (\varrho_a)_s \gg 1. \quad (236)$$

i. e., there is not much difference between the two long wave cases.

An inspection of (188) further shows that (236) holds for the quadratic layer too.

In accordance with (70 a),  $\cos \varphi_c$  actually is

$$\cos \varphi_c = \left\{ 1 - \frac{n_s^2}{(kc)^2} - \frac{n_s^4}{(kc)^4} \cdot \Delta \chi^2 e^{j2\eta} \left( \frac{\Delta h_m}{c} \right)^2 \right\}^{\frac{1}{2}}. \quad (239)$$

So far we have neglected the last term in (239). For  $s = 1$  we have  $\varrho_c \approx 1$  or 2, i. e.,  $1 - n_1^2 / (kc)^2 > 1/192$ , when  $\lambda = 5$  km. Since  $\Delta h_m / c \approx 10^{-3}$ , if  $\Delta h_m = 6$  km, we have been well justified, however, in neglecting the last term. This holds even for a half-thickness of as much as 60 km.

\* \* \*

For low losses in accordance with (234) we have very approximately

$$\beta_1 \approx \frac{y (a/3)^{\frac{1}{3}}}{a} = \frac{1}{a} \cdot \left( \frac{\Delta h_m}{6 c_0} \right)^{\frac{1}{3}} \cdot \frac{f^{\frac{2}{3}} \nu^{\frac{1}{3}}}{f_{c_m}^{\frac{2}{3}}}. \quad (240)$$

It is especially interesting to note that the frequency dependence differs but slightly from the later AUSTIN formula for long distance day-time transmission which has

$$\beta \approx 0,73 \cdot 10^{-6} \cdot f^{0,6} \text{ km}^{-1} \quad (241)$$

for transmission over sea water. This coefficient is assumed to be independent of  $\gamma_0$ , the height of the sun.

For the *E*-layer as well as the *D*-layer we may put

$$f_{c_m} = (f_{c_m})_{\max} \cdot (\sin \gamma_0)^{\frac{1}{4}}. \quad (\gamma_0 > 0).$$

The density at the level of maximum ion production of the absorbing gas roughly is

$$\varrho_0 = (\varrho_0)_{\max} \cdot \sin \gamma_0. \quad (\gamma_0 > 0).$$

Putting as an approximation  $\nu$  proportional to  $\varrho_0$ , we have

$$\nu \approx \nu_{\max} \cdot \sin \gamma_0,$$

i. e.,

$$\beta_1 \approx \frac{1}{a} \left( \frac{\Delta h_m}{6 c_0} \right)^{\frac{1}{3}} f_{\max}^{\frac{2}{3}} \nu_{\max}^{\frac{1}{3}} \cdot (\sin \gamma_0)^{\frac{1}{6}} \cdot (\gamma_0 > 0) \quad (242)$$

According to this approximation  $\beta_1$  is practically independent of  $\gamma_0$  when  $\gamma_0 > 0$ , in complete agreement with the AUSTIN formula and later field-strength data.

It next remains to be seen if acceptable values of  $(f_{c_m})_{\max}$  and  $\nu_{\max}$  yield the proper attenuation or not. If we assume that  $\lambda = 5$  km and  $(\beta_1)_{\max} \approx 0,3 \cdot 10^{-3}$ , we find  $(f_{c_m})_{\max} \approx 300$  kc/s when  $\nu_{\max} = 5 \cdot 10^7$  (a reasonable value for the *D*-layer) and  $\Delta h_m = 6$  km. This value of  $(f_{c_m})_{\max}$  is not at all improbable. AUSTIN's formula (241) yields  $\beta \approx 0,5 \cdot 10^{-3}$  for the same wavelength.

Making use of (188) we find for the high angle terms in the case of a quadratic layer when the losses are small,

$$\beta_s \approx \frac{\cos^2 \varphi_s}{2 h \sin \varphi_s} \cdot \frac{\Gamma \left( \frac{1}{4} \right)}{\Gamma \left( \frac{3}{4} \right)} \cdot \frac{1}{(c_0^2 \bar{\sigma})^{\frac{1}{4}}} \cdot \omega^{\frac{3}{4}} \nu^{\frac{1}{4}} \cdot \sin \frac{\pi}{8} \cdot \quad (243)$$

since  $\bar{\sigma}$  is proportional to  $\omega_{c_m}$ , we have the approximation

$$\beta_s \approx (\beta_s)_{\max} \cdot (\sin \gamma_0)^{\frac{1}{8}}, \quad (\gamma_0 > 0) \quad (244)$$

which corresponds to (236).

So far we have only attempted a discussion of the day-time transmission ( $\gamma_0 > 0$ ). At the present stage it is not possible to say much about the transition from day to night conditions. During the night transatlantic field strength data yield a much smaller  $\beta$ -value. This is perhaps an indication of reflection in the *E*-region where  $\nu$  only is of the order of  $3 \cdot 10^5$ . For very long waves the sun-set transition takes place quite smoothly whereas for shorter long waves ( $\lambda \approx 5000$  m) this transition is marked by a very pronounced field strength minimum as shown in fig. 27 reproduced from ESPENSCHIED, ANDERSON, and BAILEY [22].

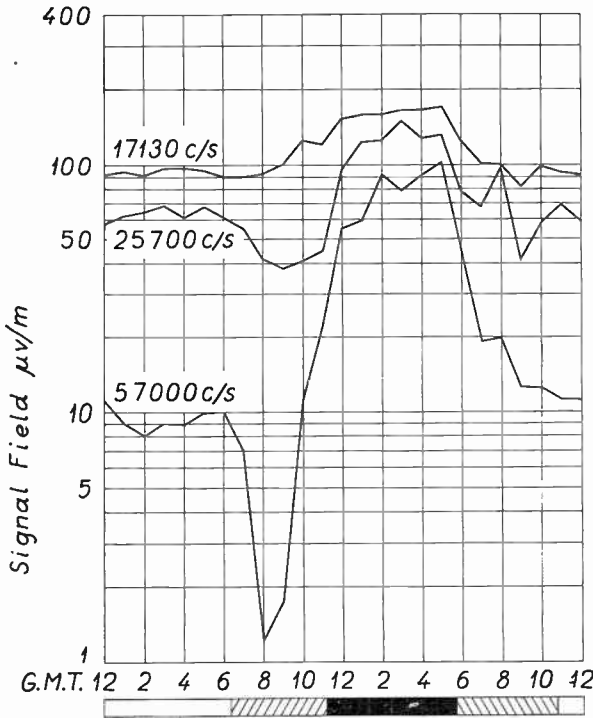


Fig. 27. Diurnal field strength data for transatlantic long wave transmission.

□ Entire path in daylight.    ■ Entire path in darkness.

When the entire path is in daylight typical field strength constancy is observed. The field strength minimum is observed only in the sunset zone and not in the sunrise zone. This phenomenon so far does not seem to have been satisfactorily explained. One remarkable feature of this field strength minimum should be mentioned, however. It appears to be more pronounced at the equinoxes than at other seasons. It is interesting to compare this circumstance with the fact that the ozone density of the *D*-region has its maxima and minima at these seasons.

It is evident that the field cannot be dependably predicted by a formula as simple as the AUSTIN one. The comparison between the attenuation coefficient of this formula and  $\beta_1$  therefore should not be taken too seriously. ESPENSCHIED, ANDERSON and BAILEY for example suggest  $\beta \approx 4 \cdot 10^{-6} \cdot f^{1.25}$ , where  $f$  in kc/s. This coefficient

is supposed to represent the experimental data better than does the AUSTIN coefficient.

Experimental data on the lower ionosphere unfortunately are extremely rare on account of the fact that the conventional echo-method of BREIT and TUVE cannot be used. BEST, RATCLIFFE and WILKES [23] measuring the phase change of ground and sky waves in long wave transmission estimate a day-time reflection level of 74 km for  $\lambda = 18,8$  km. Further research in this direction is desirable.

\* \* \*

Finally we have computed  $|U/U_{pr}|$  for  $\theta$  ranging from  $15^\circ$  to  $150^\circ$  for transmission over sea water and a homogeneous layer with  $\omega_c = 2\pi \cdot 0,768 \cdot 10^6$ ,  $\nu = 10^6$ ,  $\lambda = 5$  km and  $h = 60$  km. The result is shown in fig. 28.

For real long distance ( $\theta > 110^\circ$ ) only the first three terms in the residue series have to be considered. This means that the ground influence is quite small as we have already seen. Even if a comparison cannot be made it should be mentioned that FASSBENDER, EISNER and KURLBAUM [24] making field strength measurements in over land long wave transmission find but little difference between their attenuation coefficient and the AUSTIN value for  $\lambda \approx 3750$  m.

For  $\theta < 60^\circ$  the high angle waves also have to be considered and for  $\theta \approx 15^\circ$  it is necessary to consider twenty terms in the residue series. The high angle waves produce quite complicated interference phenomena. For  $\theta < 15^\circ$  so many terms have to be considered in the residue series that the numerical computation becomes quite cumbersome. Fig. 29 finally demonstrates the evaluation of the residue series for  $\theta = 45^\circ$ .

It is interesting to note that even for distances as long as  $45^\circ$  the third order term is the largest one numerically. For the case in question this term has  $n_s$  practically equal to  $ka$  as shown by fig. 14. For still longer distances the first and second order waves will become relatively more important.

In the case of the inhomogeneous layer the high angle waves may be less important than in the present case. Equally complicated

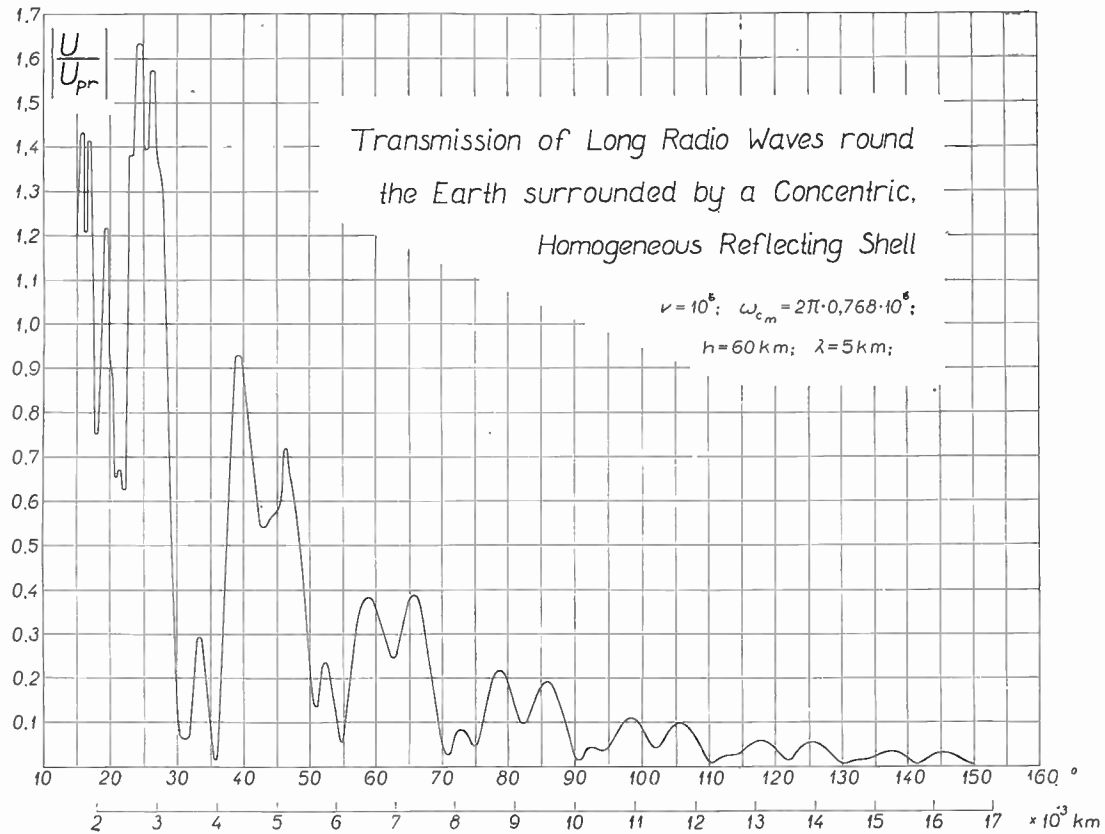


Fig. 28.

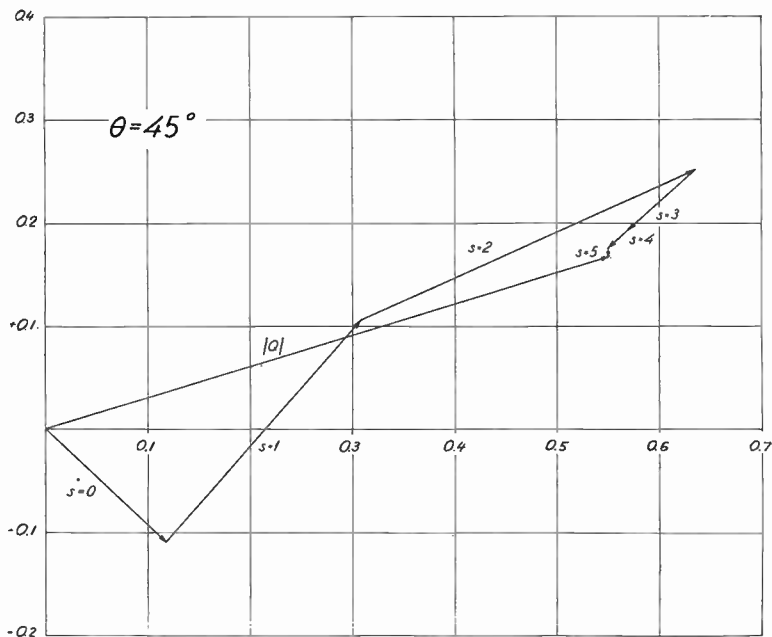


Fig. 29. Demonstrating the evaluation of the residue series.

interference phenomena are to be expected when  $\theta$  is relatively small, however.

It is finally of some interest to note the striking similarity between the  $|U/U_{pr}|$ -curve in the neighbourhood of  $\theta = 15^\circ$  and the common medium and short wave fading curves.

### The Reflection Coefficient of the Parabolic Layer in the Penetration Frequency Region.

So far we have not discussed the value of the reflection coefficient in the penetration frequency region. This frequency range is of considerable interest in connexion with investigations of the upper ionosphere.

The actual investigation of the reflection coefficient is somewhat complicated by the fact that the magnitude of the quantity  $\eta$  appearing in (55) becomes very large in this region when the losses are small. One finds (when  $a \gg 1$ )

$$(|\eta|)_{\max} \approx \frac{2}{\sin \psi}, \text{ if } (|\varrho|)_{\min} > \frac{1}{2},$$

and

$$(|\eta|)_{\max} \approx 8\alpha, \text{ if } (|\varrho|)_{\min} < \frac{1}{2}.$$

When the losses are small (as is the case in the upper ionosphere) expansion (55) therefore does not yield correct results in the penetration frequency region. This is also the region where the main deviation from the geometrical optics occurs.

Let us study the value of  $|\eta|$  in the penetration frequency region for the  $F_2$ - and  $E$ -layers. From reflection coefficient measurements the corresponding  $\nu$ -values are roughly known, viz.,  $2 \cdot 10^3$  and  $3 \cdot 10^5$ . One finds  $(|\varrho|)_{\min} \approx 0,4$  for the  $F_2$ -layer of half-thickness 120 km (such a value is not at all unusual) and a penetration wave-length of 30 m, a typical day-time value. This yields  $(|\eta|)_{\max} \approx 0,32 \cdot \pi \cdot 10^5$ . For the  $E$ -layer with a half-thickness of 12 km and a penetration wave-length of 90 m one further finds  $(|\varrho|)_{\min} \approx 12$ , i. e.,  $(|\eta|)_{\max} \approx 200$ . Expansion (55) is much less accurate for the  $F_2$ -layer than for the  $E$ -layer. For the  $D$ -layer on the other hand expansion (55) always appears to be a sufficiently accurate approximation (except of course for very long waves when the bridging approximation has to be used).

Of the quantities  $u$  and  $\varrho$  appearing in the wave functions  $u$  is practically constant in the penetration frequency region whereas  $\varrho$  generally is varying within very wide limits.

We had

$$\varrho = \alpha \{ (1 - y^2) \cos \psi - j (1 + y^2) \sin \psi \}.$$

Therefore  $|\varrho|$  is practically independent of the wave frequency in the penetration frequency region ( $y \approx 1$ ) when

$$1 - y^2 < 2 \tan \psi. \quad (246)$$

For the  $F_2$ - and  $E$ -layers, where  $\tan \psi \approx \frac{\nu}{2(\omega - \omega_H)}$ , we thus obtain the »band-width»

$$\frac{2 \Delta \omega \left( \omega_{c_m} - \frac{1}{2} \omega_H \right)}{\omega_{c_m}^2} = 2 \tan \psi \approx \frac{\nu}{\omega_{c_m} - \omega_H},$$

i. e.,

$$2 \Delta \omega \approx \nu \cdot \frac{\omega_{c_m}^2}{(\omega_{c_m} - \omega_H/2)(\omega_{c_m} - \omega_H)} > \nu. \tag{247}$$

For the  $F_2$ -layer a typical day-time »band-width» becomes about 159 c/s, whereas a typical day-time value for the  $E$ -layer is approximately 16 kc/s.

This means that it is possible to measure the maximum electron density of the  $F$ -region extremely accurately. Even for the  $E$ -layer this measurement is quite accurate, since a band-width smaller than the frequency width of the reflected pulse cannot be measured.

For the  $D$ -region, however,  $\psi \approx \frac{\pi}{4}$ , and it is obvious that the critical frequency conception has lost its meaning. In the lower ionosphere where the reflection is mainly »metallic» it is impossible to measure the maximum electron density (even if the reflection coefficient were numerically sufficient). The following table of  $|R|$  for a layer with typical  $D$  constants serves to illustrate the situation.

$$\Delta h_m = 6 \text{ km}, \lambda_{c_m} = 0,75 \text{ km}, \nu = 10^7 \text{ sec}^{-1}.$$

TABLE II.

$\omega/\omega_{c_m}$	0,125	0,250	0,500
$ R $	$1,3 \cdot 10^{-1}$	$3,5 \cdot 10^{-4}$	$1,8 \cdot 10^{-13}$

\* \* \*

Fortunately expansion (41) is well suited for application in the penetration frequency region when the losses are small. It is especially useful when

$$\left| \frac{Q^2}{2u^2} \right| \ll 1, \text{ i. e., when } \frac{|2 \Delta \omega|}{\omega_{c_m}} \ll \left( \frac{8}{\alpha} - \sin^2 2\psi \right)^{\frac{1}{2}} \cdot (\omega_H = 0) \tag{248}$$

For  $F_2$ - and  $E$ -layers with day-time characteristics as before we have

$$(2 \Delta f)_{F_2} \ll 250 \text{ kc/s,}$$

and

$$(2 \Delta f)_E \ll 460 \text{ kc/s.}$$

This means that the two expansions (41) and (55) overlap as will soon be shown in more detail.

In accordance with (41) one finds in the vertical incidence case when  $y = 1$ , that

$$\frac{d}{dz} \left\{ \ln D \left( u e^{j \frac{\pi}{4}} \right) \right\} \approx \frac{2\pi}{\lambda_{cm}},$$

$$j \varrho - \frac{1}{2}$$

proving again that there is no boundary reflection.

Denoting all terms containing  $\varrho$  within the main brackets of (41) by  $-j\Phi$ , we immediately obtain the reflection coefficient

$$R \approx - \frac{\Gamma \left( j \varrho + \frac{1}{2} \right)}{(2\pi)^{\frac{1}{2}}} \exp. \left\{ \frac{\pi \varrho}{2} + j \left( \frac{u^2}{2} - \varrho \ln u^2 + \frac{\pi}{2} \right) \right\} \cdot \frac{1 + j \Phi^*}{1 - j \Phi}, \quad (249)$$

where  $(\Phi^*)_{\nu=0}$  is the conjugate of  $(\Phi)_{\nu=0}$ .

After a simple transformation of the  $\Gamma$ -function we obtain

$$R \approx - 2^{\frac{1}{2}} \exp. \left\{ \ln \Gamma (2 j \varrho) - \ln \Gamma (j \varrho) + \frac{\pi \varrho}{2} + j \left( \frac{u^2}{2} - 2 \varrho \ln 2 u + \frac{\pi}{2} \right) \right\} \cdot \frac{1 + j \Phi^*}{1 - j \Phi}. \quad (249 \text{ a})$$

a)  $|\varrho|$  small, i. e., small losses and  $\frac{\Delta f}{f_{cm}}$  sufficiently small. The magnitude of the reflection coefficient is conveniently written

$$|R| = \frac{|\xi|}{\sqrt{2}} \exp. \left\{ \frac{\pi \varrho_{re}}{2} - 2 \operatorname{Im} \left( \frac{u^2}{4} - \varrho \ln 2 u \right) \right\},$$

where

$$\xi = e^{-j \gamma_0 \varrho} \prod_{m=0}^{\infty} \left\{ \frac{1}{1 + j \frac{2 \varrho}{2m+1}} \cdot e^{j \frac{2 \varrho}{2m+1}} \right\},$$

and  $\gamma_0$  is EULER'S constant.

We further have

$$\frac{\pi \varrho_{re}}{2} - 2 \cdot \text{Im} \left( \frac{u^2}{4} - \varrho \ln 2u \right) = \alpha [\cos \psi \cdot (1 - y^2) \cdot \frac{\pi}{2} - \sin \psi \{(1 + y^2) \ln 16a - 2\} - (1 - y^2) \psi \cos \psi]. \tag{250}$$

For small losses  $\sin \psi \approx \psi$  and therefore

$$|R| \approx \frac{|\xi|}{\sqrt{2}} \exp. \left[ -\frac{\nu}{2(\omega - \omega_H)} (1 + y^2) \{\ln(16a) - 1\} + \frac{\pi}{2} (1 - y^2) \right].$$

Remembering that

$$\frac{1}{\{\cos \pi \varrho_{re}\}^{\frac{1}{2}}} = \prod_{m=0}^{\infty} \frac{1}{\left\{ 1 + \frac{4 \varrho_{re}^2}{(2m+1)^2} \right\}^{\frac{1}{2}}},$$

and further in accordance with (22 b) that the no-loss coefficient  $(|R|)_{\nu=0} = |R_0|$ , is

$$|R_0| = \frac{\alpha \frac{\pi}{2} (1 - y^2)}{e^{\left\{ 2 \cos \alpha \frac{\pi}{2} (1 - y^2) \right\}^{\frac{1}{2}}}},$$

we finally obtain

$$|R| \approx |R_0| e^{-\frac{\nu}{\omega - \omega_H} \cdot \alpha \cdot \{\ln(16a) + \gamma_0 - 1\}} \cdot \prod_{m=0}^{\infty} \left\{ 1 + \frac{4 \nu \alpha}{\omega - \omega_H} \cdot \frac{1 + \frac{\nu}{\omega - \omega_H} \cdot \frac{\alpha}{2m+1}}{2m+1 + \frac{4 \alpha^2}{2m+1} (1 - y^2)^2} \right\}^{-\frac{1}{2}} e^{\frac{\nu}{\omega - \omega_H} \cdot \frac{\alpha}{2m+1}}. \tag{251}$$

When  $\frac{\nu}{\omega - \omega_H} \cdot \alpha \ll 1$  ( $|\varrho_{im}| \ll 1$ ) the penetration value thus becomes

$$|R| \approx \frac{1}{\sqrt{2}} \cdot e^{-\frac{\nu}{\omega - \omega_H} \cdot \alpha \{ \ln(16\alpha) - 1 \}} \cdot \underbrace{\left\{ \frac{\Gamma\left(1 + \frac{4\nu\alpha}{\omega - \omega_H}\right)^{\frac{1}{2}}}{\Gamma\left(1 + \frac{2\nu\alpha}{\omega - \omega_H}\right)} \right\}}_{\approx 1} \quad (251 \text{ a}) \quad (y = 1)$$

For a thick layer even a relatively low collisional frequency reduces  $|R|$  considerably. Thus for an  $F_2$ -layer with the same day-time characteristic as before a value of  $\nu$  as low as 200 reduces  $|R|$  with about 36 %.

b)  $|\varrho| \gg 1$ . This covers the case of  $f$  in the overlapping regions of (41), (45) and further the case of  $f$  arbitrary when the losses are considerable.

Making use of the conjugate relation of (160) we obtain from (249)

$$R \approx - \exp. j \left[ \alpha e^{-j\psi} \left\{ 2\bar{y} - (1 - \bar{y}^2) \ln \left( \frac{1 + \bar{y}}{1 - \bar{y}} \right) \right\} + \frac{\pi}{2} \right] \cdot \exp. \left\{ -j\alpha (1 - \bar{y})^2 \cdot \frac{3}{4} \right\} \quad (252)$$

Since in the useful range of (41) by (248)  $|\alpha (1 - \bar{y})^2| \ll 2$ , the result obtained is substantially the same as (161), i. e.,

$$R \sim e^{j2\xi}$$

\* \* \*

When  $\nu$  so low that  $\sin \psi \approx \psi$ , we have approximately

$$\left. \begin{aligned} \varrho_{re} &\approx \frac{\Delta h_m}{c_0} \cdot 2 \Delta \omega, \quad (\Delta \omega = \omega_{c_m} - \omega) \\ \text{and} \\ \varrho_{im} &\approx - \frac{\Delta h_m}{2 c_0} \cdot \nu. \end{aligned} \right\} \quad (253)$$

For layers with  $\Delta h_m \cdot \nu = \text{constant}$ , parameters

$$\lambda_{c_{m_1}}, \lambda_{c_{m_2}}, \dots; \nu_1, \nu_2, \dots,$$

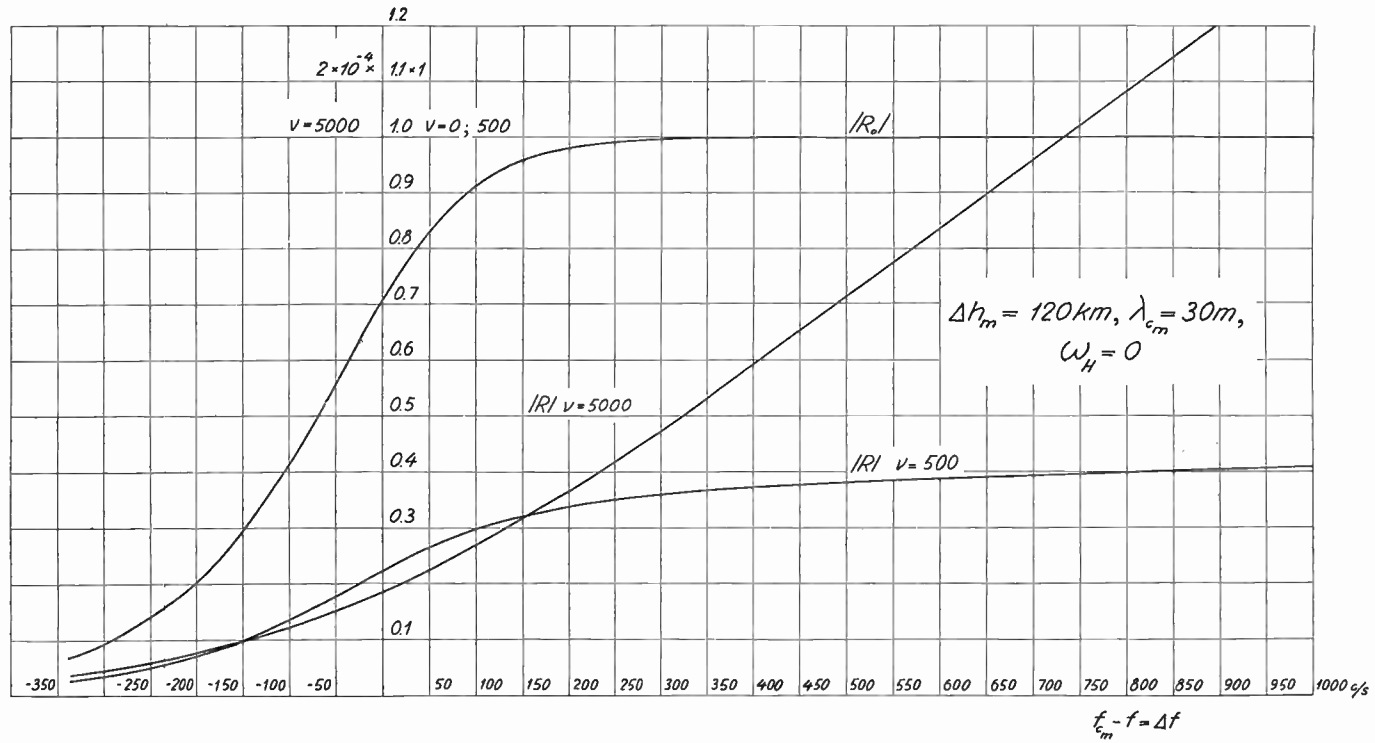


Fig. 30. The Reflection Coefficient of the Parabolic Layer.

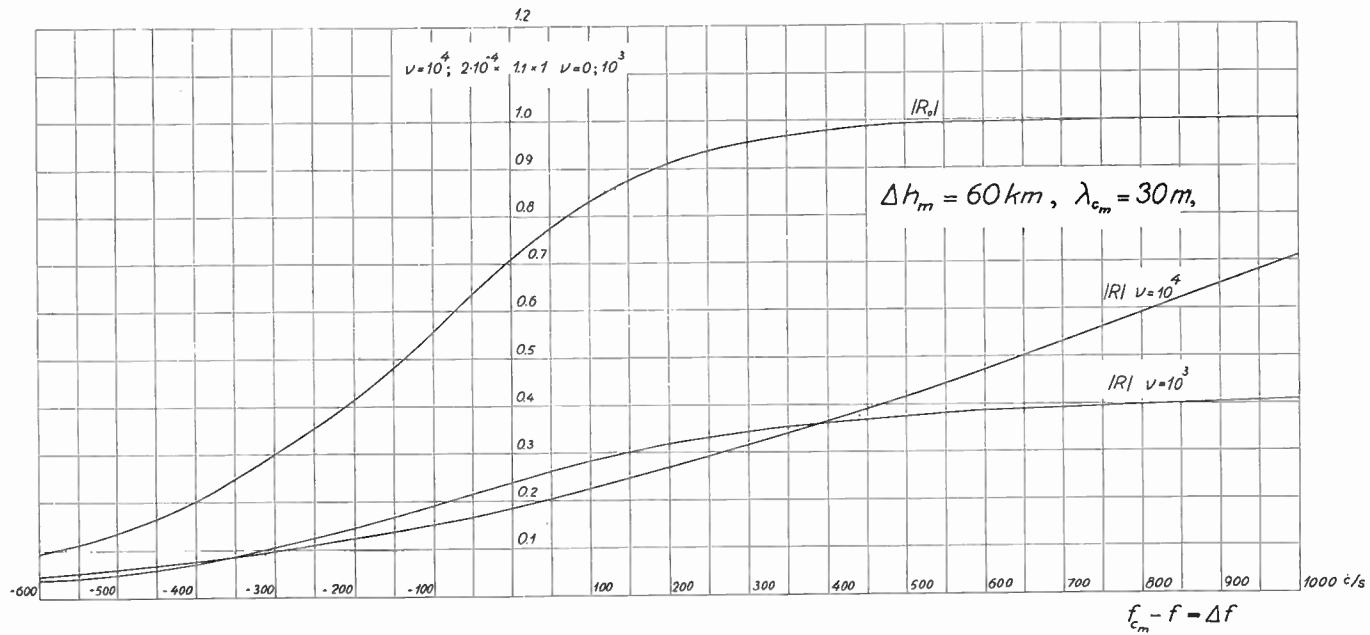


Fig. 31. The Reflection Coefficient of the Parabolic Layer.

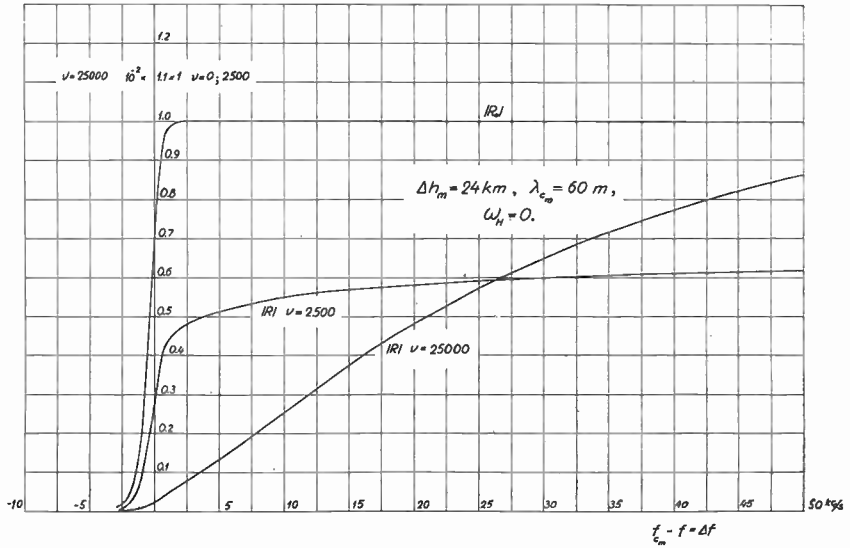


Fig. 32. The Reflection Coefficient of the Parabolic Layer.

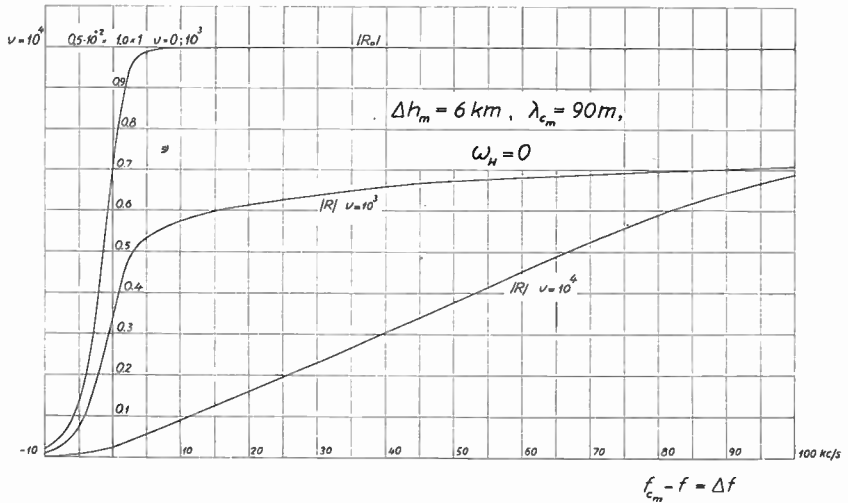


Fig. 33. The Reflection Coefficient of the Parabolic Layer.

and frequency deviations  $\Delta f_1, \Delta f_2, \dots$ , we find in accordance with (247) that

$$\frac{(|R|)_{\lambda_{c_{m_1}}, \Delta f_1}}{(|R|)_{\lambda_{c_{m_2}}, \Delta f_2 = \frac{v_2}{v_1} \cdot \Delta f_1}} = \left(\frac{\Delta h_m}{2 c_0}\right)^{\lambda_{c_{m_1}}/\lambda_{c_{m_2}}} \quad (254)$$

For a layer with changing  $\lambda_{c_m}$  but with  $\Delta h_m$  and  $v$  constant the relative variation in  $|R|$  with  $\Delta f$  always is the same.

A few typical examples of the variation of the reflection coefficient in the penetration frequency region are shown in figs 30—33.

Figs 30 and 31 show typical  $F_2$ -layer values. Since it is possible to determine  $\omega_{c_m}$  very accurately from ionospheric sweep frequency records we infer that  $v$  must be of the order of  $10^3$ . Generally it does not seem to be much in excess of this value. This is in substantial agreement with the results of FARMER and RATCLIFFE. They find  $v = 1,6 \cdot 10^3$  for the  $F_2$ -layer.

Fig. 32 depicts typical  $F_1$ -layer values. Since it is possible to determine  $\omega_{c_m}$  practically as accurately for the  $F_1$ -layer as for the  $F_2$ -layer, we further infer that for the  $F_1$ -layer  $v$  probably is less than about  $10^4$ . It should be mentioned that at an estimated  $F_1$ -height of 265 km, ECKERSLEY finds  $v = 3,6 \cdot 10^3$ .

Fig. 33 finally is plotted with special reference to the normal  $E$ -layer. The critical frequency generally cannot be measured very accurately for the  $E$ -layer. This holds for virtual height measurements as well as for reflection intensity measurements. Therefore it seems probable that  $v$  is  $10^5$  or more for the  $E$ -layer. This agrees fairly well with the value calculated for this atmospheric level.

### The Virtual Height of the Parabolic Layer.

If the wave reflected from the ionosphere experiences an increase in phase  $A(\omega)$ , one finds the time of travel of a wave-train with intensity maximum at  $\omega = \omega_0$  to be approximately  $\tau \approx \left(\frac{d A}{d \omega}\right)_{\omega = \omega_0}$  at vertical incidence (38 a). This relation is extremely accurate under most conditions. When the relative change of  $|R|$  is considerable within

the main part of the frequency spectrum of the wave-train it has to be used very carefully, however. In this connexion the reader is referred to the fundamental papers by SOMMERFELD and BRILLOUIN concerning similar problems [25].

Except when  $|Γ| \ll 1$  (which is of no interest in this connexion), when further  $f$  lies in the penetration frequency region, and the losses are small, we have at vertical incidence

$$\tau = 2 \frac{d}{d \omega} \{ \text{Re} (\xi) \} = 2 \text{Re} \left\{ \frac{d \xi}{d \omega} \right\} \tag{255}$$

i. e., the virtual height is

$$\Delta h_v \approx c_0 \cdot \text{Re} \left\{ \frac{d \xi}{d \omega} \right\}. \tag{255 a}$$

Relation (161 a) then yields

$$\begin{aligned} \Delta h_v = & \frac{\Delta h_m}{2} \cdot \frac{\omega}{\omega_r} \cdot \Delta^{-\frac{1}{2}} \left[ \frac{\omega - \omega_H - \omega \Delta^{-2}}{2 \omega_r} + \frac{1}{4 \omega_{c_m} \omega_r^2} \left\{ \frac{1}{2} \ln \left| \frac{1 + \frac{2 y \cos \psi}{1 + y^2}}{1 - \frac{2 y \cos \psi}{1 + y^2}} \right| \right. \right. \\ & \cdot \left[ \cos \psi \cdot \{ \omega_r^2 \Delta [3 (\omega - \omega_H) + \omega \Delta^{-2}] - \omega_{c_m}^2 (\omega - \omega_H - \omega \Delta^{-2}) \} - \sin \psi \cdot \{ \omega_{c_m}^2 - \omega_r^2 \Delta \} \cdot \right. \\ & \cdot \Delta^{-2} \cdot \left. \frac{\nu}{\omega - \omega_H} \cdot \omega \right] - \arctan \left\{ \sin \psi \frac{2 y}{1 - y^2} \right\} \cdot \left[ \sin \psi \{ \omega_r^2 \Delta [3 (\omega - \omega_H) + \omega^2 \Delta^{-2}] + \right. \\ & \left. \left. + \omega_{c_m}^2 (\omega - \omega_H - \omega \Delta^{-2}) \} - \cos \psi \cdot (\omega_{c_m}^2 + \omega_r^2 \Delta) \cdot \Delta^{-2} \cdot \frac{\nu}{\omega - \omega_H} \cdot \omega \right] \right], \tag{256} \end{aligned}$$

where  $\omega_r^2 = \omega (\omega - \omega_H)$ .

When  $\sin \psi \approx \psi$ , (256) is conveniently transformed and reduced to

$$\begin{aligned} \Delta h_v \approx & \frac{\Delta h_m}{2} \cdot \frac{\omega}{\omega_{c_m}} \left[ \ln \left| \frac{1 + y}{\left\{ (1 - y)^2 + \frac{y}{4} \left( \frac{\nu}{\omega - \omega_H} \right)^2 \right\}^{\frac{1}{2}}} \right| \cdot \frac{\omega_r^2 \left( \omega - \frac{3}{4} \omega_H \right) + \omega_{c_m}^2 \cdot \frac{1}{4} \omega_H}{\omega_r^3} + \right. \\ & \left. + \frac{\nu}{4 (\omega - \omega_H)} \left\{ \frac{\pi}{2} - \arctan \left( \frac{1 - y^2}{y} \cdot \frac{\omega - \omega_H}{\nu} \right) \right\} \cdot \frac{\omega_{c_m}^2 \left( \omega + \frac{1}{2} \omega_H \right) - \omega_r^2 \left( \omega - \frac{3}{2} \omega_H \right)}{\omega_r^3} - \right. \\ & \left. - \frac{\omega_H \omega_{c_m}}{2 \omega_r^2} \right]. \quad (\sin \psi \approx \psi) \tag{257} \end{aligned}$$

From this relation it is immediately found that

$$\lim_{\omega \rightarrow \infty} (\Delta h_v) = \Delta h_m. \tag{258}$$

When  $y = 1$ ,  $\Delta h_v$  becomes very large when  $v$  is low. For  $v = 0$  it becomes infinite. But this is in the region where we know that (252) cannot be correct.

In this region (249 a) yields

$$\Delta h_v \approx \frac{c_0}{2} \operatorname{Im} \left[ \left\{ 2j\psi(2j\varrho) - j\psi(j\varrho) + \frac{\pi}{2} - j \ln 4u^2 \right\} \cdot \frac{d\varrho}{d\omega} + j \left( u - \frac{2\varrho}{u} \right) \frac{d u}{d\omega} \right] + \frac{c_0}{2} \frac{d}{d\omega} (\Phi + \Phi^*),$$

where  $\psi(z)$  is the logarithmic derivative of  $\Gamma(z)$ .

When  $\sin \psi \approx \psi$  this finally yields

$$\begin{aligned} \Delta h_v \approx & \frac{\Delta h_m}{2} \cdot \frac{\omega}{\omega_{c_m}} \left[ \left\{ \ln(16a) + \gamma_0 - \sum_{m=1}^{\infty} \frac{4(2|\varrho|^2 - \varrho_{im} \cdot m)}{(m - 2\varrho_{im})^2 + (2\varrho_{re})^2} - \right. \right. \\ & \left. \left. - \frac{|\varrho|^2 - \varrho_{im} \cdot m}{(m - \varrho_{im})^2 + \varrho_{re}^2} \right\} \cdot \underbrace{\frac{\omega_r^2 \left( \omega - \frac{1}{4} \omega_H \right) - \omega_{c_m}^2 \frac{1}{4} \omega_H}{\omega_r^3}}_{\approx \frac{\omega - \frac{1}{2} \omega_H}{\omega_r}} + \frac{v}{4(\omega - \omega_H)} \left\{ \frac{\pi}{2} - \right. \right. \\ & \left. \left. - \sum_{m=1}^{\infty} \frac{4\varrho_{re} \cdot m}{(m - 2\varrho_{im})^2 + (2\varrho_{re})^2} - \frac{\varrho_{re} \cdot m}{(m - \varrho_{im})^2 + \varrho_{re}^2} \right\} \cdot \underbrace{\frac{\omega_{c_m}^2 \left( \omega + \frac{1}{2} \omega_H \right) - \omega_r^2 \left( \omega - \frac{3}{2} \omega_H \right)}{\omega_r^3}}_{\approx \frac{2\omega_H}{\omega_r}} - \right. \\ & \left. \left. - \underbrace{\frac{\omega_H (\omega_r^2 + \omega_{c_m}^2)}{4\omega_r^3}}_{\approx \frac{\omega_H}{2\omega_r}} \right] \tag{259} \end{aligned}$$

The close similarity between (259) and (257) is apparent.

At the classical penetration frequency  $y = 1$  and  $\omega_r = \omega_{c_m}$ , i. e.,

$$(\omega)_{y=1} = \frac{\omega_H}{2} + \left\{ \omega_{c_m}^2 + \left( \frac{\omega_H}{2} \right)^2 \right\}^{\frac{1}{2}} = \omega_{c_m}^x. \quad (260)$$

At this frequency  $\varrho_{re} = 0$  and therefore

$$\begin{aligned} \Delta h_v \approx & \frac{\Delta h_m}{2} \cdot \frac{\omega_{c_m}^x}{\omega_{c_m}} \cdot \left[ \left\{ \ln(16\alpha) - 2\psi(-2\varrho_{im}) + \psi(-\varrho_{im}) \right\} \cdot \frac{\omega_{c_m}^x - \frac{1}{2}\omega_H}{\omega_{c_m}} + \right. \\ & \left. + \frac{\nu}{4(\omega_{c_m}^x - \omega_H)} \cdot \frac{2\omega_H}{\omega_{c_m}} \cdot \frac{\pi}{2} - \frac{\omega_H}{2\omega_{c_m}} \right]. \quad (y = 1) \quad (261) \end{aligned}$$

The no-loss virtual height accordingly becomes

$$\Delta h_v \approx \frac{\Delta h_m}{2} \cdot \frac{\omega_{c_m}^x}{\omega_{c_m}} \cdot \left\{ (\ln(16\alpha) + \gamma_0) \cdot \frac{\omega_{c_m}^x - \frac{1}{2}\omega_H}{\omega_{c_m}} - \frac{\omega_H}{2\omega_{c_m}} \right\} \quad (y = 1; \nu = 0) \quad (262)$$

This generally is very large though not infinite as one might expect from (257).

For a thick layer  $\nu$  does not have to increase very much before  $-\varrho_{im} \gg 1$ . When this is the case it is convenient to use the asymptotic form

$$2\psi(-\varrho_{im}) - \psi(-\varrho_{im}) \sim \ln(-4\varrho_{im}), \quad (263)$$

i. e.,

$$\begin{aligned} \Delta h_v \approx & \frac{\Delta h_m}{2} \cdot \frac{\omega_{c_m}^x}{\omega_{c_m}} \left[ \ln \left\{ \frac{4(\omega - \omega_H)}{\nu} \right\} \cdot \frac{\omega_{c_m}^x - \frac{1}{2}\omega_H}{\omega_{c_m}} + \frac{\nu}{4(\omega_{c_m}^x - \omega_H)} \cdot \frac{2\omega_H}{\omega_{c_m}} \cdot \frac{\pi}{2} - \right. \\ & \left. - \frac{\omega_H}{2\omega_{c_m}} \right]. \quad (y = 1, -\varrho_{im} \gg 1). \quad (264) \end{aligned}$$

We immediately see that this result is the same as that of (257). When therefore  $-\varrho_{im} \gg 1$  in the penetration frequency region, (257) can be used throughout, i. e., the phase integral method is correct. Denoting the distance between the branch points by  $l$ , we further find that when this method can be used  $l \gg \Delta h_m (2\alpha)^{-\frac{1}{2}}$ .

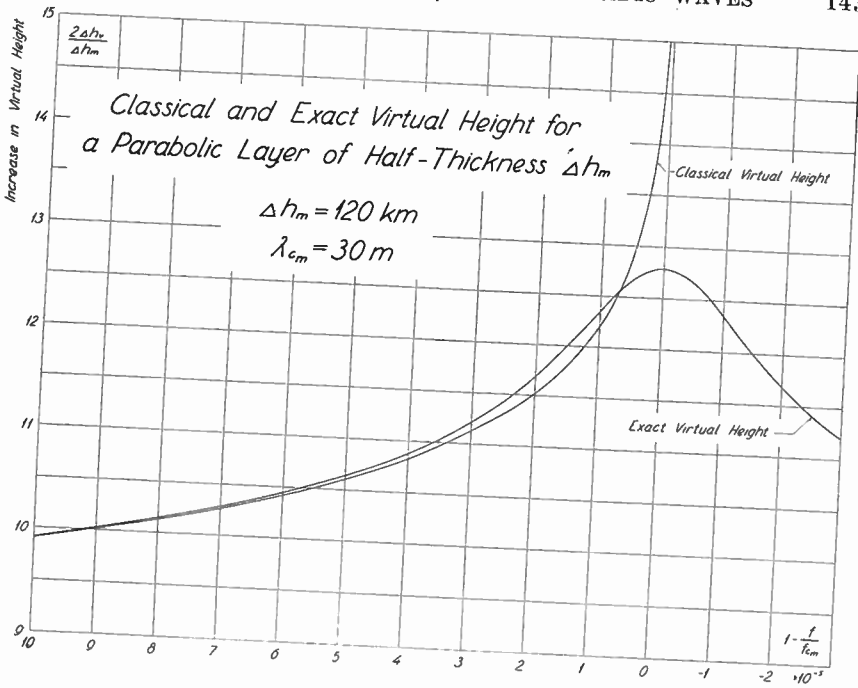


Fig. 34.

Introducing the notation virtual penetration for  $\frac{\Delta h_v}{2 \Delta h_m}$ , we find that the reduction in virtual penetration due to the introduction of  $\nu$  is

$$\delta \left( \frac{2 \Delta h_v}{\Delta h_m} \right) \approx \frac{\omega_{c_m}^x}{\omega_{c_m}} \left[ \left\{ \gamma_0 + 2 \psi(-2 \varrho_{im}) - \psi(-\varrho_{im}) \right\} \frac{\omega_{c_m}^x - \frac{1}{2} \omega_H}{\omega_{c_m}} - \frac{\nu}{4 (\omega_{c_m}^x - \omega_H)} \cdot \frac{2 \omega_H}{\omega_{c_m}} \cdot \frac{\pi}{2} \right] \quad (265)$$

For  $\omega_H = 0$  we therefore obtain the convenient expression

$$\delta \left( \frac{2 \Delta h_v}{\Delta h_m} \right) \approx \gamma_0 + 2 \psi(-2 \varrho_{im}) - \psi(-\varrho_{im}). \quad (265 \text{ a})$$

When  $\omega_H = 0$  all layers with  $\Delta h_m \cdot \nu = \text{constant}$  experience the same reduction in virtual penetration and this reduction is independent of  $\lambda_{c_m}$ .

A number of virtual height plots based on relations (257) and (259) are shown in figs. 34 to 41.

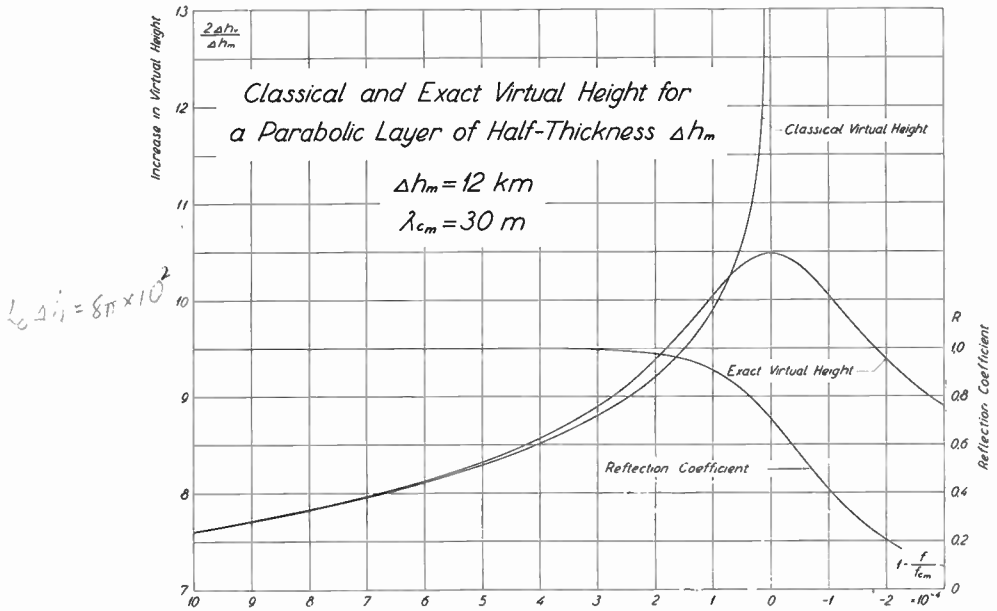


Fig. 35.

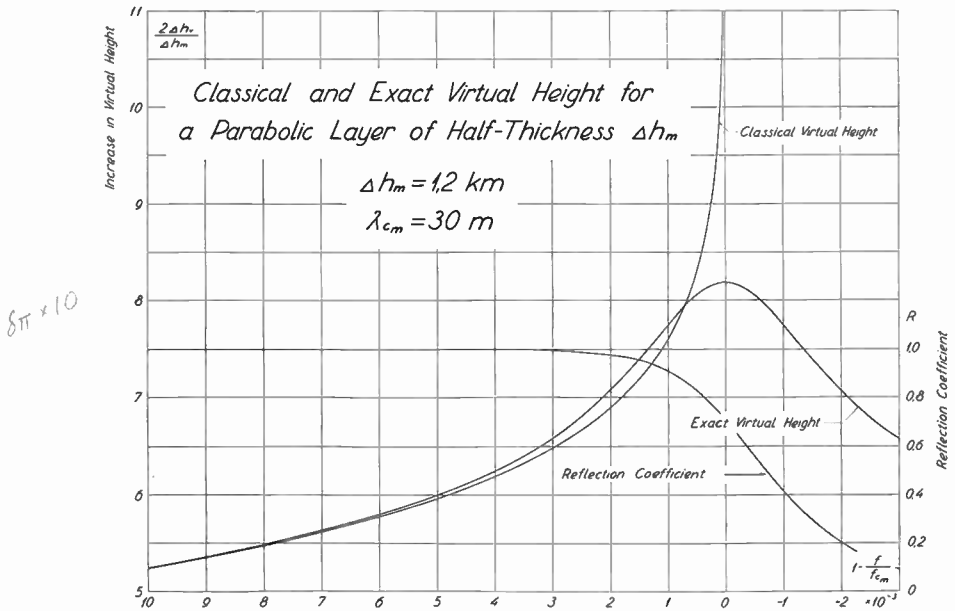


Fig. 36.

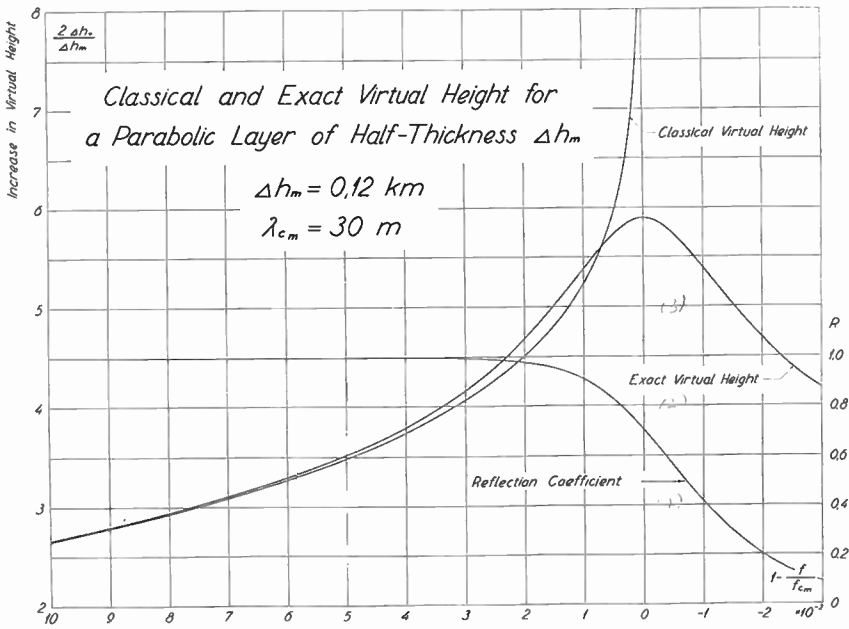


Fig. 37.

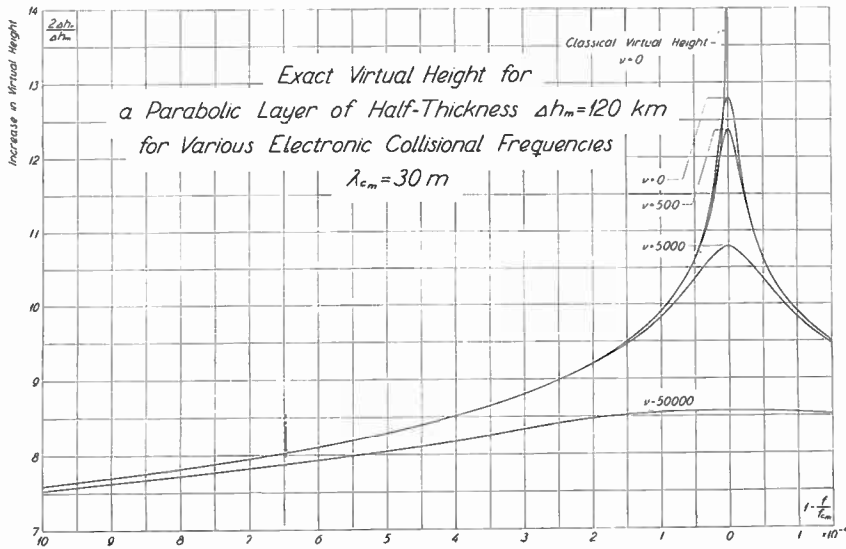


Fig. 38.

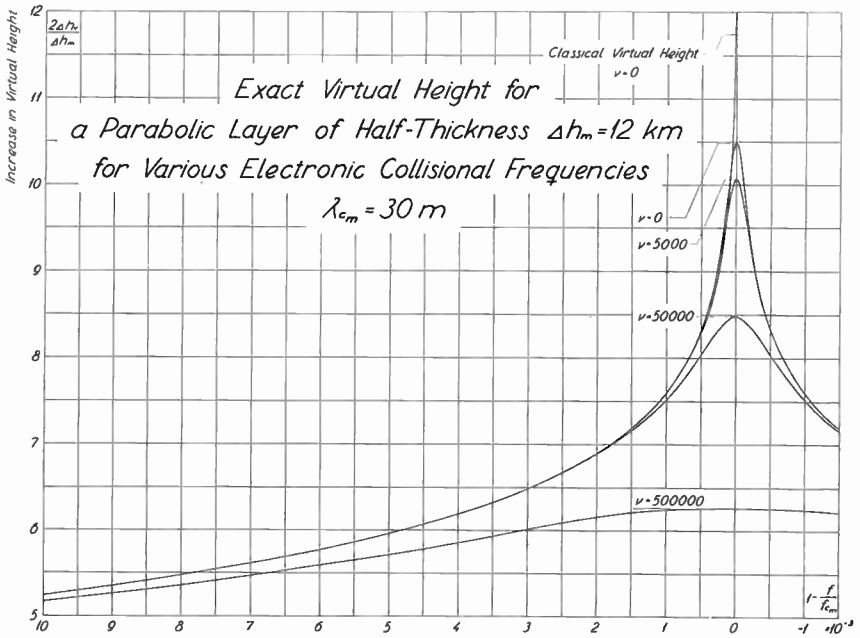


Fig. 39.

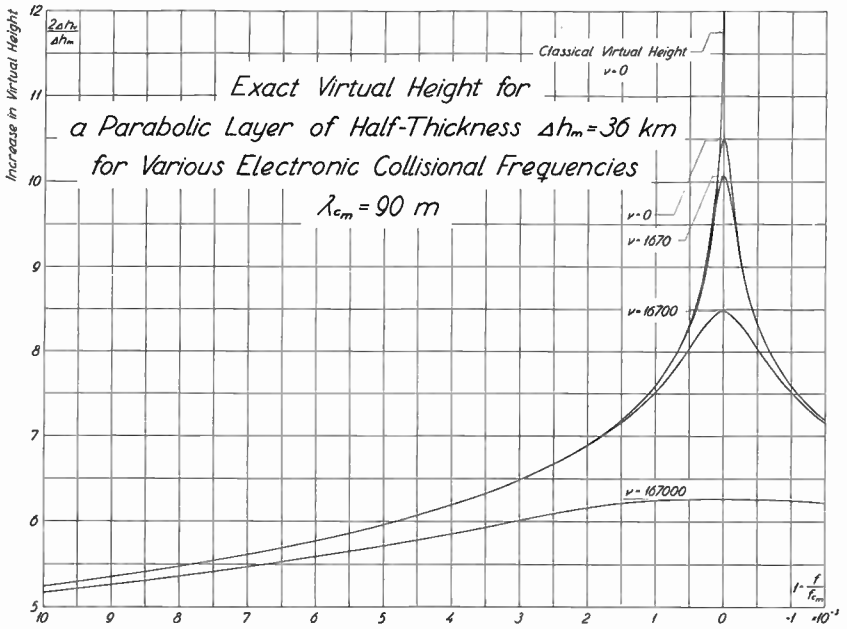


Fig. 40.

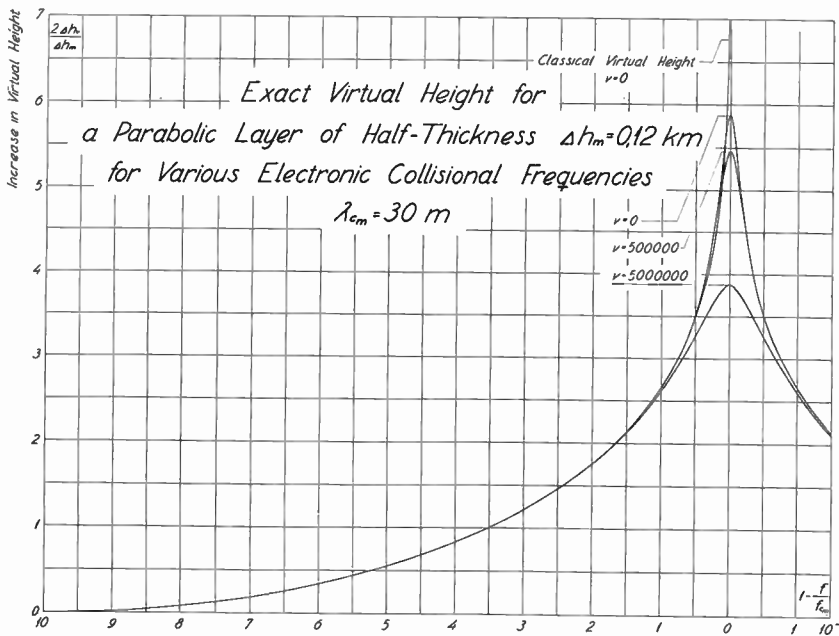


Fig. 41.

Fig. 34 shows the discrepancy between the classical and exact virtual heights for a thick  $F_2$ -layer when  $\nu = 0$ . The transition from reflection to penetration is extremely sharp. Fig. 35 shows the same thing for a considerably thinner layer.

For thin layers as shown in figs 36 and 37 the deviation from geometrical optics cannot be neglected.

Fig. 38 depicts the intrusion reducing influence of the collisional friction for the  $F_2$ -layer. On account of the fact that  $\nu$  (as mentioned before) probably is not much larger than  $2 \cdot 10^3$  it is possible to obtain experimentally practically the entire classical virtual height curve. This is extremely important, since the calculation of the true electron density distribution of the upper ionosphere is based on the classical height curve.

For a layer ten times thinner the height reducing influence of the collisional friction is about ten times smaller as shown in fig. 39.

Fig. 40 depicts the virtual height for a thick  $E$ -layer. Since  $\nu$  is  $3 \cdot 10^5$  or more the characteristic increase in virtual height near penetration generally is suppressed. It is not possible to determine the true electron density distribution with reasonable accuracy. For a

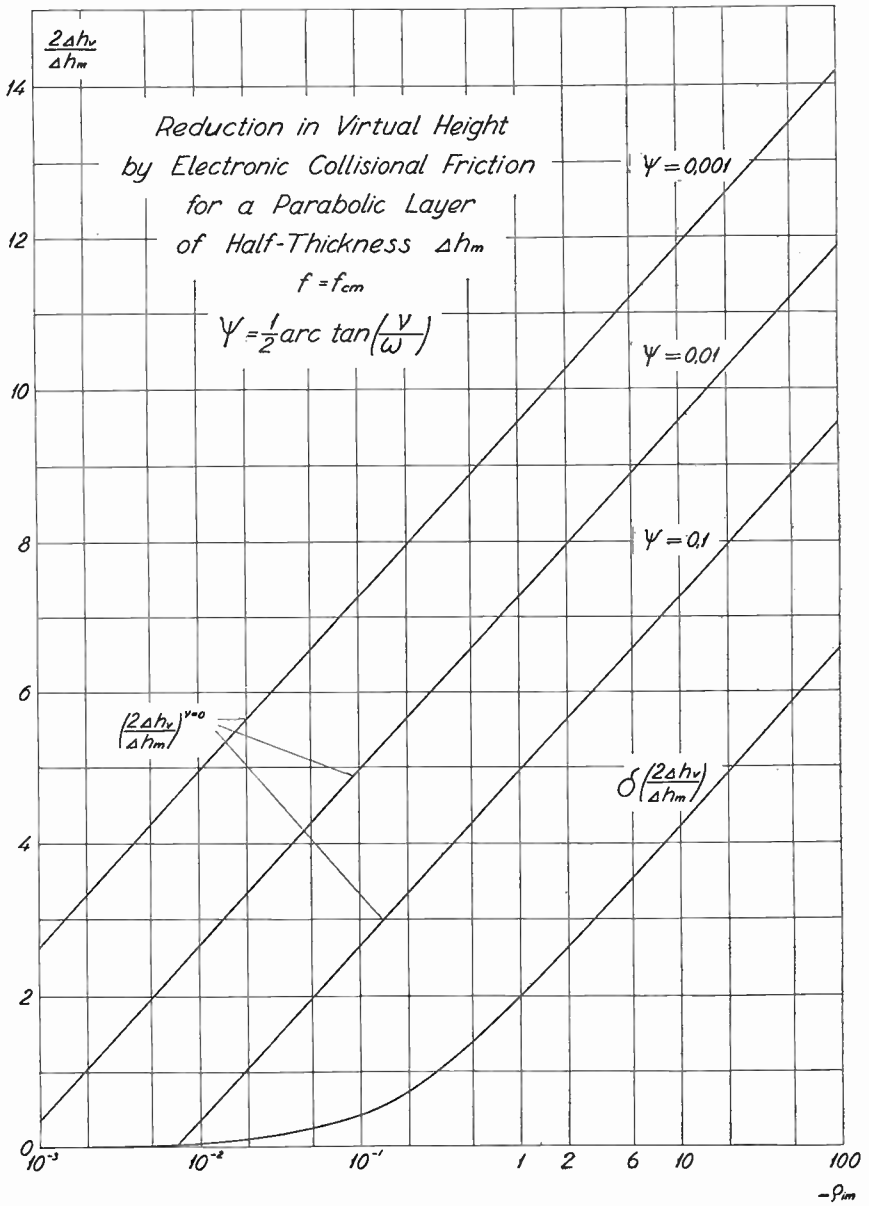


Fig. 42.

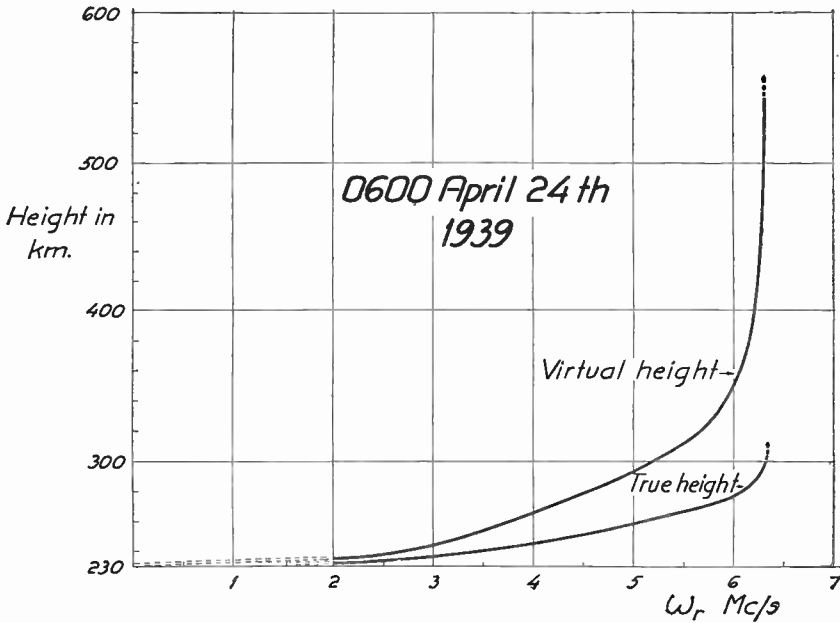


Fig. 43. Experimentally determined virtual and true heights.

thin layer the collisional friction can assume considerable values before any appreciable reduction in virtual height is observed as shown in fig. 41.

Finally the reduction in virtual intrusion is shown in fig. 42 for the special case  $\omega_H = 0$ . The corresponding no loss height has also been plotted for three characteristic  $\psi$  values.

A typical night-time virtual height curve for the *F*-layer obtained by the author at *Harvard University* is shown in fig. 43. This curve, which depicts the case  $\omega_H = 0$ , was transformed from the original virtual height data of the extra-ordinary component by a method already described [3].

The electron density distribution was found to be practically parabolic from the true height curve. In accordance with fig. 43,  $\Delta h_m \approx 70$  km and  $\lambda_{cm} \approx 47,2$  m. The no-loss virtual height

at  $y = 1$  therefore becomes  $\Delta h_v \approx \frac{\Delta h_m}{2} \cdot 11,75$ . The recording was made with a very sensitive equipment and the highest reduced virtual height recorded was  $\frac{\Delta h_m}{2} \cdot 9,20$ . We thus find from

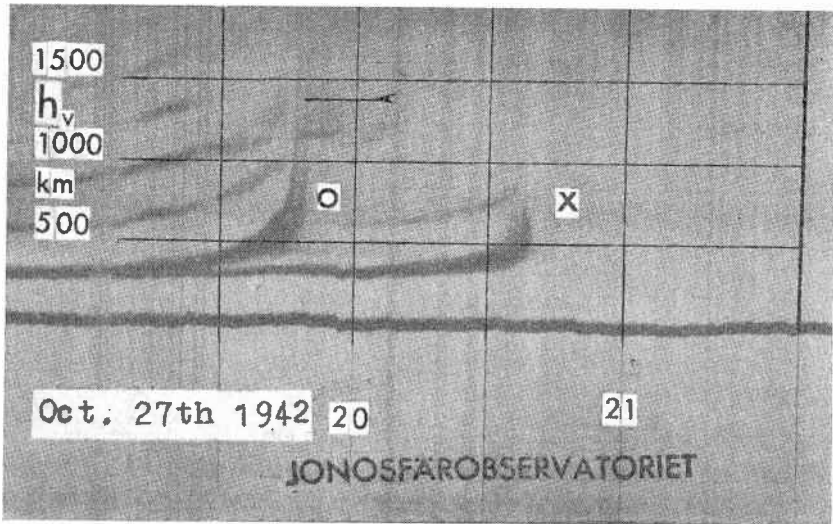


Fig. 44. Fixed frequency recording from Chalmers Ionospheric Observatory.

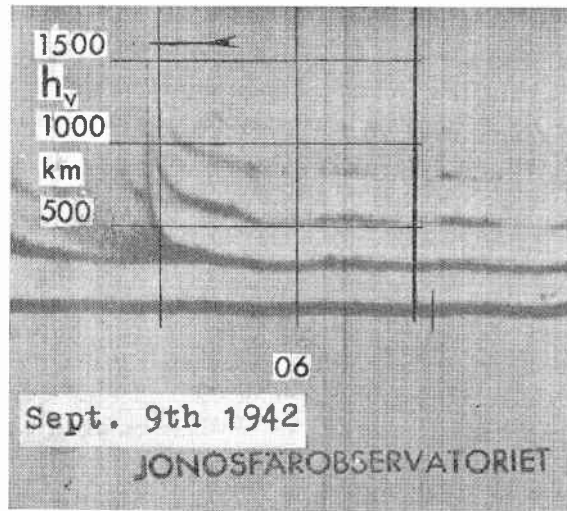


Fig. 45. Fixed frequency recording from Chalmers Ionospheric Observatory.

fig. 42 that  $-q_{im}$  must have been less than 1,7, i. e.,  $\nu$  must have been less than about 15000.

This method thus gives an idea of the upper limit of  $\nu$ . Sweep frequency records technically cannot be made sufficiently sensitive to register the delayed echo tail at the penetration frequency which generally is overtaken too rapidly.

A much better way to measure the night-time delay of the dispersed echo tail is to run an abnormally sensitive fixed frequency recording equipment when the signals just begin to penetrate at that frequency. A sweep frequency recording is made at the same time. From this recording  $\Delta h_m$  is calculated. One then finds that the upper limit of  $\nu$  certainly is appreciably lower than 15000.

Typical examples of this are shown as figs 44 and 45.

Fig. 44 shows a quiet evening recording. The dispersed pulse tail of the ordinary component at penetration was delayed to a virtual height of about 1100 km. Fig. 44 represents normal quiet conditions at the equinox sunrise. In this particular case the ordinary pulse tail was delayed to a maximum virtual height of about 1350 km. In both cases the virtual height is counted from the lower boundary of the layer. These tremendous virtual heights indicate a  $\nu$  value probably less than 3000 at the level in question.

### The Reflection of Radio Waves from an Extremely Thin Layer.

In connexion with studies of abnormal *E*-layer reflections it is of particular interest to investigate the reflection of radio waves from very thin layers. It is therefore not out of the place to study briefly the reflection of waves from a very thin parabolic layer.

a)  $\omega > \omega_H$

For the extremely thin layer we have  $\left(\frac{\pi \Delta h_m}{\lambda_{c_m}}\right)^2 \ll 1$ . When this is the case and  $\left|\frac{q u^2}{4}\right| \ll 1$ , i. e.,  $y^2 \ll \frac{1}{\alpha^2}$ , the following approximation for relation (39) certainly is sufficiently accurate, viz.,

$$D \left( u e^{j \frac{\pi}{4}} \right)_{j\rho - \frac{1}{2}} = \frac{e^{j \frac{\rho}{2} \ln 2}}{2^{\frac{1}{4}} \Gamma \left( \frac{3 - 2j\rho}{4} \right)} \cdot \pi^{\frac{1}{3}} \left[ 1 + \frac{\rho u^2}{2} - 2^{\frac{1}{2}} \bar{\beta} u e^{j \frac{\pi}{4}} \left\{ 1 + \frac{\rho u^2}{6} \right\} \right], \quad (266)$$

where

$$\bar{\beta} = \frac{\Gamma \left( \frac{3 - 2j\rho}{4} \right)}{\Gamma \left( \frac{1 - 2j\rho}{4} \right)}.$$

One further finds

$$\begin{aligned} \frac{d}{du} \left\{ D \left( u e^{j \frac{\pi}{4}} \right)_{j\rho - \frac{1}{2}} \right\} &= - \frac{e^{j \frac{\rho}{2} \ln 2}}{2^{-\frac{1}{4}} \Gamma \left( \frac{3 - 2j\rho}{4} \right)} \cdot \pi^{\frac{1}{2}} \left[ 1 + \frac{\rho u^2}{2} - \right. \\ &\quad \left. - \frac{\rho u e^{-j \frac{\pi}{4}}}{2^{1/2} \bar{\beta}} \left\{ 1 + \frac{u^2}{6} \left( \rho - \frac{2}{\rho} \right) \right\} \right] \cdot \beta e^{j \frac{\pi}{4}} \end{aligned} \quad (267)$$

This yields (26)

$$\mu = \frac{k}{j \frac{d}{dz} \left\{ \ln D \left( u e^{j \frac{\pi}{4}} \right)_{j\rho - \frac{1}{2}} \right\}} = y \cdot \left( \frac{a}{2} \right)^{\frac{1}{2}} \cdot \frac{e^{j \left( \frac{\pi}{4} + \frac{\psi}{2} \right)}}{\xi \bar{\beta}}, \quad (268)$$

with

$$\frac{1}{\xi} = \frac{1 + \frac{\rho u^2}{2} - u \bar{\beta} 2^{\frac{1}{2}} e^{j \frac{\pi}{4}} \left\{ 1 + \frac{\rho u^2}{6} \right\}}{1 + \frac{\rho u^2}{2} - \frac{u \rho e^{-j \frac{\pi}{4}}}{\bar{\beta} 2^{\frac{1}{2}}} \left\{ 1 + \frac{u^2}{6} \left( \rho - \frac{2}{\rho} \right) \right\}}.$$

We further have

$$\bar{\beta} \approx \frac{1}{3}, \text{ when } |\rho| \ll 1,$$

and

$$\bar{\beta} \sim \left(-j \frac{\varrho}{2}\right)^{\frac{1}{2}}, \text{ when } |\varrho| \gg 1.$$

When  $y^2 \ll \frac{1}{a^2}$ ,  $\xi \approx 1$ , and

$$\mu \approx y \cdot \left(\frac{a}{2}\right)^{\frac{1}{2}} \cdot \frac{e^{j\left(\frac{\pi}{4} + \frac{\varphi}{2}\right)}}{\bar{\beta}}.$$

Putting for example  $a = 0.08$ , we thus find

$$\mu \approx 0,6 \cdot y \cdot e^{j\left(\frac{\pi}{4} + \frac{\varphi}{2}\right)}, \tag{268 a}$$

when  $y \leq 1$ .

Making use of (266) and the circuit relation we find the internal reflection coefficient

$$R = - \frac{\Gamma\left(j\varrho + \frac{1}{2}\right)}{(2\pi)^{\frac{1}{2}}} \cdot e^{\frac{\pi\varrho}{2} + j\left(\frac{\pi}{4} - \varrho \ln 2\right)} \cdot \frac{\Gamma\left(\frac{3 - 2j\varrho}{4}\right)}{\Gamma\left(\frac{3 + 2j\varrho}{4}\right)} \cdot \underbrace{\frac{1 - \frac{1}{2^2} \bar{\beta}^* u e^{-j\frac{\pi}{4}} \cdot \frac{1 + \varrho u^2/6}{1 + \varrho u^2/2}}{1 - \frac{1}{2^2} \bar{\beta} u e^{j\frac{\pi}{4}} \cdot \frac{1 + \varrho u^2/6}{1 + \varrho u^2/2}}}_{\zeta},$$

where

$$\bar{\beta}^* = \frac{\Gamma\left(\frac{3 + 2j\varrho}{4}\right)}{\Gamma\left(\frac{1 + 2j\varrho}{4}\right)}.$$

Fortunately this expression for  $R$  can be simplified considerably. Making use of the duplication formula for the  $\Gamma$ -functions it is possible to show that

$$\frac{\Gamma\left(j\varrho + \frac{1}{2}\right)}{(2\pi)^{\frac{1}{2}}} \cdot \frac{\Gamma\left(\frac{3-2j\varrho}{4}\right)}{\Gamma\left(\frac{3+2j\varrho}{4}\right)} = \frac{\exp. j \left[ \varrho \ln 2 - \arctan \left\{ \frac{\overbrace{\tanh \frac{\pi \varrho_{re}}{2}}^{\eta_0}}{\tan \frac{\pi}{2} \left( \frac{1}{2} - \varrho_{im} \right)} \right\} \right]}{2 \left\{ \sin^2 \frac{\pi}{2} \left( \frac{1}{2} - \varrho_{im} \right) + \sinh^2 \frac{\pi \varrho_{re}}{2} \right\}^{\frac{1}{2}}}$$

We thus finally obtain

$$R = - \frac{e^{\frac{\pi \varrho_{re}}{2}} \cdot \exp. j \left( \frac{\pi}{4} + \frac{\pi \varrho_{im}}{2} - \arctan \eta_0 \right)}{2 \left\{ \sin^2 \frac{\pi}{2} \left( \frac{1}{2} - \varrho_{im} \right) + \sinh^2 \frac{\pi \varrho_{re}}{2} \right\}^{\frac{1}{2}}} \cdot \zeta. \quad (269)$$

When  $y^2 \ll \frac{1}{a}$ , (233) reduces to

$$R \approx - \frac{1}{2^{\frac{1}{2}}} \cdot \left( 1 + \frac{\pi \varrho_{re}}{2} + \frac{\pi \varrho_{im}}{2} \right) \cdot e^{j \left( \frac{\pi}{4} + \frac{\pi \varrho_{re}}{2} + \frac{\pi \varrho_{im}}{2} \right)} \cdot \zeta, \quad (269 a)$$

and we further obtain

$$T \approx - \frac{1}{2^{\frac{1}{2}}} \cdot \left( 1 - \frac{\pi \varrho_{re}}{2} + \frac{\pi \varrho_{im}}{2} \right) \cdot e^{j \left( -\frac{\pi}{4} + \frac{\pi \varrho_{re}}{2} - \frac{\pi \varrho_{im}}{2} \right)} \cdot \zeta. \quad (270)$$

If  $y$  increases so that  $y^2 \gg \frac{1}{a}$ , but still  $\left| \frac{\varrho u^2}{4} \right| \ll 1$ , we find

$$R = - e^{\pi \varrho_{re} + j \left( \frac{\pi}{2} + \pi \varrho_{im} \right)} \cdot \frac{1 + j 2 a y}{1 - j 2 a y} \approx - e^{\pi \varrho_{re} + j \left( \frac{\pi}{2} + \pi \varrho_{im} + 4 a y \right)} = e^{2j\xi}. \quad (271)$$

As expected relations (269) and (161) overlap. It is further to be noted that the influence of the collisional friction is practically negligible for the extremely thin layer in accordance with previous results (fig. 41, p. 147).

\* \* \*

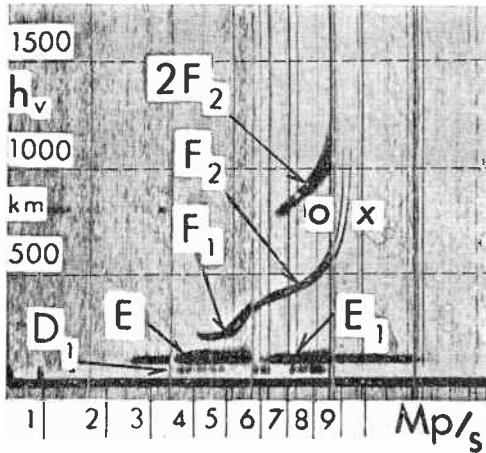


Fig. 46. Sweep frequency recording from Huancayo (Carnegie Institution), July 1 st, 12<sup>00</sup>, 1939.

We have already seen that in the case of  $a = 0,08$ , one has  $\mu \approx 0,6 \cdot y \cdot \exp. j \left\{ \frac{\pi}{4} + \frac{\psi}{2} \right\}$ . Since  $0 \leq \frac{\psi}{2} \leq \frac{\pi}{8}$ , it is apparent that  $r_0 \neq 0$ , and  $t_i \neq 0$  through a considerable frequency range. When  $y^2 \gg \frac{1}{a}$ , however,  $\mu \approx 1 = k / (d\xi/dz)_{z = \Delta h_m}$ , i. e.,  $r_0 = 0$ . From (271) we further have  $|R| = \exp. (\pi \rho_{re}) \ll 1$ . This means that boundary and internal reflections for the thin layer slowly disappear through about the same wide frequency range.

We find from (268 a) that  $t_i$  is small only when  $y$  is small. This means that incident waves penetrate the thin layer practically throughout the entire frequency range.

The reflected wave, which disappears first when  $y^2 \gg \frac{1}{a}$ , is practically independent of  $\omega_H$  as long as  $\omega \gg \omega_H$ . This is a characteristic feature of the thin layer.

Fig. 46 shows a sweep frequency recording from the *Huancayo Magnetic Observatory*. The record has kindly been placed at the author's disposal by DR. J. A. FLEMING. It is especially interesting because it shows abnormal  $E$  ( $E_1$ ) and abnormal  $D$  reflections.  $D$  signals from a cloudy but thick region should be too much absorbed (compare table II on p. 132). It is not unlikely that the abnormal  $D$ -layer is thin, perhaps also patchy. A very thin abnormal

*E*-layer (perhaps thin reflecting strata of locally greater electron density embedded in the *E*-region) is not unlikely as it would transmit and reflect signals as shown in fig. 46. If we assume that  $f_{c_m}$  of a thin abnormal *E*-layer is about 3 Mc/s at the time of the Huancayo recording, then from fig. 46 very roughly

$$\left(\frac{13}{3}\right)^2 = 18,8 \gg \frac{1}{a}.$$

Since at least  $a < 1$ ,  $a \approx 0,5$  perhaps is a reasonable guess. This makes the layer (stratum) thickness about 30 meters.

In fig. 47 is shown a fixed frequency recording from *Chalmers Ionospheric Observatory* of abnormal *E*-signals shortly before sunrise. The recording receiver was equipped with a polarization preselector. The difference in intensity between the ordinary and extraordinary components is considerable. It was further found that low level absorption very probably was not responsible for this intensity difference. In this particular case one therefore has to assume that the reflector was an electronic cloud of moderate thickness.

A further discussion of this interesting problem is outside the scope of the present communication. For extended knowledge of the abnormal *E*-layer phenomena the reader is referred to the ionospheric literature. Here may especially be mentioned *The Critical-Frequency Method of Measuring Upper-Atmospheric Ionization* by APPLETON, NAISMITH and INGRAM [26].

b)  $\omega_{c_m} < \omega < \omega_H$ .

This case is of limited practical interest. It will therefore be discussed very briefly. Making use of the notations of p. 102 and of relation (266) one immediately infers that the circuit relation yields waves progressing in both directions between the branch points. In this respect the thin and thick layers behave alike.

Thus  $\{R\}_{\omega_{c_m} < \omega < \omega_H} = 0$ , and  $D(jV)_{-n-1}$  represents the up-going wave. One finds

$$D_{-n-1}(\pm jV) = \frac{2^{-\frac{n+1}{2}}}{\Gamma\left(1 + \frac{n}{2}\right)} \cdot \pi^{\frac{1}{2}} \left[ 1 - \frac{\left(n + \frac{1}{2}\right) V^2}{2} \mp j 2^{\frac{1}{2}} \beta V \left\{ 1 - \frac{\left(n + \frac{1}{2}\right) V^2}{6} \right\} \right], \quad (272)$$

when  $\left| \left(n + \frac{1}{2}\right) \frac{V^2}{4} \right| \ll 1$ .

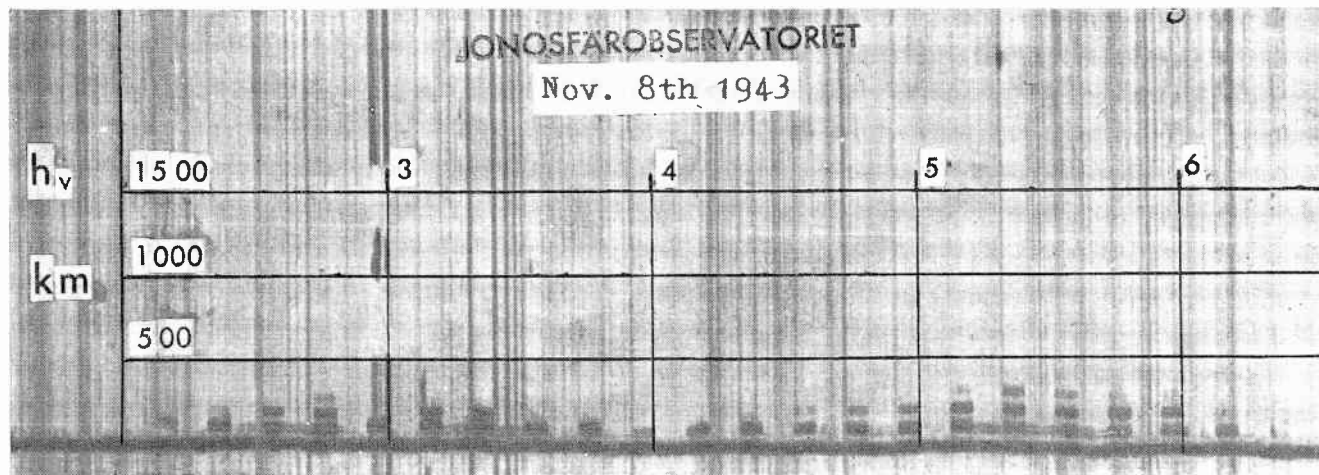


Fig. 47. Abnormal  $E$ -reflections recorded with a polarization receiver at the Chalmers Ionospheric Observatory.

This yields

$$T = \frac{1 - \frac{\left(n + \frac{1}{2}\right) V^2}{2} + j 2^{\frac{1}{2}} \bar{\beta} V \left\{ 1 - \frac{\left(n + \frac{1}{2}\right) V^2}{6} \right\}}{1 - \frac{\left(n + \frac{1}{2}\right) V^2}{2} - j 2^{\frac{1}{2}} \bar{\beta} V \left\{ 1 - \frac{\left(n + \frac{1}{2}\right) V^2}{6} \right\}}, \quad (273)$$

i. e.,

$$T \approx \frac{1 + j 2^{\frac{3}{2}} \bar{\beta} (a)^{\frac{1}{2}} e^{j \frac{\psi_1}{2}}}{1 - j 2^{\frac{3}{2}} \bar{\beta} (a)^{\frac{1}{2}} e^{j \frac{\psi_1}{2}}}, \quad (273 a)$$

and

$$(|T|)_{\nu > 0} < 1.$$

When  $y^2 \gg \frac{1}{a}$ , but  $\left| \left(n + \frac{1}{2}\right) \frac{V^2}{4} \right|$  still appreciably less than 1, we obtain

$$T \approx \frac{1 + j 2 a y}{1 - j 2 a y} \approx e^{j 4 a y} = e^{j \left\{ \pi \left(n + \frac{1}{2}\right) + 2\xi + \frac{\pi}{2} \right\}}, \quad (273 b)$$

i. e., (197) and (273) overlap.

We further finally find.

$$\mu = y \left( \frac{a}{2} \right)^{\frac{1}{2}} \cdot \frac{e^{-j \frac{\psi_1}{2}}}{\bar{\beta} \xi_1}, \quad (274)$$

where

$$\frac{1}{\xi_1} = \frac{1 - \frac{\left(n + \frac{1}{2}\right) V^2}{2} - j 2^{\frac{1}{2}} \bar{\beta} V \left\{ 1 - \frac{V^2}{6} \left(n + \frac{1}{2}\right) \right\}}{1 - \frac{\left(n + \frac{1}{2}\right) V^2}{2} - j \frac{\left(n + \frac{1}{2}\right) V}{2^{\frac{1}{2}} \bar{\beta}} \left\{ 1 - \frac{V^2}{6} \left(n + \frac{1}{2} - \frac{2}{n + \frac{1}{2}}\right) \right\}}.$$

For  $a = 0,08$ , (274) yields  $\mu \approx 0,6 y \cdot \exp. \left\{ -j \frac{\psi_1}{2} \right\}$ . When  $y^2 \gg \frac{1}{a}$ ,  $\mu \approx 1$  and the boundary reflection disappears. It is further apparent from (273 a) and (273 b) that within the frequency range of appreciable boundary reflection the phase of  $T$  is less than  $\frac{\pi}{2}$ . If we consult (200) we find that this means that the reflected light of the extremely thin layer exhibits no colour effects.

### Tables of Cylinder Functions of Order

$$\pm \frac{1}{3} \text{ and } \pm \frac{2}{3}.$$

Bessel functions  $J(x)$ ,  $J(x)$ ,  $I(x)$ , and  $I(x)$  have been tabulated by DINNIK, *Archiv der Math. u. Phys.*, XVIII, 1911, pp. 337—338 to four places of decimals from  $x = 0$  to  $x = 8,0$  with interval 0,2. This interval is not sufficiently small for our purpose, i. e., the computation of the low order poles etc. We have therefore prepared a preliminary complementary table of cylinder functions with 0,02 interval from  $x = 0$  and  $x = 1$ . This is the region where considerable accuracy is required. The functions tabulated are

$$J_{\pm \frac{2}{3}}(x), Y_{\frac{2}{3}}(x), H_{\frac{2}{3}}^{(1)}(x), I_{\pm \frac{1}{3}}(x), I_{\pm \frac{2}{3}}(x), Y_{\frac{1}{3}}\left(x e^{-j \frac{3\pi}{2}}\right), Y_{\frac{2}{3}}\left(x e^{-j \frac{3\pi}{2}}\right),$$

$$H_{\frac{1}{3}}^{(1)}\left(x e^{-j \frac{3\pi}{2}}\right), \text{ and } H_{\frac{2}{3}}^{(1)}\left(x e^{-j \frac{3\pi}{2}}\right). \quad J_{\frac{1}{3}}(x), Y_{\frac{1}{3}}(x), H_{\frac{1}{3}}^{(1)}(x) \text{ are tabu-}$$

lated with 0,02 interval in WATSON'S *Theory of Bessel Functions*, p. 714. It was further found practical to compute the HANKEL and second kind functions for the range of  $x$  values used by DINNIK.

Making use of the familiar relations (\*)

$$H_{\nu}^{(2)}(x) = H_{\nu}^{(1)}(x)^*,$$

$$H_{\frac{1}{3}}^{(2)}\left(x e^{-j \frac{3\pi}{2}}\right) = -H_{\frac{1}{3}}^{(1)}\left(x e^{-j \frac{3\pi}{2}}\right)^*,$$

$$H_{\frac{2}{3}}^{(2)}\left(x e^{-j \frac{3\pi}{2}}\right) = H_{\frac{2}{3}}^{(1)}\left(x e^{-j \frac{3\pi}{2}}\right)^*,$$

and

$$H_{-\nu}^{(2)}(z) = e^{\mp j \nu \pi} H_{\nu}^{(2)}(z),$$

one easily obtains the second kind HANKEL function and HANKEL functions of order  $-\frac{1}{3}$  and  $-\frac{2}{3}$  from the following tables.

\*) \* denotes the conjugate quantity.

TABLE III

$x$	$J_{\frac{2}{3}}(x)$	$J_{-\frac{2}{3}}(x)$	$Y_{\frac{2}{3}}(x)$	$ H_{\frac{2}{3}}^{(1)}(x) $	Phase $H_{\frac{2}{3}}^{(1)}(x)$
0,00	0,0000	$\infty$	$\infty$	$\infty$	$-90^{\circ} 0'$
0,02	0,0514	8,0398	-9,3133	9,3134	$-89^{\circ} 41'$
0,04	0,0816	5,0603	-5,8901	5,8901	$-89^{\circ} 12'$
0,06	0,1069	3,8559	-4,5141	4,5154	$-88^{\circ} 39'$
0,08	0,1294	3,1763	-3,7423	3,7446	$-88^{\circ} 1'$
0,10	0,1501	2,7298	-3,2388	3,2423	$-87^{\circ} 21'$
0,12	0,1694	2,4094	-2,8800	2,8840	$-86^{\circ} 38'$
0,14	0,1876	2,1656	-2,6089	2,6156	$-85^{\circ} 53'$
0,16	0,2049	1,9721	-2,3955	2,4042	$-85^{\circ} 7'$
0,18	0,2214	1,8137	-2,2222	2,2332	$-84^{\circ} 19'$
0,20	0,2372	1,6808	-2,0779	2,0914	$-83^{\circ} 29'$
0,22	0,2525	1,5673	-1,9554	1,9717	$-82^{\circ} 40'$
0,24	0,2672	1,4684	-1,8499	1,8691	$-81^{\circ} 47'$
0,26	0,2814	1,3814	-1,7575	1,7799	$-80^{\circ} 54'$
0,28	0,2952	1,3037	-1,6758	1,7017	$-80^{\circ} 1'$
0,30	0,3085	1,2338	-1,6027	1,6322	$-79^{\circ} 6'$
0,32	0,3215	1,1701	-1,5368	1,5701	$-78^{\circ} 11'$
0,34	0,3341	1,1121	-1,4770	1,5144	$-77^{\circ} 15'$
0,36	0,3463	1,0585	-1,4222	1,4637	$-76^{\circ} 19'$
0,38	0,3582	1,0088	-1,3717	1,4177	$-75^{\circ} 22'$
0,40	0,3698	0,9625	-1,3248	1,3755	$-74^{\circ} 24'$
0,42	0,3811	0,9191	-1,2814	1,3368	$-73^{\circ} 26'$
0,44	0,3921	0,8782	-1,2405	1,3011	$-72^{\circ} 27'$
0,46	0,4028	0,8397	-1,2022	1,2679	$-71^{\circ} 29'$
0,48	0,4131	0,8031	-1,1660	1,2370	$-70^{\circ} 29'$
0,50	0,4233	0,7684	-1,1317	1,2083	$-69^{\circ} 29'$
0,52	0,4332	0,7352	-1,0990	1,1813	$-68^{\circ} 29'$
0,54	0,4428	0,7035	-1,0680	1,1561	$-67^{\circ} 29'$
0,56	0,4521	0,6730	-1,0382	1,1324	$-66^{\circ} 28'$
0,58	0,4612	0,6437	-1,0097	1,1100	$-65^{\circ} 27'$
0,60	0,4701	0,6156	-0,9822	1,0889	$-64^{\circ} 25'$
0,62	0,4787	0,5884	-0,9557	1,0690	$-63^{\circ} 24'$
0,64	0,4870	0,5620	-0,9302	1,0501	$-62^{\circ} 22'$
0,66	0,4951	0,5366	-0,9054	1,0320	$-61^{\circ} 20'$
0,68	0,5030	0,5119	-0,8815	1,0149	$-60^{\circ} 17'$
0,70	0,5106	0,4879	-0,8582	0,9986	$-59^{\circ} 15'$
0,72	0,5180	0,4645	-0,8355	0,9830	$-58^{\circ} 12'$
0,74	0,5252	0,4418	-0,8134	0,9682	$-57^{\circ} 9'$
0,76	0,5322	0,4196	-0,7918	0,9540	$-56^{\circ} 6'$
0,78	0,5389	0,3980	-0,7707	0,9404	$-55^{\circ} 2'$
0,80	0,5453	0,3769	-0,7501	0,9274	$-53^{\circ} 59'$
0,82	0,5516	0,3563	-0,7299	0,9149	$-52^{\circ} 55'$
0,84	0,5576	0,3361	-0,7100	0,9028	$-51^{\circ} 51'$
0,86	0,5635	0,3163	-0,6906	0,8913	$-50^{\circ} 47'$
0,88	0,5690	0,2970	-0,6714	0,8801	$-49^{\circ} 43'$

Table III (contd.)

$x$	$J_{\frac{2}{3}}(x)$	$J_{-\frac{2}{3}}(x)$	$Y_{\frac{2}{3}}(x)$	$H_{\frac{2}{3}}^{(1)}(x)$	Phase $H_{\frac{2}{3}}^{(1)}(x)$
0,90	0,5744	0,2780	-0,6526	0,8694	-48° 39'
0,92	0,5796	0,2594	-0,6341	0,8591	-47° 34'
0,94	0,5845	0,2411	-0,6159	0,8491	-46° 30'
0,96	0,5892	0,2232	-0,5979	0,8394	-45° 25'
0,98	0,5937	0,2056	-0,5802	0,8301	-44° 21'
1,0	0,5980	0,1883	-0,5627	0,8212	-43° 16'
1,2	0,6290	+0,0309	-0,3986	0,7446	-32° 22'
1,4	0,6392	-0,1033	-0,2498	0,6862	-21° 21'
1,6	0,6295	-0,2163	-0,1137	0,6397	-10° 14'
1,8	0,5975	-0,3093	+0,0122	0,5976	+ 1° 10'
2,0	0,5570	-0,3823	0,1199	0,5697	12° 9'
2,2	0,4978	-0,4355	0,2154	0,5424	23° 24'
2,4	0,4266	-0,4689	0,2951	0,5187	34° 41'
2,6	0,3459	-0,4831	0,3581	0,4979	45° 59'
2,8	0,2589	-0,4789	0,4035	0,4794	57° 19'
3,0	0,1684	-0,4576	0,4312	0,4629	68° 40'
3,2	+0,0776	-0,4209	0,4412	0,4480	80° 1'
3,4	-0,0105	-0,3708	0,4342	0,4343	91° 23'
3,6	-0,0932	-0,3098	0,4115	0,4220	102° 45'
3,8	-0,1679	-0,2405	0,3746	0,4105	114° 9'
4,0	-0,2325	-0,1657	0,3256	0,4000	125° 32'
4,2	-0,2851	-0,0882	0,2663	0,3902	136° 56'
4,4	-0,3246	-0,0110	0,2001	0,3812	148° 20'
4,6	-0,3497	+0,0631	0,1290	0,3727	159° 45'
4,8	-0,3602	0,1329	+0,0546	0,3643	171° 23'
5,0	-0,3571	0,1925	-0,0161	0,3575	182° 34'
5,2	-0,3400	0,2434	-0,0847	0,3505	194° 0'
5,4	-0,3105	0,2834	-0,1480	0,3440	205° 29'
5,6	-0,2703	0,3105	-0,2025	0,3377	216° 50'
5,8	-0,2209	0,3249	-0,2476	0,3318	228° 16'
6,0	-0,1646	0,3262	-0,2816	0,3262	239° 42'
6,2	-0,1038	0,3149	-0,3037	0,3209	251° 8'
6,4	-0,0409	0,2916	-0,3132	0,3158	262° 34'
6,6	+0,0216	0,2579	-0,3102	0,3110	273° 59'
6,8	0,0814	0,2150	-0,2953	0,3063	285° 25'
7,0	0,1364	0,1651	-0,2694	0,3019	296° 51'
7,2	0,1844	0,1101	-0,2342	0,2981	308° 13'
7,4	0,2241	+0,0524	-0,1899	0,2937	319° 43'
7,6	0,2539	-0,0058	-0,1399	0,2899	331° 9'
7,8	0,2729	-0,0623	-0,0856	0,2861	342° 35'
8,0	0,2808	-0,1149	-0,0294	0,2823	354° 1'

TABLE IV

$x$	$I_{\frac{2}{3}}(x)$	$I_{-\frac{2}{3}}(x)$	$Y_{\frac{2}{3}}\left(x e^{-j\frac{3\pi}{2}}\right)$	$H_{\frac{2}{3}}^{(1)}\left(x e^{-j\frac{3\pi}{2}}\right)$	Phase $H_{\frac{2}{3}}^{(1)}\left(x e^{-j\frac{3\pi}{2}}\right)$
0,00	0,0000	$\infty$	$\infty$	$\infty$	90° 0'
0,02	0,0514	8,0446	9,3187	9,3189	90° 19'
0,04	0,0816	5,0724	5,8971	5,8978	90° 48'
0,06	0,1070	3,8767	4,5382	4,5396	91° 21'
0,08	0,1297	3,2069	3,7779	3,7802	91° 58'
0,10	0,1506	2,7710	3,2866	3,2901	92° 37'
0,12	0,1701	2,4620	2,9411	2,9460	93° 19'
0,14	0,1887	2,2301	2,6840	2,6907	94° 1'
0,16	0,2065	2,0493	2,4855	2,4940	94° 45'
0,18	0,2236	1,9039	2,3275	2,3383	95° 29'
0,20	0,2401	1,7848	2,1995	2,2126	96° 14'
0,22	0,2562	1,6853	2,0939	2,1096	96° 59'
0,24	0,2718	1,6010	2,0057	2,0240	97° 43'
0,26	0,2872	1,5289	1,9312	1,9525	98° 28'
0,28	0,3022	1,4665	1,8678	1,8922	99° 12'
0,30	0,3170	1,4123	1,8138	1,8412	99° 55'
0,32	0,3316	1,3648	1,7674	1,7982	100° 38'
0,34	0,3459	1,3230	1,7274	1,7616	101° 20'
0,36	0,3601	1,2861	1,6930	1,7309	101° 58'
0,38	0,3741	1,2534	1,6633	1,7049	102° 41'
0,40	0,3880	1,2244	1,6379	1,6837	103° 20'
0,42	0,4018	1,1987	1,6161	1,6654	103° 59'
0,44	0,4155	1,1758	1,5976	1,6508	104° 35'
0,46	0,4292	1,1554	1,5819	1,6391	105° 11'
0,48	0,4428	1,1372	1,5688	1,6301	105° 46'
0,50	0,4563	1,1212	1,5580	1,6235	106° 19'
0,52	0,4698	1,1069	1,5494	1,6190	106° 52'
0,54	0,4833	1,0944	1,5427	1,6167	107° 24'
0,56	0,4967	1,0825	1,5368	1,6151	107° 55'
0,58	0,5102	1,0738	1,5345	1,6171	108° 23'
0,60	0,5237	1,0655	1,5327	1,6197	108° 52'
0,62	0,5372	1,0585	1,5325	1,6239	109° 19'
0,64	0,5507	1,0526	1,5334	1,6293	109° 45'
0,66	0,5643	1,0477	1,5356	1,6360	110° 11'
0,68	0,5780	1,0437	1,5388	1,6437	110° 35'
0,70	0,5915	1,0406	1,5432	1,6527	110° 58'
0,72	0,6052	1,0386	1,5487	1,6628	111° 21'
0,74	0,6190	1,0373	1,5552	1,6739	111° 42'
0,76	0,6329	1,0368	1,5626	1,6860	112° 3'
0,78	0,6468	1,0370	1,5709	1,6989	112° 23'
0,80	0,6609	1,0379	1,5801	1,7127	112° 42'
0,82	0,6751	1,0395	1,5901	1,7274	113° 0'
0,84	0,6892	1,0417	1,6008	1,7430	113° 18'
0,86	0,7036	1,0446	1,6123	1,7592	113° 35'
0,88	0,7180	1,0480	1,6247	1,7763	113° 51'

Table IV (contd.)

$x$	$I_{\frac{2}{3}}(x)$	$I_{-\frac{2}{3}}(x)$	$Y_{\frac{2}{3}}\left(x e^{-j\frac{3\pi}{2}}\right)$	$\left H_{\frac{2}{3}}^{(1)}\left(x e^{-j\frac{2\pi}{2}}\right)\right $	Phase $H_{\frac{2}{3}}^{(1)}\left(x e^{-j\frac{3\pi}{2}}\right)$
0,90	0,7326	1,0520	1,6377	1,7942	114° 6'
0,92	0,7473	1,0566	1,6515	1,8127	114° 21'
0,94	0,7621	1,0617	1,6660	1,8320	114° 35'
0,96	0,7771	1,0674	1,6811	1,8522	114° 49'
0,98	0,7922	1,0735	1,6970	1,8729	115° 2'
1,0	0,8075	1,0801	1,7135	1,8942	115° 14'
1,2	0,9701	1,1720	1,9134	2,1453	116° 53'
1,4	1,1547	1,3067	2,1755	2,4632	117° 58'
1,6	1,3678	1,4836	2,5028	2,8522	118° 39'
1,8	1,6166	1,7055	2,9027	3,3223	119° 7'
2,0	1,9089	1,9778	3,3859	3,8869	119° 25'
2,2	2,2547	2,3081	3,9647	4,5613	119° 38'
2,4	2,6650	2,7065	4,6638	5,3718	119° 45'
2,6	3,1528	3,1856	5,4987	6,3386	119° 50'
2,8	3,7002	3,7343	6,4484	7,4346	119° 54'
3,0	4,4289	4,4495	7,6949	8,8794	119° 56'
3,2	5,2592	5,2755	9,1280	10,536	119° 57'
3,4	6,2530	6,2655	10,845	12,519	119° 58'
3,6	7,4423	7,4535	12,903	14,898	119° 59'
3,8	8,8698	8,8841	15,379	17,757	119° 59'
4,0	10,580	10,587	18,333	21,167	119° 59'
4,2	12,634	12,637	21,886	25,268	120° 0'
4,4	15,107	15,112	26,172	30,214	120° 0'
4,6	18,060	18,064	31,285	36,120	120° 0'
4,8	21,621	21,621	37,449	43,242	120° 0'
5,0	25,90	25,90	44,86	51,80	120° 0'
5,2	31,05	31,05	53,78	62,10	120° 0'
5,4	37,25	37,25	64,52	74,50	120° 0'
5,6	44,72	44,72	77,46	89,44	120° 0'
5,8	53,71	53,71	93,03	107,42	120° 0'
6,0	64,54	64,54	111,79	129,08	120° 0'
6,2	77,60	77,60	134,41	155,20	120° 0'
6,4	93,34	93,34	161,67	186,68	120° 0'
6,6	112,33	112,33	194,56	224,66	120° 0'
6,8	135,24	135,24	234,24	270,48	120° 0'
7,0	162,89	162,89	282,13	325,78	120° 0'
7,2	196,25	196,25	339,91	392,50	120° 0'
7,4	236,55	236,55	409,72	473,10	120° 0'
7,6	285,20	285,20	493,98	570,40	120° 0'
7,8	343,99	343,99	595,81	687,98	120° 0'
8,0	415,01	415,01	718,82	830,02	120° 0'

TABLE V

$x$	$I_{\frac{1}{3}}(x)$	$I_{-\frac{1}{3}}(x)$	$j \cdot Y_{\frac{1}{3}}\left(xe^{-j\frac{3\pi}{2}}\right)$	$H_{\frac{1}{3}}^{(1)}\left(xe^{-j\frac{3\pi}{2}}\right)$	Phase $H_{\frac{1}{3}}^{(1)}\left(xe^{-j\frac{3\pi}{2}}\right)$
0,00	0,0000	$\infty$	$\infty$	$\infty$	0° 0'
0,02	0,2413	3,4283	4,0979	4,1050	— 3° 22'
0,04	0,3041	2,7222	3,3189	3,3328	— 5° 14'
0,06	0,3482	2,3800	2,9491	2,9696	— 6° 44'
0,08	0,3834	2,1645	2,7208	2,7477	— 8° 1'
0,10	0,4133	2,0121	2,5620	2,5951	— 9° 10'
0,12	0,4396	1,8966	2,4438	2,4830	—10° 12'
0,14	0,4632	1,8051	2,3518	2,3969	—11° 9'
0,16	0,4849	1,7304	2,2780	2,3288	—12° 1'
0,18	0,5049	1,6680	2,2175	2,2743	—12° 50'
0,20	0,5237	1,6150	2,1671	2,2295	—13° 35'
0,22	0,5415	1,5693	2,1247	2,1926	—14° 18'
0,24	0,5583	1,5297	2,0887	2,1620	—14° 58'
0,26	0,5745	1,4949	2,0579	2,1366	—15° 37'
0,28	0,5901	1,4643	2,0315	2,1154	—16° 11'
0,30	0,6051	1,4371	2,0089	2,0955	—16° 47'
0,32	0,6197	1,4129	1,9893	2,0836	—17° 18'
0,34	0,6339	1,3914	1,9726	2,0720	—17° 49'
0,36	0,6478	1,3721	1,9584	2,0627	—18° 18'
0,38	0,6614	1,3550	1,9464	2,0556	—18° 46'
0,40	0,6747	1,3395	1,9362	2,0504	—19° 13'
0,42	0,6879	1,3257	1,9279	2,0470	—19° 38'
0,44	0,7008	1,3134	1,9212	2,0451	—20° 2'
0,46	0,7137	1,3026	1,9160	2,0446	—20° 26'
0,48	0,7264	1,2928	1,9122	2,0455	—20° 47'
0,50	0,7390	1,2843	1,9096	2,0478	—21° 9'
0,52	0,7515	1,2768	1,9082	2,0508	—21° 29'
0,54	0,7640	1,2703	1,9079	2,0552	—21° 49'
0,56	0,7764	1,2647	1,9086	2,0605	—22° 8'
0,58	0,7888	1,2600	1,9104	2,0668	—22° 26'
0,60	0,8013	1,2561	1,9131	2,0741	—22° 44'
0,62	0,8137	1,2530	1,9166	2,0822	—23° 0'
0,64	0,8261	1,2507	1,9211	2,0912	—23° 16'
0,66	0,8386	1,2490	1,9264	2,1010	—23° 31'
0,68	0,8511	1,2480	1,9324	2,1115	—23° 46'
0,70	0,8636	1,2476	1,9393	2,1229	—24° 0'
0,72	0,8763	1,2479	1,9468	2,1350	—24° 14'
0,74	0,8890	1,2487	1,9551	2,1477	—24° 27'
0,76	0,9017	1,2501	1,9642	2,1613	—24° 40'
0,78	0,9146	1,2521	1,9739	2,1755	—24° 52'
0,80	0,9276	1,2546	1,9842	2,1903	—25° 3'
0,82	0,9407	1,2576	1,9953	2,2059	—25° 14'
0,84	0,9539	1,2612	2,0070	2,2221	—25° 25'
0,86	0,9672	1,2652	2,0193	2,2390	—25° 36'
0,88	0,9807	1,2697	2,0323	2,2565	—25° 46'

Table V (contd.)

$x$	$I_{\frac{1}{3}}(x)$	$I_{-\frac{1}{3}}(x)$	$j \cdot Y_{\frac{1}{3}}\left(xe^{-j\frac{3\pi}{2}}\right)$	$\left H_{\frac{1}{3}}^{(1)}\left(xe^{-j\frac{3\pi}{2}}\right)\right $	Phase $H_{\frac{1}{3}}^{(1)}\left(xe^{-j\frac{3\pi}{2}}\right)$
0,90	0,9943	1,2747	2,0459	2,2747	-25° 55'
0,92	1,0080	1,2801	2,0601	2,2935	-26° 4'
0,94	1,0219	1,2860	2,0749	2,3129	-26° 13'
0,96	1,0360	1,2923	2,0904	2,3330	-26° 22'
0,98	1,0502	1,2991	2,1064	2,3537	-26° 29'
1,0	1,0646	1,3063	2,1231	2,3751	-26° 38'
1,2	1,2199	1,4018	2,3230	2,6234	-27° 43'
1,4	1,4002	1,5386	2,5850	2,9404	-28° 26'
1,6	1,6116	1,7181	2,9143	3,3304	-28° 56'
1,8	1,8617	1,9442	3,3188	3,8064	-29° 17'
2,0	2,1588	2,2231	3,8134	4,3825	-29° 31'
2,2	2,5224	2,5726	4,4269	5,0958	-29° 40'
2,4	2,9340	2,9733	5,1272	5,9070	-29° 47'
2,6	3,4370	3,4681	5,9890	6,9044	-29° 51'
2,8	4,0379	4,0624	7,0221	8,1001	-29° 54'
3,0	4,7773	4,7967	8,2969	9,574	-29° 56'
3,2	5,6147	5,6303	9,7430	11,245	-29° 57'
3,4	6,6426	6,6547	11,5193	13,298	-29° 58'
3,6	7,8727	7,8831	13,6479	15,758	-29° 58'
3,8	9,3473	9,3546	16,1984	18,706	-29° 59'
4,0	11,114	11,120	19,257	22,240	-29° 59'
4,2	13,234	13,238	22,927	26,479	-29° 59'
4,4	15,775	15,779	27,328	31,560	-29° 59'
4,6	18,827	18,831	32,614	37,661	-30° 0'
4,8	22,493	22,494	38,960	44,99	-30° 0'
5,0	26,90	26,90	46,59	53,80	-30° 0'
5,2	32,19	32,19	55,75	64,38	-30° 0'
5,4	38,56	38,56	66,79	77,12	-30° 0'
5,6	46,22	46,22	80,06	92,44	-30° 0'
5,8	55,45	55,45	96,04	110,90	-30° 0'
6,0	65,55	65,55	113,54	131,10	-30° 0'
6,2	79,93	79,93	138,44	159,86	-30° 0'
6,4	96,05	96,05	166,36	192,10	-30° 0'
6,6	115,47	115,47	200,00	230,94	-30° 0'
6,8	138,90	138,90	240,58	277,80	-30° 0'
7,0	167,15	167,15	289,51	334,30	-30° 0'
7,2	201,24	201,24	348,56	402,48	-30° 0'
7,4	242,37	242,37	419,80	484,74	-30° 0'
7,6	292,02	292,02	505,79	584,04	-30° 0'
7,8	351,97	351,97	609,63	703,94	-30° 0'
8,0	424,40	424,40	735,09	848,80	-30° 0'

## References<sup>1)</sup>.

1. P. S. EPSTEIN: Reflection of waves in an inhomogeneous absorbing medium. *Nat. Acad. Sci.*, **16**, p. 629, 1930.
2. K. RAWER: Elektrische Wellen in einem geschichteten Medium. *Ann. d. Phys.*, **35**, p. 402, 1939.
3. O. E. H. RYDBECK: A theoretical survey of the possibilities of determining the distribution of the free electrons in the upper atmosphere. *Transactions of Chalmers University of Technology* (Gothenburg, Sweden), **3**, 1942.  
O. E. H. RYDBECK: The reflection of electromagnetic waves from a parabolic friction-free ionized layer. *Journ. Appl. Phys.*, Vol. **13**, p. 577, 1942.  
O. E. H. RYDBECK: The reflexion of electromagnetic waves from a parabolic ionized layer. *Phil. Mag.*, XXXIV, p. 342, 1943.
4. T. L. ECKERSLEY: Radio transmission problems treated by phase integral methods. *Proc. Roy. Soc.*, A **136**, p. 499, 1932.
5. B. VAN DER POL and H. BREMMER: The diffraction of electromagnetic waves from an electrical point source round a finitely conducting sphere, with applications to radiotelegraphy and the theory of the rainbow. *Phil. Mag.*, XXIV, p. 825, 1937.
6. G. N. WATSON: The transmission of electric waves round the earth. *Proc. Roy. Soc.*, A **95**, p. 546, 1919.
7. K. FÖRSTERLING: Über die Ausbreitung elektromagnetischer Wellen in einem magnetisierten Medium bei senkrechter Inzidenz. *Hochfrequenztechn. u. Elektroak.*, **59**, p. 10, 1942.
8. G. BREIT and M. TUVE: A test of the existence of the conducting layer. *Phys. Rev.*, **28**, p. 554, 1926.
9. D. R. HARTREE: Optical and equivalent paths in a stratified medium. *Proc. Roy. Soc.*, A **131**, p. 449, 1931.
10. E. T. WHITTAKER and G. N. WATSON: *A Course of Modern Analysis*, p. 338.
11. E. T. WHITTAKER and G. N. WATSON; loc. cit., p. 349.
12. G. N. WATSON: *Theory of Bessel Functions*, p. 235.
13. G. N. WATSON: *Theory of Bessel Functions*, p. 236.
14. G. W. KENRICK: Radio transmission formulae. *Phys. Rev.*, **31**, p. 1040, 1928.
15. M. C. GRAY: Diffraction and refraction of a horizontally polarized electromagnetic wave over a spherical earth. *Phil. Mag.*, XXVII, p. 421, 1939.
16. B. VAN DER POL and H. BREMMER: loc. cit., p. 161 et seq.
17. G. N. WATSON: *Theory of Bessel Functions*, p. 243 et seq.

---

<sup>1)</sup> Due to the war situation this list of references cannot be regarded as complete as far as later publications are concerned.

18. G. N. WATSON: *Theory of Bessel Functions*, p. 248 et seq.
19. E. C. KEMBLE: *Fundamental Principles of Quantum Mechanics*, p. 97.
20. D. R. HARTREE: loc. cit., p. 443.
21. B. VAN DER POL and H. BREMMER: The propagation of radio waves over a finitely conducting spherical earth. *Phil. Mag.*, XXV, p. 820, 1938.
22. L. ESPENSCHIED, C. N. ANDERSON and A. BAILEY: Transatlantic radio telephone transmission. *Proc. Inst. Rad. Eng.*, 14, p. 7, 1926.
23. J. A. BEST, J. A. RATCLIFFE, and M. W. WILKES: Experimental investigations of very long waves reflected from the ionosphere. *Proc. Roy. Soc.*, A 156, p. 614, 1936.
24. H. FASSBENDER, F. EISNER u. G. KURLBAUM: Leistungs- und Strahlungsmessung an Flugzeug- und Bodenstationen. *Jahrb. drahtl. Telegr. u. Teleph.*, 31, p. 141, 1928.
25. Reports of the *Congrès International d'Electricité*, Vol. II, 1<sup>re</sup> Sec., Paris, 1932.
26. E. V. APPLETON, R. NAISMITH, and L. J. INGRAM: The critical-frequency method of measuring upper-atmospheric ionization. *Proc. Phys. Soc.*, 51, p. 81, 1939.

## Postscript.

Attention is called to the following errata in the former paper [3] in these transactions:

1. Page 17, in formula (31) read  $\int_{r_0 \sin \gamma_0}^r$  instead of  $\int_0^r$ .
2. Page 67, in formula (94) read  $\frac{\varrho^2}{2u^2} \ll 1$  instead of  $\frac{2u^2}{\varrho^2} \ll 1$ .
3. Page 72, line 11 from the bottom, read When  $\left(\frac{\nu}{\omega_0}\right)^2 \ll 1$  it is formally introduced *instead of* It is formally introduced.

## Table of Contents.

	Page
Introduction and Summary .....	5
General Considerations .....	7
On the Wave Functions of the Parabolic Layer .....	14
On the Expansions of the Parabolic Wave Functions .....	24
The Transmission of Radio Waves round a Spherical Earth surrounded by a Radially Inhomogeneous Concentric Reflecting Shell .....	36
The Transformation of the Series .....	52
The Poles of the Watson Case .....	59
The Numerical Evaluation of the Poles .....	69
The Residue Series .....	73
The Treatment of the Separate Wave Groups .....	76
The Field Strength from the Dipole Element .....	83
The Reflection Coefficient of the Parabolic Layer .....	86
On the Application of the Phase Integral .....	93
The Boundary Reflection of the Parabolic Layer .....	96
A Short Note on the Reflection Coefficient of a Layer with Quadratic Increase in Electron Density .....	99
A Short Discussion of the Case $\omega_{r_m} < \omega < \omega_H$ for the Parabolic Layer .....	101
On the Poles when the Reflecting Shell is Radially Inhomogeneous .....	105
Further Notes on the Residue Series .....	108
The Limiting Case of a Plane Boundary .....	118
A Short Discussion of the Case of the Poor Reflector .....	120
On the Attenuation Coefficient in Long Wave Transmission .....	124
The Reflection Coefficient of the Parabolic Layer in the Penetration Frequency Region .....	130
The Virtual Height of the Parabolic Layer .....	139
The Reflection of Radio Waves from an Extremely Thin Layer .....	151
Tables of Cylinder Functions of Order $\pm \frac{1}{3}$ and $\pm \frac{2}{3}$ .....	160
References .....	167
Postscript .....	169





CHALMERS TEKNISKA HÖGSKOLAS  
HANDLINGAR

TRANSACTIONS OF CHALMERS UNIVERSITY OF TECHNOLOGY  
GOTHENBURG, SWEDEN

Nr 3

(Avd. för Allmänna Vetenskaper 1)

1942

---

A THEORETICAL SURVEY OF THE POSSIBILITIES OF DETERMINING THE DISTRIBUTION OF THE FREE ELECTRONS IN THE UPPER ATMOSPHERE

BY

OLOF E. H. RYDBECK



GÖTEBORG 1942  
ELANDERS BOKTRYCKERI AKTIEBOLAG

(ES)



## Summary.

The problem of determining the variation with height of the density of the free electrons of the upper ionosphere has attracted a great deal of interest during the past two years. The same is true of the problem of determining the variation of the electronic collisional frequency with height, a problem of a very similar nature. This communication is a theoretical survey of the fundamentals which are of main interest in connexion with these problems.

The measurement of the travel-times of electromagnetic wave-packets forms the basis of almost all ionospheric measurements. As an introduction, therefore, the propagation and dispersion of the wave-packet is treated by means of well known optical methods. Several examples are shown of the actual dispersion of down-coming wave-trains. Under most conditions the dispersion is not serious and the determination of the time of travel is fairly accurate.

In a following section a closer approximation to the actual wave solution than that afforded by the geometrical optics is studied by means of B. W. K.-approximations. A practical example of standing waves between the ionosphere and ground is shown. As the difference between the classical phase and the B. W. K.-phase is independent of the wave frequency, the time of travel becomes the same in both cases. When the time of travel is known as a function of the wave frequency it is generally possible to determine the distribution of the free electrons over most of the lower part of the ionized layers. The various mathematical methods to be used for this purpose are studied fairly thoroughly. It is shown that quite accurate solutions can be obtained at places where the magnetic inclination is either great or small.

The next problem to be discussed is the calculation of the variation of the collisional frequency with height. It is interesting to find that it can be determined from sweep frequency reflection coefficient measurements, if the electron density distribution is determined at the same time. So far the method has not been applied in practice. Even though the necessary measuring equipment is fairly complicated the prospects of getting valuable results are good.

A number of ionospheric records have been examined and the corresponding electron density distribution studied. It is shown that it generally is parabolic over a quite wide density range. Examples are shown where the parabolic representation is a very good approximation for practically the whole layer. The characteristic frequencies have been obtained for each distribution and it is shown that it generally is not a permissible approximation to use a fixed characteristic frequency to critical frequency ratio in the routine scaling of ionosphere records. The total number of electrons has been integrated for several cases and it is shown that this number may decrease even though the maximum electron density increases as is often the case in the afternoon in the equatorial regions. This strongly supports the various hypotheses of the expansion of the upper atmosphere.

Finally the exact wave functions for a parabolic layer are studied briefly. It is shown that the travel time and the dispersion are finite at the critical frequency and that the reflection coefficient differs appreciably from the classical one only when the layer thickness becomes less than about four wave lengths. Asymptotic expansions of the wave functions will appear in a later communication.

## A general survey of the situation.

The problem of determining the electron distribution of the upper atmosphere has been studied with a great deal of interest in recent years by a number of investigators engaged in ionospheric research [1]. The  $F$ -region of the ionosphere, especially its upper part the  $F_2$ -layer, has attracted the main interest. Several factors make the investigation of the electron distribution of the  $F_2$ -layer fairly easy and profitable. Its main ionization is spread over a great height interval and its collisional frequency is low. Furthermore the maximum ionization of the  $F_2$ -layer generally exceeds that of the lower layers very much.

The determination of the true electron distribution of the  $F_2$ -layer appears to be one of the most important problems of the physics of the upper atmosphere. The experimental data on the electron density variation of the lower layers (the  $E$ - and the  $F_1$ -layers) is in accord with the hypothesis of ion production in a static atmosphere by solar ultra-violet light and recombination of the two-body collision type. This, however, is not true of the  $F_2$ -layer which shows a character different in several respects.

The reader not familiar with the essential features of the ionosphere may find a reference to the general literature useful [2]. It should suffice here to state the main result of the experimental data so far collected in various parts of the world. The  $E$ - and  $F_1$ -maximum ionizations are in fair accord with the following expressions, viz.

$$N_{max} = 1.45 \cdot 10^5 \cdot (\sin \gamma)^{1/2} \text{ electrons cm}^{-3} \text{ for the } E\text{-layer} \quad (1)$$

and

$$N_{max} = 2.55 \cdot 10^5 \cdot (\sin \gamma)^{1/2} \quad \gg \quad \gg \quad \gg \quad F_1\text{-layer} \quad (2)$$

according to Hulbert.  $\gamma$  denotes the height of the sun. The true heights of the maximum ionization varies with  $\gamma$ . Heights of 100 and 180 km respectively may be mentioned as typical noon values for the two layers.

---

Partly communicated at the joint meeting of the International Scientific Radio Union American Section and the Institute of Radio Engineers at the National Academy of Sciences, Washington, D. C. April 26, 1940.

As shown by (1) and (2) the ultra-violet light theory of the static atmosphere yields a single maximum in the daily variation of  $N$ . In the  $F_2$ -layer, however, a double maximum is observed in tropical latitudes. The decrease in ionization is different from day to day. If the average decrease were attributed to recombination only not affected by other factors, which is a questionable assumption, the corresponding value of the recombination coefficient would differ very much from the present theoretical value. However, the photoelectric action of the solar ultra-violet radiation seems to be adequate to produce an ionization at  $F_2$ -levels of the observed order of magnitude [3]. To explain the  $F_2$ -variations, therefore, an additional hypothesis is necessary. One of the most probable ones is the assumption of a day-time expansion of the  $F_2$ -atmosphere due to heating and dissociation of the molecules. The  $F_2$ -ionization would center about a 275-km level in the absence of the expansion and it would increase to a maximum in the early afternoon. The expansion, however, spreads the ionization to say 375 km or higher and therefore reduces the ionization density. The expansion is very slight during days when  $\gamma$  never approaches  $45^\circ$  and  $N$  reaches its maximum shortly after noon. When  $\gamma$  approaches  $90^\circ$  at noon  $N$  increases very rapidly in the morning. Soon, however, in spite of the fact that the total number of electrons continues to increase, the expansion is so rapid as really to make  $N$  decrease.  $N$  will therefore pass through one maximum in the morning and another maximum in the afternoon.

Owing to the expansion of the  $F_2$ -atmosphere it appears likely that winds will blow away in all directions in levels about 275 km directly beneath the sun. In the morning hemisphere a stream of » $F_2$ -air» should move against the rotation of the earth and gradually become turbulent whereas one expects a stream moving with the rotation of the earth in the afternoon hemisphere. It is believed by many that such an eastward wind would displace the afternoon maximum in  $N$  one hour or more towards evening.

The two hypotheses, ionization by solar ultra-violet light and expansion of the  $F_2$ -atmosphere, appear to be able to account for the main features of the  $F_2$ -ionization. Very probably too the  $F_2$ -atmosphere contracts slowly as the night progresses. This may account for the irregular recrudescence of the  $F_2$ -ionization frequently observed in the small hours of the morning.

The  $F_2$ -layer generally is quite disturbed during magnetic storms,

though not necessarily so. On some occasions the electron density of the  $F_2$ -layer is so reduced during magnetic disturbances that it tends to fall below the value of the maximum electron density of the  $F_1$ -layer. At the same time the virtual heights of reflection become abnormally great. They become much greater than should be expected by the retardation in the  $F_1$ -layer and therefore indicate an extensive expansion and diffusion of the  $F_2$ -region.

A thorough and accurate study of the electron density and collisional frequency distributions of the  $F_2$ -layer therefore is very desirable as it would give us more reliable information concerning the upper atmosphere and the magnetic storms. As practically all transatlantic short wave radio communication is conveyed by means of the  $F_2$ -layer a deeper study of its properties, especially during magnetic storms, is of technical importance.

After this survey of the general situation it should be proper to study briefly the application of well known optical methods to the description of the propagation of the radio wave-packet. This should be a fitting introduction to the following problems since the practical way of exploring the upper atmosphere is by means of recording the times of travel and the intensity of radio signals reflected from the various ionized regions.

### The Propagation of the Wave-Train.

As a further introduction to the following sections we make ourselves a little bit more familiar with the essential facts governing the transmission of arbitrary wave-trains in a dispersive medium. We restrict ourselves to the ordinary form of the wave equation, where  $\Pi$  is a function from which the characteristic quantities of the wave may be derived by suitable operations,

$$\nabla^2 \Pi + k_0^2 \cdot n^2 \cdot \Pi = 0. \quad (3)$$

The notations are the general ones, viz.  $k_0 = \frac{2\pi}{\lambda_0}$  and  $n$  = the refractive index. Here  $n$  in general is a function of the coordinates. If the change in  $n$  is sufficiently slow we may seek an approximate solution of the classical form

$$\Pi = e^{iS}, \quad (4)$$

where  $S$  represents the phase of the wave. Inserting this in (3) one gets that

$$\sum_{x, y, z} \left( \frac{\delta S}{\delta x} \right)^2 - j \nabla^2 S = k_0^2 \cdot n^2 \quad (5)$$

If

$$|\nabla S| \ll \sum_{x, y, z} \left( \frac{\delta S}{\delta x} \right)^2, \text{ i. e. } \frac{1}{n} \cdot \text{grad}(n) \cdot \lambda \cdot \cos \Psi \ll 2\pi, \quad (5a)$$

where  $\Psi$  is the angle between the direction of the ray and  $\text{grad}(n)$ , then Eq. (5) reduces to

$$\sum_{x, y, z} \left( \frac{\delta S}{\delta x} \right)^2 = k_0^2 \cdot n^2, \quad (6)$$

which in geometrical optics is called »equation of the iconal». By (5a) a reduction to the iconal equation is possible only when the relative change of the refractive index within a wavelength is very small, as is well known. Such a reduction generally is possible over most wave paths in the ionosphere. It is obvious, however, that the apex-region of a ray, especially at vertical incidence, may form an exception. Another exceptional example is the level of maximum electron density for a ray in the penetration frequency region.

An integral of the equation of the iconal will have the form

$$S = S(x, y, z, c_1, c_2) + c_3. \quad (7)$$

If we write (7) in differential form it becomes

$$\frac{\delta S}{\delta x} \cdot dx + \frac{\delta S}{\delta y} \cdot dy + \frac{\delta S}{\delta z} \cdot dz = 0, \quad (8)$$

showing that the rays are everywhere normal to the wave surfaces.

The equation of the ray is

$$\frac{dx}{\left( \frac{\delta S}{\delta x} \right)} = \frac{dy}{\left( \frac{\delta S}{\delta y} \right)} = \frac{dz}{\left( \frac{\delta S}{\delta z} \right)}. \quad (8a)$$

If the medium is absorbing  $n$  becomes complex and we consequently get two characteristic wave surfaces. One is the surface of equal phase and the other one is the surface of equal amplitude.

$$S = S_1 + jS_2.$$

It is of interest to investigate briefly how much the direction of the ray actually departs from the normal to the surfaces  $S_1 = \text{const.}$ . To fix our definitions we say that the ray is the curve in which the energy travels. If we have electromagnetic waves the direction of energy flow is given by the direction of Poynting's vector. Let us consider a two-dimensional case as outlined by Epstein [4] in which the index of refraction is independent of the coordinate  $z$ . If the electric vector is parallel to  $z$  ( $E_x = E_y = 0$ ) we get from Maxwell's equations that

$$\begin{aligned} \mu \cdot k_0 \cdot H_x &= \exp. (-S_2) \cdot \left[ \frac{\delta S_1}{\delta y} \cdot \cos (S_1 - \omega_0 t) - \frac{\delta S_2}{\delta y} \cdot \sin (S_1 - \omega_0 t) \right], \\ \mu \cdot k_0 \cdot H_y &= -\exp. (-S_2) \cdot \left[ \frac{\delta S_1}{\delta x} \cdot \cos (S_1 - \omega_0 t) - \frac{\delta S_2}{\delta x} \cdot \sin (S_1 - \omega_0 t) \right]. \end{aligned} \quad (9)$$

The Poynting vector has the components

$$P = \frac{c_0}{4\pi} [-E_z H_y, E_z H_x, 0]$$

and its direction therefore is given by the ratio

$$P_y / P_x = -H_x / H_y. \quad (10)$$

In the case of a non-dissipative medium this ratio is independent of time. We can therefore compute the curves of energy flow. In absorbing media, however,  $\text{grad} (S_2) \neq 0$  and Poynting's vector oscillates. In this case it is not possible to compute the curves of energy flow from the vector direction. When the absorption is considerable there is not much left of the conception of a ray. Although it is not too important in this connexion to make a detailed study of the ray equation in the dissipative case a short survey of the essentials certainly has some educational value. Let us therefore study the propagation of a wave-packet produced by letting an interrupted radiation pass through a suitable aperture. If we observe the interrupted ray-pencil at sufficient distance from the slit (Fraunhofer diffraction) we remember from theoretical optics that it can be represented the following way, viz.

$$\begin{aligned} H(x, y, z, t) &= A \int_{-\eta_a}^{+\eta_a} \int_{-\eta_b}^{+\eta_b} \int_{-\infty}^{+\infty} \exp. (j [2\pi (\eta_x \cdot x + \eta_y \cdot y + \eta_z \cdot z) - \\ &\quad - \omega_0 t]) \cdot \psi(\eta) \cdot d\eta_x \cdot d\eta_y \cdot d\eta_z. \end{aligned} \quad (11)$$

$\bar{\eta} = (\eta_x, \eta_y, \eta_z)$  is the vector wave number.  $\eta_a$  and  $\eta_b$  are small if the ray is directed along the  $z$ -axis. We now wish to study the behaviour of this wave-packet impinging upon an arbitrary discontinuity surface, which for example may be the boundary of an ionized medium. It is practical to change to new coordinates  $x_1, y_1$  and  $z_1$  where  $x_1$  and  $y_1$  are in the plane of the discontinuity surface. Defining the new axis by their direction cosines with respect to the old system, viz.

$$\begin{aligned} \hat{x}_1 &= [\cos \alpha_x, \cos \alpha_y, \cos \alpha_z], \hat{y}_1 = [\cos \beta_x, \cos \beta_y, \cos \beta_z], \hat{z}_1 = \\ &= [\cos \gamma_x, \cos \gamma_y, \cos \gamma_z] \end{aligned} \quad (12)$$

we have

$$\begin{aligned} \Pi &= A \int \int \int_{\substack{\text{range as} \\ \text{before}}} \exp. (j [2\pi (x_1 \overbrace{(\eta_x \cdot \cos \alpha_x + \eta_y \cdot \cos \alpha_y + \eta_z \cdot \cos \alpha_z)}^{\varrho_1} + \\ &+ y_1 \overbrace{(\eta_x \cdot \cos \beta_x + \eta_y \cdot \cos \beta_y + \eta_z \cdot \cos \beta_z)}^{\varrho_2} + \\ &+ z_1 (\eta_x \cdot \cos \gamma_x + \eta_y \cdot \cos \gamma_y + \eta_z \cdot \cos \gamma_z)) - \\ &- \omega_0 t]) \cdot \varphi(\eta) \cdot d\eta_x \cdot d\eta_y \cdot d\eta_z. \end{aligned} \quad (13)$$

According to the well known rules for the reflection of plane waves the coefficients of  $x_1$  and  $y_1$  remain unchanged when the wave enters the second medium. If  $\eta_1$  is the wave number of the second medium corresponding to  $\eta$  in the first medium we must have that

$$\begin{aligned} \Pi &= A \int \int \int \exp. (j [2\pi (x_1 \cdot \varrho_1 + y_1 \cdot \varrho_2 + z_1 \cdot \sqrt{\eta_1^2 - \varrho_1^2 - \varrho_2^2}) - \\ &- \omega_0 t]) \cdot \varphi(\eta) \cdot d\eta_x \cdot d\eta_y \cdot d\eta_z \end{aligned} \quad (14)$$

in the second medium if we neglect the change in amplitude of the refracted ray for the time being. Because  $\eta_x$  and  $\eta_y \ll \eta_z$  in the important range of wave numbers, we can write that  $\varphi(\eta) = \varphi(\eta_z)$ , and

$$\begin{aligned} \sqrt{\eta_1^2 - \varrho_1^2 - \varrho_2^2} &\simeq \eta_z - \frac{\eta_z}{\eta_2} [\eta_x (\cos \alpha_x \cdot \cos \alpha_z + \cos \beta_x \cdot \cos \beta_z) + \\ &+ \eta_y (\cos \alpha_y \cdot \cos \alpha_z + \cos \beta_y \cdot \cos \beta_z)] \end{aligned}$$

where  $\eta_2^2 = \eta_1^2 - \eta_z^2 \cdot \sin^2 \gamma_z$ .

Introducing

$$T_1 = 2 \pi \left[ \left( x_1 - z_1 \cdot \cos \alpha_z \cdot \frac{\eta_z}{\eta_2} \right) \cos \alpha_x + \left( y_1 - z_1 \cdot \cos \beta_z \cdot \frac{\eta_z}{\eta_2} \right) \cos \beta_x \right]$$

and

$$T_2 = 2 \pi \left[ \left( x_1 - z_1 \cdot \cos \alpha_z \cdot \frac{\eta_z}{\eta_2} \right) \cos \alpha_y + \left( y_1 - z_1 \cdot \cos \beta_z \cdot \frac{\eta_z}{\eta_2} \right) \cos \beta_y \right]$$

and remembering that  $\eta_z / \eta_1 \sim \eta / \eta_1 = n / n_1$ , where  $n$  and  $n_1$  are the respective refractive indices, (14) reduces to

$$H \simeq 4 A \cdot \frac{\sin(T_1 \cdot \eta_a)}{T_1} \cdot \frac{\sin(T_2 \cdot \eta_b)}{T_2} \int_{-\infty}^{+\infty} \exp. \left( j \left[ 2 \pi \cdot \eta \left\{ x_1 \cdot \cos \alpha_z + y_1 \cdot \cos \beta_z + z_1 \sqrt{\left( \frac{n_1}{n} \right)^2 - \sin^2 \gamma_z} \right\} - \omega_0 t \right] \right) \cdot \varphi(\eta) \cdot d\eta. \quad (15)$$

In order to find the direction of the ray we have to search for the direction that makes

$$\left| \frac{\sin(T_1 \cdot \eta_a)}{T_1} \right| \cdot \left| \frac{\sin(T_2 \cdot \eta_b)}{T_2} \right|$$

as large as possible. In this direction the real part of  $T_1$  and  $T_2$  will vanish.

Therefore

$$\frac{x_1}{\cos \alpha_z} = \frac{y_1}{\cos \beta_z} = z_1 \cdot \operatorname{Re} \left( \frac{1}{\sqrt{\left( \frac{n_1}{n} \right)^2 - \sin^2 \gamma_z}} \right), \quad (16)$$

that is the direction of the ray is given by the set

$$\operatorname{Re} \left[ \frac{dx}{\delta S / \delta x} = \frac{dy}{\delta S / \delta y} = \frac{dz}{\delta S / \delta z} \right] \quad (16 a)$$

in a homogeneous medium as was originally shown by Epstein. In general orthogonal coordinates, with the absorption constant for  $U_3 = \text{const.}^1$ ), the direction is given by

<sup>1)</sup> The surfaces  $U_3 = \text{const.}$  are constant intensity surfaces.

$$\operatorname{Re} \left[ \frac{h_1^2 \cdot du_1}{\delta S / \delta u_1}, \frac{h_2^2 \cdot du_2}{\delta S / \delta u_2}, \frac{h_3^2 \cdot du_3}{\delta S / \delta u_3} \right]. \quad (16b)$$

As  $\varphi(\eta)$  is the shape of the packet in the non-dispersive medium we put  $n = 1$ . We introduce the absorption by writing

$$n_1^2 = \alpha + j\beta. \quad (17)$$

After a little bit of juggling we get the following direction cosines of the refracted ray, viz.

$$\left[ \cos \alpha_z^\nu, \cos \beta_z^\nu, \cos \gamma_z^\nu \right] = \left[ \frac{\cos \alpha_z}{\sqrt{\xi}}, \frac{\cos \beta_z}{\sqrt{\xi}}, \right. \\ \left. \frac{\sqrt{(a - \sin^2 \gamma_z)^2 + \beta^2}}{\sqrt{\frac{1}{2}(a - \sin^2 \gamma_z)(2a - \sin^2 \gamma_z) + \beta^2} + \frac{1}{2} \sin^2 \gamma_z \sqrt{(a - \sin^2 \gamma_z)^2 + \beta^2}}} \right] \\ \varrho_3 \quad (18)$$

where

$$\xi = \frac{2\varrho_3}{a - \sin^2 \gamma_z + \sqrt{(a - \sin^2 \gamma_z)^2 + \beta^2}}.$$

It is especially convenient to change from  $\cos \gamma_z^\nu$  to  $\operatorname{tang} \gamma_z^\nu$ . It is easily established that

$$\operatorname{tg} \gamma_z^\nu = \sin \gamma_z \sqrt{\frac{a - \sin^2 \gamma_z + \sqrt{(a - \sin^2 \gamma_z)^2 + \beta^2}}{2(a - \sin^2 \gamma_z)^2 + 2\beta^2}}. \quad (18a)$$

From this expression we see that the ray never becomes horizontal when the medium is dissipative.<sup>1)</sup> At the classical reflection level

$$a = \sin^2 \gamma_z$$

and

$$\operatorname{tang} \gamma_z^\nu = \sin \gamma_z \cdot \frac{1}{\sqrt{2\beta}}. \quad (19)$$

Practically always  $\beta \ll 1$ , i. e. the absorption is negligible in a wavelength, and  $\gamma_z^\nu$  therefore approximately  $90^\circ$ . Below the classical reflection level the correction is even smaller, so we are fairly well

<sup>1)</sup> This is not unexpected as the lower rays of the pencil travel greater distances to reach the same height and consequently become more absorbed than the higher ones.

justified in computing the ray-path neglecting the absorption. (One always has to be careful, of course, when speaking of the ray path near the reflection level. It happens that inequality (5 a) does not hold and then the ray treatment is no longer correct). It is apparent from the direction expressions so far deduced that it is a great complication to consider the absorption in computing the ray paths. To illustrate this further we calculate the signal velocity along the path of maximum intensity.

We assume that  $\varphi(\eta)$  has a maximum for  $\eta = \eta_0$  which is the carrier wave number of the sender. We further suppose that it approaches zero monotonically as  $|\eta - \eta_0|$  increases. To have a definite limit we state that  $\varphi(\eta)$  is practically zero outside the wave number range  $\eta'$  to  $\eta''$ . The wave function (15) therefore gets the following form, if  $f_0 =$  carrier frequency and  $\eta = \eta_0 + \Omega$ , viz.

$$\begin{aligned}
 H \simeq & 4 A \cdot \frac{\sin(T_1 \cdot \eta_a)}{T_1} \cdot \frac{\sin(T_2 \cdot \eta_b)}{T_2} \\
 & \cdot \exp. \left( j 2 \pi f_0 \left[ \frac{x_1 \cdot \cos \alpha_z + y_1 \cdot \cos \beta_z + z_1 \sqrt{n_1^2 - \sin^2 \gamma_z}}{c_0} - t \right] \right) \\
 & + \int_{-\infty}^{+\infty} \exp. \left( j \left[ 2 \pi \Omega \left[ \frac{\varrho_4}{x_1 \cdot \cos \alpha_z + y_1 \cdot \cos \beta_z + z_1 \left( \sqrt{n_1^2 - \sin^2 \gamma_z} + \right. \right.} \right. \right. \right. \\
 & \left. \left. \left. + f \frac{d}{df} \left( \sqrt{n_1^2 - \sin^2 \gamma_z} \right) \right) - c_0 t \right] \right)_{f=f_0} \\
 & + z_1 \cdot \pi \cdot \Omega^2 \cdot c_0 \left[ \frac{2 \frac{d}{df} \sqrt{n_1^2 - \sin^2 \gamma_z} + f \cdot \frac{d^2}{df^2} \sqrt{n_1^2 - \sin^2 \gamma_z}}{\varrho_5} \right]_{f=f_0} \\
 & \left. + \dots \right] \cdot \varphi_0(\eta_0 + \Omega) \cdot d \Omega . \tag{20}
 \end{aligned}$$

At the center of the wave-packet  $\text{Re}(\varrho_4) = 0$ . Following the ray direction  $x_1 = r \cdot \cos \alpha_z^y$ , etc.,  $\text{Re}(\varrho_4)$  gets the following form, viz.

$$\text{Re}(\varrho_4) = (r/v_g - t) \cdot c_0 , \tag{21}$$

where  $v_g$  is the group velocity and is equal to

$$v_g = \frac{c_0 \cdot \sqrt{\xi}}{\sin^2 \gamma_z + \sqrt{(a - \sin^2 \gamma_z)^2 + \beta^2} + \frac{f}{2} \left( \frac{d\alpha}{df} + \frac{\beta}{a - \sin^2 \gamma_z + \sqrt{(a - \sin^2 \gamma_z)^2 + \beta^2}} \cdot \frac{d\beta}{df} \right)} \quad (21 a)$$

For negligible absorption it reduces to the well known

$$v_g = \frac{c_0 \cdot n}{n^2 + \frac{f}{2} \frac{d(n^2)}{df}} \quad (21 b)$$

The introduction of absorption complicates matters very much as was stated before. In the  $F$ -layer of the ionosphere the electronic collisional frequency is so low that we are practically always justified in neglecting the absorption for most angular frequencies  $\omega_0$  of the ray used for the exploration of the layer. The corrections in our expressions so far deduced therefore generally will be so small that they are insignificant compared to the error involved in the experimental methods used for the exploration of the ionosphere.

The length of the wave-packet is determined by the fact that the principal phase factor  $2\pi\Omega\rho_4$  should not range through more than about  $2\pi$  from end to end of the packet if the various components are not to cancel each other mutually through interference. Calling the length of the packet  $\Delta s$  and the corresponding time of travel  $\Delta\tau$  this means that

$$(\eta' - \eta'') \cdot \Delta s \cdot \frac{c_0}{v_g} = \frac{\Delta f \cdot \Delta s}{v_g} = \Delta f \cdot \Delta\tau \sim 1. \quad (22)$$

of which the last expression is familiar as the wave-mechanical uncertainty relation. This expression shows us that it is impossible to make the experimental error as small as possible. If we for example wish to register the time of travel of the signal it is desirable to make  $\Delta\tau$  as small as possible. The smaller  $\Delta\tau$  is compared to the actual time of travel the more accurate will be the determination of that time. If  $\Delta\tau$  is made very small, however, the frequency width of the packet or pulse becomes so large that it is comparable to  $f_0$  and it becomes difficult to produce the packet. In practical applications  $\Delta\tau$  is made as small as the limitations of the sender and the recording receiver will permit.

Finally let us study briefly the dispersion the wave-packet will suffer in a friction free ionosphere. Then

$$n^2 = 1 - f_c^2 / f^2, \quad (23)$$

where  $f_c$  is the so called critical frequency of the medium. If the dispersion is to be negligible the magnitude of the phase correction

$$z_1 \cdot \pi \cdot \Omega^2 \cdot c_0 \cdot \rho_s$$

should not increase to more than about  $2\pi$  from center to end of the packet. For negligible dispersion, therefore,

$$r \ll v_g \cdot \frac{8}{(\Delta f)^2} \cdot \frac{\cos^2 \gamma_z - f_c^2 / f_0^2}{\cos^2 \gamma_z} \cdot f_0^3 / f_c^2. \quad (24)$$

As a typical example we take vertical incidence with a carrier frequency of 4 mc/s and a frequency width of 10 kc/s. If a)  $f_c = 0.7 f_0$ , the dispersion is negligible as long as

$$r \ll 70000 \text{ km}$$

and b) if  $f_c = 0.95 f_0$ , the same is true if

$$r \ll 3000 \text{ km.}$$

The dispersion, therefore, always is negligible except very close to the apex of the ray where  $f_c = f_0 \cdot \cos \gamma_z$ . The actual path-length in the principally dispersing region generally is so small, when the electronic gradient is of average magnitude, that the total dispersion is unimportant. During magnetic storms, however, when the  $F_2$  electronic gradient may be abnormally low dispersion is frequently noticeable. The calculation of the total dispersion from experimental travel-time data is shown in the following section.

The propagation of the wave-packet will, under certain circumstances, be reduced to a mechanical problem when the medium is non-dissipative. This analogy is, of course, quite accidental and presents nothing new. It was known already to Hamilton that there generally is a close analogy between geometrical optics and mechanics. In modern times a treatment similar to Hamilton's was introduced by Brunn about 1872 and has been extensively used ever since. The mechanical interpretation offers many advantages to the practi-

cal engineer even though it is an approximation in practical applications. A short recapitulation of the essential transformation therefore must have its educational value. To fix our ideas we introduce the mass  $m$  of the electro-magnetic photon

$$m \cdot c_0^2 = h \cdot f_0 . \quad (25)$$

If we further write  $n_1^2 = 1 - \Delta \varepsilon$ , where  $\Delta \varepsilon$  is the reduction of the dielectric constant,  $\varepsilon$ , and  $S_1 = S \cdot h/2\pi$ , the iconal equation gets the following form

$$\sum_{x, y, z} \left( \frac{\delta S_1}{\delta x} \right)^2 = 2m(E - V) \quad (26)$$

where  $E = h \cdot f_0/2$  is the initial energy and  $V = \Delta \varepsilon \cdot h \cdot f_0/2$  is the potential energy of the representative particles. Eq. (26) can also be written

$$\frac{h^2}{\eta_1^2} = 2m(E - V) . \quad (26 a)$$

Another expression for the signal velocity equivalent to (21 b) is

$$v_g = \left( \frac{df}{d\eta_1} \right)_{f_0} . \quad (27)$$

It is, as has been shown on page 10, normal to the constant phase surface in the non-dissipative case. Making use of (26 a) the momentum of the representative particles turns out to be

$$P = m \cdot v_g = \frac{\delta S_1}{\delta r} + \frac{2}{h \cdot c_0^2} \left[ \frac{d}{d\eta_1} (E \cdot V) \right]_{f_0} \quad (28)$$

directed along the normal to the constant phase surface. When either  $V = 0$  or the product  $E \cdot V$  is independent of frequency, the momentum is equal to the gradient of  $S_1$  and (26) is the Hamilton-Jacobi differential equation for the abbreviated action function  $S_1$ , of a masspoint of energy  $E$  and mass  $m$  moving in a force field with potential energy  $V$ . The only time when  $E \cdot V$  is independent of frequency is when  $n^2$  is of the form given by (23).  $V$  then becomes

$$V = \frac{h \cdot f_c}{2} \cdot \frac{f_c}{f_0} . \quad (29)$$

As  $f_c^2 = e^2 N/\pi m_0$ , where  $e$  and  $m_0$  are charge and mass of the electron, we may visualize the wave-packet as a masspoint  $m$  experiencing a force

$$\vec{F} = -\frac{h \cdot e^2}{2 \pi \cdot m_0 \cdot f_0} \cdot \text{grad } N. \quad (30)$$

In the case of a symmetrical, spherical ionized region as shown on Fig. 1 the propagation is a case of central motion.

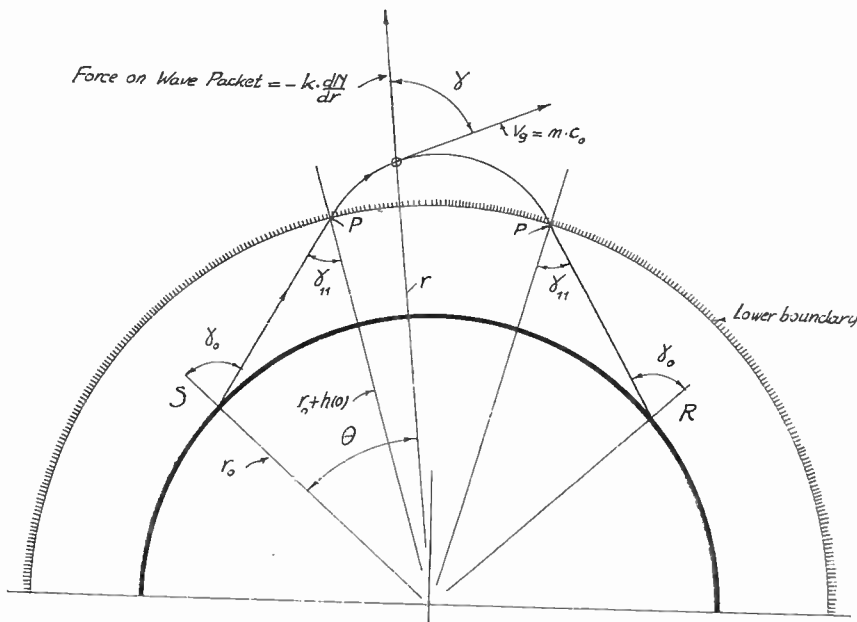


Fig. 1.

In this case the Hamilton—Jacobi equation has the following solution

$$S_1 = c_1 \cdot \theta + \int_0^r \sqrt{2 m (E - V(r)) - \frac{c_1^2}{r^2}} \cdot dr. \quad (31)$$

The angular momentum  $P_\theta$  is constant as is always the case at central motion. This determines the integration constant  $c_1$ .

$$P_\theta = \frac{\delta S_1}{\delta \theta} = c_1 = \sqrt{2 m E} \cdot r_0 \cdot \sin \gamma_0. \quad (31 a)$$

As  $v_g = c_0 \cdot n$ , the appropriate form of Snellius law means nothing else than that  $P_\theta$  or the surface velocity is constant. At the apex of the ray  $P_r$  is zero. This determines the electron density needed to return the ray.

$$P_r = \frac{\delta S_1}{\delta r} = \left\{ 2m \left[ E - V - E \cdot \left( \frac{r_0}{r} \sin \gamma_0 \right)^2 \right] \right\}^{1/2}. \quad (31 \text{ b})$$

At the apex

$$V = E \cdot \cos^2 \gamma_0 + \frac{r^2 - r_0^2}{r^2} \cdot E \cdot \sin^2 \gamma_0, \quad (32)$$

which is the initial radial kinetic energy plus the work performed on the wave-packet by the centrifugal force. This relation is the same as

$$(n)_{\text{apex}} = r_0/r \cdot \sin \gamma_0, \quad (32 \text{ a})$$

which is immediately obtained from Snellius' law. Finally reference should be made to de Groot [5] who wrote one of the first notes on the mechanical interpretation of the propagation of electromagnetic waves with special reference to radio waves. Communications of similar kind have also been given by Eckersley [6].

It should be stressed again that the mechanical analogy should not be pushed too far. The wave equation is not equivalent to the motion of one particle but to the motion of many, a so called statistical ensemble. It is, as we have seen, only in the non-dissipative case that the iconal equation gives correctly the direction of the ray and even when it so does the mechanical interpretation is only correct when  $E \cdot V$  is independent of frequency.

## The Dispersion of the Down-Coming Radio Echoes.

In the exploration of the ionosphere short wave-trains are transmitted from the sending station. Their eventual return is then registered by some kind of recording device which records the time of travel as a function of the carrier frequency of the sending station. The frequency range generally is so wide that the rays always penetrate at the highest frequencies. When the time of travel is known as a function of frequency it is possible to calculate the

actual electron density distribution fairly accurately. The accuracy of these calculations depends upon the accuracy with which the time of travel of the wave-train can be determined. A computation of the actual dispersion of the down-coming wave-trains therefore is of interest.

To begin with let us study the dispersion of a simple wave-train of rectangular envelope. At the time  $t = 0$  the key is pressed at the sending station and a wave-train is sent out. At time  $\tau$  the key is opened and we get a train  $\tau$  seconds long.

Thus

$$\begin{aligned} H_0(t) &= e^{j\omega_0 \cdot t} & 0 < t < \tau, \\ H_0(t) &= 0 & t < 0 \text{ and } t > \tau. \end{aligned} \tag{33}$$

Next we form the image of  $H$ , i. e.

$$f(\omega) = \int_{-\infty}^{+\infty} e^{-j\omega t} H_0(t) \cdot dt = \frac{1 - e^{-j\Omega \tau}}{j\Omega}, \tag{34}$$

where  $\Omega = \omega - \omega_0$ .

Now, every component experiences a change in phase  $S(x, y, z, \omega)$  which we write as

$$S(\omega) = S(\omega_0) + \Omega \cdot S'(\omega_0) + \frac{1}{2!} \Omega^2 \cdot S''(\omega_0) + \frac{1}{3!} \Omega^3 \cdot S'''(\omega_0) + \dots$$

The resultant wave-train at the receiving station therefore is of the form

$$H(t) = \frac{1}{2\pi} \exp. \left( j [\omega_0 t - S(\omega_0)] \right). \tag{35}$$

$$\int_{-\infty}^{+\infty} \frac{e^{jT\Omega} - e^{j(T-\tau)\Omega}}{j\Omega} \exp. \left( j \left[ \overbrace{-\frac{\Omega^2}{2} S''(\omega_0) - \frac{\Omega^3}{6} S'''(\omega_0) - \dots}^{\Delta S} \right] \right) \cdot d\Omega,$$

where  $t = T + t_0$  and  $t_0 = S'(\omega_0)$  is the time of arrival of the undispersed wave-train. The solution of this can be obtained fairly simply if only one of the terms of the phase correction  $\Delta S$  is considered. The results were given by Carson in a note on the building up of sinusoidal currents in long periodically loaded lines [7].

The time of travel times the velocity of light in vacuum generally is called the virtual path-length,  $L_v$ .

$$L_v = c_0 \cdot t_0. \quad (36)$$

If we only consider the first term of the phase correction the solution of (35) becomes

$$\begin{aligned} H(t) = \frac{\exp. (j [\omega_0 t - S(\omega_0) - \pi/4])}{\sqrt{2}} & \left[ C\left(\frac{T}{\sqrt{B}}\right) - C\left(\frac{T-\tau}{\sqrt{B}}\right) + \right. \\ & \left. + j \left( S\left(\frac{T}{\sqrt{B}}\right) - S\left(\frac{T-\tau}{\sqrt{B}}\right) \right) \right], \quad (37) \end{aligned}$$

where  $S(u)$  and  $C(u)$  are the Fresnel integrals<sup>1)</sup> to argument  $u$ .  $B$  is given by the relation

$$B = \frac{\pi}{c_0} \cdot \left( \frac{dL_v}{d\omega} \right) \omega_0. \quad (37 a)$$

Now, let us take a typical example from vertical incidence  $F$ -layer »sounding».  $L_v$  then means twice the so called virtual height  $h_v$ .

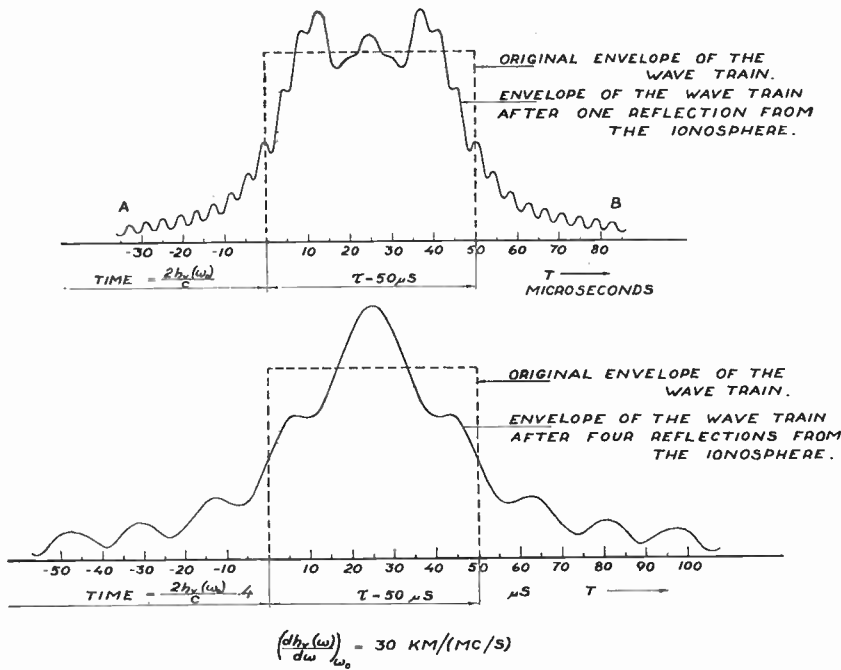
A very normal value of  $\frac{dh_v}{df}$ , i. e. the tangent of the virtual height versus frequency curve of the recorder<sup>2)</sup>, is 30 km/mc/s. Fig. 2 shows a plot of the envelope of the received wave-train when the original envelope is  $0.5 \cdot 10^{-4}$  seconds long.

The upper part of Fig. 2 shows the received envelope after one reflection. Tail  $A$  consists of the lowest frequency components of the wave train and  $B$  the highest as  $\frac{dh_v}{df}$  is positive. A normal receiver does not have transmission characteristics to reproduce much of the tails and ripples of  $A$  and  $B$ . If the tuning of the receiver circuits is too sharp one has to be careful to adjust the tuning to the point of maximum response. Otherwise the time of travel might be slightly too great or too small.

The lower part of Fig. 2 shows the appearance of the envelope after four reflections. The dispersion is worse but it still holds that a tuning for maximum intensity gives the correct time of travel. The dispersion, therefore, is not serious as was indicated on page 15.

1) Jahnke & Emdé: Tables of Functions, p. 35.

2) By many writers called  $P'$  —  $f$  recording which in terms of our symbols might be called an  $S'$  —  $f$  recording.



**DISPERSION OF WAVE TRAINS REFLECTED FROM THE IONOSPHERE**

Fig. 2.

Generally the wave-train is modulated. As almost all envelopes lie somewhere between the rectangular and the sinusoidal shape an investigation of the dispersion of the latter type should complete our study.

The original train thus is of the form

$$H_0(t) = e^{j\omega_0 t} \cdot \sin\left(\frac{\pi}{\tau} t\right) = \frac{1}{2j} \left[ e^{j\left(\omega_0 + \frac{\pi}{\tau}\right) t} - e^{j\left(\omega_0 - \frac{\pi}{\tau}\right) t} \right] \quad (38)$$

for  $0 < t < \tau$  and

$$H_0(t) = 0 \quad \text{for } t < 0 \text{ and } t > \tau.$$

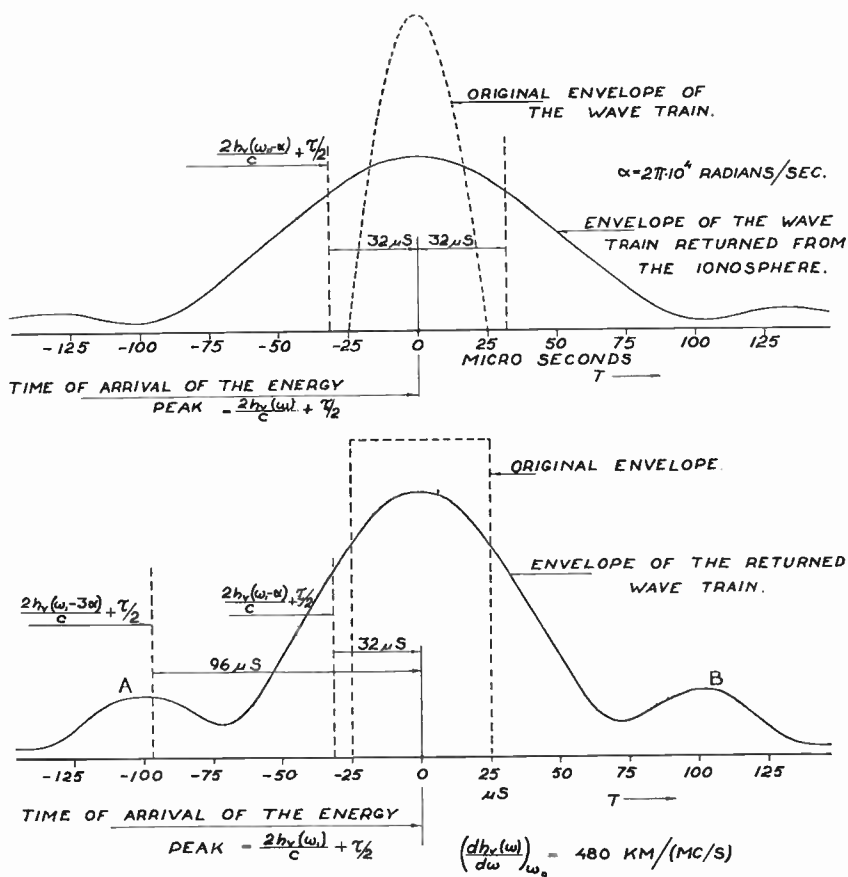
The resultant pulse at the receiver is produced by interference between the two wave-trains of angular frequency  $\omega_0 + \pi/\tau$  and

$\omega_0 - \pi/\tau$  respectively. The greater  $\frac{dh_v}{df}$  the greater will be the difference in time of arrival between the two trains and the broader will be the recorded pulse. Adding the two solutions for the respective wave-trains it is not difficult to show that the resulting wave-train is expressed by

$$\begin{aligned}
 H_0(t) = & \frac{1}{(2)^{3/2}} \exp. \left( j \left[ \omega_0 t - S(\omega_0) - \frac{1}{c_0} \left( \frac{dh_v}{d\omega} \right) \omega_0 \cdot \left( \frac{\pi}{\tau} \right)^2 \right] \right) \\
 & \left[ e^{+j \frac{\pi}{\tau} \cdot T} \left[ C \left( \frac{T}{\sqrt{B}} - \frac{\sqrt{B}}{\tau} \right) - C \left( \frac{T-\tau}{\sqrt{B}} - \frac{\sqrt{B}}{\tau} \right) + \right. \right. \\
 & \quad \left. \left. + j \left\{ S \left( \frac{T}{\sqrt{B}} - \frac{\sqrt{B}}{\tau} \right) - S \left( \frac{T-\tau}{\sqrt{B}} - \frac{\sqrt{B}}{\tau} \right) \right\} \right] - \right. \\
 & \left. - e^{-j \frac{\pi}{\tau} \cdot T} \left[ C \left( \frac{T}{\sqrt{B}} + \frac{\sqrt{B}}{\tau} \right) - C \left( \frac{T-\tau}{\sqrt{B}} + \frac{\sqrt{B}}{\tau} \right) + \right. \right. \\
 & \quad \left. \left. + j \left\{ S \left( \frac{T}{\sqrt{B}} + \frac{\sqrt{B}}{\tau} \right) - S \left( \frac{T-\tau}{\sqrt{B}} + \frac{\sqrt{B}}{\tau} \right) \right\} \right] \right]. \quad (39)
 \end{aligned}$$

If we use the same train-length as before, i. e.  $50 \mu S$ , and the slope of the virtual height curve is  $30 \text{ km/mc/s}$ , the time difference between the two components is as little as  $4 \mu S$ . For a slope of  $480 \text{ km/mc/s}$ , which may be found on the rising part of the curve near the  $F_2$ -critical frequencies, the time difference is  $64 \mu S$  and this is  $14 \mu S$  more than the original train-length. It might be of interest to examine the shape of the received envelope under this condition of appreciable dispersion.

The upper part of Fig. 3 shows a plot of the received pulse. The pulse is broadened approximately four times, i. e. from  $50$  to  $200 \mu S$ . The lower part of Fig. 3 shows the dispersion of a rectangular wave-train under the same conditions. It has a more pronounced energy peak but it is broader at the same time with tails of appreciable energy peaks. Typical peaks are shown at  $A$  and  $B$ . They appear about the time of arrival of energy pulses of frequency  $\omega_0 - 3\pi/\tau$  and  $\omega_0 + 3\pi/\tau$  respectively. These »sideband» components are prominent in the rectangular pulse of width  $\tau$ . At such



DISPERSION OF WAVE TRAINS REFLECTED FROM THE IONOSPHERE.

Fig. 3.1)

a high dispersion the pulses more and more look like their original Fourier image. For the rectangular pulse its magnitude is

$$|f(\omega)| = \left| \frac{2 \sin\left(\frac{\Omega \tau}{2}\right)}{\Omega} \right| \tag{40}$$

with »sideband» peaks at  $\Omega \simeq \pm \frac{\pi}{\tau} (2n + 1)$ . ( $n = 1, 2, \dots$ )

1) Note:  $a = \frac{\pi}{\tau}$  and  $\omega_1 = \omega_0$ .

Finally it should be mentioned that the lower part of Fig. 3 also represents the wave-train of Fig. 2 after sixteen reflections. The comparison is interesting. It gives a good picture of the dissolution of a wave-train.

Finally we study briefly the case when the second term of the phase correction  $\Delta S$  dominates. In this case the curvature of the virtual height curve is a measure of the dispersion. The received wave-train becomes

$$H(t) = \frac{1}{2\pi j} \exp. \left( j \left[ \omega_0 t - S(\omega_0) \right] \right) \int_{-\infty}^{+\infty} \frac{1}{\Omega} \left\{ \exp. \left( j \left[ \Omega T - \frac{\Omega^3}{6 \cdot c_0} L_v''(\omega_0) \right] \right) - \exp. \left( j \left[ \Omega (T - \tau) - \frac{\Omega^3}{6 \cdot c_0} L_v''(\omega_0) \right] \right) \right\} d\Omega \quad (41)$$

in the rectangular case. The solution can easily be expressed by means of Airy's rainbow integral,  $A(u)$ , where

$$A(u) = \int_0^{\infty} \cos \left( \frac{\pi}{2} (u \cdot w - w^3) \right) \cdot dw. \quad (42)$$

It first appeared in a study of the rainbow by Airy in 1838 [8]. It is easily verified that

$$H(t) = \exp. \left( j \left[ \omega_0 t - S(\omega_0) \right] \right) \int_{U_1}^{U_2} A(u) du, \quad (43)$$

where

$$U_2 = \frac{T}{(B_1)^{1/3}}, \quad U_1 = \frac{T - \tau}{(B_1)^{1/3}} \quad \text{and} \quad B_1 = \frac{L_v''(\omega_0) \cdot \pi^2}{c_0 \cdot 24}.$$

$A(u)$  was first tabulated by Airy for values of  $u$  ranging from  $-5.6$  to  $+5.6$ . Later it was found that  $A(u)$  could be expressed by Bessel functions of order  $\pm 1/3$ .<sup>1)</sup>

$$A \left( u \left[ \frac{2}{\pi} \right]^{2/3} \right) = \left( \frac{2}{\pi} \right)^{1/3} \cdot \frac{\pi}{3} \cdot \sqrt{\frac{u}{3}} \left\{ J_{+1/3} \left( 2 \left[ \frac{u}{3} \right]^{3/2} \right) + J_{-1/3} \left( 2 \left[ \frac{u}{3} \right]^{3/2} \right) \right\}. \quad (44)$$

<sup>1)</sup> See Theory of Bessel Functions by Watson, pp. 188 and 712, where Bessel functions of order  $1/3$  are tabulated.

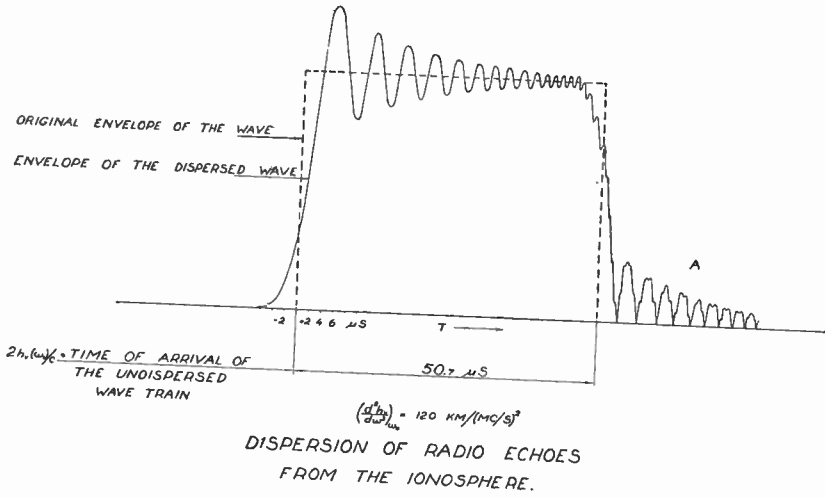


Fig. 4.

Fig. 4 shows a plot of the received envelope for  $\left(\frac{d^2 h_p}{d\omega^2}\right)_{\omega_0} = 120 \text{ km}/(\text{mc}/\text{s})^2$ . For the sake of convenience the original wave-train was made  $50.7 \mu\text{S}$  long. The result is quite different from Figs. 2 and 3. The received envelope is not symmetrical any longer due to the fact that both the low and high frequency components of the wave-train are more delayed than the components around the carrier frequency. Therefore the beginning of the pulse is a smooth rise followed by a typical diffraction ripple. The lowest and highest frequency components of the original wave-train appear in the tail A where they form a complex pattern.

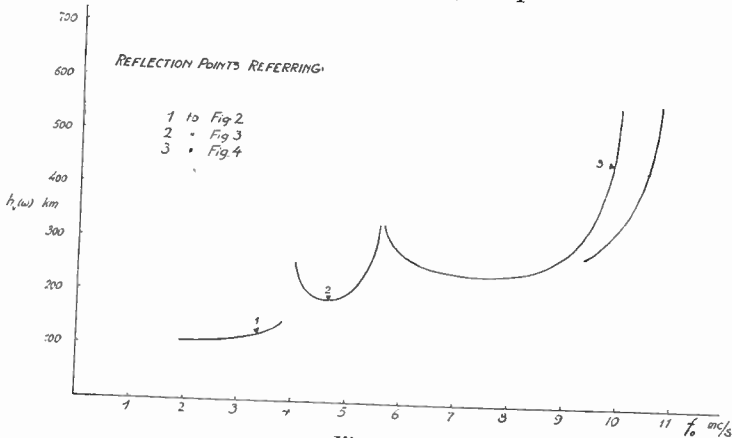


Fig. 5.

Fig. 5 shows the appearance of the ionosphere record to which the pulse shapes on Figs. 2, 3, and 4 refer. As a conclusion we can say that under most practical conditions the dispersion is not serious. Comparing the arguments of the Fresnel and the Airy integrals one finally easily finds that the Fresnel integral is the proper form of the solution when

$$\left( \frac{1}{c_0} \frac{d h_v}{d \omega} \right)^{1/2} \gg \left( \frac{1}{c_0} \frac{d^2 h_v}{d \omega^2} \right)^{1/3}$$

and the Airy integral when

$$\left( \frac{1}{c_0} \frac{d h_v}{d \omega} \right)^{1/2} \ll \left( \frac{1}{c_0} \frac{d^2 h_v}{d \omega^2} \right)^{1/3}$$

### The Phase Relations and the Virtual Path-Length.

As long as inequality (5 a) holds the phase-integral is obtainable from the iconal equation. In the regions where this is not the case a different treatment has to be used. An exact solution of the wave equation can be obtained only for certain kinds of electron density distributions. To begin with we will have to seek a solution that is the closest possible approximation as we do not know anything about the distribution.

Let us study the two-dimensional case of the plane homogeneous ionosphere. The electron density is a function of  $z$  only and the wave normal is parallel to the  $z-x$  plane. If we split the phase in its two components we can write

$$H = \exp. \left( j \left( S_a(z) + S_b(x) \right) \right) = \exp. \left( j \left( S_a(z) + k_0 \cdot \sin \gamma_0 \cdot x \right) \right), \quad (45)$$

where  $\gamma_0$  is the angle of incidence and  $x$  is the distance from the  $z-y$  plane through the apex of the ray. Eq. (3) thereby gets the following form, where the arbitrary constant,  $\delta$ , has to be put equal to unity, viz.

$$\left( \frac{d S_a}{d z} \right)^2 + \frac{\delta}{j} \cdot \frac{d^2 S_a}{d z^2} = k_0^2 (n^2 - \sin^2 \gamma_0) = k_0^2 \cdot q^2. \quad (46)$$

This is a first-order Riccati equation in  $\frac{d S_a}{d z}$ . If we put  $\delta$  equal to zero (46) reduces to the iconal equation. Using therefore

the methods of Brillouin, Wentzel and Kramers [9]  $\frac{d S_a}{d z}$  is expanded in a power series in  $\delta$ . Using only the first two terms of an expansion of the form

$$\frac{d S_a}{d z} = \sum_{n=0}^{\infty} \delta^n \cdot \sigma_n(z)$$

and inserting the value of  $\frac{d S_a}{d z}$  for  $\delta = 1$  in (45), the wave function is obtained in the form of a B. W. K.-approximation, viz.

$$H = a \cdot (k_0 \cdot q)^{-1/2} \exp. \left( j \left[ k_0 \cdot (\sin \gamma_0 \cdot x + \int_0^z q \cdot dz) \right] \right) + \\ + b \cdot (k_0 \cdot q)^{1/2} \cdot \exp. \left( j \left[ k_0 \cdot (\sin \gamma_0 \cdot x - \int_0^z q \cdot dz) \right] \right) . \quad (47)$$

Multiplied by the time factor (47) yields progressive waves in the classical region travelling up and down respectively. One has to put  $b$  equal to zero in the non-classical region ( $z > h_t$ , where  $h_t$  is the true classical height of reflection) because the probability of penetration must decrease very rapidly with depth. The solutions in the two regions have to be joined at the classical reflection level at  $h_t$ . This is difficult, however, on account of the fact that the B. K. W.-approximations generally »blow up» near  $h_t$ . This gap therefore must be bridged.

In the case of the ionosphere it is practically always a permissible approximation to write

$$N = (N)_{h_t} + \left( \frac{d N}{d z} \right)_{h_t} (z - h_t) \quad (48)$$

for the electron density in the bridging region. Remembering that

$$\alpha = 1 - \frac{4 \pi N e^2}{m_0} \cdot \frac{1}{\omega_0^2 + \nu^2} \quad (49)$$

and

$$\beta = \frac{4 \pi}{\omega_0} \cdot \frac{N e^2}{m_0} \cdot \frac{\nu}{\omega_0^2 + \nu^2}, \quad (50)$$

where  $\nu$  is the collisional frequency, the wave equation is easily transformed to

$$\frac{d^2 \xi}{d u^2} + \frac{u}{3} \xi = 0. \quad (51)$$

Here  $\xi = \exp. (j \cdot S_a)$  and

$$u = (3 \delta)^{1/3} [h_t - z + \mu] \quad (51 a)$$

is the new variable with

$$\delta = k_0^2 \cdot \cos^2 \gamma_0 \cdot \left( \frac{1}{N} \frac{d N}{d z} \right)_{h_t} \cdot \left( 1 - j \frac{\nu}{\omega_0} \right) \quad (51 b)$$

and

$$\mu = \frac{+ j \nu / \omega_0}{1 - j \nu / \omega_0} \left[ \left( \frac{1}{N} \frac{d N}{d z} \right)_{h_t} \right]^{-1}. \quad (51 c)$$

It was already noted by Stokes that the operator  $\frac{d^2}{d u^2} + \frac{u}{3}$  annihilates Airy's integral to argument  $u \left( \frac{2}{\pi} \right)^{2/3}$ . The solution in the classical region suitable to our special case is

$$\begin{aligned} H = A \cdot (u)^{1/2} \left\{ \exp. \left( j \left[ k_0 \cdot x \cdot \sin \gamma_0 - \frac{\pi}{6} \right] \right) \cdot H_{1/3}^{(2)} \left( 2 \left[ \frac{u}{3} \right]^{3/2} \right) + \right. \\ \left. + \exp. \left( j \left[ k_0 \cdot x \cdot \sin \gamma_0 + \frac{\pi}{6} \right] \right) \cdot H_{1/3}^{(1)} \left( 2 \left[ \frac{u}{3} \right]^{3/2} \right) \right\}, \quad (52) \end{aligned}$$

which in fact for  $x = 0$  is equal to the Airy integral according to (44). The Hankel function of the second kind yields the up-going wave and the first kind function the down-coming wave.

In the non-classical region at the top of the rays the solution is the surface wave<sup>1)</sup>

$$H = A \cdot \frac{3^{1/2}}{\pi} \cdot (-u)^{1/2} \cdot K_{1/3} \left( 2 \left[ -\frac{u}{3} \right]^{3/2} \right) \cdot e^{j \cdot k_0 \cdot x \cdot \sin \gamma_0}, \quad (53)$$

which for  $x = 0$  is another expression of Airy's integral when the real part of the argument is negative.

<sup>1)</sup> The symbol  $K$  is that of Basset, see Theory of Bessel Functions, p. 78, and p. 714 where  $K_{1/3}$  is tabulated.

For large values of the argument in the classical region we can use the Hankel asymptotic series for both Hankel functions. To begin with we note that

$$\begin{aligned}
 2 \left( \frac{u}{3} \right)^{3/2} &= \int_z^{h_t} k_0 \cdot q \cdot dz + \overbrace{\delta^{1/2} \cdot \mu^{3/2} \cdot \frac{2}{3}}^{\Delta} \simeq \\
 &\simeq \int_z^{h_t} k_0 \cdot q \cdot dz + \frac{4\pi}{3} \cdot \cos \gamma_0 \cdot \frac{(v/\omega_0)^{3/2}}{\left( \frac{1}{N} \frac{dN}{dz} \right)_{h_t} \cdot \lambda_0} \cdot \frac{-1 + j}{\sqrt{2}}. \quad (54)
 \end{aligned}$$

Putting the arbitrary phase,  $\psi$ , of the time factor equal to the classical phase difference between the bottom and the reflection level our solution in the classical bridging region therefore gets the form

$$e^{-j(\omega_0 t - \psi)} \cdot H \sim$$

$$\begin{aligned}
 &\sim \frac{A \cdot (81 \cdot \delta)^{1/6}}{(\pi \cdot k_0 \cdot q)^{1/2}} \left[ \underbrace{\exp. \left( j \left[ \int_0^z k_0 \cdot q \cdot dz + k_0 \cdot \sin \gamma_0 \cdot x - \Delta + \frac{\pi}{4} - \omega_0 t \right] \right)}_{\text{up-going wave}} \right] + \\
 &+ \underbrace{\exp. \left( j \left[ \int_0^{h_t} k_0 \cdot q \cdot dz + \int_z^{h_r} k_0 \cdot q \cdot dz + k_0 \cdot \sin \gamma_0 \cdot x + \Delta - \frac{\pi}{4} - \omega_0 t \right] \right)}_{\text{down-coming wave}} \quad (55)
 \end{aligned}$$

if

$$2 \left( \frac{u}{3} \right)^{3/2} \gg 1, \text{ i. e. } \frac{4\pi}{3} \cdot \cos \gamma_0 \cdot \frac{h_t - z}{\lambda_0} \left[ (h_t - z) \left( \frac{1}{N} \frac{dN}{dz} \right)_{h_t} \right]^{1/2} \gg 1. \quad (56)$$

If this is the case at the boundary of the bridging region we do not have to bother about connecting our solution to the B. K. W.-approximations because it reduces to the same as is evident when comparing Eqs. (47) and (55).

If we for example assume that the relative change in  $N$  is 10 % per km, and such a value is not abnormally high in the lower portion of the layer, and if further  $\lambda_0 = 86.5$  m, then

$$2 \left( \frac{|u|}{3} \right)^{3/2} \sim \cos \gamma_0 \cdot 5.4.$$

500 m above and below the reflection level. As  $N$  in most cases is very well represented by (48) through an interval of this length we are justified in considering (52) the proper solution in the whole classical region. 500 m above the reflection level the disturbance is reduced to about one three hundredth of its maximum value and therefore can be neglected for heights above this level. Practically, therefore, no disturbance penetrates more deeply than this into the layer for the values given.

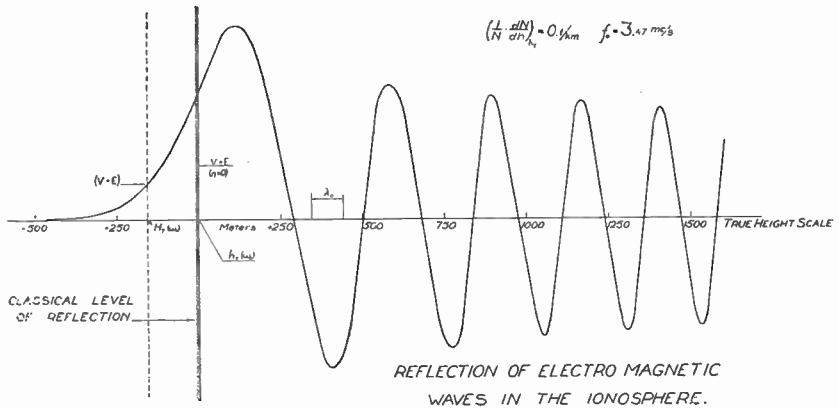


Fig. 6.

Fig. 6 shows a plot of the standing wave between the arbitrary bottom and the reflection level at vertical incidence for the non-dissipative case, i. e.  $\nu = 0$ . If we have another classical region higher up, as marked by the dashed boundary line, transmission through the layer is possible if the distance between the boundaries is less than about 500 m. To many physicists this transmission through the non-classical region is also known as the »tunnel effect». It will be treated exactly for a parabolic layer in the last section of this communication.

The complex phase difference between the down-coming and the up-going waves at the bottom is

$$\Delta S = 2 \int_0^{h_1} k_0 \cdot q \cdot dz + k_0 \cdot \sin \gamma_0 \cdot 2x - \frac{\pi}{2} + 2\Delta. \quad (57)$$

Using the mechanical notations of Eqs. (26) and (28) for the non-dissipative case the conditions for standing waves between two ionized regions as obtained from (57)

$$\oint P_r \cdot dr = h(n + 1/2) \quad (57 a)$$

is formally identical with the Bohr-Sommerfeld phase integral as expected.

The total phase difference between the down-coming and the up-going waves is

$$\begin{aligned} \Delta S_1 = 2 \int_0^{h_t} k_0 \cdot \sqrt{\frac{a - \sin^2 \gamma_0}{2} + \frac{1}{2} \sqrt{(a - \sin^2 \gamma_0)^2 + \beta^2}} \cdot dz + \\ + 2x \cdot k_0 \cdot \sin \gamma_0 - \frac{\pi}{2} + \text{Re}(2 \Delta) \end{aligned} \quad (58)$$

and the virtual path-length<sup>1)</sup>

$$\begin{aligned} L_e = 2 \int_0^{h_t} \frac{d}{d\omega_0} \left( \omega_0 \cdot \sqrt{\frac{a - \sin^2 \gamma_0}{2} + \frac{1}{2} \sqrt{(a - \sin^2 \gamma_0)^2 + \beta^2}} \right) dz + \\ + 2x \cdot \sin \gamma_0 - \text{Re}(2 \Delta) \frac{3}{4\pi} \cdot \lambda_0. \end{aligned} \quad (59)$$

In the  $F$ -layer the following approximation therefore often is sufficient, viz.

$$L_v \simeq 2 \int_0^{h_t} \frac{\cos^2 \gamma_0 \cdot dz}{\sqrt{a - \sin^2 \gamma_0}} + 2x \cdot \sin \gamma_0, \quad (59 a)$$

further

$$L_e = \frac{2x}{\sin \gamma_0} \quad \text{for } \nu = 0$$

as immediately follows from the mechanical interpretation. This result was given by Breit and Tuve already in 1926 [10].

The total attenuation is

$$\Delta S_2 = 2 \int_0^{h_t} \frac{\omega_0}{c_0} \frac{1/2 \beta \cdot dz}{\sqrt{\frac{a - \sin^2 \gamma_0}{2} + \frac{1}{2} \sqrt{(a - \sin^2 \gamma_0)^2 + \beta^2}}} + \text{Im}(2 \Delta). \quad (60)$$

<sup>1)</sup> The last term is unimportant even when the collisional frequency is fairly high. For our example on p. 29 it becomes about  $14 \cdot \cos \gamma_0 \cdot (\nu/\omega_0)^{3/2}$  km, which is negligible even for  $\nu$  as high as  $10^6$ .

Using the approximate refraction relations one gets the classical attenuation expression

$$\Delta S_2 \simeq \int_{\text{Path}} \frac{\omega_0 \cdot \beta}{2 \cdot c_0 \cdot \sqrt{\alpha}} \cdot dr = \int_{\text{Path}} \gamma \cdot dr,$$

where  $\gamma$  is the so called attenuation coefficient.

As a conclusion we may say that even the more exact treatment of the wave equation justifies the use of the classical attenuation and path-length formulae. It should be remarked at this point, however, that this may not necessarily be true in the region of maximum electron density near the critical penetration frequencies of the ionized layer. In this region a somewhat different treatment has to be used as is shown in the last section. In the following sections we will proceed to determine the actual electron and collisional frequency distribution using the phase and attenuation relations just shown.

### The Calculation of the True Height of Reflection and the True Electron Density Distribution.

Let us to begin with assume that the square of the collisional frequency is negligible compared to the square of the important wave frequencies of the exploring spectrum. This must be a permissible approximation at least for the  $F_2$ -layer under most conditions. Thereby  $\alpha$  is reduced to  $n$  for the friction free medium. To accentuate the historical background of the problem we use the mechanical interpretation. This we are free to do because  $E \cdot V$  is independent of frequency.

The vertical incidence virtual height then gets the form

$$h_r(E) = h(0) + \int_{h(0)}^{h_t(V=E)} \frac{dz}{\sqrt{1 - V/E}} \quad (61)$$

where  $h(0)$  is the distance from ground to the lower boundary of the ionized layer.

$$\Delta h_v(E) = h_r(E) - h(0) \quad (61 a)$$

is the increase in virtual height for a given primary energy,  $E$ .

The problem of finding the height of return of a particle sent vertically upwards into a gravitational field of unknown character is exactly the same. Once the heights of return are known as a function of the initial energy, the potential energy is known as a function of height and thereby the gravitational force. It is quite well known that mechanical problems of this kind lead to Abel's integral equation [11]. Abel's equation was developed for the purpose of finding that form of friction free path for which the time of fall is a given function of height; a problem similar to ours.

A very similar problem occurs in seismology [12] when the depth of penetration of a seismic wave has to be determined. To this problem we will have occasion to return briefly a little later.

Quite recently, too, Abel's equation has found another entirely different application, viz. to determine the pitch-function of a variable- $\mu$  vacuum tube grid so that the tube gets a predetermined control-grid characteristic [13].

It is of historical interest to study Abel's problem briefly in this connexion. Assume that the height of fall is  $h$ , the vertical axis  $z$  and the horizontal  $x$ . Under friction free fall we have

$$dt = - \frac{dl}{\sqrt{2g(h-z)}}$$

where  $g$  is the acceleration of the gravitational force and  $dl^2 = dx^2 + dz^2$ . As the velocity of arrival is  $\sqrt{2gh}$  we get the following expression for the virtual path-length, viz.

$$L_v(h) = \int_{z=0}^{z=h} \frac{dl}{\sqrt{1 - \frac{mgz}{mgh}}} = \int_{v=0}^{v=E} \frac{dl}{\sqrt{1 - V/E}}$$

When this is solved the true path-length,  $L_t = \int dl$  becomes known as a function of  $h$ . Thereby the shape of the path is known. It is evident that Abel's original problem is formally identical with ours.

Appleton and de Groot were the first to apply Abel's integral equation to problems of the propagation of electromagnetic waves [14]. It has been frequently used by the present author in connection with the study of ionosphere records [15]. Lately Pekeris has made use of Appleton's solution in a study of the electron density distribution [1].

Before we extend our study to the more general cases of the wave propagation let us examine the mathematical side of the vertical incidence problem a little bit more carefully. This will give us a wider basis when trying to solve the more general problems.

We will find it convenient to introduce the following notation, viz.

$$\Delta h_v(\omega_0, \omega_a) = h_v(\omega_0, \omega_a) - h(0), \quad (62)$$

for the increase in virtual height for a wave-train of angular frequency  $\omega_0$  travelling from the bottom of the ionosphere to an electron density corresponding to an angular critical frequency  $\omega_a$ . If we regard the true height,  $h_v$ , as a function of the electron density, as we very well can do, then (61) can instead be written

$$\Delta h_v(\omega_0, \omega_0) - \Delta h_v(\omega_0, \omega_a) = \omega_0 \int_{\omega_a^2}^{\omega_0^2} \frac{h'_T(\omega_c^2) \cdot d(\omega_c^2)}{(\omega_0^2 - \omega_c^2)^{1/2}}, \quad (63)$$

where  $h'_T(\omega_c^2) = \frac{d h_T}{d(\omega_c^2)}$  and  $\omega_a$  is the lower limit of integration, usually somewhat higher than the critical frequency of the nearest layer below.

Multiplying the identity

$$\Delta h_T(\omega_0^2) - \Delta h_T(\omega_a^2) = \int_{\omega_a^2}^{\omega_0^2} h'_T(\omega_c^2) \cdot d(\omega_c^2)$$

with a suitable form of the  $B$ -function (Eulerian Integral of the First Kind), viz.

$$B(1/2, 1/2) = \int_{\omega_c^2}^{\omega_0^2} \frac{d(\omega^2)}{(\omega^2 - \omega_c^2)^{1/2} (\omega_0^2 - \omega^2)^{1/2}},$$

then

$$\Delta h_T(\omega_0^2) - \Delta h_T(\omega_a^2) = \frac{1}{\pi} \int_{\omega_a^2}^{\omega_0^2} d(\omega_c^2) \int_{\omega_c^2}^{\omega_0^2} \frac{h'_T(\omega_c^2) \cdot d(\omega^2)}{(\omega^2 - \omega_c^2)^{1/2} (\omega_0^2 - \omega^2)^{1/2}}.$$

If we assume that  $h'_T$  is continuous for values of  $\omega_c$  ranging from  $\omega_a$  to  $\omega_0$  we can apply Dirichlet's formula<sup>1)</sup> to the inversion of the integral equation. Under this condition then it can be inverted to

$$\Delta h_T(\omega_0^2) - \Delta h_T(\omega_a^2) = \frac{1}{\pi} \int_{\omega_a^2}^{\omega_0^2} d(\omega^2) \int_{\omega_a^2}^{\omega^2} \frac{h'_T(\omega_c^2) \cdot d(\omega_c^2)}{(\omega^2 - \omega_c^2)^{1/2} (\omega_0^2 - \omega^2)^{1/2}} \cdot$$

But by Eq. (63) this yields

$$\Delta h_T(\omega_0^2) = \Delta h_T(\omega_a^2) + \frac{2}{\pi} \int_{\omega_a}^{\omega_0} \frac{[\Delta h_v(\omega, \omega) - \Delta h_v(\omega, \omega_a)] \cdot d\omega}{(\omega_0^2 - \omega^2)^{1/2}} \quad (64)$$

which is the required solution.

It very often happens that the retardation caused by the electrons below  $h_T(\omega_a^2)$  and in the lower layers is so small compared to the retardation for the rest of the path that it is a good approximation to replace  $\Delta h_v(\omega, \omega_a)$  by  $\Delta h_v(\omega_a, \omega_a)$ . Eq. (64) then gets the simple form

$$h_T(\omega_0^2) = h_T(\omega_a^2) + \frac{2}{\pi} \int_{\omega_a}^{\omega_0} \frac{\Delta h_v \cdot d\omega}{(\omega_0^2 - \omega^2)^{1/2}}, \quad (65)$$

where  $\Delta h_v$  is the increase in virtual height when the frequency of the wave is increased from  $\omega_a$  to  $\omega$ . This is the quantity actually registered on the ionosphere records. It may also happen that  $\omega_a$  is so low and the character of the  $h_v$ -curve is such in that region that it is a permissible approximation to extend the curve by its tangent down to zero frequency. Under such a condition  $\Delta h_v$  may be regarded as known down to the lowest frequencies and (65) can be written

$$h_T(\omega_0^2) = h(0) + \frac{2}{\pi} \int_0^{\pi/2} \Delta h_v(\omega_0 \sin \xi) d\xi = \frac{2}{\pi} \int_0^{\pi/2} h_v(\omega_0 \sin \xi) \cdot d\xi \quad (66)$$

<sup>1)</sup> Whittaker & Watson: A Course of Modern Analysis, p. 77.

which is the Schlömilch integral equation. This is a very useful form of the solution. It neglects the influence of the low-density electrons at the bottom of the layer and therefore does not give the correct distribution of the electrons there. These electrons are »shadowed» by the lower layers and therefore their distribution can never be obtained exactly. Usually, however, one is interested in obtaining the general character of the main portion of the layer and for these purposes (66) is very useful provided it is carefully applied. Applications of this will be shown.

\* \* \*

Of theoretical interest is the oblique incidence case for a symmetrical, spherical ionosphere as being the most general one. From Eq. (31 b) the following expression for the virtual path-length is obtained, viz.

$$L_v = 2 \int_{r_0}^{r_0 + h_T} c_0 \cdot dt = 2 \int_{r_0}^{r_0 + h_T} \frac{dr}{\left(1 - \left(\frac{\omega_c}{\omega_0}\right)^2 - \left(\frac{r_0}{r}\right)^2 \cdot \sin^2 \gamma_0\right)^{1/2}} \quad (67)$$

It is suitable to rewrite it in the following form

$$L_v = r_0 \int_{r_0}^{r_0 + h_T} \frac{d(r/r_0)^2}{(\cos^2 \gamma_0 - \chi^2)^{1/2}}, \quad (67 a)$$

where  $\chi^2 = 1 - \left(\frac{r}{r_0}\right)^2 \left[1 - \left(\frac{\omega_c}{\omega_0}\right)^2\right]$ . In order to adopt our previous method of solution we have to restrict ourselves to a range of integration where  $(r/r_0)^2$  is a single valued function of  $\chi^2$ . Calling the lower limit of integration for  $r_x$ , we therefore get that

$$r_x = r_0/n(r_x) \quad (68)$$

$r_x$  thus is the radial distance to the apex of the path of a ray sent horizontally from the transmitter as shown by Fig. 7. We also have to assume that the electron density increases at least at such a rate that the refractive index will decrease more rapidly than  $r_0/r$ .

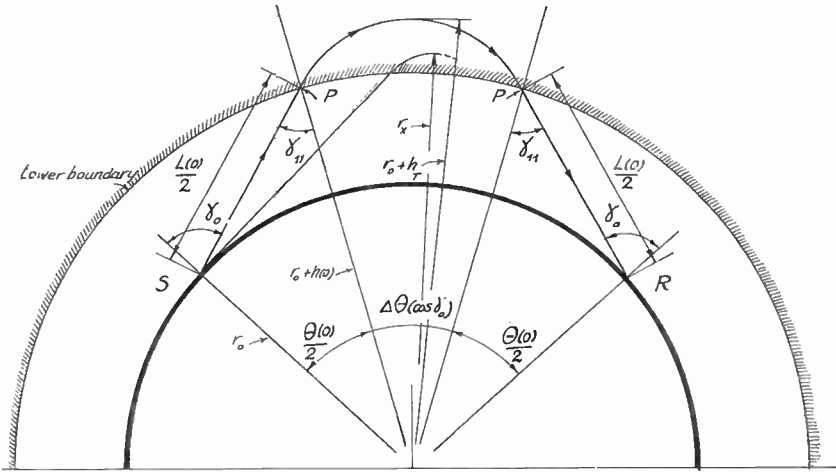


Fig. 7.

Otherwise no rays will return to the earth. In the limiting case that  $n$  decreases as  $r_0/r$  the ray path will be an exponential spiral.

It is useful to introduce a notation similar to the one in the previous example, viz.  $L_v(\cos \gamma_0, \cos \gamma_1)$  for the virtual path of a ray leaving the earth at a normal angle  $\gamma_0$  to an electron density level where a ray of initial normal angle  $\gamma_1$  is returned.  $L_v(\cos \gamma_0, \cos \gamma_0)$  therefore is the complete virtual path of the ray. The integral equation thus gets the following form

$$\frac{L_v(\cos \gamma_0, \cos \gamma_0) - L_v(\cos \gamma_0, 0)}{r_0} = \int_0^{\cos^2 \gamma_0} \frac{f_1'(\chi^2) \cdot d(\chi^2)}{(\cos^2 \gamma_0 - \chi^2)^{1/2}}, \quad (69)$$

where  $(r/r_0)^2 = f_1(\chi^2)$ . Comparing this to Eq. (63) we see that the solution is

$$\left(\frac{r_T}{r_0}\right)^2 - \left(\frac{r_x}{r_0}\right)^2 = \frac{2}{\pi} \int_0^{\pi/2} \frac{\cos \gamma_0 \cdot \sin \xi}{r_0} \left[ L_v(\cos \gamma_0 \cdot \sin \xi, \cos \gamma_0 \cdot \sin \xi) - L_v(\cos \gamma_0 \cdot \sin \xi, 0) \right] \cdot d\xi. \quad (70)$$

In this case the curvature of the layer »shields» the low density electrons even if we do not have any layers below.

For reasons just discussed in connexion with the plane vertical case it generally should be a good approximation to replace  $L_v(\cos \gamma_0, 0)$  by  $L(0)$  which is the path-length between the earth and the lower boundary of the layer. If we neglect the retardation caused by the lower layers this is equal to  $2(S - P)$  on Fig. 7. For practical purposes we therefore get the following solution

$$\begin{aligned} \Delta h_T(\omega_0, \cos \gamma_0) & \left( 1 + \frac{2h(0) + \Delta h_T(\omega_0, \cos \gamma_0)}{2r_0} \right) = \\ & = \frac{2}{\pi} \int_0^{\pi/2} \frac{\Delta L_v(\cos \gamma_0 \cdot \sin \xi) \cdot \cos \gamma_0 \cdot \sin \xi \cdot d\xi}{2}, \end{aligned} \quad (71)$$

where  $\Delta L_v$  is the virtual path in the ionized layer. Therefore the electron distribution is determined for all penetrations up to an initial normal angle of  $\gamma_0$  when the time of travel or the virtual path is known for all angles of arrival from  $\gamma_0$  to  $90^\circ$ . In the case of the plane ionosphere ( $r_0 \rightarrow \infty$ ) it is easily seen that (71) reduces to

$$\Delta h_T(\omega_0, \cos \gamma_0) = \frac{2}{\pi} \int_0^{\pi/2} \Delta h_v(\cos \gamma_0 \cdot \sin \xi) \cdot d\xi. \quad (71 a)$$

For the special case of  $\cos \gamma_0 = 1$ , i. e. vertical incidence, we get

$$\Delta h_T(\omega_0) = \frac{2}{\pi} \int_0^{\pi/2} \Delta h_v(\sin \xi) \cdot d\xi.$$

This shows us that the true penetration at vertical incidence at a given angular frequency  $\omega_0$  is the average of the virtual penetrations for all angles of incidence. This gives a physical significance to the Schlömilch integral.

\* \* \*

The time of travel or the virtual height, which is the quantity generally measured, has always been the essential thing in our previous calculations. As the virtual path has to be known as a function of the angle of arrival it is more practical to use the fact that the angle of arrival is known as a function of the distance (angular) from the sender. This makes the travel time determination unnecessary.

It is easy to deduce from Eq. (31) that the central angle of the ray path (see Fig. 7) is

$$\theta = 2 \sin \gamma_0 \int_{r_0}^{r_0 + h_T} \frac{d(\ln(r/r_0))}{(\cos^2 \gamma_0 - \chi^2)^{1/2}} \quad (72)$$

Using the same range of integration as before we introduce  $\ln(r/r_0) = f_2(\chi^2)$  and by this (72) yields

$$\left[ \frac{\theta(\cos \gamma_0, \cos \gamma_0) - \theta(\cos \gamma_0, 0)}{2 \sin \gamma_0} \right] = \int_0^{\cos^2 \gamma_0} \frac{f_2'(\chi^2) \cdot d(\chi^2)}{(\cos^2 \gamma_0 - \chi^2)^{1/2}} \quad (72 a)$$

For the same reasons as before we can put  $\theta(\cos \gamma_0, 0) = \theta(0)$ . This is the central angle covered by the path between the earth and the bottom of the ionized layer. Applying the same method as before we get the following solution, viz.

$$\frac{\Delta h_T(\omega_0, \cos \gamma_0)}{r_0 + h(0)} \sim \exp. \left[ \frac{1}{\pi} \int_0^{\pi/2} \frac{\Delta \theta(\cos \gamma_0 \cdot \sin \xi) \cdot \cos \gamma_0 \cdot \sin \xi \cdot d\xi}{(1 - \cos^2 \gamma_0 \cdot \sin^2 \xi)^{1/2}} \right] - 1 \quad (73)$$

Therefore, if we know the angle of arrival (of the first reflection) as a function of the angular distance from the sender the electron density distribution is determined with the same exception as before of the lowest electron densities at the bottom of the layer.

This corresponds closely to the problem of determining the paths of seismic rays. When the virtual surface velocity, i. e. the angle of arrival, is known as a function of the angular distance from the source of the disturbance then the true depths of penetration will be known providing the interior of the earth is symmetrical and homogeneous. The practical aspects of this problem are discussed in the literature given by the reference [12].

Although the application of the spherical solution does not seem to be of any practical value at present its study is worth while from a theoretical point of view. It makes the treatment complete.

\* \* \*

When the effect of the terrestrial magnetic field is taken into account conditions become more complicated. First of all only vertical incidence paths have to be selected as the angle between the direction of propagation and the magnetic field otherwise will change appreciably over the path. Strictly speaking the vertical incidence integral (65) can be used only at the magnetic equator where the direction of propagation is perpendicular to the magnetic field. The virtual height data to be used are those of the ordinary ray, of course. Most ionospheric observatories, however, are located far from the magnetic equator and therefore cannot use Eq. (65) for the ordinary ray if accuracy is desired. Very often the propagation angle<sup>1)</sup> is as low as 20° to 15°. Under such conditions a solution for the extra-ordinary ray must be found. It can be obtained reasonably simply as has already been shown by the present author (16).

In the longitudinal case, where  $\theta_{prop} = 0$ , it is well known that

$$n^2 = 1 - \frac{\omega_c^2}{\omega_0 (\omega_0 - \omega_H)} \tag{75}$$

for the extraordinary ray. Here  $\omega_H = \frac{e \cdot H}{m_0 \cdot c_0}$  is the gyro frequency of the electrons in the terrestrial magnetic field of strength  $H$ . The phase integral therefore becomes

$$S(\omega_0) = 2 \left[ \frac{\hbar(0) \cdot \omega_0}{c_0} + \int_{\hbar(0)}^{\hbar_T} \frac{\omega_0}{c_0} \left( 1 - \frac{\omega_c^2}{\omega_0 (\omega_0 - \omega_H)} \right)^{1/2} dz - \frac{\pi}{4} \right]. \tag{76}$$

This leads to the following expression for the virtual height, viz.

<sup>1)</sup> The propagation angle is the angle between the direction of the terrestrial magnetic field and the wave normal.

$$h_r(\omega_0) = h(0) + \int_{\omega_c^2=0}^{\omega_c^2=\omega_0(\omega_0-\omega_H)} \frac{dz}{\left(1 - \frac{\omega_c^2}{\omega_0(\omega_0-\omega_H)}\right)^{1/2}} \cdot \left[1 + \frac{1}{2} \cdot \frac{\omega_c^2}{\omega_0(\omega_0-\omega_H)} \cdot \frac{\omega_H}{\omega_0-\omega_H}\right].$$

This is much more complicated than the previous integral equations. However, we can solve it in a somewhat different way.

We introduce an »effective» frequency  $\omega_r$ , defined by

$$\omega_r = \left(\omega_0(\omega_0 - \omega_H)\right)^{1/2}. \tag{77}$$

Multiplying the phase integral by

$$\frac{d}{d\omega_r} \cdot \frac{\omega_r}{\omega_0},$$

and remembering that

$$\frac{d}{d\omega_r} = \frac{\omega_r}{\omega_0 - \omega_H/2} \cdot \frac{d}{d\omega_0},$$

we get

$$\begin{aligned} \frac{\omega_H}{2\omega_0 - \omega_H} \left[ \frac{S(\omega_0) + \pi/2}{2\omega_0} - h_v(\omega_0) \right] + \frac{h_r(\omega_0)}{c_0} &= \\ &= \frac{h(0)}{c_0} + \frac{1}{c_0} \int_{\omega_c^2=0}^{\omega_c^2=\omega_r^2} \frac{dz}{\left(1 - \omega_c^2/\omega_r^2\right)^{1/2}}. \end{aligned}$$

But as we must have that

$$S(\omega_0) + \pi/2 = \frac{2h(0) \cdot \omega_0}{c_0} + \frac{2}{c_0} \int_{\omega_H}^{\omega_0} \Delta h_r(\omega) \cdot d\omega,$$

we finally get

$$\begin{aligned} \Delta h_v(\omega_0) - \frac{\omega_H}{2\omega_0 - \omega_H} \left[ \Delta h_v(\omega_0) - \frac{1}{\omega_0} \int_{\omega_H}^{\omega_0} \Delta h_v(\omega) \cdot d\omega \right] &= \\ &= \int_{\omega_0^2 = 0}^{\omega_c^2 = \omega_r^2} \frac{dz}{(1 - \omega_c^2/\omega_r^2)^{1/2}}, \end{aligned} \quad (78)$$

or

$$\Delta H_v(\omega_0) = \Delta h_v(\omega_0) - \Delta H(\omega_0) = \int_{\omega_c^2 = 0}^{\omega_c^2 = \omega_r^2} \frac{dz}{(1 - \omega_c^2/\omega_r^2)^{1/2}}, \quad (78 a)$$

where

$$\Delta H(\omega_0) = \frac{\omega_H}{2\omega_0 - \omega_H} \left[ \Delta h_v(\omega_0) - \overline{\Delta h_c(\omega_0)} \right]$$

and

$$\overline{\Delta h_c(\omega_0)} = \frac{1}{\omega_0} \int_{\omega_H}^{\omega_0} \Delta h_c(\omega) \cdot d\omega \quad (78 b)$$

$\Delta H(\omega_0)$  thus is the correction we must apply to  $\Delta h_v$  before we can translate it into the effective frequency,  $\omega_r$ , for application of the solution in the form of the Schlömilch integral.

At Cambridge, Mass., for example

$$\frac{\omega_H}{2\omega_0 - \omega_H} \simeq 0.68, 0.26 \text{ and } 0.13$$

for a wave frequency of 2, 4 and 7 mc/s respectively. This should give an idea of the magnitude of the correction.

Comparing Eq. (78 a) to Eq. (66) we immediately see that the solution is

$$\Delta h_T(\omega_0^2) = \frac{2}{\pi} \int_0^{\pi/2} \Delta H_v \left( \frac{\omega_H}{2} + \sqrt{\omega_0(\omega_0 - \omega_H) \cdot \sin^2 \xi + \frac{\omega_H^2}{4}} \right) \cdot d\xi \quad (79)$$

For the sake of simplicity we have considered the values of  $\Delta h_r$  known down to  $\omega_0 = \omega_H$  as they of course never are. Our method does not give us any information about the very lowest density electrons at the bottom of the layer as before. It is in the nature of things that they must be shadowed by the lower layers.

The value of the present solution lies in the fact that it can be applied with surprisingly small errors even up to propagation angles as large as  $25^\circ$ . A computation of the error will be shown on page 64.

### The Calculation of the Variation of the Collisional Frequency with Height.

From the close similarity between the virtual height integral (59 a) and the attenuation integral (60) one naturally expects that the collision frequency distribution will be determined by similar methods as the electron density distribution, as soon as the latter is known. This was noticed by Pekeris [1]. Quite generally, when the integral equation of the electron distribution has been solved, the collisional frequency distribution can be obtained when the attenuation is known for the frequency range or, at a fixed frequency, for all angles of incidence throughout the range.

In accordance with Eq. (60) the attenuation at vertical incidence is

$$\Delta S_2 = \frac{1}{c_0} \int_0^{h_T} \frac{\omega_0 \cdot \beta \cdot dz}{\sqrt{\frac{\alpha}{2} + \frac{1}{2} \sqrt{\alpha^2 + \beta^2}}} \approx \frac{1}{c_0} \int_0^{h_T} \frac{\omega_0 \cdot \beta \cdot dz}{\sqrt{\alpha}}.$$

Let us study the case of longitudinal transmission for the extraordinary ray. Then

$$\alpha \cong 1 - \frac{\omega_c^2}{\omega_0 (\omega_0 - \omega_H)}, \tag{80 a}$$

and

$$\beta \cong \frac{\omega_c^2}{(\omega_0 - \omega_H)^2} \cdot \frac{r}{\omega_0}. \tag{80 b}$$

This makes

$$\Delta S_2(\omega_r^2) = \frac{\omega_r}{c_0} \int_0^{\omega_r^2} \frac{\omega_c^2 \cdot \nu(\omega_c^2) \cdot h'_T(\omega_c^2) \cdot d(\omega_c^2)}{(\omega_0 - \omega_H)^2 (\omega_r^2 - \omega_c^2)^{1/2}}.$$

We consider  $\nu(\omega_c^2)$  a function of the electron density ( $\omega_c^2$ ) which we can do whenever  $h'_T(\omega_c^2)$  is a single valued function. Comparing the integral equation to our earlier ones we easily see that the solution is

$$\nu(\omega_r^2) = \frac{2 \cdot c_0}{\pi} \cdot \frac{1}{\omega_r^2 h'_T(\omega_r^2)} \cdot \frac{d^2}{d(\omega_r^2)} \cdot \int_0^{\omega_r} \frac{\Delta S_2(\omega_{r_1}^2) \cdot \omega_{r_1}^4}{\left(\frac{\omega_H}{2} + \left(\omega_{r_1}^2 + \frac{\omega_H^2}{4}\right)^{1/2}\right)^2} \cdot \frac{d\omega_{r_1}}{(\omega_r^2 - \omega_{r_1}^2)^{1/2}}. \quad (81)$$

Therefore, when the absorption  $\Delta S_2$  is known throughout the frequency range the variation of the collisional frequency with height is also known by Eq. (81).

Next let us study briefly the case of oblique incidence at a fixed frequency ( $\omega_H$  necessarily = 0). From Eq. (60).

$$\Delta S_2(\omega_0^2 \cos^2 \gamma_0) = \frac{1}{c_0 \cdot \omega_0} \cdot \int_0^{\omega_0^2 \cos^2 \gamma_0} \frac{\nu(\omega_c^2) \cdot \omega_c^2 \cdot h'_T(\omega_c^2) \cdot d(\omega_c^2)}{(\omega_0^2 \cos^2 \gamma_0 - \omega_c^2)^{1/2}}.$$

In the same way as before we get the solution

$$\nu(\omega_0^2 \cos^2 \gamma_0) = \frac{2 c_0}{\pi} \cdot \frac{1}{\omega_0^2 \cdot \cos^2 \gamma_0 \cdot h'_T(\omega_0^2 \cos^2 \gamma_0)} \cdot \frac{d}{d(\cos^2 \gamma_0)} \left[ \int_0^{\pi/2} \cos \gamma_0 \cdot \sin \xi \cdot \Delta S_2(\cos^2 \gamma_0 \cdot \sin^2 \xi) \cdot d\xi \right]. \quad (82)$$

Therefore, when the attenuation is known for all angles of incidence from  $\pi/2$  to  $\gamma_0$  the variation of the collisional frequency is known

for all levels of reflection up to the level where a ray of incidence  $\gamma_0$  is reflected.

Even for simple electron distributions the calculation is not notably easy. Let us take an example.

If the attenuation is of the following form, viz.

$$\Delta S_2 = \frac{\pi}{2} \cdot \frac{r_0 \cdot h}{c_0} \cdot \omega_0 \cdot \cos^2 \gamma_0 \left[ I_0'' \left( \frac{h \cdot \omega_0}{H} \cdot \cos \gamma_0 \right) - L_0'' \left( \frac{h \cdot \omega_0}{H} \cdot \cos \gamma_0 \right) \right], \tag{83}$$

where  $L_0(u)$  bears the same relation to Struve's function  $II_0(u)$  as  $I_0(u)$  bears to  $J_0(u)$ <sup>1)</sup>, then by means of Theisinger's integral<sup>2)</sup>

$$\nu (\omega_0^2 \cos^2 \gamma_0) \cdot h_T' (\omega_0^2 \cos^2 \gamma_0) = \frac{r_0 \cdot h}{2} \cdot \frac{e^{-\frac{h \cdot \omega_0}{H} \cdot \cos \gamma_0}}{\omega_0 \cdot \cos \gamma_0} \tag{84}$$

If the electron distribution is such that for  $h_T < h_{T_1}$

$$\frac{4 \pi e^2 N}{m_0} = \omega_c^2 = \left( \frac{h_T}{h} \right)^2,$$

then  $h_T' (\omega_c^2) = \frac{h}{2 \omega_c}$  and (84) yields

$$\nu = r_0 \cdot e^{-\frac{h_T}{H}} \tag{85}$$

for all penetrations  $h_T < h_{T_1}$ . Under this condition the absorption can also be written

$$\Delta S_2 = \cos \gamma_0 \cdot \frac{\pi \cdot r_0}{2 c_0} \cdot h_T \cdot \left[ I_0'' \left( \frac{h_T}{H} \right) - L_0'' \left( \frac{h_T}{H} \right) \right] \tag{86}$$

indicating the fact that for the same intrusion, the oblique ray suffers less attenuation than the vertical one.

It is clear from the following that an experimental determination of the attenuation, especially as a function of frequency for the application of Eq. (82), should be very valuable. If we possessed sufficient knowledge regarding the distribution of  $r$  in the  $F$ -layer,

<sup>1)</sup> G. N. Watson: Theory of Bessel Functions, p. 329.

<sup>2)</sup> G. N. Watson: l. c., p. 338.

we should no doubt be helped a great deal towards a better understanding of its physics. This should be of value also to the cosmic ray research. It is to be hoped that radio exploration will some day give us the desired information about the attenuation function. At present there are some experimental difficulties to be overcome. However, they are not serious and the problem is a question of experimental facilities and time rather than anything else.

Finally it should be mentioned that a few experimental determinations of the collisional frequency have already been carried out under the simple assumption that it is constant through the important part of the layer. It is easily established that the attenuation relation can be written in the following approximate form when this is the case, viz.

$$\frac{\delta}{\delta t}(\Delta S_2) \simeq \frac{\nu}{2c_0} \cdot \frac{\delta}{\delta t} \left( 2 \Delta h_v - \frac{\Delta S_1}{k_0} \right).$$

By measuring corresponding time-changes of  $\Delta S_2$  and  $\Delta h_v$ , and neglecting changes of the optical path,  $\frac{\Delta S_1}{k_0}$ , Eckersley has found that in the  $F_1$ -layer, at an estimated height of 265 km,  $\nu = 3.6 \cdot 10^3$ . Farmer and Ratcliffe, working along similar lines, have found the value  $\nu = 1.6 \cdot 10^3$  for the  $F_2$ -layer. This should at least give an idea of the order of magnitude of the collisional frequency.

### Typical Electron Density Distributions.

The ionospheric records from the magnetic equator are fairly simple to analyze because the Schlömilch equation (66) can be used for the ordinary component. A number of typical smooth records from quiet days at Huancayo ( $12^\circ$  S,  $75^\circ$  W) have kindly been placed at the author's disposal by the director of the Department of Terrestrial Magnetism of the Carnegie Institution, Dr J. A. FLEMING. Several typical ones will be shown in what follows.

As is evident from the Schlömilch equation one simply has to plot the virtual heights as functions of  $\omega_0 \cdot \sin \xi$  and then take the respective mean values (by a good planimeter) which are the true heights.

Fig. 8 shows the virtual height curve for the ordinary ray at Huancayo, Jan. 2nd 1515 local time, 1939. The virtual height curve

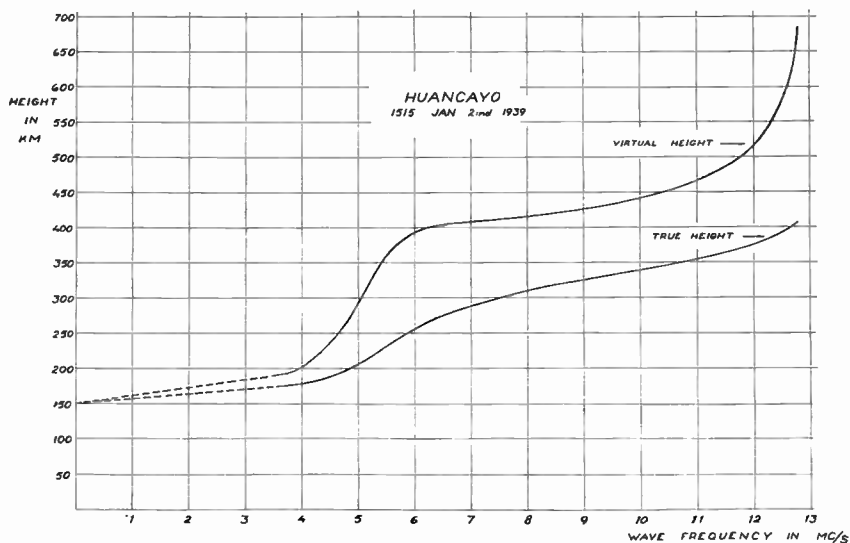


Fig. 8.

was extended by its tangent at its lowest point. There is no distinct difference between the  $F_1$ - and  $F_2$ -layers and the true height is fairly large.

Fig. 9 shows the electron density distribution as obtained from the true height curve. The reliable limits of the curve are marked by  $m$ . The upper portion of the distribution, i. e. the distribution

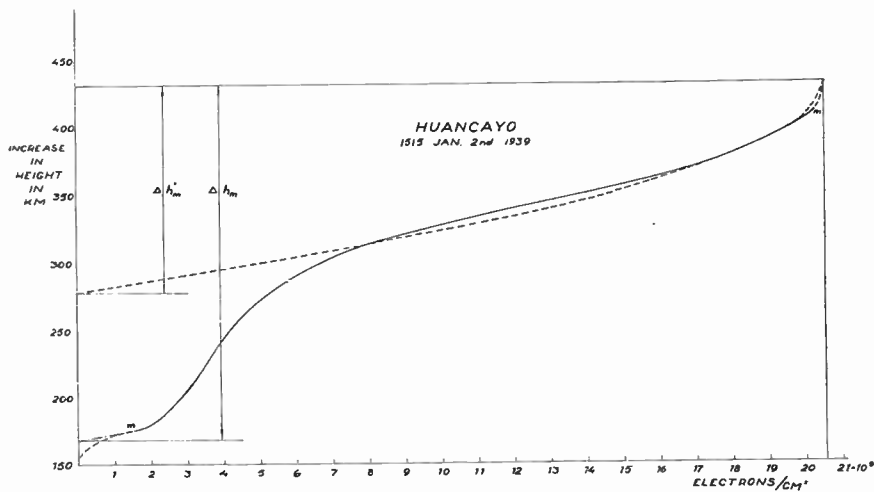


Fig. 9.

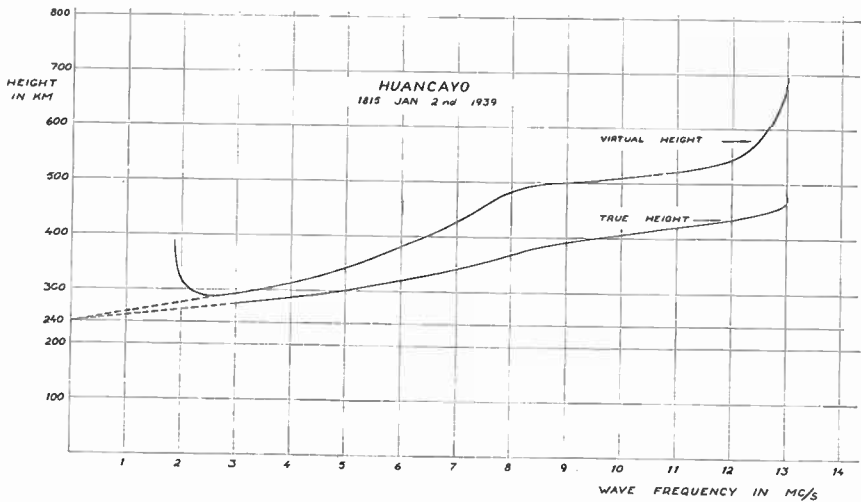


Fig. 10.

mainly of  $F_2$ -character, is essentially parabolic as shown by the dashed parabola drawn for comparison.

Now for a Chapman layer the ionization  $N$  in the vicinity of the level of maximum ionization varies as

$$N = N_{max} \left( 1 - \frac{z^2}{(2H)^2} \right). \quad (86)$$

$H$  thus should be equal to about  $\frac{\Delta h'_m}{2}$ ,<sup>1)</sup> For the electron distribution just shown it becomes about 76 km. This determination of  $H$  is, of course, very approximate subject as it is to the individual selection of the comparison parabola,<sup>2)</sup> However, it should serve as an indication of the magnitude of  $H$ .

Three hours later the same day, as shown on Fig. 10, the virtual and true height curves were slightly different, the change in the virtual height curve being more noticeable of course.

Fig. 11 shows the corresponding electron density distribution. The upper part, as before, is represented reasonably well by a parabola. It yields  $H$  equal to about 56 km, a fairly low value.

<sup>1)</sup>  $H$  is the local scale height of the gas from which the layer is formed.

<sup>2)</sup> It should also be added that it always is very difficult to record the virtual heights near the critical frequency. The true electron density distribution near the maximum level therefore can not be determined accurately.

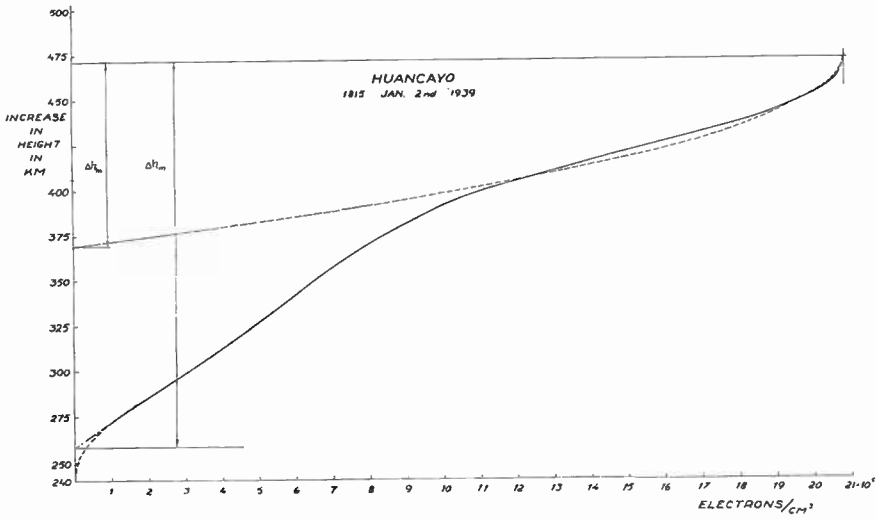


Fig. 11.

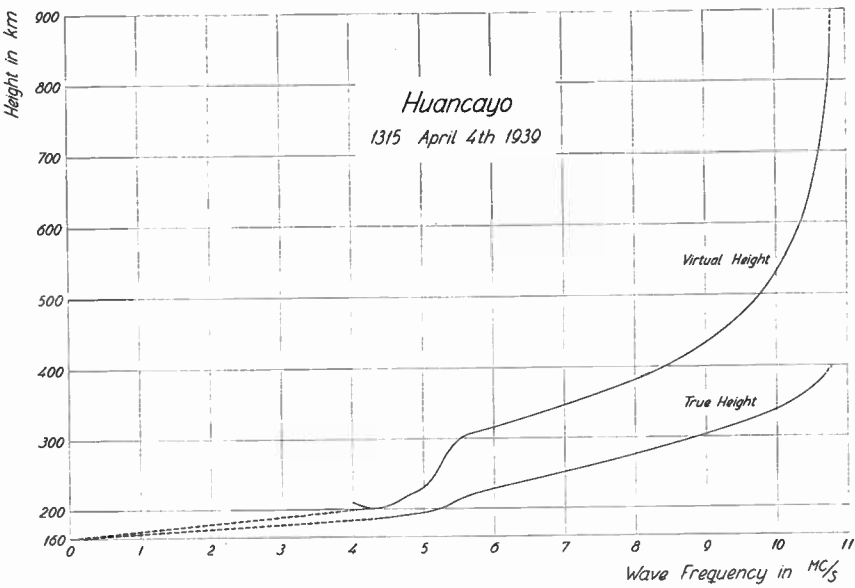


Fig. 12.

Fig. 12 indicates a not inconsiderable expansion of the  $F_2$ -layer. It is noticeable that the true heights still are great.



Fig. 13.

Fig. 13, showing the corresponding electron density distribution, indicates this even more clearly. The parabolic approximation is fairly good over an appreciable frequency range and it yields  $H$  about 105 km.

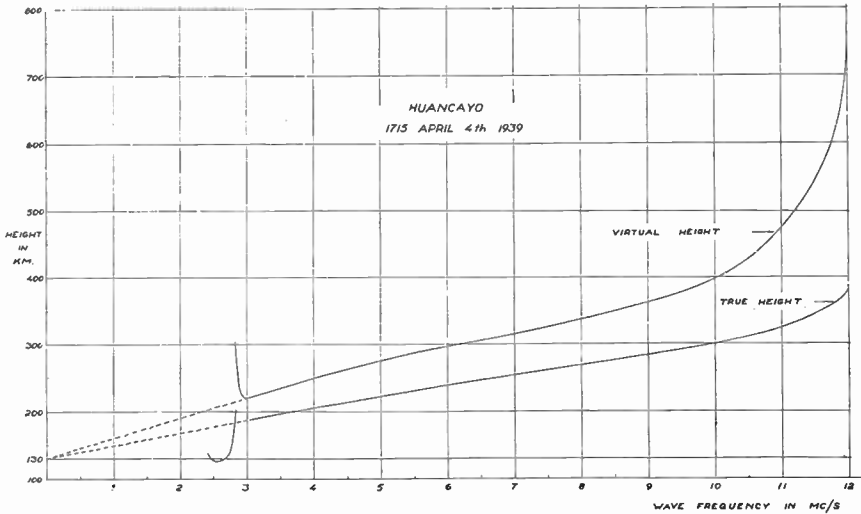


Fig. 14.

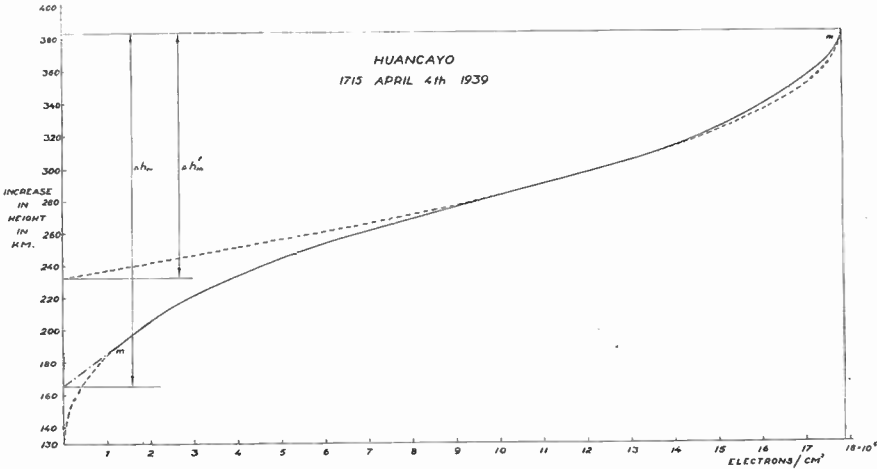


Fig. 15.

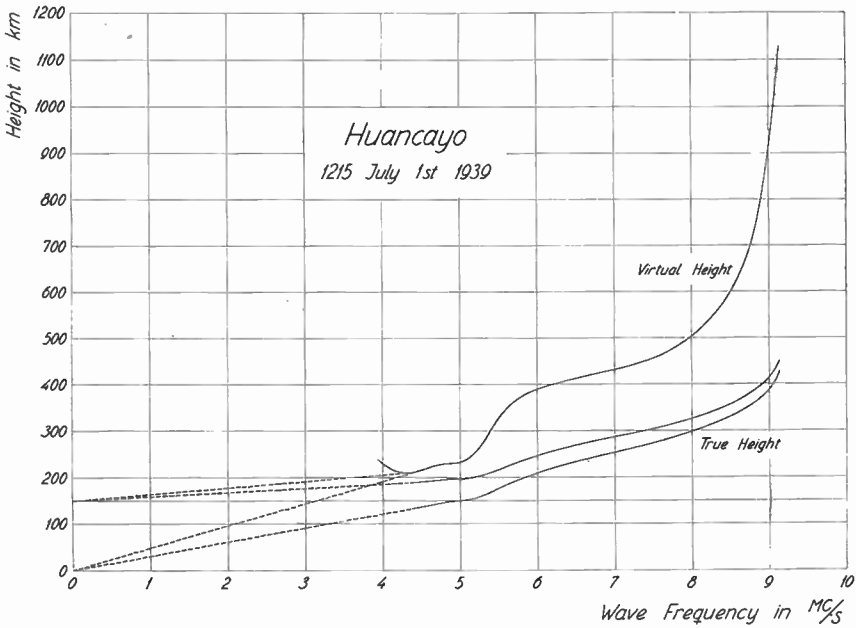


Fig. 16.

Fig. 14 shows a virtual height record three hours later the same day. The general characteristic is the same. The true height still is fairly great.

Fig. 15 shows the corresponding electron density distribution. It remains essentially parabolic over an important frequency range and the dashed parabola yields  $H$  about 76 km.

Fig. 16 shows a noon recording obtained on July 1st at 1215. The expansion is considerable. In order to show how much the final result is affected by the direction of the tangent extending the virtual height curve to zero frequency, plots were made for two drastically different cases.

1) The lowest portion of the virtual height curve was extended by a suitable tangent to a zero frequency height of about 150 km, a fairly probable direction.

2) Another tangent was drawn to the curve extending it down to zero height at zero frequency, this being the most improbable direction.

It is clearly shown, as is also demonstrated by the nature of the integral equation, that the true height curve is not affected very much in the higher frequency region near the penetration frequency.

The probable electron density distribution, corresponding to the more probable case 1), is of the same character essentially as the distributions just shown.  $H$  becomes approximately 130 km.

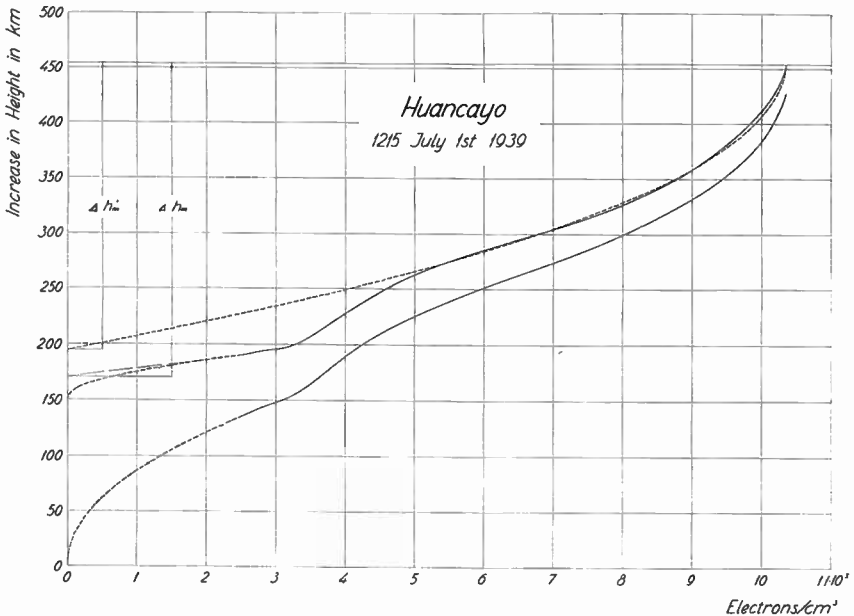


Fig. 17.

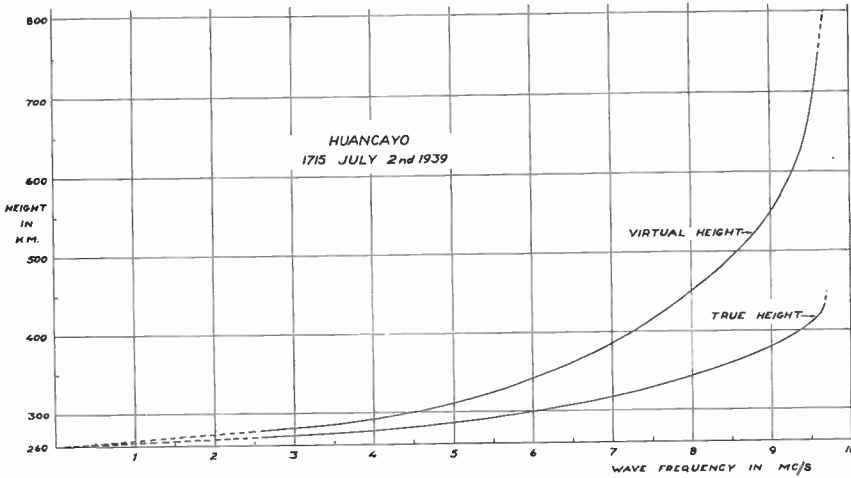


Fig. 18.

Fig. 18 shows a smooth «mid-winter» afternoon recording from Huancayo. It is very similar in appearance to the quiet Cambridge recordings shown later.

The corresponding electron density distribution is practically parabolic over the entire frequency range. The dashed parabola yields  $H$  approximately 86 km. The deviation from the parabola is of the same order of magnitude, generally, as the experimental error although greater.

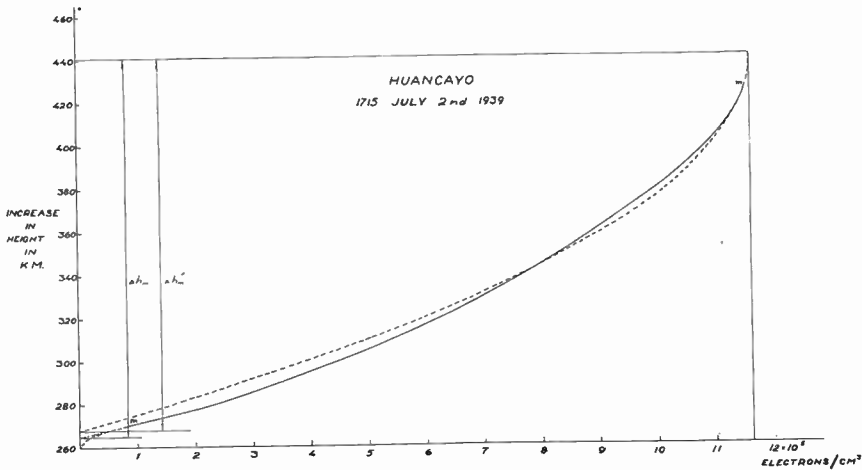


Fig. 19.

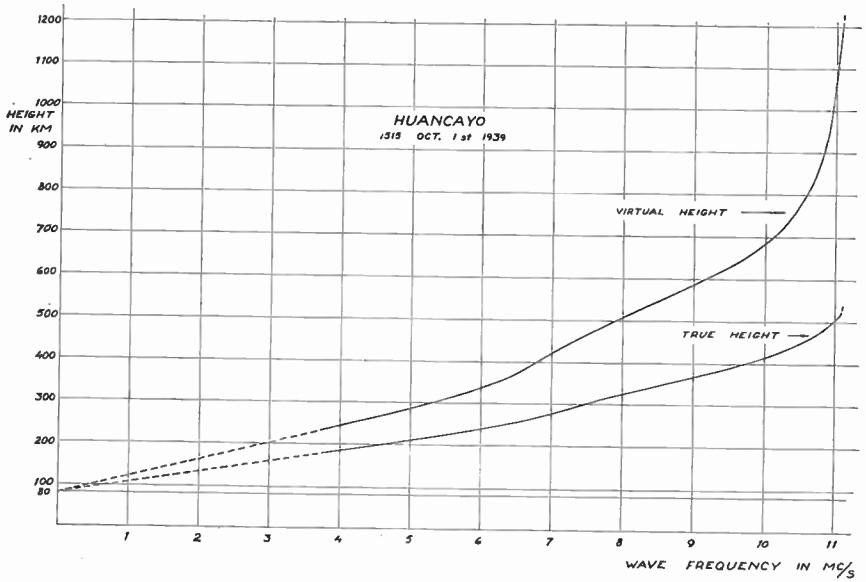


Fig. 20.

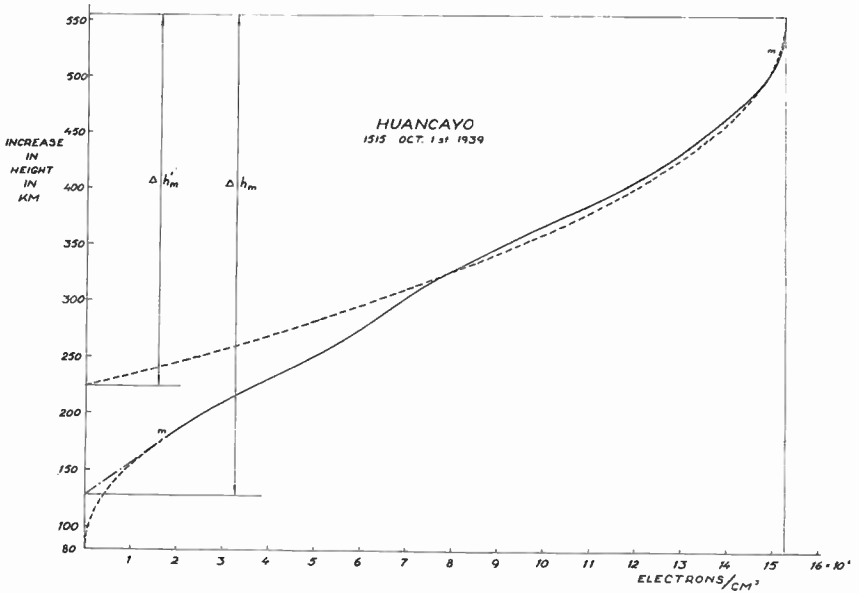


Fig. 21.

Fig. 20 indicates a very great expansion, the maximum true height being more than 500 km. Consequently the corresponding  $H$  value is great as indicated by Fig. 21. The approximate value is 165 km.

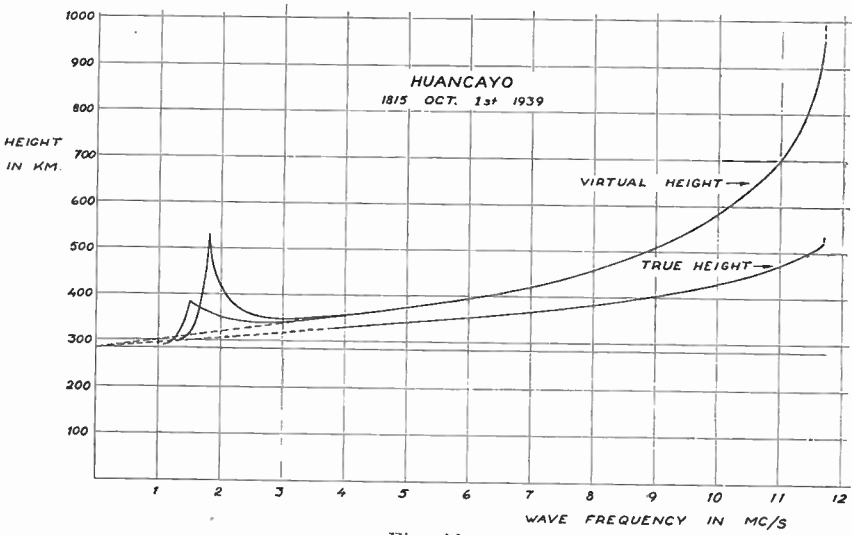


Fig. 22.

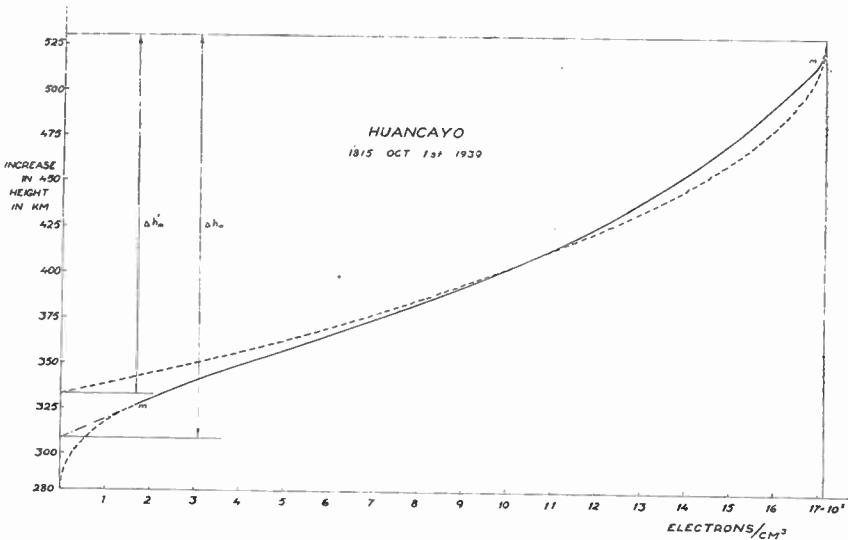


Fig. 23.

This seems very great compared to values normally obtained at northern observatories. The uncertainty regarding the construction of the tangent extension was especially troublesome in this case. The low density distribution therefore is very uncertain.

The expansion was much smaller in the early evening the same day as indicated by Fig. 22. The distribution function, shown by

Fig. 23, did not change much. The corresponding value of  $H$  is 98 km, approximately, a fairly great value so late in an undisturbed day.

\* \* \*

Next, let us for comparison study a few records from Cambridge, Mass. ( $42^\circ$  N,  $71^\circ$  W), obtained by the author at Harvard University. As the propagation angle is about  $16^\circ$  at Cambridge we have to use Eq. (79) as the proper solution. The solution, strictly speaking, applies only to the extraordinary ray when the angle of propagation is zero and the path is assumed to be vertical. However, the error we make by applying Eq. (79) to the Cambridge recordings is very small, in fact smaller than the experimental error. A plot of the propagation angles will be shown at the end of this section for two typical propagation angles, viz.  $15^\circ$  and  $25^\circ$ .

The first thing to do is to construct the *corrected* virtual height in accordance with Eq. (78 a).

Fig. 24 shows a quiet afternoon recording from Cambridge obtained on April 20th, 1939, at 1700. The corrected height curve clearly indicates the importance of the correction. The corrected virtual height is then plotted against the «effective» frequency,  $f_r$ , as shown by Fig. 25.

From this the true height curve is obtained in the usual manner by plotting the virtual heights against  $\omega_r \cdot \sin \xi$  and integrating the mean value. The result is shown by the dashed curve. The maximum increase in true height is slightly more than 140 km while the

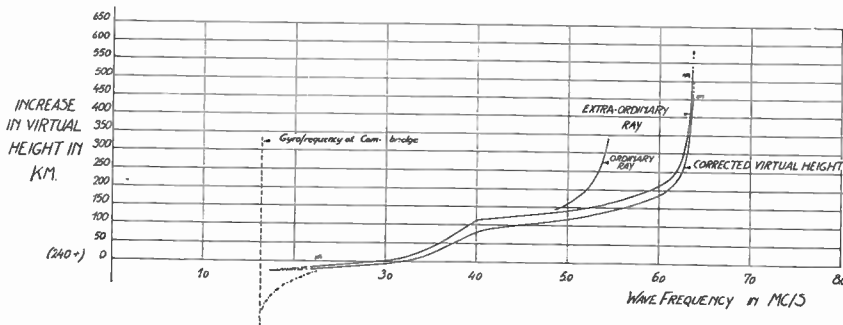


Fig. 24.

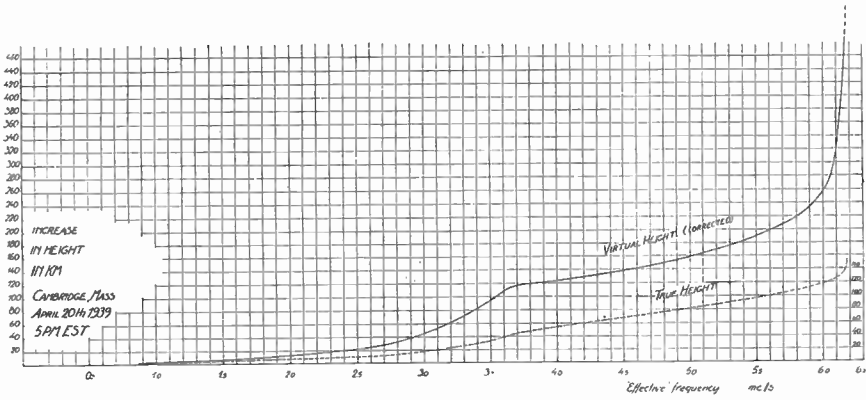


Fig. 25.

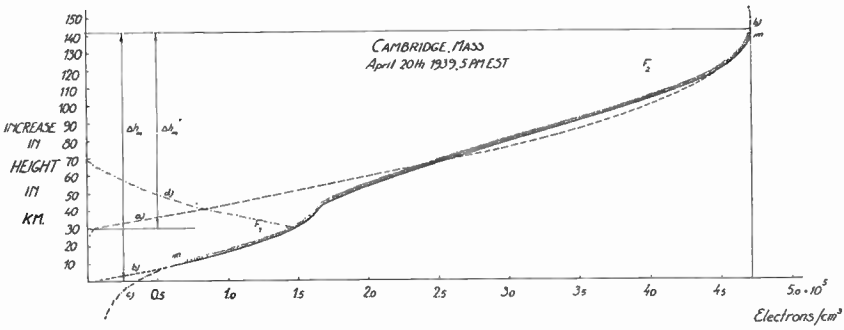


Fig. 26.

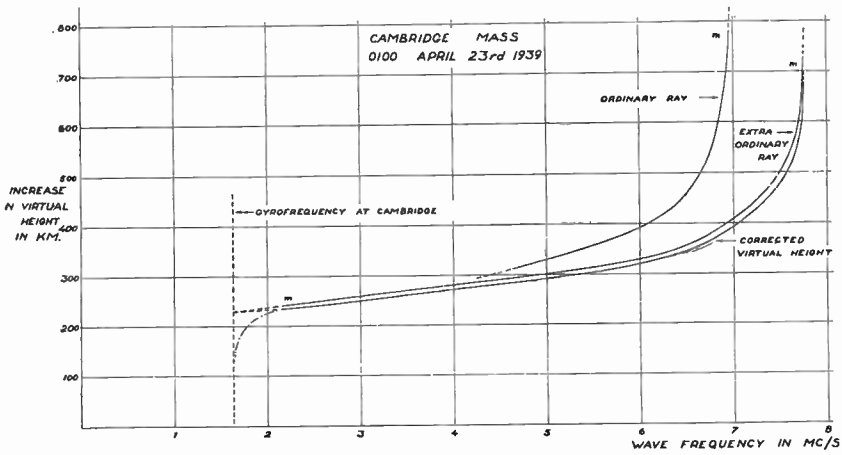


Fig. 27.

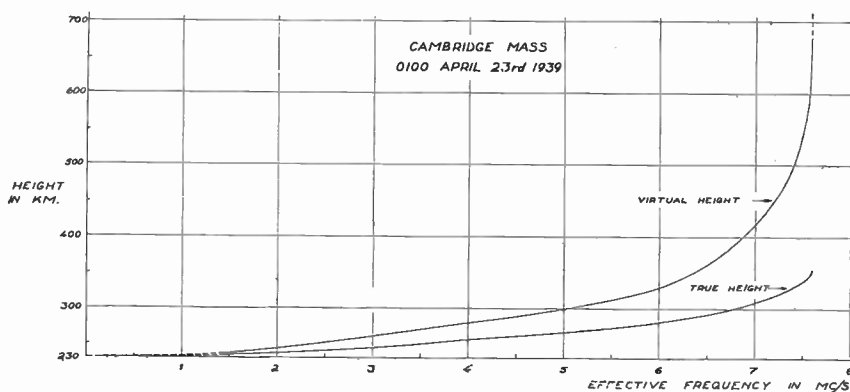


Fig. 28.

corresponding increase in virtual height is about 475 km. Fig. 26 shows the electron density distribution drawn from the true height curve.

The essential portion of the distribution (the  $F_2$ -layer) is fairly closely represented by a parabola. This yields  $H$  about 60 km.

Fig. 27 is another Cambridge example taken a few days later one hour past mid-night (local time). The corrected height curve is constructed as before and the true height is plotted against the »effective» frequency as shown by Fig. 28.

Fig. 29 finally shows the resulting electron density distribution. It is essentially parabolic throughout the frequency range. To represent such a layer by a parabola should be a very good approximation. The approximate value of  $H$  is 58 km.

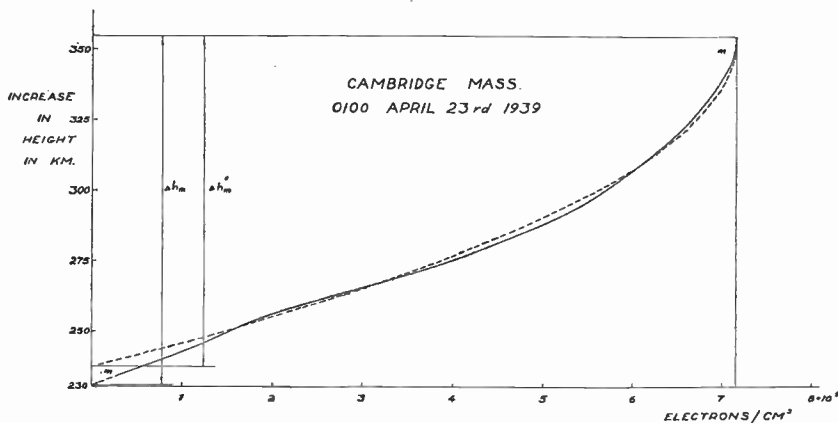


Fig. 29.

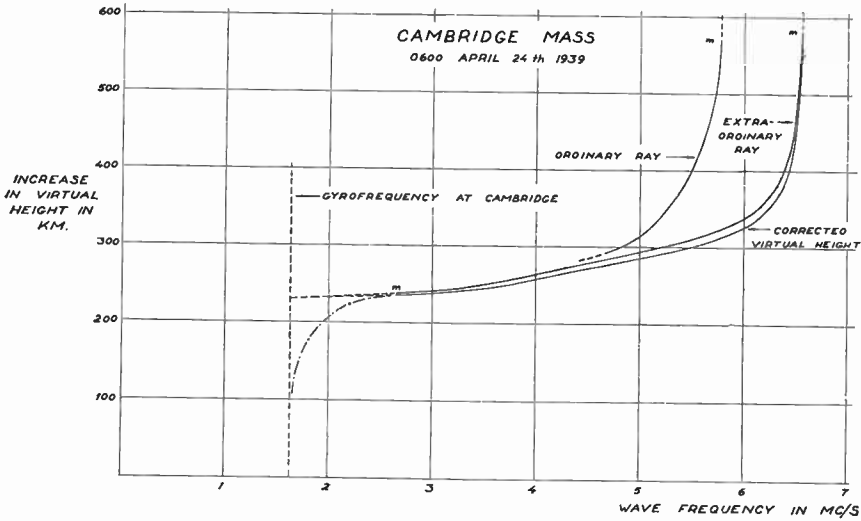


Fig. 30.

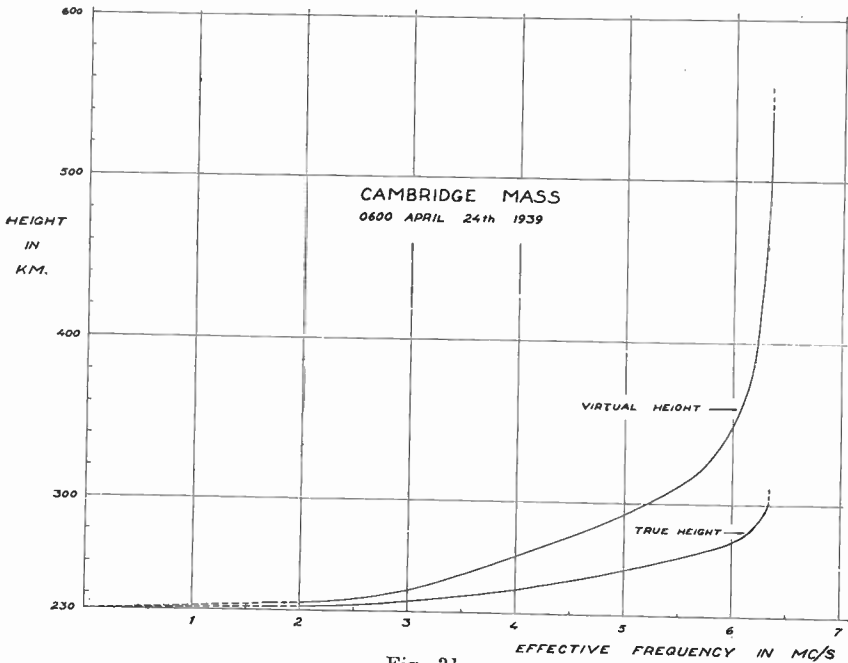


Fig. 31.

Fig. 30 shows the virtual height curve in the early morning a day later. The height correction is about the same as before. The virtual and true heights plotted against the »effective frequency» are shown

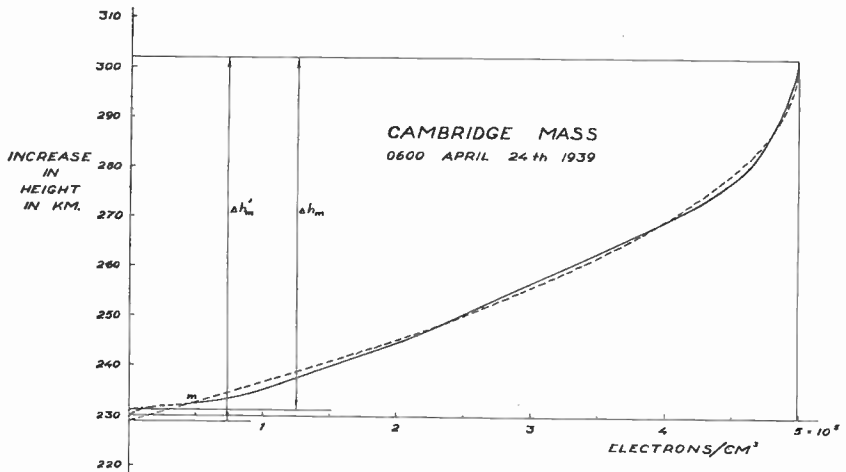


Fig. 32.

by Fig. 31. The maximum increase in true height is very small, approximately 70 km. At the same time the increase in virtual height is about 310 km.

The electron density distribution is shown on Fig. 32. As before it is essentially parabolic throughout the frequency range.  $H$  is small, or only about 37 km.

Finally another typical Cambridge distribution is shown on Fig. 33. This one too is a typical parabolic distribution with an  $H$  value of about 58 km.

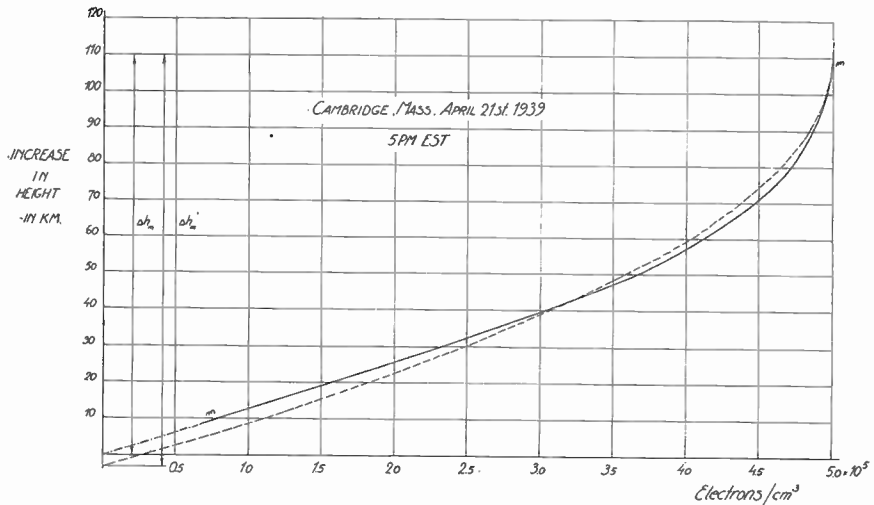


Fig. 33.

As a conclusion a few words should be said about the interpretation of the Cambridge recordings. Naturally it often happens that the lower part of the virtual height curves is registered by the ordinary ray and not by the extra-ordinary ray which may be much absorbed at frequencies in the neighbourhood of the gyro-frequency. As the sweep-frequency equipment used by the author had no polarisation indication (such an indication should, although it makes the apparatus more complex, be of value even for the attenuation measurement discussed on page 46), a low frequency virtual height curve might have been recorded even if the extra-ordinary ray were absent. As the difference in retardation between the components is very small, even though the difference in attenuation may be great, one is allowed to make use of the virtual height curve down to the very vicinity of the gyro-frequency. The tangent to the virtual height curve is thereby, so to speak, drawn by the ordinary ray itself.

\* \* \*

The total number of electrons in the  $F_2$ -layer is of special interest as is obvious from our earlier discussions. A study only of the variation of the maximum electron density may be misleading on account of the expansion. We have therefore computed the total number of electrons,  $N_t$ , in a column of  $1 \text{ cm}^2$  cross section for the Huancayo recordings. The variation in  $N_{max}$  has also been tabulated for comparison.

We have also tabulated the ratio between the so called characteristic frequency,  $f_k$ , and the critical frequency,  $f_{c_m}$ . This indicates the shape of the layer. The characteristic frequency of the distribution is the frequency at which the virtual height equals the true height of the maximum electron density. The assumption that the electron density distribution is parabolic is especially convenient as was pointed out by Booker and Seaton [1]. For a parabolic layer such that

$$N = N_{max} \left[ 1 - \left( \frac{\Delta h_m - z}{\Delta h_m} \right)^2 \right]$$

the classical virtual height is given by the familiar relation

$$\Delta h_e = \frac{\Delta h_m}{2} \cdot \frac{f_0}{f_{c_m}} \cdot \ln \left( \frac{f_{c_m} + f_0}{f_{c_m} - f_0} \right). \quad (87)$$

Booker and Seaton selected three characteristic frequencies, viz.  $0.648 f_{c_m}$ ,  $0.834 f_{c_m}$ , and  $0.925 f_{c_m}$ , at which the virtual height is equal to

$$h(0) + \frac{\Delta h_m}{2}, h(0) + \Delta h_m, \text{ and } h(0) + \frac{3}{2} \cdot \Delta h_m$$

respectively. Rawer, in Germany [17], working with the so called Epstein distribution mentions  $0.707 f_{c_m}$  as a characteristic frequency, corresponding to  $0.834 f_{c_m}$  in the parabolic case, but points out that the magnitude of this characteristic frequency is liable to change quite a lot with the layer shape.

#### Huancayo (1939)

Day	Local Time	$N_t$	Change in $N_t$	$N_{max}$	Change in $N_{max}$	$H$	$\frac{f_k}{f_{c_m}}$
Jan. 2nd	151 $\frac{1}{2}$	$2.50 \cdot 10^{13}$	0 pct.	$2.06 \cdot 10^6$	0 pct.	76 km	0.58
Jan. 2nd	181 $\frac{1}{2}$	$1.97 \cdot 10^{13}$	-22 »	$2.08 \cdot 10^6$	1 »	51 »	0.60
April 4th	131 $\frac{1}{2}$	$2.19 \cdot 10^{13}$	0 »	$1.45 \cdot 10^6$	0 »	105 »	0.78
April 4th	171 $\frac{1}{2}$	$1.96 \cdot 10^{13}$	-11 »	$1.79 \cdot 10^6$	23 »	76 »	0.81
July 1st	121 $\frac{1}{2}$	— —	— —	— —	— —	125 »	0.81
July 2nd	171 $\frac{1}{2}$	— —	— —	— —	— —	86 »	0.80
Oct. 1st	151 $\frac{1}{2}$	$3.68 \cdot 10^{13}$	0 pct.	$1.53 \cdot 10^6$	0 pct.	165 »	0.75
Oct. 1st	181 $\frac{1}{2}$	$2.30 \cdot 10^{13}$	-38 »	$1.71 \cdot 10^6$	12 »	99 »	0.79

It is interesting to see from the table that the variation in  $N_t$  and  $H$  show a similar character. It is further clearly demonstrated how different the variations in  $N_t$  and  $N_{max}$  are. This indicates the importance of the expansion, the nature of which we do not know much about at present. A very typical example is furnished by the October recordings. In spite of the fact that the total number of electrons actually decreased about 38 pct. in the late afternoon the maximum electron density increased 12 pct. The decrease in  $H$  was of the same order of magnitude as the decrease in  $N_t$ , viz. about 40 pct.

It should be evident from these results that it is necessary to compute the true electron density distribution from hour to hour if misleading conclusions regarding the essential processes in the  $F_2$ -layer are to be avoided. The construction of a suitable inte-

grating machine should facilitate this very much. When the present serious times so will permit we hope to present an account of the hourly and daily variation of the total number of electrons of the  $F_2$ -layer in Sweden.

The ratio between the characteristic frequency and the critical frequency is far from constant as shown by the table. The use of a fixed characteristic frequency ratio in the routine scaling of ionosphere records as suggested by Booker and Seaton ( $f_k = 0.834 f_{c_m}$ ) therefore easily leads to erroneous conclusions, convenient as the method otherwise may be. The method of using the integral equations is not as cumbersome as it may appear. Once one is used to the procedure it works quite fast.

The Cambridge  $\frac{f_k}{f_{c_m}}$  ratios are tabulated below together with the corresponding  $H$ -values for the sake of completeness. It should be

Cambridge (1939)<sup>1)</sup>

Date	Time	$H$	$\frac{f_k}{f_{c_m}}$ <sup>2)</sup>
April 20th	17 <sup>00</sup>	56 km	0.75
April 21st	17 <sup>00</sup>	58 »	0.83
April 23rd	01 <sup>00</sup>	58 »	0.84
April 24th	06 <sup>00</sup>	37 »	0.82

added that the quantity  $H$  may be entirely fictitious as in the earlier case. It serves merely as an indication of the thickness of the layer or of the expansion of the  $F_2$ -air. We do not yet possess sufficient knowledge about the formation of the  $F_2$ -layer to state anything definite about  $H$  or the temperature of the  $F_2$ -air. It is possible that, at least in the daytime in summer, the temperature attains high values, perhaps exceeding 1200° K. The probability of such high temperatures in the upper atmosphere was originally suggested by Maris and Hulburt [18]. The temperature gradient in the  $F$ -atmosphere therefore may be considerable since the tempera-

<sup>1)</sup> On account of the limited frequency range of the recording equipment used by the author at Cambridge no complete noon-time sweeps could be taken at the year in question.

<sup>2)</sup> Referred to the effective frequency.

ture at 120 km probably is less than 300° K. Vegard [2], on the other side, considers that the higher layers of the atmosphere extend far upwards on account of electrical forces, and that they are not at a high temperature. This would, of course, also lead to an abnormal increase in  $H$ . Although the temperature expansion seems very probable it is not unlikely that the great  $H$ -values of the  $F_2$ -layer indicate not only such an expansion but also the expansion suggested by Vergard. One therefore has to be very careful not to draw too rapid conclusions regarding the temperature from the  $H$ -values. Further research is needed regarding this matter.

\* \* \*

In order to study the general usefulness of Eq. (79) we have plotted the phase integral as a function of frequency for a parabolic layer. The propagation angle is zero and the gyro-frequency is put equal to  $1/6 \cdot f_c$ , an arbitrary typical value. Making use of the complete expression for the refractive index of the extraordinary ray,<sup>1)</sup> viz.

$$n^2 = 1 - \frac{2x(1-x)}{2(1-x) - y^2 \sin^2 \theta - \sqrt{y^4 \sin^4 \theta + 4y^2 \cos^2 \theta (1-x)^2}} \quad (89)$$

where  $x = \frac{\omega_c^2}{\omega_0^2}$ ,  $y = \frac{\omega_H}{\omega_0}$  and  $\theta =$  the angle of propagation, the correction in the phase integral for  $\theta = 15^\circ$  and  $25^\circ$  has been plotted on the same chart as a function of frequency as shown on Fig. 34. The correction is somewhat smaller than was originally expected.

It is easy to construct the error  $\varepsilon = \frac{\Delta S'}{S'}$  in the virtual height from these data. A plot of the error is shown on Fig. 35 where the original virtual height curve for  $\theta = 0$  has also been drawn.

The correction curves are fairly accurate except near the penetration frequency. The error for a propagation angle of  $15^\circ$  is insignificant compared to the experimental errors in determining  $\Delta h_p$ . At a propagation angle of  $25^\circ$  the errors are much greater, of course, but still generally not as large as the experimental error. Eq. (79) therefore must be useful even at observatories where the magnetic dip is as low as  $65^\circ$ .

<sup>1)</sup> For a deduction of this expression see for example H. R. Mimno: The Physics of the Ionosphere, Rev. Mod. Phys., Vol. 9, Jan. 1937.

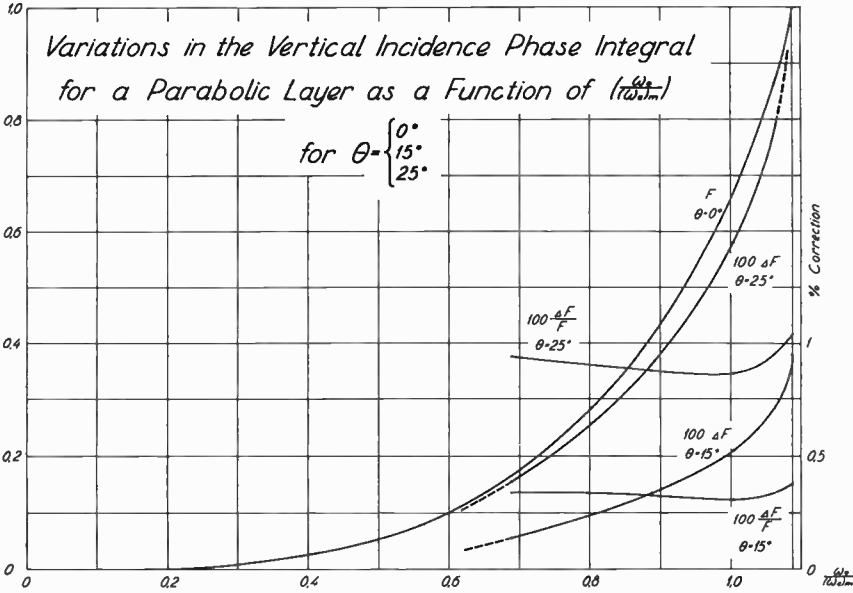


Fig. 34.1)

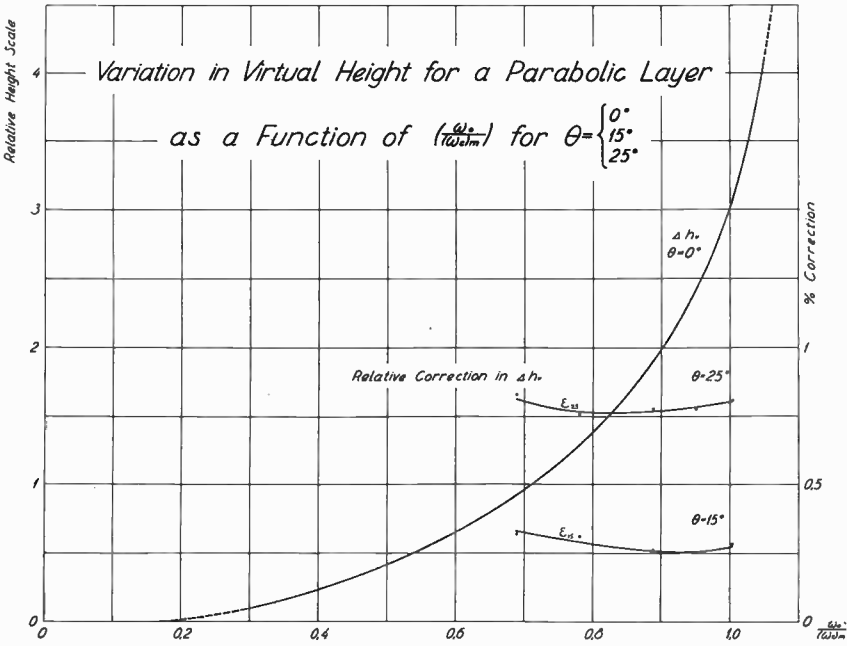


Fig. 35.

1) Note:  $F'$  means  $S$  in accordance with our previous notations.

## The Exact Wave Functions for a Parabolic Layer.

As we have seen, the undisturbed  $F_2$ -layer very often is essentially parabolic, at least at sufficient distances from the equator. However, the electron density distributions in the equatorial regions too appear to be notably parabolic at the level of maximum electron density. The main results of the following calculation can therefore be applied to equatorial cases as well.

Let us assume a parabolic electron density distribution of half-thickness,  $\Delta h_m$ , i. e.

$$f_c^2 = f_{c_m}^2 \left[ 1 - \left( \frac{z}{\Delta h_m} \right)^2 \right],$$

where  $z$  is counted from the level of maximum electron density.

Let us further, for the sake of simplicity, study the case of vertical incidence upon a non-dissipative layer.

It is convenient to introduce the following notations, viz.

$$\lambda_s = \lambda_{c_m} \cdot \frac{f_{c_m}^2}{f_{c_m}^2 - f_0^2}; \quad \varrho = \pi \cdot \frac{\Delta h_m}{\lambda_s}; \quad (90)$$

$$V = \left( \frac{4\pi \cdot \Delta h_m}{\lambda_{c_m}} \right)^{1/2} \cdot \frac{z}{\Delta h_m} \cdot e^{j \frac{\pi}{4}} = u \cdot e^{j \frac{\pi}{4}}.$$

Thereby the wave equation can be written

$$\frac{d^2 \Pi}{dV^2} + \left( j\varrho - \frac{V^2}{4} \right) \cdot \Pi = 0. \quad (91)$$

$\Delta h_m / \lambda_{c_m}$  always is large, 2 to  $5 \cdot 10^3$  is a typical day-time value.  $\varrho$  is large except near the penetration frequency. Eq. (91) is satisfied by Weber's parabolic cylinder functions. One of them is<sup>1)</sup>

$$\Pi = D \left( u \cdot e^{j \frac{\pi}{4}} \right)_{j\varrho - 1/2}. \quad (92)$$

<sup>1)</sup> The symbol used is that of Whittaker. See Whittaker & Watson: A Course of Modern Analysis, p. 347.

From Whittaker's integral representation one easily gets the following asymptotic expansion, viz.

$$\begin{aligned}
 & D \left( u \cdot e^{j \frac{\pi}{4}} \right) \simeq \\
 & j \rho^{-1/2} \\
 \simeq e^{-j \left( \frac{u^2}{4} - \varrho \cdot \ln u + \frac{\pi}{8} \right)} \cdot \frac{e^{-\frac{\pi \rho}{4}}}{\sqrt{u}} & \left( \overbrace{1 - j \frac{(\varrho + j^{1/2})(\varrho + j^{3/2})}{2u^2} + \dots}^{\text{Phase angle } - \Phi} \right). \quad (93)
 \end{aligned}$$

As  $u$  always is large the only restriction is that  $\varrho$  must be sufficiently small. A safe limit is marked by

$$\frac{2u^2}{\varrho^2} \ll 1 \text{ or } |\Delta f_0| = |f_{cm} - f_0| \ll \left( \frac{2c_0}{\pi \cdot \Delta h_m} \right)^{1/2} \cdot (f_{cm})^{1/2}. \quad (94)$$

For  $f_{cm} = 10^7$  c/s and  $\Delta h_m = 100$  km,  $|\Delta f_0|$  becomes less than about  $1.4 \cdot 10^5$  c/s. The present expansion, therefore, can only be used in the neighbourhood of the penetration frequency,  $f_{cm}$ , of the layer. As this is the frequency range where we know that our earlier methods are likely to be too approximate we do not have to develop another expansion in this connexion, although a complete study of the solution should make it necessary.

Multiplying by the time factor we see that

$$e^{-j\omega_0 \cdot t} \cdot D \left( u \cdot e^{j \frac{\pi}{4}} \right) \simeq j \rho^{-1/2}$$

yields an up-going wave.

Another solution is

$$\begin{aligned}
 & D \left( u \cdot e^{-j \frac{\pi}{4}} \right) \simeq \\
 & -j \rho^{-1/2} \\
 \simeq e^{+j \left( \frac{u^2}{4} - \varrho \cdot \ln u + \frac{\pi}{8} \right)} \cdot \frac{e^{-\frac{\pi \rho}{4}}}{\sqrt{u}} & \left( \overbrace{1 + j \frac{(\varrho - j^{1/2})(\varrho - j^{3/2})}{2u^2} - \dots}^{\text{Phase angle } + \Phi} \right), \quad (95)
 \end{aligned}$$

which multiplied by the same time-factor yields a down-coming wave.

Next we have to find a suitable »circuit relation» of the differential equation connecting the incident, the reflected and the refracted wave. Fortunately enough, there exists a fairly simple one, viz.

$$\begin{aligned}
 \underbrace{D \left( u \cdot e^{j \frac{\pi}{4}} \right)}_{\text{incident wave}} &= \underbrace{\frac{\Gamma(j \varrho + 1/2)}{\sqrt{2 \pi}} \cdot e^{\frac{\pi \varrho}{2} + j \frac{\pi}{4}} \cdot D \left( u \cdot e^{-j \frac{\pi}{4}} \right)}_{\text{reflected wave}} + \\
 &+ \underbrace{\frac{\Gamma(j \varrho + 1/2)}{\sqrt{2 \pi}} \cdot e^{-\frac{\pi \varrho}{2} - j \frac{\pi}{4}} \cdot D \left( u \cdot e^{j \frac{3}{4} \pi} \right)}_{\text{refracted wave}}. \quad (96)
 \end{aligned}$$

Mathematically speaking, the above expression gives the analytical continuation of the function of the refracted ray, represented by an asymptotic series for instance, beyond the region for which this special representation is valid. The law of reflection gives us, therefore, a physical visualization of the rather abstract concept of analytical continuation. This was mentioned already by Epstein [19] in a fundamental paper on the reflection of waves in an inhomogeneous medium.

We are primarily interested in the phase difference between the up-going and down-coming rays at the bottom of the layer ( $z = \Delta h_m$ ). This is

$$\begin{aligned}
 \Delta S &= \frac{u^2}{2} - \varrho \cdot \ln u^2 + \text{phase} \left[ \Gamma(j \varrho + 1/2) \right] + 2 \cdot \Phi + \pi/2; \\
 2 \Phi &\sim \varrho^2 / u^2. \quad (97)
 \end{aligned}$$

But by Gauss' multiplication theorem it becomes

$$\Delta S \simeq \frac{u^2}{2} - \varrho \cdot \ln(4 u^2) + \text{phase} \left[ \frac{\Gamma(2 j \varrho)}{\Gamma(j \varrho)} \right] + \frac{\varrho^2}{u^2} + \pi/2.$$

The virtual height therefore becomes

$$\begin{aligned}
 \Delta h_c &= \frac{c_0}{2} \frac{d}{d \omega_0} (\Delta S) = \frac{c_0}{4 \pi} \left[ -\ln(4 u^2) + \frac{2 \varrho}{u^2} + \right. \\
 &\left. + \text{Re} \left( 2 \Psi(2 j \varrho) - 1 \Psi(j \varrho) \right) \right] \frac{d \varrho}{d f_0},
 \end{aligned}$$

where  $\Psi(a)$  is the logarithmic derivative of  $\Gamma(a)$ . This finally yields

$$\Delta h_v = \frac{\Delta h_m}{2} \cdot \frac{f_0}{f_{c_m}} \cdot \left[ \gamma + \ln \left( 16 \cdot \pi \cdot \frac{\Delta h_m}{\lambda_{c_m}} \right) - \right. \\ \left. - \varrho \left( \frac{2}{a^2} + \operatorname{Re} \sum_{n=1}^{\infty} j \cdot \frac{3n + 2j\varrho}{n(n + j\varrho)(n + 2j\varrho)} \right) \right], \quad (98)$$

where  $\gamma$  is Euler's constant = 0.5772.

At the penetration frequency the *exact* virtual height becomes

$$\Delta h_v = \frac{\Delta h_m}{2} \left[ \gamma + \ln \left( 16 \cdot \pi \cdot \frac{\Delta h_m}{\lambda_{c_m}} \right) \right]. \quad (98 a)$$

This is not infinite. The classical virtual height expression for a parabolic layer

$$\Delta h_v = \frac{\Delta h_m}{2} \cdot \frac{f_0}{f_{c_m}} \cdot \ln \left( \frac{f_{c_m} + f_0}{f_{c_m} - f_0} \right)$$

yields infinite virtual height at the penetration frequency. The exact virtual height is very great. For a half-thickness of 100 km and a critical wave-length of  $10\pi$  m it becomes about 630 km. It should be noted that this is the increase in virtual height and the total virtual height therefore, as registered on the ionosphere records, should become 900 or 1000 km depending upon the value of  $h(0)$ . As the absorption is too strong for these signals to be recorded, except perhaps when the transmitter is very powerful, it generally is impossible to note the correct critical height even on the very best records. As an example let us return to Fig. 26. The maximum virtual height is about 680 km. Eq. (98 a) yields a height of 950 km for the corresponding parabolic layer as shown on Fig. 29. Similarly for the recording shown on Fig. 27 the maximum virtual height is about 550 km whereas the exact virtual height turns out to be 670 km. The absorption at the penetration frequency

is so strong for the recordings in question that it is never possible to register the discrepancy between classical and exact virtual heights near the penetration frequency.

That the dispersion becomes finite at the penetration frequency is obvious from Eq. (98). When the wave frequency equals the penetration frequency, however, only the lower side-bands of the Fourier representation of the wave-train are reflected with noticeable intensity. Fig. 36 shows a plot of the classical and exact virtual heights in the neighbourhood of the penetration frequency,  $f_{c_m} = 10^7$  c/s, for a layer of 120 km half-thickness. It should be noticed that the deviation from geometrical optics is of importance only in a very narrow frequency region for such a thick layer. We are therefore very well justified to use our integral equations for the determination of the true electron density distribution. It should further be added that it is easily proved from Eq. (98) that

$$\lim_{\left(\frac{\Delta h_m}{\lambda_{c_m}} \rightarrow \infty\right)} \frac{(\Delta h_v)_{\text{exact}}}{(\Delta h_v)_{\text{classical}}} = 1.$$

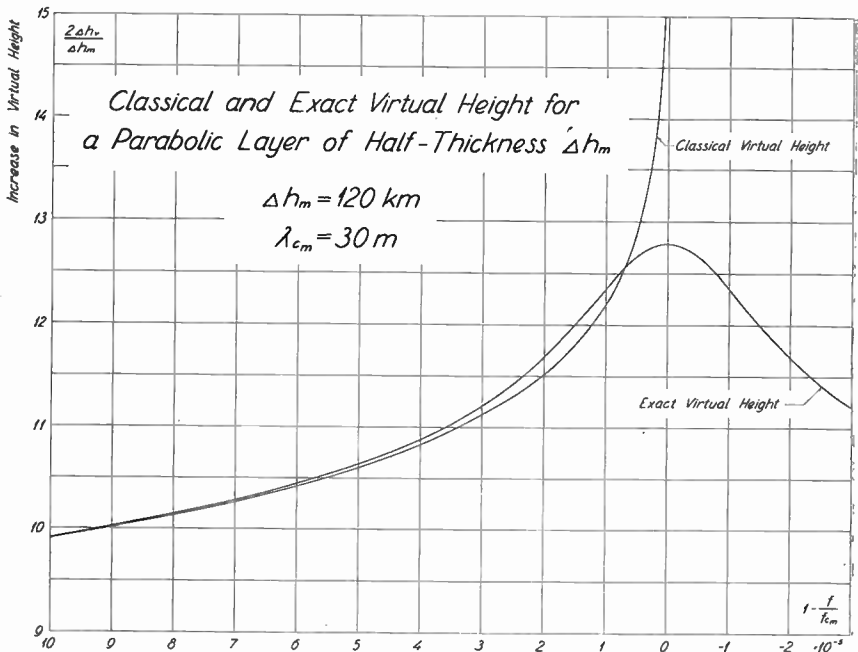


Fig. 36.

This shows mathematically the transition to diffractionless optics when the geometrical dimensions become infinitely large.

Finally it should be noted that results closely similar to Eq. (98) were obtained already in 1939 by Rawer in an excellent paper treating the general wave propagation in dissipative Epstein layers [20]. The interested reader is referred to his paper for a complementary study.

As the medium is non-dissipative one immediately obtains from the circuit relation that the reflection coefficient,  $R$ , is determined by the relation

$$\frac{R^2}{1 - R^2} = e^{2\pi q} = e^{4\pi^2 \frac{\Delta h_m}{\lambda_{cm}} \cdot \frac{f_{cm}^2 - f_0^2}{2f_{cm}^2}} \quad (99)$$

This holds throughout the frequency range. Fig. 37 shows several plots of the reflection coefficient for layers of different thickness. The critical frequency is  $10^7$  c/s, i. e.  $\lambda_{cm} = 30$  m. The deviation from geometrical optics is practically noticeable first for a

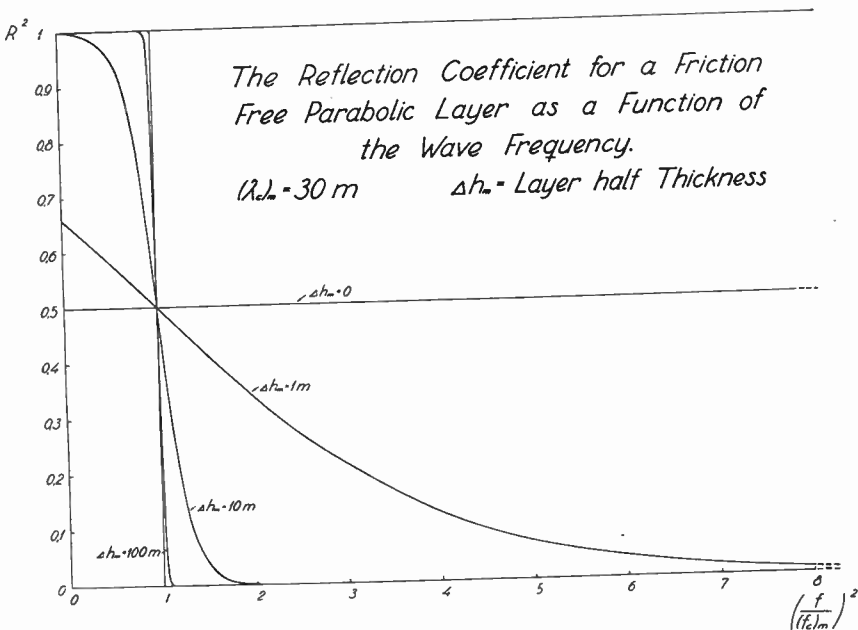


Fig. 37.

half-thickness of about three to four wave-lengths. As the thickness becomes even smaller (maximum electron density constant) appreciable reflection appears at frequencies well above the critical frequency. It is obvious that the critical frequency conception may be misleading for a very thin layer.

The night-time abnormal *E*-layer reflections often appear to come from such thin layers and reflection is obtained over a surprisingly wide frequency range.

\* \* \*

When the layer is parabolic only in its upper part, as shown on Fig. 13, it is convenient to use the parabolic wave functions in the upper part and the BKW-approximations in the lower part. They have to be joined at the proper level, about 275 km on Fig. 13 for example, which is a fairly simple matter.

An extended study of the parabolic solutions for other values of frequency, i. e. frequencies not necessarily close to the critical frequency of the layer, necessitates the expansion of the parabolic wave functions in asymptotic series which can be used when not only  $u$  but also  $q$  is large. Interesting as such a study may be, it is outside the scope of the present communication. An account of these expansions will be given in a later communication to which those especially interested are referred.

In conclusion a few words should be said about the collisional friction. It is formally introduced in the wave functions if  $f_{c_m}$  is replaced by  $\bar{f}_{c_m} = f_{c_m} \cdot \exp.(-j\alpha)$ , where  $\alpha = \frac{1}{2} \arctan\left(\frac{\nu}{\omega_0}\right)$ . When  $\left(\frac{\nu}{\omega_0}\right)^2 \ll 1$ , as is generally the case in the  $F_2$ -layer, the introduction of  $\nu$  is hardly noticeable as far as  $\Delta h_p$  is concerned. The mathematical results, which therefore are of mainly theoretical interest, will appear in a forthcoming paper.

---

The author wishes to express his thanks to *Alice and Knut Walenberg's Foundation*, Stockholm, for their generous support of the investigation. The author's thanks are also due, and are cordially extended, to *TORSTEN JÖNSSON*, M. Ph., who carefully assisted in correcting the proof.

## References<sup>1)</sup>.

1. F. H. Murray and J. B. Hoag: Heights of reflection of radio waves in the ionosphere. *Phys. Rev.*, **51**, pp. 333—341, 1937.  
O. E. H. Rydbeck: Jonosfärens fysik och dess betydelse för radiokommunikationerna. *Tekniska Samfundets Handlingar* (Gothenburg), **3**, p. 155, 1939.  
H. G. Booker and S. L. Seaton: Relation between actual and virtual ionospheric heights. *Phys. Rev.*, **57**, pp. 87—94, 1940.  
O. E. H. Rydbeck: *Vertical and Non-Vertical Ionospheric Reflections at Fixed and Variable Frequencies*. Dissertation, Harvard University, 1940.  
C. L. Pekeris: The vertical distribution of ionization in the upper atmosphere. *Terr. Mag.*, **45**, pp. 205—211, 1940.  
O. E. H. Rydbeck: The propagation of electromagnetic waves in an ionized medium and the calculation of the true heights of the ionized layers of the atmosphere. *Phil. Mag.* XXX, pp. 282—293, 1940.
2. P. O. Pedersen: *The Propagation of Radio Waves along the Surface of the Earth and in the Atmosphere*. Danmarks Naturvidenskabelige Samfund. Nr. 15 a/b, Copenhagen, 1927.  
J. Bartels: Überblick über die Physik der hohen Atmosphäre. *Elektr. Nachrichten-Technik*, **10**, Sonderheft. 40 pp. Berlin, 1933.  
S. Chapman and W. C. Price: The upper atmosphere, *Reports on Progress in Physics*, **3**, 42—65, Cambridge Univ. Press, 1937.  
H. R. Mimno: The physics of the ionosphere, *Rev. Mod. Phys.*, **9**, 1—43, 1937.  
B. Haurwitz: The physical state of the upper atmosphere, reprinted from *Journ. Roy. Astron. Soc. Canada*, Oct. 1936 to Feb. 1937. 96 pp., Toronto Univ. Press, 1937.  
L. Vegard: Die Deutung der Nordlichterscheinungen und die Struktur der Ionosphäre. *Ergebn. exakt. Naturw.*, **17**, pp. 229—281, 1938.  
O. E. H. Rydbeck: Jonosfärens fysik och dess betydelse för radiokommunikationerna. *Tekniska Samfundets Handlingar* (Gothenburg), **3**, pp. 135—192, 1939.  
*Terrestrial Magnetism and Electricity*, pp. 434—656, edited by J. A. Fleming, 1939.  
S. Chapman and S. Bartels: *Geomagnetism*. Vol. I, pp. 487—542, 1940.
3. *Terrestrial Magnetism and Electricity*, p. 526.
4. P. S. Epstein: Geometrical optics in absorbing media. *Proc. Nat. Acad. Sci.*, **16**, pp. 40, 43., 1930.

<sup>1)</sup> As the mail service has been very irregular during the past year the list of references necessarily can not be regarded as complete as far as later publications are concerned.

5. W. de Groot: Some remarks on the analogy of certain cases of propagation of electromagnetic waves and the motion of a particle in a potential field. *Phil. Mag.*, **10**, p. 521, 1930.
6. T. L. Eckersley: On the connection between the ray theory of electric waves and dynamics. *Proc. Roy. Soc.*, **A132**, p. 83, 1931.
7. J. R. Carson: The building up of sinusoidal currents in long periodically loaded lines. *Bell. Syst. Techn. Journ.*, p. 559, 1924.
8. G. B. Airy: On the intensity of the light in the neighbourhood of the caustic. *Trans. Camb. Phil. Soc.*, **VI**, pp. 379—402, 1838.
9. A. Sommerfeld: *Atombau und Spektrallinien*. II Band, pp. 707—714.
10. G. Breit and M. Tuve: A test of the existence of the conducting layer. *Phys. Rev.*, **28**, p. 554, 1926.
11. N. H. Abel: *Oeuvres Complètes*, Tome 1, Christiania (Oslo), p. 11, 1881. (Solution de quelques problèmes à l'aide d'intégrales définies, 1823).
12. J. B. Macelwane and F. W. Sohon: *Introduction to Theoretical Seismology I*. p. 180.  
G. Angenhoister: Seismik. *Handbuch d. Physik*, VI Band, pp. 605, 606.
13. M. J. O. Strutt: *Moderne Mehrgitter-Elektronenröhren*, p. 32.
14. E. V. Appleton: Some notes on wireless methods of investigating the electrical structure of the upper atmosphere. *Proc. Phys. Soc.*, **42**, pp. 321—339, 1930.  
W. de Groot: Loc. cit.
15. O. E. H. Rydbeck: *Tekniska Samfundets Handlingar* (Gothenburg), **3**, p. 155, 1939.
16. O. E. H. Rydbeck: *Phil. Mag.* loc. cit.
17. K. Rawer: Zur Frage der Auswertung von Ionosphärenbeobachtungen. *Hochfrequenztechnik und Elektroakustik*, **58**, p. 50, 1941.
18. H. B. Maris: The upper atmosphere. *Terr. Magn.*, **33**, pp. 233—255,  
H. B. Maris and E. O. Hulburt: A theory of aurorae and magnetic storms. *Phys. Rev.*, **33**, pp. 412—431, 1929.
19. P. S. Epstein: Reflection of waves in an inhomogeneous absorbing medium. *Nat. Acad. Sci.*, **16**, p. 629, 1930.
20. K. Rawer: Elektrische Wellen in einem geschichteten Medium. *Ann. d. Phys.*, **35**, p. 402, 1939.

## Table of contents.

Summary.....	3
A General Survey of the Situation .....	5
The Propagation of the Wave-Train .....	7
The Dispersion of the Down-Coming Radio Echoes .....	18
The Phase Relations and the Virtual Path-Length .....	26
The Calculation of the True Height of Reflection and the True Electron Density Distribution .....	32
The Calculation of the Variation of the Collisional Frequency with Height .....	43
Typical Electron Density Distributions .....	46
The Exact Wave Functions for a Parabolic Layer .....	66
References .....	73



CHALMERS TEKNISKA HÖGSKOLAS HANDLINGAR  
TRANSACTIONS OF CHALMERS UNIVERSITY OF TECHNOLOGY  
GOTHENBURG, SWEDEN

Nr 74

(Avd. Elektroteknik 12)

1948

---

ON THE PROPAGATION OF WAVES IN  
AN INHOMOGENEOUS MEDIUM

I

BY

OLOF E. H. RYDBECK



REPORTS FROM  
THE RESEARCH LABORATORY OF ELECTRONICS

Nr 7

LUND 1948  
HÅKAN OHLSSONS BOKTRYCKERI



## Introduction and summary

The propagation of waves through inhomogeneous or stratified media was studied already by RAYLEIGH in 1912 [1] and by FÖRSTERLING [2] and GANS [3] 1913/1915. FÖRSTERLING later, in 1931, returned to the same theme with application to the new problem, the propagation of short radio waves in an inhomogeneous atmosphere [4]. Slightly earlier EPSTEIN published a fundamental paper concerning the same problem with exact results for certain types of dielectric constant variation profiles [5].

In the following years with the rapid advance of quantum mechanics and of the experimental investigation of the propagation of radio waves in the inhomogeneous upper atmosphere a great number of papers appeared concerning special kinds of wave propagation or wave functions. The problems were attacked by various methods and this, no doubt, frequently was due to the fact that very different physical quantities were desired.

In the subsequently developed theory of reaction rates [6] problems very similar to those of the radio case have been studied by the introduction of ECKART-EPSTEIN type potential energy profiles.

In a comparatively recent communication SCHELKUNOFF considered the problem of wave propagation in a slightly inhomogeneous medium [7]. It seems that there is a definite need for a further development of the various theories both for propagation in slightly inhomogeneous media as well as in strongly inhomogeneous media and also for a deeper discussion of the connection between the different theoretical methods. When, for example, does the elementary form of phase integration originally developed by ECKERSLEY yield a sufficiently accurate result?

In the present communication first and higher order approximations for the reflection coefficient are developed for slightly inhomogeneous media. The results of these approximations, applied to cases which can be solved exactly, demonstrates the usefulness and range of the former.

The methods of ZWAAN, KEMBLE [8] and others of connecting the layer or barrier boundaries with a so called good path is discussed as an introduction to the connection of wave functions of LANGER type developed from the branch points of the refractive index,  $n$ . The general agreement between the two methods when the branch points are sufficiently apart is shown and it is further demonstrated that the complete method of phase integration must consider all waves "running" up and down between the branch points. The result is physically clear.

In a following section it is proved that the reflection intensity as calculated by the good path method is correct even when the branch points come very close (transition from reflection to penetration or vice versa) if only the minimum in  $n^2$  is parabolic. In practically all applications this is the case. A complete expression for the wave phase is shown.

In the final section of this communication the application of the circuit relation of the wave equation is demonstrated in two topical applications, viz. the propagation of ALFVEN's magneto hydro dynamic waves in the Sun [9] and the duct propagation of micro waves in the lower troposphere.

It is shown that from the circuit relation the actual value of the reflection coefficient can be obtained for any level even though the wave functions, forming the circuit relation, themselves can not be considered as purely progressive waves well inside the inhomogeneous medium. As RAYLEIGH once remarked: In the full sense of the phrase there is not such a thing as a progressive wave (in an inhomogeneous medium). By means of the methods demonstrated in this communication, however, it is possible to follow the continuous deformation and reflection of the progressive wave if only the circuit relation is known.

O. E. H. R.

*Research Laboratory of Electronics  
May 1948.*

## Fundamental theory

Let us start with the one-dimensional monochromatic wave equation

$$\frac{d^2 II}{dx^2} + k_0^2 n^2 II = 0, \tag{1}$$

where  $II$  is a wave potential,  $k_0 = 2\pi/\lambda_0$  and  $\lambda_0$  the vacuum wave length. The refractive index  $n$  is supposed to be a function  $n(x)$  of the coordinate  $x$ .

The first-order approximation to a solution of (1) is the so called WENTZEL-KRAMER-BRILLOUIN-JEFFREYS approximation\*

$$II_1^{(1)} = n^{-1/2} e^{\mp j \int_a^x k_0 n(s) ds - \pi/4}, \tag{2}$$

Making use of the time-factor  $e^{-j\omega t}$  we note that  $II_1^{(1)}$  represents a wave traveling in the positive  $x$ -direction.

The general solution of (1) thus takes the form

$$II = a^{(1)}(x) II_1^{(1)}(x) + a^{(2)}(x) II_1^{(2)}(x), \tag{3}$$

where the coefficients  $a^{(1)}(x)$  and  $a^{(2)}(x)$  change very slowly except in regions of considerable reflection.

The first order approximations (2) do not themselves give us any information about the partial reflection in the medium. However, they contain the "impedance" transforming factor  $n^{-1/2}$  so that for sufficiently short waves

$$\frac{1}{jk_0} \frac{dII_1^{(1)}}{dx} \sim n II_1^{(1)}, \tag{4}$$

i. e. the energy flow

$$\left\{ \frac{1}{jk_0} \frac{dII_1^{(1)}}{dx} \cdot II_1^{(1)*} \right\} \sim 1 = \text{constant}. \tag{5}$$

Thus if  $n(x)$  is a slowly varying function  $\left\{ \frac{1}{|n|} \cdot \frac{d|n|}{dx} \lambda \ll 1 \right\}$  one can ignore the reflections

---

\* As a matter of fact used long ago by RAYLEIGH and GANS.

and in the first approximation consider the medium as continuously "matched" and thus acting as a transformer.

Let us now return to Equation (3). We will necessarily have to complement it by

$$\frac{d\Pi}{dx} = a^{(1)}(x) \frac{d\Pi_1^{(1)}(x)}{dx} + a^{(2)}(x) \frac{d\Pi_1^{(2)}(x)}{dx}. \quad (6)$$

Eqs. (3) and (6) are evidently the equations we should have to employ if we were fitting a *fixed* linear combination to  $\Pi$  at the point  $x$  and wished the combination to cling to  $\Pi$  as closely as possible in the neighbourhood of  $x$ . We assume that the coefficients  $a^{(1)}(x)$  and  $a^{(2)}(x)$  thus defined reduce to  $A^{(1)}$  and  $A^{(2)}$  at one end of the path (the incidence side) and to  $B^{(1)}$  and  $B^{(2)}$  at the other.

Introducing

$$W(x, b) = k_0 \int_b^x n(s) ds - \pi/4, \quad (7)$$

we find from (3) and (6)

$$\frac{da^{(1)}}{dx} = -\frac{da^{(2)}}{dx} \cdot e^{-j2W}. \quad (8)$$

We further find from (3) and (6) that\*

$$a^{(1)}(x) = \frac{\mp j}{2k_0} \{ \Pi \Pi_1^{(2)'} - \Pi' \Pi_1^{(1)} \}. \quad (9)$$

As further

$$\Pi_1^{(1)''} + (k_0^2 n^2 - Q) \Pi_1^{(1)} = 0, \quad (10)$$

where

$$Q = \frac{3}{4} \left( \frac{n'}{n} \right)^2 - \frac{1}{2} \frac{n''}{n}, \quad (11)$$

we finally have

$$\frac{da^{(1)}}{dx} = \frac{j}{2k_0} \cdot \frac{Q}{n} \{ a^{(1)} + a^{(2)} e^{-j2W} \}, \quad (12)$$

and

$$\frac{da^{(2)}}{dx} = \frac{-j}{2k_0} \cdot \frac{Q}{n} \{ a^{(1)} e^{j2W} + a^{(2)} \}, \quad (13)$$

which also proves (8).

It is convenient to introduce

$$b^{(2)}_{(1)} = a^{(2)}_{(1)} e^{\pm j \int_b^x \Pi^{(s)} ds} = a^{(2)}_{(1)} e^{\pm j\Gamma}, \quad (14)$$

where

$$H(x) = \frac{Q(x)}{2k_0 n(x)}. \quad (14 a)$$

\* Note:  $\Pi' = \frac{d\Pi}{dx}$ ,  $\Pi'' = \frac{d^2\Pi}{dx^2}$ .

Eqs (12) and (13) thus yield

$$\boxed{\frac{db^{(1)}}{dx} = Hb^{(2)} e^{\pm j2\theta}}, \tag{15}$$

and 
$$\Theta = W + \Gamma - \pi/4. \tag{16}$$

Eqs (15) describe the partial or infinitesimal reflection in the medium and prove that a change in  $n$ , even if small and slow, always produces a fractional reflection.

When  $n$  real, one further easily finds from (15) that

$$|b^{(1)}|^2 - |b^{(2)}|^2 = \text{const.}, \tag{17}$$

proving that the net energy transfer through the medium is constant. If we select the fundamental case of waves incident from one direction only, for example in positive direction, we evidently have  $B^{(2)} = 0$ , and

$$|b^{(1)}|^2 - |b^{(2)}|^2 = |B^{(1)}|^2, \tag{18}$$

i. e. the magnitude of the reflection coefficient becomes

$$|R| = \sqrt{1 - |B^{(1)}|^2 / |b^{(1)}|^2}. \tag{19}$$

This demonstrates how the reflection coefficient gradually falls to zero as we leave the inhomogeneous region in positive direction.

Introducing  $b = \infty$ ,

$$z = He^{+j2\theta} \text{ and } z^* = He^{-j2\theta}, \tag{20}$$

we obtain from (15) after successive integrations

$$b^{(2)}(x) = B^{(1)} \cdot \{I_1(x) + I_3(x) + I_5(x) + \dots\}, \tag{21}$$

where

$$I_1(x) = \int_{\infty}^x z dx, \quad I_{2n+1}(x) = \int_{\infty}^x z I_{2n}^*(x) dx, \tag{21 a}$$

and

$$I_{2n}^*(x) = \int_{\infty}^x z^* I_{2n-1}(x) dx. \tag{21 b}$$

Similarly

$$b^{(1)}(x) = B^{(1)} \cdot \{1 + I_2^*(x) + I_4^*(x) + \dots\}, \tag{22}$$

i. e. the reflection coefficient becomes \*

$$R(x) = \frac{I_1(x) + I_3(x) + I_5(x) + \dots}{1 + I_2^*(x) + I_4^*(x) + \dots} e^{-j2\theta}. \tag{23}$$

This formula, however, is useful only when the variations in  $n$  are relatively small as will be shown in the following section.

\* Note: Time factor  $e^{-j\omega t}$ .

### Propagation in a medium with small variations in refractive index

As an introduction let us study the nature of  $Q$  briefly. With

$$n = \sqrt{1 + f(x)}, \quad (24)$$

we have

$$Q = -\frac{1}{4} \frac{f''(x)}{1+f(x)} + \frac{5}{16} \cdot \left\{ \frac{f'(x)}{1+f(x)} \right\}^2. \quad (25)$$

However, as

$$\frac{n''}{n} = \frac{1}{2} \left[ \frac{f''(x)}{1+f(x)} - \frac{1}{2} \left\{ \frac{f'(x)}{1+f(x)} \right\}^2 \right] \quad (25 \text{ a})$$

but

$$\frac{n''}{n} = \frac{1}{2} \frac{f''(x)}{1+f(x)/2}, \quad \text{if } n = 1 + f(x)/2; \quad (26)$$

we infer that neglect of the last term in (25) practically is the same as assuming that  $1 + f(x)/2$  is a good approximation for (24).

Let us next consider two typical cases, viz.

a)  $f(x) = \delta_1 \tanh x/x_0, \quad (27)$

and

b)  $f(x) = \frac{\delta_2}{4} \cdot \frac{1}{\cosh^2 x/x_0}. \quad (28)$

as depicted in fig. 1. Cases a) and b) can also be written

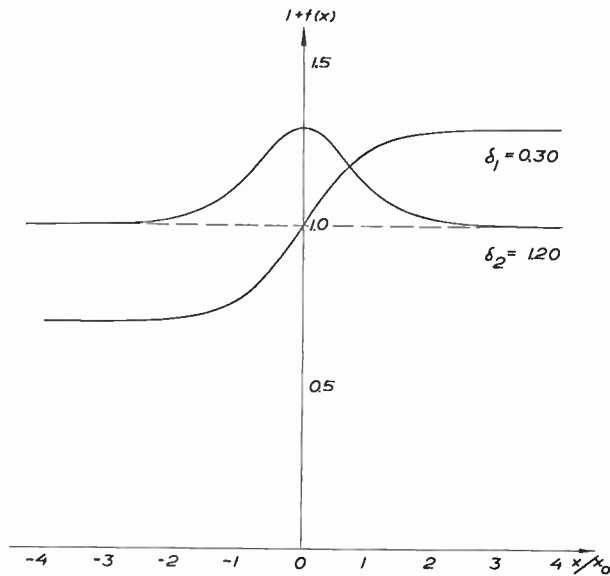


Fig. 1.

$$f(x) = -\delta_1 + \frac{2\delta_1}{1 + e^{-\eta}}, \quad (27 \text{ a})$$

and

$$f(x) = \delta_2 \cdot \frac{e^{-\eta}}{(1 + e^{-\eta})^2}, \tag{28 a}$$

where

$$\eta = 2x/x_0. \tag{29}$$

Both are special cases of the general EPSTEIN-ECKART function (or potential-function) [5, 6]

$$f_E(\eta) = A + \frac{B}{1 + e^{-\eta}} + \frac{C}{(1 + e^{-\eta})^2} \cdot e^{-\eta}, \tag{30}$$

for which the wave equation can be solved in terms of hypergeometric functions.

Returning now to case a) we assume that  $\delta_1 \ll 1$ , i. e.

$$H(x) \cong -\frac{1}{8k_0} f''(x), \text{ and } \Theta \cong k_0(x - b) - \pi/4.$$

The first order approximation for  $R$ , i. e.  $R^{(1)}$ , in accordance with (23) becomes

$$R^{(1)}(x) = -\frac{e^{-j2k_0x}}{8k_0} \int_{-\infty}^x e^{j2k_0x} f''(x) dx. \tag{31}$$

If we assume that we are well on the negative  $x$ -side of the main reflection region ( $-x \gg x_0$ ), the upper limit  $x$  can safely be replaced by  $-\infty$ . Therefore, after partial integration,

$$R^{(1)}(x) = -\frac{\delta_1 e^{-j2(k_0x - \pi/4)}}{2} \int_0^{\infty} \frac{t^{-j k_0 x_0} dt}{(1+t)^2} = -e^{-j2(k_0x - \pi/4)} \cdot \frac{\delta_1}{2} \cdot \frac{\pi k_0 x_0}{\sinh \pi k_0 x_0}. \tag{32}^*$$

$(-x \gg x_0)$

The reflected wave thus appears to come from the level  $x=0$  with a BKW-type phase shift of  $2 \cdot \pi/4$ . The amplitude of the first order reflection coefficient

$$|R^{(1)}| = \frac{\delta_1}{2} \cdot \frac{\pi k_0 x_0}{\sinh \pi k_0 x_0}, \tag{32 a}$$

for very long waves becomes  $|R^{(1)}| \cong |\delta_1/2|$ , i. e. the discontinuity result as one should expect.

The exact value of the reflection coefficient can be obtained from the circuit relation, involving hypergeometric functions, of the differential equation. One finds [5]

$$|R| = \frac{\sinh \{ \pi k_0 x_0 (\sqrt{1 + \delta_1} - \sqrt{1 - \delta_1}) / 2 \}}{\sinh \{ \pi k_0 x_0 (\sqrt{1 + \delta_1} + \sqrt{1 - \delta_1}) / 2 \}} \tag{33}$$

and thus for very long waves the discontinuity result  $|R| = \frac{\sqrt{1 + \delta_1} - \sqrt{1 - \delta_1}}{\sqrt{1 + \delta_1} + \sqrt{1 - \delta_1}} \approx \frac{\delta_1}{2}$ .

\* Note:  $\int_0^{\infty} \frac{t^z dt}{(1+t)^{w+1}} = \frac{\Gamma(z+1) \Gamma(w-z)}{\Gamma(w+1)}$ . ( $\text{Re } w > \text{Re } z > -1$ ).

When  $\delta_1 \ll 1$ , and  $\delta_1 \ll \lambda/\pi^2 x_0$ , (33) thus is identical with (32a). This demonstrates the usefulness of the first order approximation of (23) for small steps,  $\delta_1$ .

Next, let us study case b) briefly. Integrating partially twice we find

$$R^{(1)}(x) = -\frac{\delta_2}{2} \cdot \frac{k_0 x_0}{2} \cdot e^{-j2k_0 x} \int_0^\infty \frac{t^{-jk_0 x_0} dt}{(1+t)^2} = -\frac{\delta_2}{2} \cdot \frac{k_0 x_0}{2} \cdot \frac{\pi k_0 x_0}{\sinh \pi k_0 x_0} \cdot e^{-j2k_0 x_0}, \quad (34)$$

( $-x \gg x_0$ )

i. e.

$$|R^{(1)}| = \frac{|\delta_2|}{2} \cdot \frac{k_0 x_0}{2} \cdot \frac{\pi k_0 x_0}{\sinh \pi k_0 x_0}. \quad (34a)$$

For very long waves we thus have  $|R^{(1)}| \cong \delta_2 k_0 x_0 / 4$ . For very low frequencies  $|R^{(1)}|$  thus is proportional to the wave frequency ( $\delta_2$ , as  $\delta_1$ , have throughout been assumed independent of frequency) and not constant as in case a). This is due to the fact that the wave groups reflected at the rear of the hump ( $x > 0$ ) will be practically out of phase with the groups reflected at the front.

The same is true in the case of real discontinuities. If for example  $n = 1$ , for  $x < x_1$  and  $x > x_1 + s$ ;  $n = \sqrt{1 + \delta}$ , for  $x_1 < x < x_1 + s$ , and  $\delta \ll 1$  we find

$$|R| = \left| \frac{\delta}{2} \sin(k_0 s) \right|, \quad (35)$$

showing the characteristic colour effects except for long waves, when  $|R| \cong \delta k_0 s / 2$ . The low frequency dependence therefore is the same as in case b).

Finally, let us for comparison consider the result of the exact theory for case b). One finds

$$|R| = \frac{|\cos \pi d|}{\sqrt{\cos^2 \pi d + \sinh^2 \pi k_0 x_0}}, \quad * \quad (36)$$

where

$$d = \frac{1}{2} \sqrt{1 + (k_0 x_0)^2 \delta_2}. \quad (36a)$$

When  $\delta_2 \ll \lambda^2 / (2\pi x_0)^2$  therefore (36) reduces to (34a), proving again the usefulness of the first order approximation when the  $\delta$  is small.

In ALFVEN's theory of the development of solar magneto-hydrodynamic waves [9] these waves propagate from the photosphere towards the chromosphere in a medium with decreasing refractive index approximately of the type

$$n = \sqrt{1 + U e^{-x/x_0}}, \quad (37)$$

where  $x_0$  may be regarded as a scale-height of the medium. It is of particular interest to investigate how much of the wave will reach the chromosphere and at what level the main reflection will take place. As  $U$  is very large we can use our first-order approxi-

\* It is interesting to note from (36) that the colour effects disappear when the minimum in refractive index is sufficiently low, i. e. when  $-\delta_2 > 1/(k_0 x_0)^2$ .

mation only when  $x \gg x_0$ , i. e. for the weak, remaining reflection when  $n \cong 1$ . In a following section we will study the reflection in a much wider  $x$ -range.

As

$$H(x) \cong -\frac{U}{8k_0 x_0^2} \cdot e^{-x/x_0}, \quad (38)$$

when  $x \gg x_0$ , we have

$$R^{(1)} = -\frac{U e^{-j2k_0 x}}{8k_0 x_0^2} \int_{-\infty}^x e^{-(j2k_0 + 1/x_0)x} dx = j \frac{1}{16k_0^2 x_0^2} \frac{U e^{-x/x_0}}{1 + j^{1/2} k_0 x_0}. \quad (39)$$

The reflecting power, which at this level is very small, thus falls exponentially with distance. Relation (39) will be compared with the result of the exact theory in a following section.

### Propagation in a medium with large variations in refractive index

So far we have only considered small changes in  $n^2$  which has been assumed  $> 0$ . If, however  $n$  becomes very small, or zero for real values of  $x$ , the propagation problem has to be attacked by different methods.

Let us assume that  $n^2$  has two zeros,  $z_1$  and  $z_2$ , at  $x = -x_1$  and  $+x_2$  respectively. This corresponds to the problem of the transmission of matter waves through a potential barrier or normal incidence transmission of electro-magnetic waves through an ionized layer at frequencies below the critical frequency.

Instead of considering  $n(x)$  as a function of  $x$  only we now consider it as a function  $n(z)$  of  $z = x + jy$ . We assume that it is possible to select in the  $z$ -plane a good path,  $P$ , connecting the regions  $-x > x_1$  and  $x > x_2$  such that  $H$  is small over the entire path. This means that the variation in  $I$  can be neglected and consequently

$$\frac{d\alpha^{(1)}}{dx} = H\alpha^{(2)} e^{\pm j(2W - \pi/2)}. \quad (40)$$

As before we use the time factor  $e^{-j\omega t}$  so that a wave incident from the negative  $x$  side is represented by  $\alpha^{(2)}(x)H^{(2)}(x)^*$ . We further choose such a path,  $P$ , that  $e^{+j2W}$  is dominant over  $e^{-j2W}$  ( $b > x_2$ ). We have in fig. 2 sketched such a path for a parabolic barrier or layer as a typical example. Several curves  $\text{Re}(n^2) = \text{const.} = c$ , and  $\text{Im}(n^2) = \text{const.} = d$  have also been drawn in the picture, based on the general form

$$f(z) = -m^2 \left\{ 1 - \left( \frac{z}{x_0} \right)^2 \right\}, \quad (m^2 > 1) \quad (41)$$

where  $x_0$  is the semi-thickness of the barrier (layer). In order to make  $n(z)$  one valued over the entire plane cuts have been made round its branch points  $z_1$  and  $z_2$ .

\* Note:  $n$  real and negative on the negative side of the axis of reals when  $-x > x_1$ .

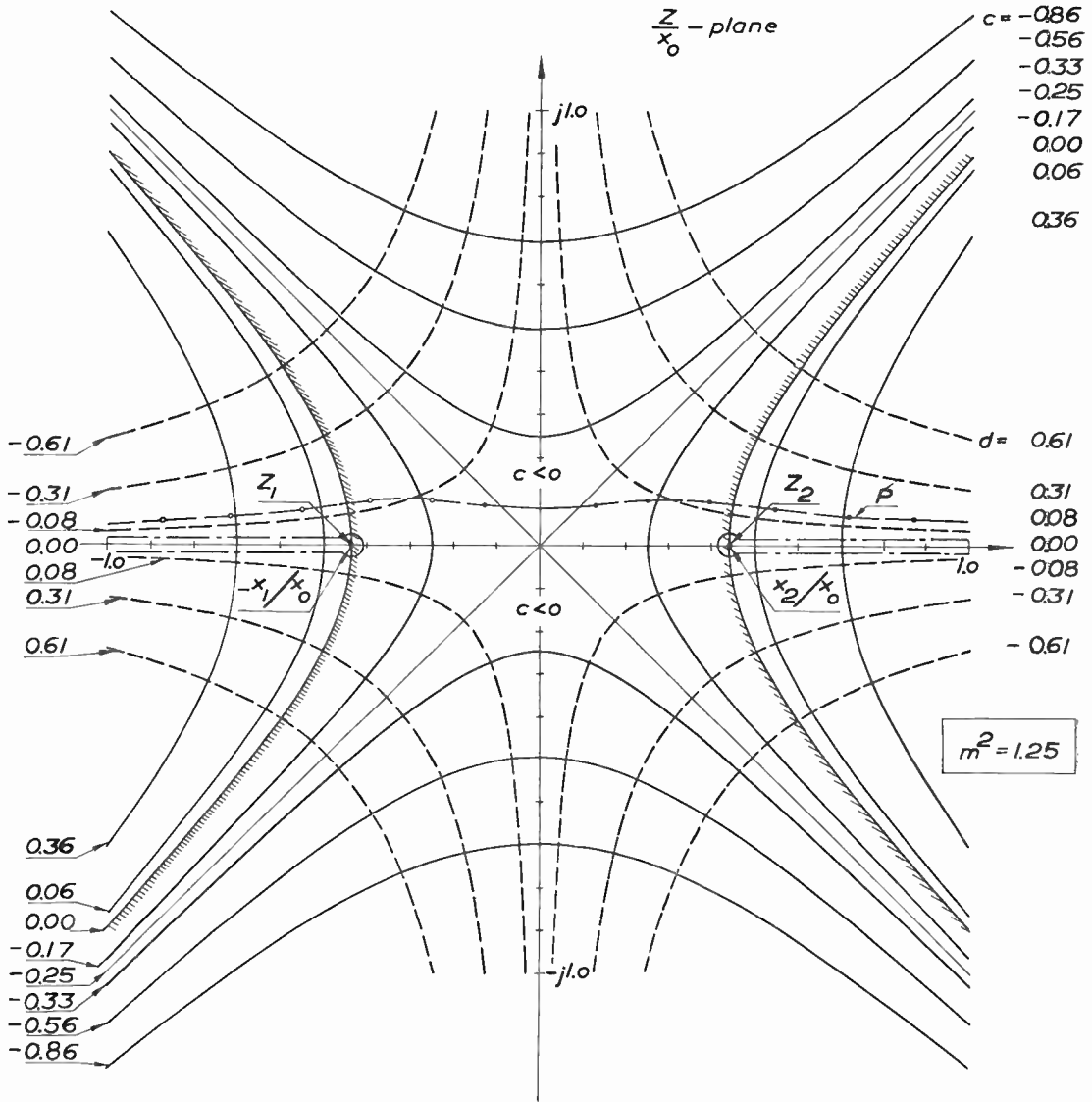


Fig. 2. The parabolic barrier in the  $z/x_0$ -plane ( $m^2 = 1.25$ ).

As  $e^{+j2W}$  is dominant over  $e^{-j2W}$

and

$$\left. \begin{aligned} \frac{da^{(1)}}{dx} &\approx 0, \text{ i. e. } a^{(1)} = \text{const.} = A^{(1)} = B^{(1)} \\ \frac{da^{(2)}}{dx} &\approx A^{(1)} He^{+j(2W - \pi/2)}. \end{aligned} \right\} \quad (42)$$

Now if we follow  $P$  from right (positive  $x$ -side) to left  $a^{(2)}$  according to (42) changes from 0 to  $A^{(2)}$ , because there is no wave assumed to approach the barrier from the right and we remain on the  $+j \cdot 0$  side of the cuts so that  $n$  is real and negative for  $x > x_2$ . With

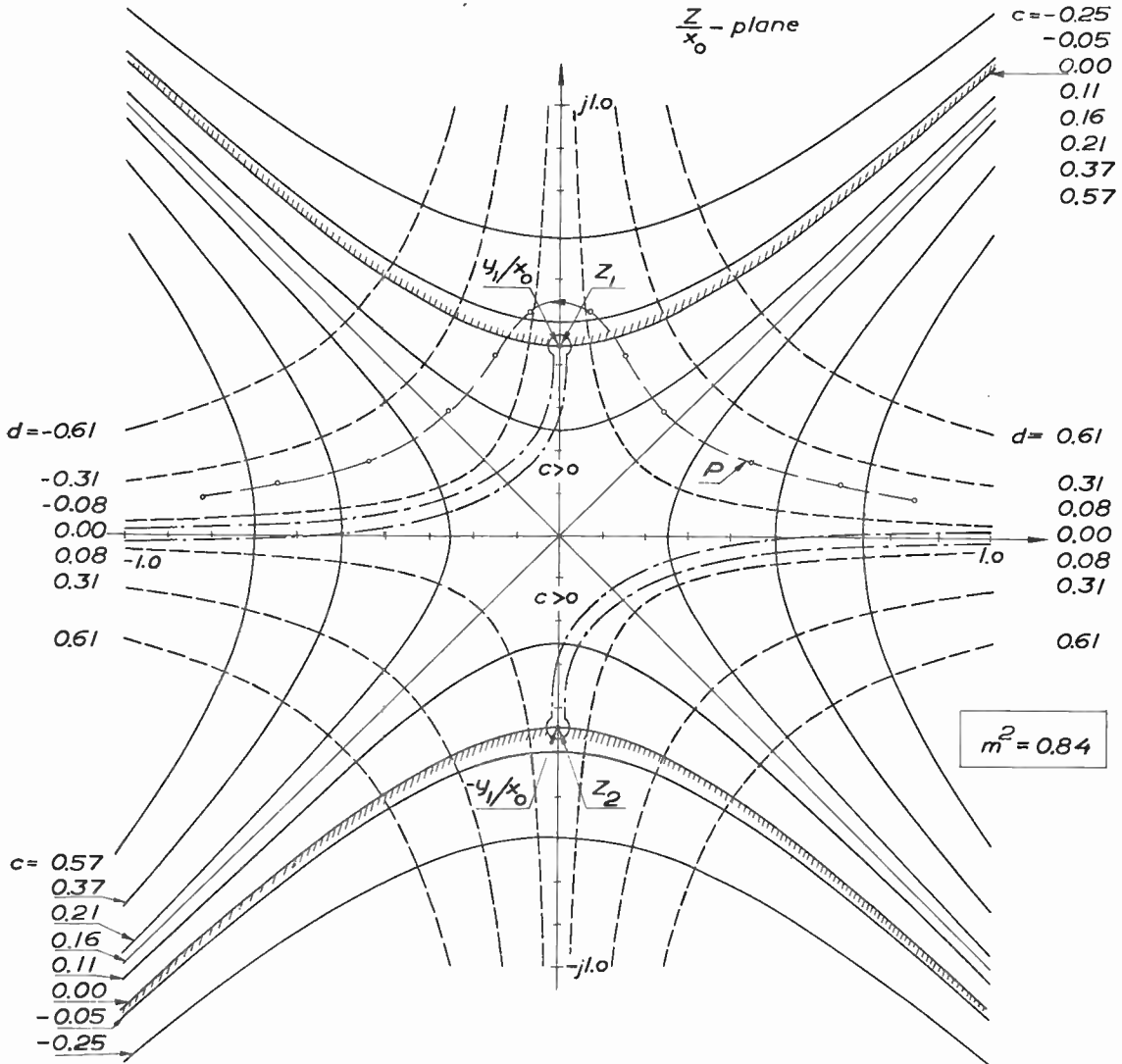


Fig. 3. The parabolic layer in the  $z/x_0$ -plane ( $m^2 = 0.84$ ).

the time-factor chosen  $\Pi^{(2)}(x)$  thus always represents a wave penetrating into the barrier, from the left or right.

The important change in  $a^{(2)}$  takes place in the STOKES' region where  $e^{+j2W}$  is dominant. We have approximately

$$a^{(2)} \approx A^{(1)} \int_P^x e^{+j(2W - \pi/2)} H dx, \quad (43)$$

where we again recognize the first order approximation. If, however, path  $P$  is good enough this is a very good approximation. Thus

$$R \cong \int_P^{\infty} e^{+j(2W - \pi/2)} H dx \quad (44)$$

Although formally simple this relation is not very useful.

However, as  $n$  is one valued over the  $z$ -plane

$$|II^{(1)}(x_b)| = |II^{(1)}(x_a)| \sqrt{\frac{n(x_a)}{n(x_b)}} e^{-k_0 \int_{x_1}^{x_2} |n| dx} \quad (45)$$

where  $-x_a > x_1$  and  $x_b > x_2$ , and as both  $II^{(1)}$ -functions represent waves leaving the barrier (layer), viz. the  $x_a$ -one the reflected wave and  $x_b$ -one the transmitted wave, we must have

$$|A^{(2)}|^2 = |A^{(1)}|^2 + |A^{(1)}|^2 e^{-2k_0 \int_{x_1}^{x_2} |n| dx} \quad (46)$$

i. e.

$$|R| = \left| \frac{A^{(1)}}{A^{(2)}} \right| = \frac{1}{\sqrt{1 + e^{-2k_0 \int_{x_1}^{x_2} |n| dx}}} \quad (47)$$

This is the familiar expression for the reflection coefficient of the potential barrier. Except when the branch points, levels of geometrical reflection, are very close (fraction of wave-length), the reflection, according to (47) is practically total.

The transmission coefficient is

$$|T| = \left| \frac{A^{(1)}}{A^{(2)}} \right| e^{k_0 \int_{x_1}^{x_2} |n| dx} = \frac{1}{\sqrt{1 + e^{+2k_0 \int_{x_1}^{x_2} |n| dx}}} \quad (47 a)$$

In the general cases of wave propagation we are also interested in the problem of transmission through a minimum in  $n$ , even though  $n$  never becomes zero for real values of  $x$ . This corresponds to  $m^2 < 1$  (but positive) in (41) for the parabolic case as shown in fig. 3 where the  $c$ - and  $d$ -curves are drawn for  $m^2 = 0.84$ . As before the good path,  $P$ , must approach the cuts from the  $+j \cdot 0$  side. If we deform the cut round  $z_1$  to enclose 0, we immediately infer that this time

$$|II^{(1)}(x_b)| = |II^{(1)}(x_a)| \sqrt{\frac{n(x_a)}{n(x_b)}} e^{+2k_0 \int_{y_2}^{y_1} |n| dx} \quad (48)$$

or

$$|R| = \left| \frac{A^{(1)}}{A^{(2)}} \right| = \frac{1}{\sqrt{1 + e^{2k_0 \int_{y_2}^{y_1} |n| dy}}} \quad (49)$$

because  $n$  is negative along the negative real axis on the  $+j \cdot 0$  side of the cut.

Results (47) and (49) can of course be combined in one formula

$$|R| = \frac{1}{\sqrt{1 + |e^{jk_0 \int_{z_1}^{z_2} n dz}|^2}} \quad (50)$$

which holds quite accurately as long as path  $P$  is good enough. The quality of the path has to be examined in dubious cases.

Even if one *a priori* is doubtful as to the application of (50) in the case  $z_2 = z_1$ , it nevertheless yields the physically proper result  $|R| = 1/\sqrt{2}$ . In the following section we will return to this question and show that (50) is substantially correct even if the branch points are very close together.

Relation (50), however, only yields the amplitude of the reflection coefficient not the phase. In order to estimate the phase one can, of course, as a first order approximation make use of expressions involving BESSEL functions of order  $\pm 1/3$ . Wave approximations of this kind were used already in 1915 by GANS in a fundamental paper, *Fortpflanzung des Lichts durch ein inhomogenes Medium* [3]. They have been used in much later applications by several writers including the present author [10, 11] and they have been discussed in mathematical detail by LANGER in several papers [12, 13, 14].

If  $n^2$  has a zero of the first order at  $z = z_2$ , we introduce the following approximate wave function

$$\psi_{1/3}^{(1)}(W_2) = \left(\frac{W_2}{n}\right)^{1/2} \cdot H_{1/3}^{(2)}(W_2) \cdot e^{\mp j\pi/6}. \tag{51}$$

where

$$W_2 = k_0 \int_{z_2}^z n(z) dz. \tag{52}$$

One easily finds that (51) is a solution of

$$\frac{d^2\psi}{dx^2} + (k_0^2 n^2 - Q_2)\psi = 0, \tag{53}$$

where

$$Q_2 = Q - \frac{5}{4} \left(\frac{W_2'}{3W_2}\right)^2. \tag{54}$$

The last term in (54) normally is very small except at or near the first order zero of  $n$  at  $z_2$  where it is  $\cong 5/8(z - z_2)$  and thus serves to make  $Q_2$  equal to zero or very small.

At the other branch point this is by no means the case and the  $\psi_{1/3}^{(2)}(W_2)$  - function can not be used. The proper form of course is  $\psi_{1/3}^{(2)}(W_1)$  where  $W_1$  denotes

$$W_1 = k_0 \int_{z_1}^z n(z) dz = W_2 + k_0 \int_{z_1}^{z_2} n(z) dz. \tag{55}$$

The connection of the  $\psi_{1/3}^{(1)}(W_2)$  - and  $\psi_{1/3}^{(2)}(W_1)$  - functions requires special consideration on account of the STOKES phenomenon.

a) *Considerable reflection* ( $m^2 > 1$  in the parabolic case)

For the sake of simplicity we assume that the transmission is loss-less so that  $z_1$  and  $z_2$  are situated on the axis of reals. If thus  $z_1 = x_1$ , and  $z_2 = x_2$  we have

$$W_1 = \left\{ \begin{array}{l} |W_1| e^{j\pi/2}, \quad x > x_1 \\ |W_1| e^{j2\pi}, \quad x < x_1 \end{array} \right\}$$

and

$$W_2 = \left\{ \begin{array}{l} |W_2|, \quad x > x_2 \\ |W_2| e^{j3\pi/2}, \quad x < x_2 \end{array} \right\} \tag{56}$$

With the same time factor,  $e^{-j\omega t}$ , as before  $\psi_{1/3}^{(2)}(W_2)$  represents a wave approaching the barrier (layer) from the right, and  $\psi_{1/3}(W_2)$  a reflected wave. As further

$$\psi_{1/3}^{(2)}(|W_1| e^{j2\pi}) = e^{j\pi/2} \psi_{1/3}^{(1)}(|W_1|)$$

$\psi_{1/3}^{(2)}(W_1)$  represents the wave penetrating the barrier, i. e. the connection relations become

$$\left. \begin{array}{l} \psi_{1/3}^{(2)}(|W_0| e^{j3\pi/2}) + A \psi_{1/3}^{(1)}(|W_0| e^{j3\pi/2}) = B \psi_{1/3}^{(2)}(|W_0| e^{j\pi/2}) \\ \psi_{-2/3}^{(2)}(|W_0| e^{j3\pi/2}) - A \psi_{-2/3}^{(1)}(|W_0| e^{j3\pi/2}) = B \psi_{-2/3}^{(2)}(|W_0| e^{j\pi/2}) \end{array} \right\} \tag{57}$$

where

$$|W_0| = \frac{k_0}{2} \left| \int_{x_1}^{x_2} n(x) dx \right|. \tag{57 a}$$

The above relations are good approximations only when the branch points  $x_1$  and  $x_2$  are so distant from each other (counted in wavelengths) that both  $\psi_{1/3}^{(2)}(W_2)$  and  $\psi_{1/3}^{(1)}(W_1)$  are good approximations to the solutions of (1) at the connection level  $W_1 = |W_0| e^{j\pi/2}$ .

As

$$\psi_{1/3}^{(2)}(W_2) \sim \frac{e^{\pm j\pi/2} |n|^{-1/2}}{(\pi/2)^{1/2}} \left\{ e^{|\omega_2|} \mp j \frac{1}{2} e^{-|\omega_2|} \right\} \tag{58}$$

when  $x < x_2$  and  $|W_2| \gg 1$ , we have the connection formula from right to left ( $x > x_2 \rightarrow x < x_2$ )

$$(n)^{-1/2} e^{\mp j(\omega_2 - \pi/4)} \rightarrow e^{\pm j\pi/2} |n|^{-1/2} \left\{ e^{|\omega_2|} \mp j \frac{1}{2} e^{-|\omega_2|} \right\}. \tag{59}$$

From right to left of  $x_1$  we similarly have { for  $\psi_{1/3}^{(2)}(W_1)$  }

$$|n|^{-1/2} \left\{ e^{|\omega_1|} + j \frac{1}{2} e^{-|\omega_1|} \right\} \rightarrow e^{j\pi/2} |n|^{-1/2} e^{j(|\omega_1| - \pi/4)}. \tag{60}$$

Relations (57) therefore yield

$$A \sim \frac{1 - \delta^2}{1 + \delta^2}, \text{ and } B \sim \frac{2\delta}{1 + \delta^2} \tag{61}$$

where

$$\delta = \frac{1}{2} e^{-2|W_0|}. \tag{62}$$

Thus

$$R \sim \frac{1 - \delta^2}{1 + \delta^2} e^{2j(W_2 - \pi/4)} \tag{63}$$

and the transmission coefficient

$$T \sim \frac{2\delta}{1 + \delta^2} e^{j(|W_1| + W_2)}. \tag{64}$$

It is well illustrated by fig. 4 that (63) yields substantially the same  $|R|$ -value as (50) ( $|R| = 1/\sqrt{1+4\delta^2}$ ) even when  $|W_0|$  is fairly small.

It is quite interesting to note that the result of (63) and (64) really can be interpreted in "geometrical" terms with the reflection virtually concentrated to the two branch points. If the virtual wave impedance at  $x = x_2 + |Ax|$  is represented by  $z_0$  the corresponding impedance at  $x = x_2 - |Ax|$  should be  $-jz_0$ .

Denoting the intervals  $x > x_2$ ,  $x_1 < x < x_2$ , and  $x < x_1$  by 1, 2 and 3 respectively we are led to introduce the following reflection and transmission coefficients, viz.

$$\left. \begin{aligned} R_{12} &= -\frac{1+j}{1-j} = e^{-j\pi/2}, & R_{32} &= e^{-j\pi/2}, \\ T_{12} &= \frac{-2j}{1-j} = \sqrt{2} e^{-j\pi/4}, & \dots & \dots \dots \dots \text{etc.} \\ T_{21} &= \frac{2}{1-j} = \sqrt{2} e^{+j\pi/4}, \\ R_{21} &= e^{j\pi/2}, \end{aligned} \right\} \tag{65}$$

$R_{12}$  denotes the branch point reflection coefficient for a wave approaching the branch point in interval 1,  $R_{21}$  the corresponding coefficient for a wave approaching the same branch point in medium 2, etc. If the virtual amplitude and phase change of the wave when progressing from branch point to branch point is represented by the coefficient  $\xi$  we can collect the following waves returning from the layer, viz.

$$e^{j|W_1|} [R_{12} + T_{12} \xi R_{23} \xi T_{21} \{1 + (R_{21} R_{23} \xi^2)^2 + (\dots)^4 + \dots\}] = e^{j(|W_1| - \pi/2)} \frac{1 - \xi^2}{1 + \xi^2}. \tag{66}$$

In this particular case the transmission of waves through the layer apparently roughly corresponds to transmission through three successive high pass ladder networks of which the central one has a cut off frequency above the wave frequency.

The reflection coefficient thus becomes

$$R = e^{2j(|W_1| - \pi/4)} \frac{1 - \xi^2}{1 + \xi^2},$$

i. e.  $\xi = \delta$ . The wave thus experiences no phase change when progressing from branch point to branch point but an attenuation

$$d = -\ln \xi = 2|W_0| + \ln 2. \tag{67}$$

b) *Considerable transmission* ( $m^2 < 1$  in the parabolic case)



If we this time for a change select the conjugate time factor  $e^{+j\omega t}$  we find that

$$\psi_{i/3}^{(2)}(W_1) = -\psi_{i/3}^{(1)}(|W_1| e^{-j\eta}) e^{-j\eta/2} \quad (x > 0) \quad (70)$$

represents a wave approaching the layer from the right ( $x < 0$ ) whereas

$$\psi_{i/3}^{(2)}(W_2) = \psi_{i/3}^{(2)}(|W_2|) e^{j\eta} e^{j\eta/2} \quad (x > 0)$$

represents a reflected wave. On the other hand

$$\psi_{i/3}^{(1)}(W_1) = -j \psi_{i/3}^{(2)}(|W_1| e^{j\eta}) e^{j\eta/2} \quad (x < 0) \quad (71)$$

represents a wave transmitted through the layer.

Our connection equations therefore become

$$\left. \begin{aligned} \psi_{i/3}^{(2)}(|W_0| e^{j3\pi/2}) + A \psi_{i/3}^{(2)}(|W_0| e^{j\pi/2}) &= B \psi_{i/3}^{(1)}(|W_0| e^{j3\pi/2}) \\ \psi_{-z/3}^{(2)}(|W_0| e^{j3\pi/2}) + A \psi_{-z/3}^{(2)}(|W_0| e^{j\pi/2}) &= -B \psi_{-z/3}^{(1)}(|W_0| e^{j3\pi/2}) \end{aligned} \right\} \quad (72)$$

As

$$\left. \begin{aligned} \psi_{i/3}^{(2)}(|W_0| e^{j3\pi/2}) &\sim \pm \frac{n^{-1/2}}{(\pi/2)^{1/2}} \left\{ 1 \mp j \frac{1}{2} e^{-2|W_0|} \right\} e^{j3\pi/4} \\ \psi_{i/3}^{(2)}(|W_0| e^{j\pi/2}) &\sim \frac{n^{-1/2}}{(\pi/2)^{1/2}} \left\{ 1 + j \frac{1}{2} e^{-2|W_0|} \right\} e^{j\pi/4}, \quad \text{etc.} \end{aligned} \right\} \quad (73)$$

we obtain from (71)

$$A = -\frac{2\delta}{1 + \delta^2}, \quad \text{and} \quad B = \frac{1 - \delta^2}{1 + \delta^2}. \quad (74)$$

Therefore, with the time factor  $e^{+j\omega t}$

$$R \sim \frac{2\delta}{1 + \delta^2} e^{-j(2|W_x| - \pi/2)}, \quad (75)$$

and

$$T \sim \frac{1 - \delta^2}{1 + \delta^2} e^{-j(|W_x| + |W_x|)} \quad (76)$$

It appears that even in this case the expressions for  $R$  and  $T$  can be interpreted in geometrical terms. Denoting the intervals  $y > y_1$ ,  $-y_2 < y < y_1$ , and  $y < -y_2$  by 1, 2 and 3 respectively we see that (74) can be interpreted as a series of reflections between the branch points according to the formula

$$R = e^{-j2|W_x|} [R_{23} \xi \{1 + (R_{21} R_{23} \xi^2) + (\dots)^2 + \dots\} + R_{21} \xi \{1 + (R_{23} R_{21} \xi^2) + (\dots)^2 + \dots\}]. \quad (77)$$

If the branch points are sufficiently remote, i. e.  $\delta^2 \ll 1$ , which means that  $e^{-4|W_0|} \ll 4$ , it appears that it is sufficient to consider only the first terms in the expansions of  $R$  and  $T$ . When therefore  $|e^{-2k_0 \int_{z_1}^{z_2} ndz}| \ll 4$ ,  $R$  and  $T$  can be obtained by elementary phase integration, in the case of  $R$  round the nearest branch point and back to the incidence

boundary, in the case of  $T$  from boundary to boundary. The older methods of phase integration, used by ECKERSLEY and others, which as a matter of fact do not explain the reflection phase shift  $-\pi/2$ , thus only are first order approximations of the *complete* method of phase integration which consider all waves running between the branch points.

A few words should be said about the wave propagation in dissipative media. Although the ray concept and a law such as SNELL's hardly are applicable, as discussed in detail by the present author in a previous communication [10, 11], the approximate method of phase integration nevertheless generally can be used with an accuracy better than in the non dissipative case. This is due to the characteristic circumstance that the introduction of losses prevent the branch points from coming very close to each other in the critical case when conditions shift from reflection (mainly) to penetration. This is well illustrated by a typical example, the parabolic ionized layer, for which

$$n^2 = 1 - \frac{\omega_{c_m}^2}{\omega^2} \frac{1 - \left(\frac{z}{x_0}\right)^2}{1 + j\nu/\omega}, \quad (\text{time factor } e^{-j\omega t}) \quad (78)$$

where  $\nu$  is the collisional frequency of the free electrons,  $\omega_{c_m}$  the maximum angular critical frequency, i. e. the vertical incidence "penetration" angular frequency, and  $x_0$  as before the layer half thickness. Also according to (41)

$$m^2 = \omega_{c_m}^2 / \omega^2 (1 + j\nu/\omega) = \chi^2 / (1 + j\nu/\omega). \quad (78 a)$$

As the no — loss branch point is  $x_2 = x_0 \sqrt{1 - 1/\chi^2}$ , we have for moderate losses ( $\nu^2 \ll \omega^2$ ) and  $\chi > 1$

$$z_2 \cong x_2 - j\nu/2\omega \chi^2 \sqrt{1 - 1/\chi^2}. \quad (79)$$

The shortest distance between the branch points ( $\chi \approx 1$ ) approximately becomes

$$|z_2 - z_1|_{\min} \cong 2x_0 \sqrt{\nu/\omega}. \quad (80)$$

For the  $E$ -layer of the ionosphere with  $\nu \cong 2 \cdot 10^5$  and a wave frequency of 3 Mc/s we find  $|z_2 - z_1|_{\min} \sim 0.2x_0$ . As  $x_0$  at least of the order 10 km the minimum distance at the frequency chosen is about 20 wave lengths. The phase integral therefore can be used as a first order approximation practically through the entire frequency range in this particular case.

#### A few examples

1) Let us consider case (27), viz.  $n = \sqrt{1 + \delta_1 \tanh x/x_0}$ . The proper branch points are easily verified to be

$$z_{\frac{1}{2}} = x_0 (\pm j\pi/2 - \arctan \delta_1). \quad (81)$$

One further after elementary transformations finds

$$\text{Re} \left\{ 2jk_0 \int_{-x}^{z_1} \sqrt{1 + \delta_1 \tanh(z/x_0)} dx \right\} = \pi k_0 x_0 \sqrt{1 - \delta_1}$$

and thus as a first order approximation of the phase integral method

$$|R| \sim e^{-\pi k_0 x_0 \sqrt{1-\delta_1}}. \tag{82}$$

This is identical with the exact result (33) when the wave length is so short that  $\pi k_0 x_0 \delta_1/2 \gg 1$ .

2) In the friction free parabolic case with the branch points  $z_1 = \pm j\sqrt{1/\chi^2 - 1}$  ( $\chi < 1$ ) we easily find

$$\operatorname{Re}\left\{ 2jk_0 \int_{-x}^{\dot{z}_1} n(z) dz \right\} = \frac{\pi}{2} k_0 x_0 \left( \frac{1}{\chi} - \chi \right)$$

and thus as a first order approximation of the phase integral method

$$|R| \sim e^{-\frac{\pi}{2} k_0 x_0 (1/\chi - \chi)}. \tag{83}$$

Formula (50) accordingly yields

$$|R|^2 = \frac{e^{-\pi k_0 x_0 (1/\chi - \chi)}}{1 + e^{-\pi k_0 x_0 (1/\chi - \chi)}} \tag{84}$$

which is exact as previously shown by the author [11]. The close agreement between (83) and (84) is evident. In the communication just referred to the parabolic case has been considered in detail for various degrees of friction and it has been proved that generally the phase integral method yields a sufficiently accurate approximation.

3) In ALFVEN'S case (37) we have  $n = \sqrt{1 + Ue^{-x/x_0}}$  with the proper branch points

$$z_1 = x_0 (\ln U \pm j\pi). \tag{85}$$

The first order approximation of the phase integral method becomes for a wave coming from the right ( $x > x_0$ )

$$|R| \sim e^{-2 \operatorname{Re} \int_x^{z_1} n(z) dz} = e^{-2k_0 x_0 \pi}. \tag{86}$$

It will later be shown that this is identical with the exact result when the wave length is short.

### Transmission properties when the waves begin to penetrate the reflecting barrier

So far we have not thoroughly discussed the transmission properties when the branch points are very close to each other, i. e. when, roughly speaking, the layer transmits and reflects equally well.

It is only natural and practical to assume that the branch points are now located in a region where  $n^2$  is parabolic. For a so called CHAPMAN layer in the ionosphere, for example, we have

$$n^2 \approx 1 - \frac{\omega_{c_m}^2}{\omega^2} \cdot \frac{1 - \left(\frac{z}{2H}\right)^2}{1 + j\nu/\omega}, \quad (e^{-j\omega t})$$

if  $|z|^2 \ll (2H)^2$ , where  $H$  is the local scale height of the gas from which the layer is formed. When therefore the wave frequency lies in the vicinity of the penetration frequency ( $\omega_{c_m}/2\pi = f_{c_m}$ ) the branch points of  $n$  are very close and located in a parabolic region.

In the case of (28) we have a similar example with  $x_0$  roughly corresponding to  $2H$ . It should also be noted in this connection that for the  $F_2$ -layer of the upper ionosphere  $\omega_{c_m}^2$  frequently has a parabolic variation practically through the entire layer.

We now introduce the parabolic wave equation

$$\frac{d^2\psi}{dv^2} + k_0^2 \{1 - \chi^2(1 - v^2)\} \psi = 0 \tag{87}$$

where

$$v = x/x_0, \tag{87 a}$$

$$\chi = \frac{\omega_{c_m}}{\omega} \cdot \frac{e^{-j\varphi}}{\sqrt{\sigma}}, \tag{88}$$

$$\varphi = \frac{1}{2} \arctan(\nu/\omega), \tag{89}$$

and

$$\sigma = \sqrt{1 + (\nu/\omega)^2}. \tag{90}$$

The case of wave transmission through a non dissipative parabolic barrier has been studied by Voss [15] and in the general dissipative case under widely different conditions by the present author [10, 11, 16] who has shown that the following parabolic cylinder functions\*

$$\left. \begin{aligned} D(u e^{j\pi/4}), \quad D(u e^{-j\pi/4}), \quad \text{and} \quad D(u e^{j3\pi/4}) \\ j_2^{-1/2}, \quad -j_2^{-1/2}, \quad -j_2^{-1/2} \end{aligned} \right\} \tag{91}$$

represent the incident, the reflected and the penetrating wave respectively if the time factor is  $e^{-j\omega t}$ . We have

$$\left. \begin{aligned} u &= r \sqrt{4\alpha} e^{-j\varphi/2}, \\ \varrho &= \alpha e^{-j\varphi} (1 - 1/\chi^2), \\ \alpha &= \frac{\pi x_0}{\lambda_{c_m}} \cdot \frac{1}{\sqrt{\sigma}} = \frac{k_0 x_0}{2} \cdot |\chi| \cdot (\lambda_{c_m} = c_0/f_{c_m}) \end{aligned} \right\} \tag{92}$$

where

\* The notation of WHITTAKER is used.

The circuit relation connecting these three waves is [10]

$$D(u e^{j\pi/4})_{j\varrho - 1/2} = \frac{\Gamma(j\varrho + 1/2)}{\sqrt{2\pi}} \left\{ \begin{matrix} e^{\pi\varrho/2 + j\pi/4} D(u e^{-j\pi/4})_{-j\varrho - 1/2} + e^{-\pi\varrho/2 - j\pi/4} D(u e^{j\pi/4})_{-j\varrho - 1/2} \end{matrix} \right\}, \tag{93}$$

from which it immediately appears that in the case of zero losses

$$(\varphi=0) \text{ when } D(u e^{-j\pi/4})_{-j\varrho - 1/2} = \text{conjug. } D(u e^{j\pi/4})_{j\varrho - 1/2}$$

$$|R|^2 = \frac{1}{1 + e^{-2\pi\varrho}} = \frac{1}{1 + e^{\pi k_0 x_0 (1/\chi - \chi)}} \tag{94}$$

in complete agreement with (50).

In order to "connect" equation (87) with the actual wave equation we introduce

$$W = k_0 x_0 \int_{v_2}^v n(v) dv = \frac{k_0 x_0 \chi}{2} \int_{v_2}^v \{ v \sqrt{v^2 - \beta^2} - \beta^2 \ln(v + \sqrt{v^2 - \beta^2}) \}, \tag{95}$$

where

$$\beta^2 = 1 - 1/\chi^2. \tag{95 a}$$

We further assume that

$$W = k_0 \int_{x_2}^x n(x) dx. \tag{96}$$

Denoting the solutions (91) of (87) by  $\psi^{(1)}(v)$ ,  $\psi^{(2)}(v)$  and  $\psi^{(3)}(v)$  respectively we easily find that

$$\psi_0^{(1)}(v) = \sqrt{\mu} \psi^{(1)}(v) \tag{97}$$

where

$$\mu = \chi \sqrt{v^2 - \beta^2} / n(x) \tag{97 a}$$

satisfies the wave equation

$$\frac{d^2 \psi_0}{dx^2} + \psi_0 \left\{ k_0^2 n^2 + \frac{1}{2} \frac{\mu''}{\mu} - \frac{3}{4} \left( \frac{\mu'}{\mu} \right)^2 \right\} = 0. \tag{98}$$

In the parabolic range, where we assume that  $x_2$  and  $v_2$  are located, we thus have  $v_2 = x_2/x_0$  and  $v \approx x/x_0$ . Within this range therefore  $\mu = 1$  and  $Q = 0$ . If the zeros of  $n^2$  as assumed are located within the parabolic range  $Q(\mu)$  is very small outside this range, where  $v$  is no longer equal to  $x/x_0$ . *When therefore the zeros of  $n^2$  lie within the parabolic range  $\psi_0(v)$  is a very good approximation to the proper wave function.*

The reflection coefficient thus becomes

$$R = - \frac{\Gamma(j\varrho + 1/2)}{\sqrt{2\pi}} e^{\pi\varrho/2 + j\pi/4} \frac{\psi^{(2)}(v)}{\psi^{(1)}(v)}. \tag{99}$$

For a thick layer  $|\varrho|$  is very large except in the penetration-reflection range where  $|\chi| \approx 1$ . Therefore when  $|\varrho| \gg 1$ , (99) should yield the same result as the phase integral method. It is easy to show that this is the case.

With

$$v_2 = +\beta \tag{100}$$

we have by (95)

$$W_0(x) = k_0 x_0 \left\{ 1 - \frac{x^2 - 1}{2x} \ln \frac{x+1}{x-1} \right\} + k_0 \int_{x_0}^x n(x) dx. \tag{101}$$

Let us first consider the case of a non-dissipative medium, i. e.  $\varphi = 0$ . Naturally we assume that the layer (or barrier) is many penetration wave lengths thick. This means that  $\alpha \gg 1$ . We can then use asymptotic expansions for  $D(u e^{j\pi/4})$  already developed by the author [11]. Two different expansions have to be used, viz. one type when  $|e^2/2u^2| \ll 1$  (wave frequency lies in the penetration region) and another one when this is not the case ( $|e|$  very large).

However, it is possible, by several transformations, to obtain a bridging formula which can be used practically without restrictions in the no loss case. One finds

$$R = \frac{1}{\sqrt{1 + e^{-2\pi e}}} e^{j[2W_0(x) - \pi/2 + \xi]}, \tag{102} \quad (\varphi = 0)$$

where

$$\xi = \text{Phase} \{ \Gamma(2je) / \Gamma(je) \} + e \{ 1 - \ln(4|e|) \}. \tag{102 a}$$

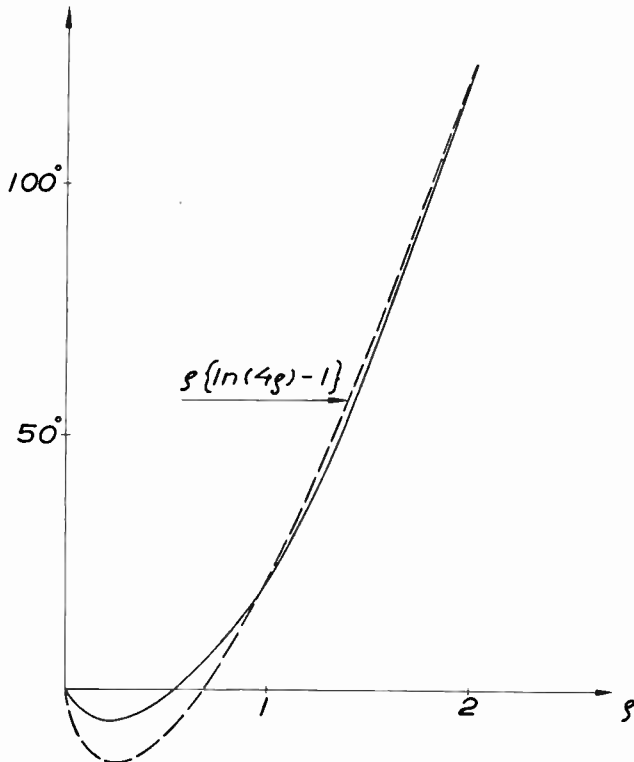


Fig. 5. Phase  $\{ \Gamma(2je) / \Gamma(je) \}$  as a function of  $e$ .

It is interesting to note that (102), as far as  $|R|$  is concerned, yields identically the same result as (50) of the "good path" method. Relation (102) only holds when the branch points are inside the parabolic range. When they are outside this range, however, the complete method of phase integration can be used. As has been shown the results of this method are identical with (50) to a high degree of accuracy. *We have therefore proved that the result of the "good path" method*

$$|R| = \frac{1}{\sqrt{1 + |e^{jk_0 z_1} \int_{z_1}^{z_2} n^2 dz|^2}}$$

is an extremely good approximation for all layers or barriers for which the zeros of  $n^2$  approach each other in a parabolic region. This covers the main cases of practical interest. It should be stressed in this connection that we have throughout assumed the layer to be many wave lengths thick, i. e.  $x_0 \gg \lambda_0$ . In the case of atmospheric radio wave propagation this is practically always the case. In the rare cases of very long waves ( $\lambda \sim 20000$  m) the wave equation has to be examined separately for each kind of  $n^2$ -variation. If this variation can be represented (approximately) by the general ERSTEIN-ECKART function the wave equation is easily solved.

It appears from (102) that in the penetration-reflection range layers with the same  $x_0$  have the same reflection properties in the no loss case. This is important. This means that layers with the same curvature at the  $n^2$ -minimum level change their transmission properties from reflection to penetration and vice versa in the same fashion because  $\varrho$  is proportional to  $\sqrt{L}$  where  $L$  is the radius of curvature of the  $n^2$ -curve at the minimum level.

Next let us discuss the phase angle of  $R$ . This is equal to the phase of the complete phase integral method,  $2\{W_0(x) - \pi/4\}$  when  $\xi$  is very small. One immediately finds from the STIRLING expansions of Phase  $\{\Gamma(2j\varrho)/\Gamma(j\varrho)\}$  and from fig. 5 that  $\xi \cong 0$  when  $|\varrho| > 1/2$ , i. e. when

$$\left| \frac{z_1 - z_2}{2x_0} \right|^2 \gg \frac{1}{k_0 x_0}$$

The shorter the wave length the closer will it be possible for the branch points to come without correction in the geometrical phase  $2\{W_0(x) - \pi/4\}$ , as expected.

In the field of radio wave propagation the time of travel  $t = d/d\omega\{|Phase(R)|\}$  is frequently measured. One defines the virtual height of the reflector as  $h_v = c_0 t/2$ . If the  $\xi$ -term in (102) is not considered this height becomes infinite at the penetration frequency. When the  $\xi$ -term is considered, however, one obtains a finite but considerable height as already demonstrated by the author [10].

When the losses are considered we obtain in stead of (102) the useful formula

$$R = \frac{\Gamma(j\varrho + 1/2) e^{\pi\varrho/2 + j\varphi(1 - \ln \varrho)}}{\sqrt{2\pi}} \cdot e^{j2\{W_0(x) - \pi/4\}} \tag{103}$$

where this time, as  $\varphi \neq 0$ , both  $W_0(x)$  and  $\varrho$  are complex according to (88) and (101).

As exp.  $[j2\{W_0(x) - \pi/4\}]$  is the first order approximation of the complete method of phase integration and

$$\frac{\Gamma(j\varrho + 1/2)}{\sqrt{2\pi}} e^{\pi\varrho/2 + j\varrho(1 - \ln \varrho)} \sim 1 \quad (|\varrho| \gg 1)$$

when  $|\varrho| \gg 1$  and as further according to (92)  $\varrho$  never becomes small when the losses are considerable we find that for a thick layer with at least moderate losses

$$R \sim e^{j2\{W_0(x) - \pi/4\}}. \quad (103a)$$

When the losses are moderate we find from (92) that the minimum  $|\varrho|$ -value becomes

$$|\varrho|_{\min} \cong \frac{k_0 x_0}{2} \cdot \frac{\nu}{\omega}. \quad (\omega \cong \omega_{c_m}). \quad (104)$$

When therefore the loss angle of the medium

$$\frac{\nu}{\omega} \gg \frac{2}{k_0 x_0} \cong \frac{\lambda_{c_m}}{\pi x_0} \quad (\omega \cong \omega_{c_m})$$

the first order approximation (103a) of the complete phase integral method is a good approximation even through the penetration frequency range.

Let us consider two examples from the ionosphere. For an  $E$ -layer with  $\lambda_{c_m} = 100 m$  and  $x_0 = 20 km$  we find that (103a) can be used even through the penetration frequency range if  $\nu \gg 3 \cdot 10^4$ . For a low  $E$ -layer where  $\nu$  at least  $3 \cdot 10^5$  (103a) thus can be used with considerable accuracy. For a  $F_2$ -layer with  $\lambda_{c_m} = 30 m$  and  $x_0 = 100 km$ , on the other hand, we find that  $\nu \gg 6 \cdot 10^3$  if (103a) could be used. As  $6 \cdot 10^3$  just is about the order of  $\nu$  for the  $F_2$ -layer we infer that for this layer the exact result (102) has to be used for detailed reflection property studies in the penetration frequency range. Compare *On the propagation of radio waves* [11] p. 143 et seq.

Finally the general formula for the transmission coefficient  $T$  should be written down. From (93) we have for the path  $v_j \rightarrow -v_0$

$$T = \frac{\Gamma(j\varrho + 1/2)}{\sqrt{2\pi}} e^{-\pi\varrho/2 - j\pi/4} \frac{\psi^{(3)}(-v_0)}{\psi^{(1)}(v_j)}. \quad (105)$$

or

$$T = \frac{\Gamma(j\varrho + 1/2)}{\sqrt{2\pi}} e^{\pi\varrho/2 + j\varrho(1 - \ln \varrho)} e^{j\{W_0(x_i) + W_0(-x_0)\} - \pi\varrho}. \quad (106)$$

As

$$e^{j\{W_0(x_i) + W_0(-x_0)\} - \pi\varrho} = e^{jk_0 \int_{x_i}^{-x_0} n(z) dz} \quad (107)$$

is equal to the first order approximation of the complete phase integral method we find again that when  $|\varrho| \gg 1$  this method is a good approximation.

### Application of the circuit relation of the wave equation

When the exact solution of the wave equations is known the remaining problem simply is to find the circuit relation, for example (93) in the parabolic case, which connects the incident, the reflected, and the penetrating waves. It is then possible to investigate in detail how the reflection coefficient varies in the medium.

a) *The ALFVEN case*

This case has already been studied approximately by two different methods, p. 20. The corresponding wave equation

$$\frac{d^2\Pi}{dx^2} + k_0^2 \left( 1 + \frac{Ue^{-x/x_0}}{U_1} \right) \Pi = 0, \tag{108}$$

is satisfied by the following wave functions, viz.  $H_{j2k_0 x_0}^{(1)}(2k_0 x_0 \sqrt{U_1})$ ,  $H_{j2k_0 x_0}^{(2)}(2k_0 x \sqrt{U_1})$ , and  $J_{j2k_0 x_0}(2k_0 x_0 \sqrt{U_1})$  representing the incident wave (traveling in positive  $x$ -direction, i. e.

towards the chromosphere), the reflected wave and the transmitted wave respectively (time factor  $e^{j\omega t}$ ). Naturally the circuit relation connecting these wave functions is

$$H_{j2k_0 x_0}^{(1)}(2k_0 x_0 \sqrt{U_1}) + H_{j2k_0 x_0}^{(2)}(2k_0 x_0 \sqrt{U_1}) = 2 J_{j2k_0 x_0}(2k_0 x_0 \sqrt{U_1}). \tag{109}$$

In order to allow also such short waves that  $2k_0 x_0 \gg 1$  we make use of the proper DEBYE-expansions of the HANKEL functions which can be written in the following suitable form, viz.

$$H_{j2k_0 x_0}^{(2)}(2k_0 x_0 \sqrt{U_1}) \sim e^{\mp j [2k_0 x_0 \{ \sqrt{1+U_1} + \ln(\sqrt{1+1/U_1} + \sqrt{1/U_1}) \} - \pi/4]} \frac{e^{\mp k_0 x_0 \pi}}{\sqrt{k_0 x_0 \pi \sqrt{1+U_1}}} \cdot (2k_0 x_0 \sqrt{U_1} > 1) \tag{110}$$

It is readily seen that these expansions are of B-K-W-J-type (2). When therefore  $2k_0 x_0 \sqrt{U_1} > 1$  the reflection coefficient becomes

$$R = \frac{H_{j\beta}^{(2)}(\beta \sqrt{U_1})}{H_{j\beta}^{(1)}(\beta \sqrt{U_1})} \sim e^{-j [2\beta \{ \sqrt{1+U_1} + \ln(\sqrt{1+1/U_1} + \sqrt{1/U_1}) \} - \pi/2] - \pi\beta} \tag{111}$$

$(e^{\pm 1/2x_0} \ll \beta \sqrt{U_1})$

where

$$\beta = 2k_0 x_0. \tag{111 a}$$

When  $U_1 \gg 1$  this result is the same as the first order approximation of the phase integral method (86). With the phase included (86) namely becomes

$$R \sim e^{-j [2\beta \{ \sqrt{1+U_1} - \frac{1}{2} \ln(1+2/\sqrt{U_1}) \}] - \pi\beta}. \tag{86 a}$$

Let us next consider the transmitted wave penetrating into the "thin" medium where  $U_1 \ll 1$ . As

$$\frac{1}{\Gamma(j\beta + 1)} = \sqrt{\frac{\sin h \pi\beta}{\pi\beta}} e^{-j \text{Phase} \{ \Gamma(j\beta + 1) \}} \quad (112)$$

and

$$\text{Phase} \{ \Gamma(j\beta + 1) \} \sim \pi/4 + \beta(\ln \beta - 1) \quad (\beta \gg 1) \quad (113)$$

when  $\beta \gg 1$ , we obtain

$$2J_{j\beta}(\beta\sqrt{U_1}) \sim \frac{e^{-j} \left[ k_0 \left[ x - 2x_0 \left\{ \ln \left( \sqrt{\frac{U_1}{2}} + 1 \right) \right\} + \pi/4 \right] + \pi\beta/2 \right] \sqrt{1 - e^{-2\pi\beta}}}{\sqrt{\pi\beta}} \left\{ 1 - \frac{\left( \frac{\beta\sqrt{U_1}}{2} \right)^2}{1 + j\beta} + \dots \right\} \quad (114)$$

$$(\beta \gg 1, e^{x/2x_0} \gg \beta\sqrt{U_1})$$

The transmission coefficient (counted from  $x=0$  to  $x \gg x_0$ ) thus becomes

$$T = \frac{2J_{j\beta}(\beta\sqrt{U_1})}{H_{j\beta}^{(1)}(\beta\sqrt{U_1})} \sim \sqrt{1 - e^{-2\pi\beta}} \cdot e^{-jk_0 \left[ x + 2x_0 \left\{ \sqrt{1 + U_1} + \ln \left\{ \frac{2}{\sqrt{1 + U_1}} (\sqrt{1 + U_1} + 1) \right\} - 1 \right\} \right]} \quad (115)$$

$$(\beta \gg 1, e^{x/2x_0} \gg \beta\sqrt{U_1}).$$

Thus  $|R|^2 + |T|^2 = 1$  as expected.

One naturally raises the question where does the main reflection take place? In order to investigate this matter we have to resort to relation (9) because we do not know what the HANKEL and BESSEL functions really represent in the transition range where  $\beta\sqrt{U_1}$  is neither large nor small. Due to the partial reflection in the medium these functions gradually change character.

In accordance with (9) we therefore introduce

$$\frac{a^{(1)}(x) \Pi_1^{(1)}(x)}{a^{(2)}(x) \Pi_1^{(2)}(x)} = R(x) = - \frac{\Pi_1^{(2)'} / \Pi_1^{(2)} - \Pi' / \Pi}{\Pi_1^{(1)'} / \Pi_1^{(1)} - \Pi' / \Pi} \quad (116)$$

where  $H = 2J_{j\beta}(\beta\sqrt{U_1})$  and  $\Pi_1^{(1)}$  and  $\Pi_1^{(2)}$  are the B-K-W-J-approximations (2).

It is easily shown from (116) that in our specific case we obtain the general result

$$R(x) = - \frac{\frac{1}{2} \frac{n'}{n} - jk_0 n + jk_0 - k_0 \sqrt{U_1} \cdot M}{-\frac{1}{2} \frac{n'}{n} + jk_0 n + jk_0 - k_0 \sqrt{U_1} \cdot M} \quad (117)$$

where  $n' = dn/dx$ ,  $n = \sqrt{1 + U_1}$ , and

$$M = J(\beta\sqrt{U_1})_{j\beta+1} / J(\beta\sqrt{U_1})_{j\beta} \quad (118)$$

1)  $e^{x/2x_0} \ll \beta\sqrt{U_1}$

Applying the DEBYE-expansions to the evaluation of  $M$  we find

$$M \sim -j \frac{1 - H_{j\beta}^{(2)}(\beta \sqrt{U_1}) / H_{j\beta}^{(1)}(\beta \sqrt{U_1})}{1 + H_{j\beta}^{(2)}(\beta \sqrt{U_1}) / H_{j\beta}^{(1)}(\beta \sqrt{U_1})}, \tag{119}$$

i. e.

$$R(x) \sim H_{j\beta}^{(2)}(\beta \sqrt{U_1}) / H_{j\beta}^{(1)}(\beta \sqrt{U_1}) \tag{e^{x/2x_0} \ll \beta \sqrt{U}}$$

as expected

$$2) \ e^{x/2x_0} \gg \beta \sqrt{U}$$

We now have  $n \cong 1 + \frac{1}{2} U_1$ , and, as is easily shown,

$$k^0 \sqrt{U_1} M \cong \frac{k_0}{2} \frac{\beta U_1}{j\beta + 1} \{1 + (U_1 \dots)\}. \tag{120}$$

Relation (117) therefore yields

$$R \cong -j \frac{U e^{-x/x_0}}{4\beta^2 (1 - j1/\beta)} \tag{e^{x/2x_0} \gg \beta \sqrt{U}} \tag{121}$$

This result is identical with the first order approximation  $R^{(1)}$  of (39) deduced for the conjugate time factor. This demonstrates the usefulness of approximations of this type (31) for weak reflectors when  $n \cong 1$ .

The variation of  $|R|$  with  $x$  is sketched in fig. 6. As  $R(x)$  is defined as the ratio between the down-coming (reflected) and up-going waves the main reflection thus takes place in the region where  $|R|$  decreases rapidly as  $x$  is increased. Roughly speaking the main reflection takes place in the neighbourhood of the level where  $U e^{-x/x_0} = 1/\beta^2$ , i. e. where  $n^2 = 1 + 1/\beta^2$ .

Returning to the DEBYE-forms of the wave functions (110) we notice that the denominator term  $\sqrt{1 + U_1}$  may be regarded as an impedance transforming factor (see also page 5). It might therefore be of interest to study briefly the "reduced" field strength  $|\Pi| \sqrt{1 + U_1} = |\Pi_{\text{red}}(x)|$ , where  $\Pi = J_{j\beta}(\beta \sqrt{U_1})$ .

When  $e^{x/2x_0} \ll \beta \sqrt{U}$  we find

$$\frac{|\Pi_{\text{red}}(x)|}{|\Pi_{\text{red}}(0)|} \sim \sqrt{\frac{1 - \sin^2 \varphi / \cos^2 h^2 \beta \pi / 2}{1 - \sin^2 \varphi_1 / \cos^2 h^2 \beta \pi / 2}}$$

and when  $e^{x/2x_0} \gg \beta \sqrt{U}$

$$\frac{|\Pi_{\text{red}}(x)|}{|\Pi_{\text{red}}(0)|} \sim \sqrt{\frac{1 - 1/\cos^2 h^2 \beta \pi / 2}{1 - \sin^2 \varphi_1 / \cos^2 h^2 \beta \pi / 2}} \sqrt{\cot h \beta \pi / 2},$$

where

$$\varphi = \beta \sqrt{1 + U_1} - \pi/4, \text{ and } \varphi_1 = \beta \sqrt{1 - U} - \pi/4.$$

These results are sketched in fig. 7 which demonstrates how the "standing wave" portion disappear as one proceeds into the "thin" medium where  $n \cong 1$ .

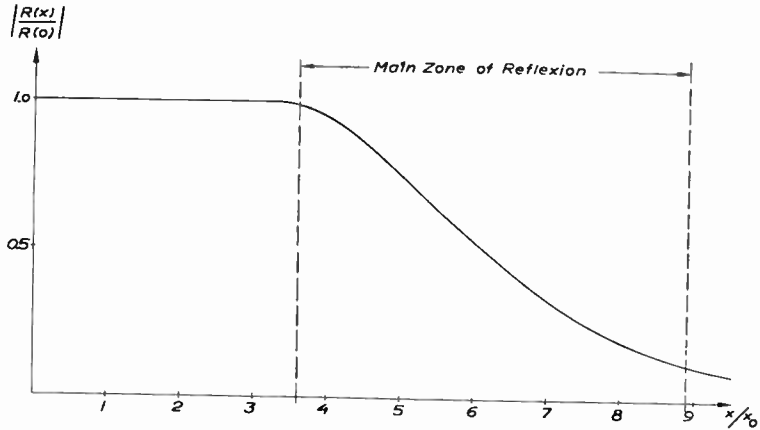


Fig. 6. Sketch of  $|R(x)|$  as a function of  $x$ .

b) *Duct propagation of micro waves*

Not only the upper atmosphere (the ionosphere) but also the lower troposphere, according to radar experiments, can act as a wave guide under certain circumstances. Such duct propagation has been studied during the war by several authors using phase integral methods and mode theories [17, 18].

The radio wave transmission theory developed by the present author 1943—1944 [11], which in a closed formula contains the degree of excitation of each mode, is especially suited for an exact study of this kind of propagation. To this question we will probably return in a later communication in this series. For the present we are only interested in a study of the circuit relation connecting the radial waves of the spherical propagation case.

The essential features of the inhomogeneity of the lower troposphere under meteorologically very stable conditions can be described by the following height function for the dielectric constant, viz.

$$\varepsilon = \varepsilon_0 \left\{ 1 - 2 \frac{r_0}{r} + 2 \left( \frac{r_0}{r} \right)^2 \right\}. \quad (122)$$

In this expression  $r_0 = a + h$  is the radial level (counted from the centre of the earth) below which rising rays can be bent down towards the earth. According to geometrical optics the penetration elevation angle of the ray (counted at the earth) becomes

$$\varphi_p = \arcsin \frac{h/a}{\sqrt{1 + 2(h/a)^2 + 2h/a}} \cong h/a, \quad (123)$$

if  $\varepsilon(a) = 1$ .

At this limiting angle the ray leaving the transmitter approaches  $r_0$  asymptotically.

The approximate cut off wave length,  $\lambda_c$ , is easily calculated when one remembers that the vertical distance between consecutive constant phase surfaces  $\lambda/4$  apart should never be more than about  $h$ , i. e.

$$\lambda_c \sim 4h^2/a. \quad (124)$$

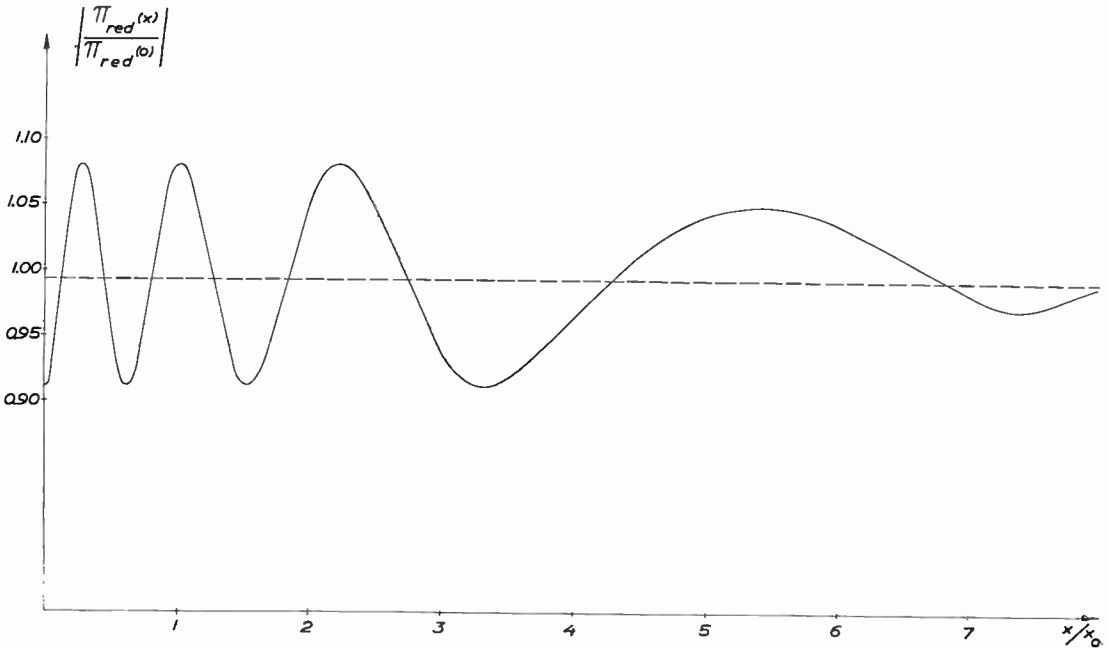


Fig. 7. "Reduced" wave field strength as a function of distance  $x$ .

Thus for a duct width of about 300 m we find  $\lambda \sim 6$  cm proving that only micro waves are short enough for this kind of propagation. The corresponding cut off or limiting wave length for the transmission of very long radio waves between  $D$ - or  $E$ -layer (of the ionosphere) and ground was discussed by the author in connection with the development of the radio wave transmission theory already mentioned [11].

Inserting the dielectric profile (122) in the wave equation we immediately find that the wave functions describing the propagation are of the type

$$\Pi_l = P_n(\cos \Theta) \xi^{(2)}_{(1)}(k_0 r). * \tag{125}$$

where 0 is counted from the transmitter and  $\xi^{(2)}_{(1)}(k_0 r)$  are the radial wave functions satisfying

$$\frac{1}{r^2} \frac{d}{dr} \left( \frac{d\xi}{dr} \right) + k_0^2 \epsilon_0 \left\{ 1 - 2 \frac{r_0}{r} - \frac{l(l+1)}{r^2} \right\} \xi = 0. \tag{126}$$

In the above equation  $l(l+1)$  denotes

$$l(l+1) = n(n+1) - 2(k_0 r_0)^2 = n(n+1) - 2\rho_0^2. \tag{126 a}$$

The circuit relation connecting  $\Pi^{(1)}(r)$  and  $\Pi^{(2)}(r)$  formally is almost as simple as (109) of ALFVEN's case. However, in order not to complicate the situation in this connection

\* This actually describes waves running in both clock wise and counter clock wise direction as  $P_n(\cos \Theta)$  is an angular standing wave function.

we select the simplest circuit relation which we know connects the waves from the outside, viz.

$$\xi^{(2)} + \frac{\Gamma\left(\frac{1}{2} + j\{\varrho_2 + \varrho_0\}\right)}{\Gamma\left(\frac{1}{2} + j\{\varrho_2 - \varrho_0\}\right)} e^{-j\pi\left[\frac{1}{2} + j\{\varrho_2 + \varrho_0\}\right]} \xi^{(1)} = \frac{\xi^{(3)}}{\Gamma(1 + j2\varrho_2)}, \tag{127}$$

where

$$\varrho_2 = \sqrt{2\varrho_0^2 - n(n+1) - 1/4}. \tag{127 a}$$

Introducing

$$k_1 = k_0 \sqrt{\varepsilon_0} \tag{128}$$

we have

$$\xi^{(3)} = \frac{e^{j\{k_1 r + \varrho_2 \ln(2k_1 r) + \pi/4\} + \pi\varrho_2/2}}{\sqrt{2k_1 r}} \cdot {}_1F_1\left\{\frac{1}{2} + j(\varrho_2 + \varrho_0); 1 + j2\varrho_2; 2jk_1 r\right\} \tag{129}$$

where  ${}_1F_1$  denotes a KUMMER function.

Let us introduce

$$n(n+1) = \varrho_0^2 \sin^2 \zeta_0, \tag{130}$$

where  $\zeta_0$  to a very high degree of approximation represents the angle between the wave direction and  $\bar{r}_0$ . When  $\varrho_2^2 - \varrho_0^2 \ll \varrho_0$ , i. e. when

$$\cos \zeta_0 < 1/\varrho_0 \tag{131}$$

we can use the following asymptotic expansions for  $\xi^{(1)}$  and  $\xi^{(2)}$ , viz.

$$\xi^{(1)}(k_0 r) \sim \frac{e^{\mp j\{k_1 r - \varrho_0 \ln(2k_1 r) - \pi/2\} \pm \pi\varrho_0/2}}{2k_1 r} \left[ 1 - \frac{r_0}{2r} \left\{ 1 \mp j \frac{\varrho_2^2 - \varrho_0^2}{\varrho_0} \right\} + \dots \right]. \tag{132}$$

As  $\varrho_0 \gg 1$ ,  $\cos \zeta_0$  therefore must be very well when (132) is used. This means that (132) can only be used with reasonable accuracy when the ray elevation is close to the limiting angle  $\varphi_p$ . However, it is in this ray direction that the sudden change from reflection to penetration takes place when  $\varphi_p$  is increased and it is therefore completely sufficient for our present purpose to limit ourselves to the limited direction range for which (132) can be used. When  $\varrho_2^2 - \varrho_0^2$  no longer  $\ll \varrho_0$  the saddle point method has to be used to obtain the proper expansion of  $\xi^{(1)}$ . However, it is outside the scope of the present communication to discuss this question further. In conclusion it should be mentioned that exactly the same problem is encountered in the discussion of the transmission of waves through a barrier or layer with parabolic maximum in potential function (or parabolic minimum in dielectric constant). Outside the penetration frequency region special saddle point expansions of the wave equation have to be used as shown by the present author [11]. Relation (112) actually is a bridging expression connecting the results of the saddle point series and the penetration range expansion corresponding to (132).

It appears from (132) that when  $k_1 r$  is very very large  $\xi^{(2)}$ , as expected, reduce to ordinary spherical waves with the minor correction of a slowly changing phase factor. At the top of the duct, however, where the wave penetrates or breaks through,  $r = r_0$ , and

$$\frac{\partial}{\partial r} \{k_1 r - \varrho_0 \ln(2k_1 r)\} = 0, \tag{133}$$

$(r = r_0)$

i. e. with the time factor  $e^{-j\omega t}$ ,  $\xi^{(1)}(k_0 r)$  represents a wave approaching the duct boundary  $r_0$  from the outside or from the inside. This is a very interesting property. The reverse is true of  $\xi^{(2)}(k_0 r)$ .

In this respect  $\xi^{(2)}$  closely resemble the wave functions (93), (97) of the parabolic barrier. When therefore  $\varrho_0 \gg 1$ , and this is always the case, circuit relation (127) can be used to study transmission properties up and down through the duct boundary.

By (127) and (132) the reflection coefficient therefore becomes

$$R = \frac{\Gamma\{1/2 + j(\varrho_2 - \varrho_0)\}}{\Gamma\{1/2 + j(\varrho_2 + \varrho_0)\}} \cdot e^{-\pi\varrho_2 - j2\{k_1 r - \varrho_0 \ln(2k_1 r) + \pi/4\}}. \tag{134}$$

Using the multiplication rule of the  $\Gamma$ -functions we easily verify from (134) that very accurately

$$|R|^2 = \frac{1}{1 + e^{2\pi(\varrho_2 - \varrho_0)}}. \tag{135}$$

As

$$\sin \zeta_0 = \cos \varphi / \cos \varphi_p, \tag{136}$$

where  $\varphi$  is the elevation of the wave normal at ground level, we have

$$2\pi(\varrho_2 - \varrho_0) = -\pi k_1 r_0 \cdot \frac{\cos^2 \varphi - \cos^2 \varphi_p}{\cos^2 \varphi_p} \cong -2\pi k_1 r_0 \frac{\cos \varphi - \cos \varphi_p}{\cos \varphi_p}. \tag{137}$$

As further  $k_1 r_0$  is a very very large quantity we see that according to (135) there is an almost sudden (very sharp) transition from reflection to penetration when the elevation increases above the limit direction  $\varphi_p$ .

It is easily shown that phase integration between the branch points yields

$$\left| e^{jk_0 \int_{z_1}^{z_2} n dz} \right|^2 = e^{2\pi(\varrho_2 - \varrho_0)},$$

i. e. the results of (135) and (50) are identical. This is not surprising because we have already shown that (50) holds good for a thick layer with parabolic minimum in  $\epsilon$ , such as in the present case with profile (122).

## References

1. LORD RAYLEIGH: On the propagation of waves through a stratified medium, with special reference to the question of reflection. *Proc. Roy. Soc., A* **86**, 1912.
2. K. FÖRSTERLING: Lichtfortpflanzung in inhomogenen Medien. *Phys. Zeits.*, **14**, 1913, **15**, 1914.
3. R. GANS: Fortpflanzung des Lichts durch ein inhomogenes Medium. *Ann. d. Phys.* **47**, 1915.
4. K. FÖRSTERLING: Über die Ausbreitung des Lichtes in inhomogenen Medien. *Ann. d. Phys.*, **11**, 1931.
5. P. S. EPSTEIN: Reflection of waves in an inhomogeneous absorbing medium. *Nat. Acad. Sci.*, **16**, 1930.
6. H. EYRING, J. WALTER and G. KIMBALL: *Quantum Chemistry*, p. 311.
7. S. A. SCHELKUNOFF: Solution of linear and slightly non linear differential equations. *Quart. Appl. Math.*, **3**, 1946.
8. E. C. KEMBLE: A contribution to the theory of the B. K. W. method. *Phys. Rev.*, **48**, 1935.
9. H. ALFVEN: Granulation, magneto-hydrodynamic waves, and the heating of the solar corona. *Mon. Not. Roy. Astro. Soc.* **107**, 1947.
10. O. E. H. RYDBECK: A theoretical survey of the possibilities of determining the distribution of the free electrons in the upper atmosphere. *Trans. Chalmers University of Technology*, **3**, 1942.
11. O. E. H. RYDBECK: On the propagation of radio waves. *Trans. Chalmers Univ.*, **34**, 1944.
12. R. E. LANGER: The asymptotic solutions of certain linear ordinary differential equations of the second order. *Trans. Amer. Math. Soc.*, **36**, 1934.
13. R. E. LANGER: The asymptotic solutions of ordinary linear differential equations of the second order, with special reference to the Stokes phenomenon. *Bull. Amer. Math. Soc.*, **40**, 1934.
14. R. E. LANGER: On the connection formulas and the solutions of the wave equation. *Phys. Rev.* **51**, 1937.
15. W. VOSS: Bedingungen für das Auftreten des Ramsauereffektes. *Zeits. f. Phys.*, **83**, 1933.
16. O. E. H. RYDBECK: The reflexion of electromagnetic waves from a parabolic ionized layer. *Phil. Mag.* XXXIV, 1943.
17. C. L. PEKERIS: Wave theoretical interpretation of propagation of 10-centimeter and 3-centimeter waves in low-level ocean ducts. *Proc. Inst. Rad. Eng.*, May, 1947.
18. H. G. BOOKER and W. WALKINSHAW: The mode theory of tropospheric refraction and its relation to wave-guides and diffraction. *Meteorological factors in radio wave propagation*, London, 1946.

## Table of Contents

	Page
Introduction and Summary .....	3
Fundamental theory .....	5
Propagation in a medium with small variations in refractive index .....	8
Propagation in a medium with large variations in refractive index .....	11
Transmission properties when the waves begin to penetrate the reflecting barrier .....	21
Application of the circuit relation of the wave equation .....	27
References .....	32

*Reports from the Research Laboratory of Electronics:*

1. RYDBECK, OLOF E. II., *The theory of the traveling wave tube*, 1947.\*
2. TOMNER, J. SIGVARD A., *The experimental development of traveling-wave tubes*, 1947.
3. SVENSSON, S. INGVAR, *Pulser and water load for high power magnetrons*, 1947.
4. INGÅRD, UNO, *On the radiation of sound into a circular tube with an application to resonators*, 1948.
5. STRANZ, DIETRICH, *A study of impressive wave formation in the atmosphere*, 1948.
6. STRANZ, DIETRICH, *Ozonradiosonde*, 1948.
7. RYDBECK, OLOF E. II., *On the propagation of waves in an inhomogeneous medium*, I, 1948.

---

\* Not published in the Chalmers Transactions but in Ericsson Technics. Copies can be obtained upon request from the Research Laboratory of Electronics, Chalmers University of Technology.

*Earlier publications from the Research Laboratory of Electronics:*

- RYDBECK, OLOF E. H., *A theoretical survey of the possibilities of determining the distribution of the free electrons in the upper atmosphere*, 1942, Trans. Chalmers Univ. of Technology no. 3, 1942.
- RYDBECK, OLOF E. H., *On the propagation of radio waves*, Trans. Chalmers Univ. of Technology no. 34, 1944.
- RYDBECK, OLOF E. H., *On the spherical and spheroidal wave functions*, Trans. Chalmers Univ. of Technology no. 43, 1945.
- RYDBECK, OLOF E. H., *A simple Kerr modulator for ionospheric recording*, Trans. Chalmers Univ. of Technology no. 44, 1945.
- RYDBECK, OLOF E. H., *Chalmers solar eclipse ionospheric expedition 1945*, Trans. Chalmers Univ. of Technology no. 53, 1946.

Copies can be obtained upon request from the Chief Librarian, Chalmers University of Technology.

